UNIVERSITY OF LEEDS

Thermofluid Engineering of the Honey bee (*Apis Mellifera*) nest

Derek Morville Mitchell

Submitted in accordance with the requirements for the
degree of Doctor of philosophy

University of Leeds

School of Mechanical Engineering

01/2024

The candidate confirms that the work submitted is his own and that appropriate credit has been given where reference has been made to the work of others

Acknowledgements

Thanks for the assistance of my supervisors for guidance in navigating the processes (Harvey Thompson, Jon Summers), Catherine Elaine Mitchell for the proof reading of the many papers and documents that have formed this thesis, Thomas Seeley for kind words of encouragement in 2011 and to the many beekeepers who assisted in providing honey bee colonies and apiary space.

The thesis was proof-read before submission by a third-party proof-reader. The PGR confirms that the third-party proof-reading undertaken was in accordance with the Postgraduate Researcher Proof-reading Policy.

Abstract

Honey bees refine flower nectar into honey in summer and maintain humidity and 20°C within their nest in -40°C winters, but their interactions with quantified nest thermal properties are not studied. Our core hypothesis is that the nest enclosure is an intrinsic part of the honey bee colony, which uses nest properties to manipulate the thermofluids within, which have in turn shaped the honey bee. This has not been understood in either academia or agriculture and has led to adverse consequences in both the study and husbandry of this important pollinator. Thus, in order to understand, and design for the honey bee we need to understand its manipulation of the thermofluid environment i.e. its thermofluid engineering. Analysis of the thermofluid engineering of honey bees shows:

- The range, diversity and efficiency of their nectar foraging is linked to the thermal efficiency of their nest.
- The nest thermal properties are major factors in the temperature and humidity regulation (homeostasis) for the diverse requirements of the production of honey, the raising of new honey bees and the suppression of parasites.
- The expansion of honeybees into different climatic regions is a result of subspecies adapting by changing their body size and hence resistance to convection within the nest.
- Honey bees' natural nests within tree cavities have thermofluid properties which allow them to avoid forced clustering. In contrast, man made hives have non-optimal design characteristics such that forced clustering is frequent and unavoidable.
- Basic assumptions about heat transfer in the honey bee nest in cold climates, which have been prevalent since before World war 1, are incorrect and as a consequence honey bees in winter are refrigerated (in North America) or kept in hives which provide not much more protection than a metal box.

Table of Contents

Index of Tables

Table of Figures

This page is intentionally bank

This page is intentionally bank

Chapter 1 Introduction

1.1 Apis Mellifera and Daughters Sugar Refining and Air-conditioning Engineers Established -6×10^6

What is the thermofluid control domain of an animal? A grey seal slips off a sunny rock on the coast of Scotland into cold seawater below 10°C. It has to keep its main organs at around 37°C despite the chilling water. To do this it has to reduce its heat loss. It achieves this by constricting blood vessels above the thick fatty layer in its body so that its skin and some of that fat is almost at the same temperature as the water. When it regains the sunny rock it has the opposite problem of managing solar heat gain and therefore reverses the process, some seals even turn pink (Erdsack et al., 2012). The seal also has to maintain the humidity of its internal air spaces i.e. its lungs and upper digestive tract at a level close to saturation at 37°C. The outside air would rapidly dessicate these organs so it has a heat exchanger/water reclamation unit i.e. its sinuses (Mason et al., 2020). A seal's thermofluid control domain volume is only its body and fur.

In contrast, a honey bee colony temperature regulates its brood volume closely to 34°C (Seeley, 1985) and some non-brood volume to at least 18°C, even if the outside temperature is -40°C. It maintains 50% relative humidity (RH) where its stores its energy reserves, and up to 90% RH at 34°C in its brood (Doull, 1976). However, its thermofluid control domain (in a tree nest) is a ~40 litre cavity (Seeley and Morse, 1976) and a significant part of the tree wood surrounding it. The tree wood being used as insulation and thermal buffer, and support for a vapour retarding barrier (Mitchell, 2016).

This control volume is approximately a million times that of an individual honey bee and a hundred times that of the combined volume of the colony’s members. A domain in which they spend more than 80% of their total lifetime, which in relative volume and control sophistication, has only been surpassed by humans in the early 20th century, while Apis mellifera has been doing this for 6 million years. They increased their range of climates by dividing into subspecies at least 600,000 years ago (Whitfield et al., 2006).

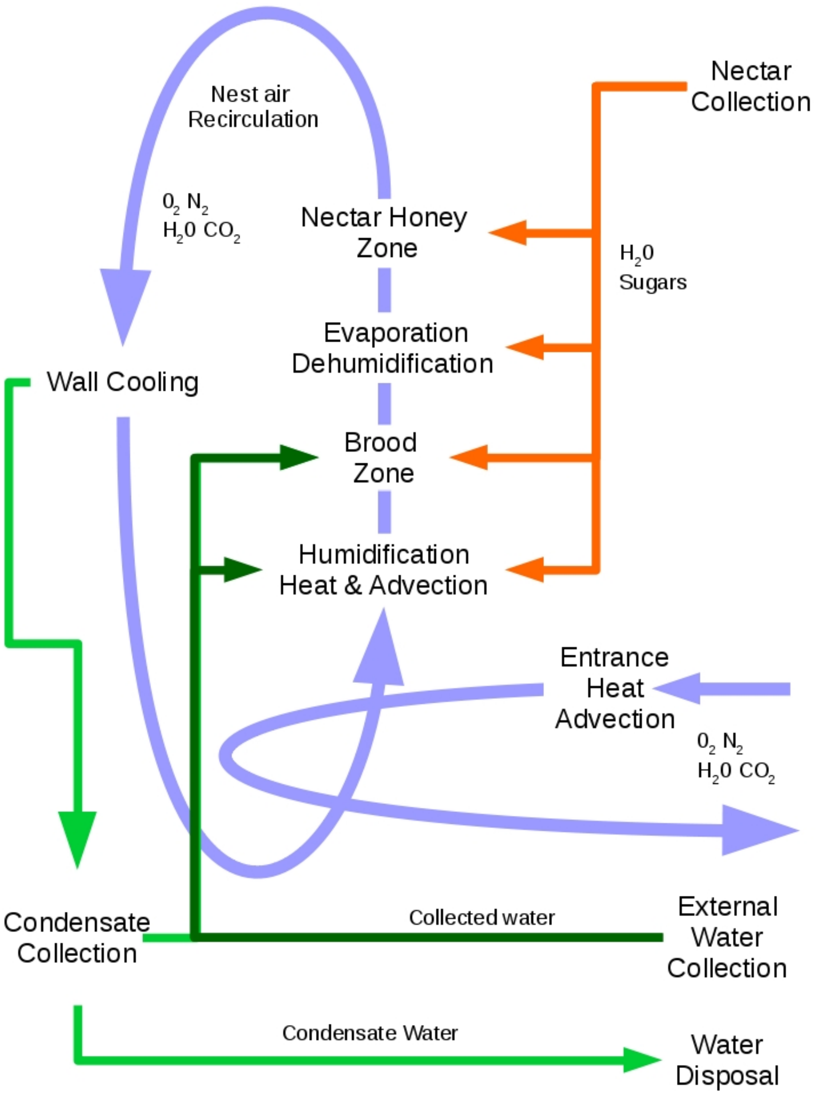

Figure 1.1: Honey bee thermofluid control domain (Mitchell, 2019).

Chapter 1 Introduction

The honey bee thermofluid control domain features (figure 1.1):

- Temperature regulation on a micro and macro scale including very precise zoned control +/- 0.1K) (Debnam, 2022).
- Humidity regulation/vapour retardation barriers and evaporating water collected for the purpose (Ellis et al., 2008; Hagenmaier and Shaw, 2019).
- Local heat generation and cooling.
- Construction of composite insulating structures for gross insulation and micro-climates.
- Sugar refining.
- Fuel storage – honey encapsulated in wax.
- Forced circulation and ventilation – fanning their wings in cooperating groups to control temperature humidity and carbon dioxide inside the hive.
- Condensate reclamation.

The honey bee colony achieves this initially with a combination of sophisticated balanced multi-variable nest site selection (Seeley, 2010), nest site excavation, and extensive internal constructions including the installation of a vapour retarding lining. It is then followed by active manipulation of temperature and humidity of the air flows within.

All of this enables the survival of these small insects, without hibernating, to withstand long winters, with temperatures below -40ºC, and summer temperatures above 40ºC while refining prodigious amounts (up to 500kg per colony per year) of dilute sugar solution to the concentrate we know as honey. Honey bees construct structures in which they perform honey refining, they construct structures in which they perform climate control. In short honey bees, specifically the females, perform all the functions of sugar refiners and air conditioning engineers, and have been doing so for 6 million years. They can be therefore validly be described as thermofluid engineers. This thesis is an analysis of their work in thermofluids and in particular how their enclosure impacts them.

The honey bee has been of great importance to humans for its pollination as well as its honey for thousands of years. However our lack of understanding of its thermofluid engineering has led to misconceptions that adversely impact the honey bee, which is also a subject for this thesis.

1.2 Human impact

There is a marked difference between the nest enclosures honey bees evolved with i.e. tree cavities and those that result from human intervention i.e. thin walled wooden hives with removable frames within stackable boxes (figure 1.2). The changes that impact the heat transfer can be categorised as follows:

1. Enclosure material, construction and apertures: 19mm walls vs 150mm walls, high aspect ratio vs low aspect ratio, closed floor vs 0.2m^2 meshed floor opening, entrance length to effective diameter (L/D) ratio of 1 vs 7 (Mitchell, 2016).

Figure 1.2: Typical tree nest and wooden hive compared.

2. Internal structures: from wall attached comb to removable frames with almost continuous air gap (Seeley and Morse, 1976; Cushman, 2011).
3. Vertical organisation: from a constant volume and aspect ratio to adding and removing boxes (Seeley and Morse, 1976; Mitchell, 2016).

These changes impact the honey bee in the following ways (Seeley, 2019):

- Increased metabolic rate (Southwick, 1982).

- Require more effort in storing food.
- Reduced winter survival for smaller colonies.
- Increased susceptibility to disease (Flores et al., 1996).
- Increased number of parasites (Kraus and Velthuis, 1997).
- Reduced hygienic activity in the nest (Tahmasbi, 2009).
- Reduced adult forager life (Wang et al., 2016).

1.3 Engineering an Extended Phenotype

Why has the interaction of the nest enclosure with the honey bee attracted so little attention in honey bee research, one of the most researched animals on the planet? In biological terms the objects outside of the animals body that are intrinsic to the existence of an animal are termed the extended phenotype (Dawkins, 2016), however, the most frequently cited animal is the beaver, that builds dams in watercourses for protection and transport. Amongst insects the one associated with the term extended phenotype is the mound building termite e.g. *Macrotermes* (Abou-Houly, 2010). So why is not the honey bee amongst those with an extended phenotype. This can first simply be put down to the fact that while the others are very obvious to the human observer, for the honey bee it is hidden within a tree and involves the manipulation (in the dark) of fluids that are invisible, and which are not always correctly interpreted (Alwan, 2011; Fitzallen et al., 2016). However, thermofluids have been extensively researched for other animals (Mason et al., 2020; Flekkøy et al., 2023; Yuk et al., 2023) some which are even extinct (Bourke et al., 2018) though it seems this is restricted to inside the body envelope, with the possible exception of macrotermes. Secondly, early research focused on the cluster as being the limit of the thermal envelope (Phillips and Demuth, 1914), and this view has been propagated since, with heavy reinforcement in the 1940's (Farrar, 1943; Anderson, 1943; Anderson, 1948) and 1980's (Southwick, 1982) and continues to this day (DeGrandi-Hoffman et al., 2023). Thus the idea that the nest enclosure is part of the thermofluid control domain has been closed out. Two examples, First, research into energy expensive internal coating of the nest (propolis) by the honey bees has been restricted to its chemical and biocidal properties (Simone et al., 2009). Second, the weight of the enclosure is not considered in calculations of metabolism per unit mass (Southwick and Mugaas, 1971; Southwick, 1985; Southwick and Heldmaier, 1987)

1.4 Motivation & goals

On the morning of the first day of being somewhat reluctantly introduced to beekeeping, the author was pleasantly informed of the details of honey bee life, but the afternoons confrontation with a wooden hive jarred. It was obvious something was amiss and did not add up. More inspection reinforced this suspicion to the extent of the "boy staring at the emperors new clothes", yet it appeared that all of the sage bee keepers and learned honey bee researchers were apparently convinced that all honey bee nest enclosures did little more than keep off the wind and the rain. This could not stand, and thus became a course of research to prove that: the properties of honey bee nest enclosures mattered to honey bees, the enclosure was part of the extended phenotype of the honey bee, and the tool to prove it was thermofluid engineering. During the exploration of the problem the following hypotheses or goals became evident:

1. The range, diversity and efficiency of their nectar foraging is linked to the thermal efficiency of their nest.
2. The nest thermal properties are major factors in the temperature and humidity regulation (homeostasis) for the diverse requirements of the production of honey, the raising of new honey bees and the suppression of parasites.
3. The expansion of honey bees into different climatic regions is a result of subspecies adapting by changing their body size and hence resistance to convection within the nest.
4. Honey bees' natural nests within tree cavities have thermofluid properties which allow them to avoid forced clustering. In contrast, man made hives have non-optimal design characteristics such that temperature mandated clustering is frequent and unavoidable.
5. Basic assumptions about heat transfer in the honey bee nest in cold climates, which have been prevalent since before World War 1, are incorrect and as a consequence honey bees in winter are refrigerated (in North America)

(McCutcheon, 1984; Hopkins et al., 2023) or kept in hives which provide not much more protection than a metal box.

1.5 Thesis summary

This thesis consists of following chapters with those based on published or submitted works in italics:

1. Introduction.
2. Literary review.
3. *Thermal efficiency extends distance and variety for honey bee foragers*
   The frequent assumption in the literature is that the nest enclosure characteristics matter little except perhaps in winter. This chapter demonstrates, via analysis, the impact of the nest thermal characteristics stretches to behaviour outside the nest in winter. It is based on:
   Mitchell, D. 2019. Thermal efficiency extends distance and variety for honeybee foragers: Analysis of the energetics of nectar collection and desiccation by Apis mellifera. Journal of the Royal Society Interface. ***16****(150).*
4. *Nectar, Humidity, Honey bees (Apis mellifera) and Varroa in summer:*
   This demonstrates that the nest enclosure has a direct effect on the honey bees' ability to control humidity and consequently affects honey production, brood rearing and the fate of a key parasite. This is based on:
   Mitchell, D. 2019. Nectar, humidity, honey bees (Apis mellifera) and varroa in summer: A theoretical thermofluid analysis of the fate of water vapour from honey ripening and its implications on the control of Varroa destructor. Journal of the Royal Society Interface. ***16****(156).*
5. *Honey bee (Apis mellifera) size determines colony heat transfer when brood covering or distributed.*
   This shows, via computational fluid dynamics, the thermofluids within the nest have actually shaped the evolution of the honey bee sub species. It is based on:
   Mitchell, D.M. 2022. Honey bee (Apis mellifera) size determines colony heat transfer when brood covering or distributed. International Journal of Biometeorology. ***66****(8), pp.1653–1663.*

6. *Simulating the built environment for another globally distributed species.*
   This focuses on the validation of the CFD model used in this research. It is an extension of :
   Mitchell, D. 2022. Simulating the built environment for another globally distributed species In: Proceedings of BSO Conference 2022: 6th Conference of IBPSA-England [Online]. BSO Conference. Bath, UK: IBPSA-England. Available from: https://publications.ibpsa.org/conference/paper/?id=bso2022_40.

7. *Are Man-Made Hives valid thermal surrogates for natural Honey Bee nests*
   Via CFD, the key differences between the performance of man made hives and tree hollows are explored and shows that tree hollows have significant advantages for the honey bee. Based on:
   Mitchell, D.M. 2023. *Are Man-Made Hives valid thermal surrogates for natural Honey Bee nests [in review] Journal of Thermal Biology*.

8. *Honey Bee Cluster – not insulation but stressful heat sink*
   Via analytical models and the results of CFD and previous experiments this work rebuts an assumption upon which bee keeping and academic research has been based for over the last 100 years i.e. that the honey bee cluster mantle is insulation. To achieve this it produces a model which shows the contributions of the elements of the honey bee nest to large temperature differences observed, and resolves why some attempts at providing insulating hives have had ambiguous results. In addition the model provides a method for rapidly assessing hive design performance. This is an extension of :
   Honey Bee Cluster – not insulation but stressful heat sink Mitchell, D.M. 2023 Journal of the Royal Society Interface.

9. Further work
   This exploration of the thermofluid engineering of honey bees has opened new area of research.

10. Conclusions.

11. Appendices.

1.6 References

Abou-Houly, H.E. 2010. Investigation of flow through and around the Macrotermes michaelseni termite mound skin. , p.273.

Alwan, A.A. 2011. Misconception of heat and temperature Among physics students. *Procedia - Social and Behavioral Sciences*. **12**, p.600.

Anderson, E.J. 1948. Hive Humidity and Its Effect Upon Wintering of Bees1. *Journal of Economic Entomology*. **41**(4), pp.608–616.

Anderson, E.J. 1943. Some Research on the Wintering of Bees. *Gleanings in Bee Culture*. **71**, pp.681–683.

Bourke, J.M., Ruger Porter, W. and Witmer, L.M. 2018. Convoluted nasal passages function as efficient heat exchangers in ankylosaurs (Dinosauria: Ornithischia: Thyreophora). *PLoS ONE*. **13**.

Cushman, D. 2011. Drawings of Hives and Hive Parts. *Dave Cushman's Beekeeping and Bee Breeding Website*.

Dawkins, R. 2016. *The Extended Phenotype: The Long Reach of the Gene*. Oxford, New York: Oxford University Press.

Debnam, S. 2022. *Juvenile temperature regulation in Apis mellifera (Honey bee) and the impacts of brood temperature requirements on the colony*. Phd, Missoula: University of Montana.

DeGrandi-Hoffman, G., Corby-Harris, V., Graham, H., Watkins-deJong, E., Chambers, M. and Snyder, L. 2023. The survival and growth of honey bee (Hymenoptera: Apidae) colonies overwintered in cold storage: the effects of time and colony location J. Rangel, ed. *Journal of Economic Entomology*., p.toad103.

Doull, K.M. 1976. the Effects of Different Humidities on the Hatching of the Eggs of Honeybees. *Apidologie*. **7**(1), pp.61–66.

Ellis, M.B., Nicolson, S.W., Crewe, R.M. and Dietemann, V. 2008. Hygropreference and brood care in the honeybee (Apis mellifera). *Journal of Insect Physiology*. **54**(12), pp.1516–1521.

Erdsack, N., Hanke, F.D., Dehnhardt, G. and Hanke, W. 2012. Control and amount of heat dissipation through thermal windows in harbor seals (Phoca vitulina). *Journal of Thermal Biology*. **37**(7), pp.537–544.

Farrar, C.L. 1943. An interpretation of the problems in wintering the honey bee colony. *Gleanings in Bee Culture*. **September**, p.513.

Fitzallen, N., Wright, S., Watson, J. and Duncan, B. 2016. YEAR 3 STUDENTS' CONCEPTIONS OF HEAT TRANSFER.

Flekkøy, E.G., Folkow, L.P., Kjelstrup, S., Mason, M.J. and Wilhelmsen, Ø. 2023. Thermal modeling of the respiratory turbinates in arctic and subtropical seals. *Journal of Thermal Biology*. **112**, p.103402.

Flores, J.M., Ruiz, J.A., Ruz, J.M., Puerta, F., Bustos, M., Padilla, F. and Campano, F. 1996. Effect of temperature and humidity of sealed brood on chalkbrood development under controlled conditions. *Apidologie*. **27**(4), pp.185–192.

Hagenmaier, R.D. and Shaw, P.E. 2019. Gas Permeability of Fruit Coating Waxes. *Journal of the American Society for Horticultural Science*. **117**(1), pp.105–109.

Hopkins, B.K., Long, J., Naeger, N.L. and Sheppard, W.S. 2023. Comparison of indoor (refrigerated) versus outdoor winter storage of commercial honey bee, *Apis mellifera* (Hymenoptera: Apidae), colonies in the Western United States J. Rangel, ed. *Journal of Economic Entomology*. **116**(4), pp.1063–1068.

Kraus, B. and Velthuis, H.H.W. 1997. High humidity in the honey bee (Apis mellifera L.) brood nest limits reproduction of the parasitic mite Varroa jacobsoni Oud. *Naturwissenschaften*. **84**(5), pp.217–218.

Mason, M., Wenger, L., Hammer, O. and Blix, A. 2020. Structure and function of respiratory turbinates in phocid seals. *Polar Biology*. **43**, pp.1–17.

McCutcheon, D.M. 1984. Indoor wintering of hives. *Bee World*. **65**(1), pp.19–37.

Mitchell, D.M. 2019. Nectar, humidity, honey bees (Apis mellifera) and varroa in summer: A theoretical thermofluid analysis of the fate of water vapour from honey ripening and its implications on the control of Varroa destructor. *Journal of the Royal Society Interface*. **16**(156).

Mitchell, D.M. 2016. Ratios of colony mass to thermal conductance of tree and man-made nest enclosures of Apis mellifera: implications for survival, clustering, humidity regulation and Varroa destructor. *International Journal of Biometeorology*. **60**(5), pp.629–638.

Phillips, E.F. and Demuth, G.S. 1914. *The temperature of the honeybee cluster in winter*. U.S. Dept. of Agriculture.

Seeley, T.D. 2019. Darwinian Beekeeping. *The Lives of Bees*. (March), pp.277–292.

Seeley, T.D. 2010. *Honeybee Democracy*. Princeton University Press.

Seeley, T.D. 1985. *Honeybee Ecology: A Study of Adaptation in Social Life*. New Jersey, United States: Princeton University Press.

Seeley, T.D. and Morse, R.A. 1976. The nest of the honey bee (Apis mellifera L.). *Insectes Sociaux*. **23**(4), pp.495–512.

Simone, M., Evans, J.D. and Spivak, M. 2009. Resin collection and social immunity in honey bees. *Evolution*. **63**(11), pp.3016–3022.

Southwick, E.E. 1985. Allometric relations, metabolism and heat conductance in clusters of honey bees at cool temperatures. *Journal of Comparative Physiology B*. **156**(1), pp.143–149.

Southwick, E.E. 1982. Metabolic energy of intact honey bee colonies. *Comparative Biochemistry and Physiology -- Part A: Physiology*. **71**(2), pp.277–281.

Southwick, E.E. and Heldmaier, G. 1987. Temperature Control in Honey Bee Colonies. *BioScience*. **37**(6), pp.395–399.

Southwick, E.E. and Mugaas, J.N. 1971. A hypothetical homeotherm: The honeybee hive. *Comparative Biochemistry and Physiology -- Part A: Physiology*. **40**(4), pp.935–944.

Tahmasbi, G.H. 2009. The effect of temperature and humidity on grooming behaviour of honeybee , Apis mellifera (Hym .: Apidae) colonies against varroa mite , Varroa destructor (Acari : Varroidae). *Journal of Entomological Society of Iran*. **28**(2), pp.7–23.

Wang, Q., Xu, X., Zhu, X., Chen, L., Zhou, S., Huang, Z.Y. and Zhou, B. 2016. Low-temperature stress during capped brood stage increases pupal mortality, misorientation and adult mortality in honey bees. *PLoS ONE*. **11**(5), AR.

Whitfield, C.W., Behura, S.K., Berlocher, S.H., Clark, A.G., Johnston, J.S., Sheppard, W.S., Smith, D.R., Suarez, A.V., Weaver, D. and Tsutsui, W.D. 2006. Thrice out of Africa: Ancient and recent expansions of the honey bee, Apis mellifera. *Science*. **314**(5799), pp.642–645.

Yuk, J., Akash, M.M.H., Chakraborty, A., Basu, S., Chamorro, L.P. and Jung, S. 2023. Morphology of pig nasal structure and modulation of airflow and basic thermal conditioning. *Integrative and Comparative Biology*. **63**(2), pp.304–314.

Chapter 2 Literature review

Table 2.1: Chapter nomenclature.

Symbol	**Description**	**Units**
c_P	Heat capacity per unit mass	Jkg^{-1}
d_f	Particle diameter derived from volume	m
d_p	Particle diameter	m
$\bar{d}$	Effective particle diameter	m
d_{sd}	Sauter mean diameter	m
e	Internal energy	J
f_j	Bulk force in j direction	N
k	Conductivity	$Wm^{-1}K^{-1}$
k	Turbulent kinetic energy	m^2s^{-2}
p	Pressure	Nm^{-2}
$\dot{q}$	Rate of heat input	W
u, v, w	Velocity components in x, y, z	ms^{-1}
u*	Friction velocity	ms^{-1}
y^+	Limit of boundary flow	-
y	Direction away from wall	m
A	Area	m^2
A_p	Particle area	m^2

Symbol	**Description**	**Units**
C_f	Particle factor	-
C_f	Skin friction coefficient	-
D	Darcy OpenFOAM coefficient of non turbulent flow through porous medium	-
F	Forchheimer OpenFOAM coefficient for turbulent flow in porous material	-
G_r	Grashof number $\frac{g \Delta T L^3}{T \nu^2}$	-
K	Permeability	m^2
L	Characteristic length	m
P_r	Prandtl number ratio of kinematic viscosity to thermal diffusivity	-
P	Pressure per unit length of porosity	Nm^{-3}
R_a	Rayleigh number G_rP_r	-
R_e	Reynolds number $\frac{LU}{\nu}$	-
S	Momentum source term	
T	Temperature	K
T_S	Temperature at surface	K
T_∞	Temperature at distance	K
$\vec{U}$	Vector of fluid flow velocity	ms^{-1}
U	Scalar velocity of fluid flow	ms^{-1}
$U_{freestream}$	Velocity away from wall	ms^{-1}

Symbol	Description	Units
α	Irgun equation coefficients	
β	Irgun equation coefficients	
τ_{ij}	Shear force in j direction in the plane normal to i direction	N
ε	Dissipation of turbulent energy	m^2s^{-3}
ρ	Density	kgm^{-3}
ρ_f	Density of fluid	kgm^{-3}
φ	Porosity	-
ψ	Shape factor	-
μ	Dynamic Viscosity	$kgm^{-1}s^{-1}$
τ_w	Wall shear stress	Pa
ζ	Resistance coefficient (Idelchik, 2006)	
ν	Kinematic Viscosity $\frac{\mu}{\rho}$	m^2s^{-1}
ω	Turbulence frequency/specific dissipation $\frac{\epsilon}{k}$	s^{-1}

2.1 Introduction

Honey bees have an extensive and sophisticated heat control domain and its study requires a wide range of both biological and engineering knowledge to come to grips with how the physics of heat transfer is exploited by honey bees and to understand the changes brought about by man.

The heat production of honey bees both singly and as colonies has been studied intensively (Corkins and Gilbert, 1932; Southwick, 1982; Stabentheiner et al., 2003; Kovac et al., 2014). However, the study of how honey bee colonies exercise the heat control, while attempted (Owens, 1971), has not been characterised by the rigour that would be expected from a calorimetric perspective e.g. not quantifying heat loss from vents or measuring changes in heat transfer from adding insulation. Additionally, those studies have utilised environments that differ by orders of magnitude from naturally occurring nests (Mitchell, 2016).

To date there has been only one study that has a quantitative heat transfer comparison of man made and natural nests of honey bees (Mitchell, 2016). That study by the author, was confined to nest enclosures with lower apertures and without internal structures. It measured the lumped conductance of a range of man made hives in design (British national, Langstroth, Warre, Kenyan top bar, skep) and materials (wood, polystyrene, straw) and both full sized and scale physical thermal models of a tree nest.

Thus the literature review will cover basic CFD and biological backgrounds, the history of research into heat and honey bee colonies and then the areas of heat transfer that apply to this problem and the known impact of heat control on the biology of honey bees.

The literature review is organised into the following structure:

1. CFD background.
2. Biological background.
3. Heat and temperature studies on honey bees and their nests.
4. Heat transfer of similar structures to honey bee nests or their components.
5. Heat transfer of honey bee structures.
6. Biological impact of heat transfer performance on honey bees.

2.1.1 CFD background

Computational fluid dynamics takes the governing partial differential equations of fluid flow and for a given problem solves them for discrete points or small volumes in time and space. The numbers for the solutions can then be visualised as the flows of fluids (Anderson, 1995a). The technique became viable in the 1970’s with the advent of more powerful computers when it enabled a third approach to solving fluid dynamic problems in addition to experiment and theory. It has been used since in diverse areas such as visualising blood flow in heart valves, design of submarine propellers as well as aerospace. Its great advantages are being a low cost alternative to experiment, and enabling fine or inaccessible detail to be discovered. This property of showing fine or difficult to measure detail is the prime reason for its use in this research. The basic CFD elements considered here are:

1. Governing equations – these describe the physics of the fluids in question.
2. Turbulence – chaotic flow arising from abrupt changes in section or high velocity.
3. Geometry Capture - Definition of the objects and spaces involved usually a CAD suite, in this case FreeCAD V1.8.
4. Numerical solution of equations - usually in a suite of software, in this case OpenFOAM V4.1.
5. Discretization - a problem broken down in time and space.
6. Visualization and post-processing.

How the theory and the practice come together in the context of OpenFOAM and the mechanics of using and modifying OpenFOAM have been described (Höpken et al., 2014; Moukalled et al., 2016).

2.1.2 Governing equations

A concise form of the conservative form of governing equations for a fluid similar to air has been produced (Anderson, 1995b) on pages 83 to 87. This, in slightly amended matrix form below, gives the continuity, the three momentum and the energy equations. For brevity let (equations 2.1, 2.2, and 2.3):

$$h=\rho\left(e+\frac{V^2}{2}\right)+p \tag{2.1}$$

$$\Pi_\alpha^b=hb-k\frac{\partial T}{\partial a}-\left(u\tau_{\alpha x}+v\tau_{\alpha y}+w\tau_{\alpha z}\right) \tag{2.2}$$

$$N_a=\rho a^2+p \tag{2.3}$$

Then for viscous flow equation 2.4

$$\begin{bmatrix} \rho & \rho u & \rho v & \rho w \\ \rho u & N_u - \tau_{xx} & \rho uv - \tau_{yx} & \rho uw - \tau_{zx} \\ \rho v & \rho vu - \tau_{xy} & N_v - \tau_{yy} & \rho vw - \tau_{zy} \\ \rho w & \rho wu - \tau_{xz} & \rho wv - \tau_{yz} & N_w - \tau_{zz} \\ h - p & \Pi_x^u & \Pi_y^v & \Pi_z^w \end{bmatrix} . \begin{bmatrix} \frac{\partial}{\partial t} \\ \frac{\partial}{\partial x} \\ \frac{\partial}{\partial y} \\ \frac{\partial}{\partial z} \end{bmatrix} = \begin{bmatrix} 0 \\ \rho f_x \\ \rho f_y \\ \rho f_z \\ \rho \left(u f_x + v f_y + w f_z + \dot{q} \right) \end{bmatrix} \tag{2.4}$$

Inviscid flow equation 2.5

$$\begin{bmatrix} \rho & \rho u & \rho v & \rho w \\ \rho u & N_u & \rho uv & \rho uw \\ \rho v & \rho vu & N_v & \rho vw \\ \rho w & \rho wu & \rho wv & N_w \\ h - p & hu & hv & hw \end{bmatrix} . \begin{bmatrix} \frac{\partial}{\partial t} \\ \frac{\partial}{\partial x} \\ \frac{\partial}{\partial y} \\ \frac{\partial}{\partial z} \end{bmatrix} = \begin{bmatrix} 0 \\ \rho f_x \\ \rho f_y \\ \rho f_z \\ \rho \left(u f_x + v f_y + w f_z + \dot{q} \right) \end{bmatrix} \tag{2.5}$$

On to these basic equations, extensions are made for phenomena such as porosity, turbulence, internal heat generation and radiation.

2.1.3 Turbulence

Flow in fluid near a wall is slowed by friction. If the flow near the wall slows in a gradual, ordered, layered manner in the same direction as the flow, then the layers near the wall are said to be laminar. In contrast, if the interaction results in flow in the vicinity of the wall moving in various directions to the overall direction of flow then the flow in the vicinity is said to be turbulent (Bergman and Lavine, 2017). Similarly if a jet of moving air interacts with a body of still air, so as to cause part of the flow to move in all directions, it is said to be turbulent (figure 2.1). Whether a flow is turbulent or laminar can greatly affect how heat is transferred from the flow to the surroundings. Thus a key consideration in any heat transfer involving a fluid is whether the flow is turbulent or laminar (Incropera et al., 2007). This applies both when the air is in motion from natural convection caused by a heat source (honey bee thorax) or from an air moving device such as honey bee wings.

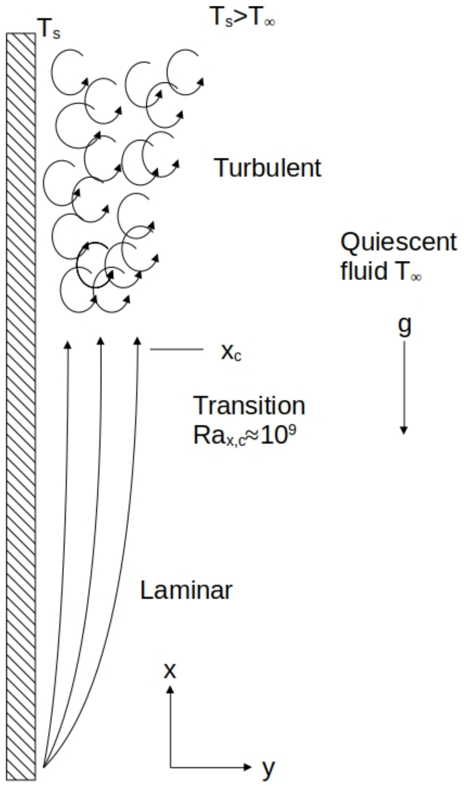

Figure 2.1:Free convection boundary layer transition on a vertical plate (Bergman and Lavine, 2017).

The mathematics of turbulence modelling is discussed at length in the available literature. A concise description is given in (Moukalled et al., 2016). Turbulence is only of consequence at $R_e > 10^3$ or $R_a > 10^7$ for impingement flow. For tangential flow this increases to $R_e > 10^7$ or $R_a > 10^9$. The turbulence modelling under consideration for this problem space is at the low end of turbulence or in the laminar regions i.e. externally: $R_e < 10^5$, $R_a < 10^9$ with abrupt changes in section; internally $R_e < 10^3$, $R_a < 10^4$ with abrupt changes in section.

Turbulence models fall into 3 main categories ranked in order of increasing computational cost (Sodja, 2007).

1. Reynolds Averaged Napier Stokes (RANS).
2. Large Eddy Simulation(LES).
3. Direct numerical Simulation (DES).

Several papers discuss the suitability of turbulence models to low R_e problems (Cable, 2009; Aksouh et al., 2010; Mathur and He, 2013). The RANS models reviewed include:

1. Standard κ-ε (kε) this assumes the flow to be fully turbulent and viscosity is of negligible effect, hence it does not give good results near a wall. The following 3 are attempts to ameliorate this restriction and to cope with large strain rates.
    1. Realizable k-ε (kε-RE) adds terms to better satisfy constraints of turbulent flows.
    2. Renormalized k-ε (kε-RNG) this adds terms based on strain rate.
    3. Launder–Sharma κε (kε Launder–Sharma) this includes a damping function to account for viscous and near wall effects.
2. Standard k-ω (kω). Uses a specific dissipation rate ω i.e. a dissipation rate related to the turbulent energy k which works better at low R_e, but with sensitivity to initial values of free stream ω.
3. Shear-stress k-ω (kω-SST) this is a blend of both k-ε and k-ω approaches with additional refinements for adverse pressure gradients.

Of these kω-SST is often recommended for low R_e convection flows (Aounallah et al., 2007; Aksouh et al., 2010).

Porosity, internal heat generation and radiation are discussed later.

2.1.4 y^+ wall distance estimation

"y^{+}" is the non-dimensional wall distance for a wall-bounded flow.It is used to determine optimal nearest cell placement. A single point y^+ estimation can be made, however with the wide variety of conditions being simulated, it became necessary to implement a more rigorous method of estimation based on the utilities within OpenFOAM.

To estimate the wall distance, needed to obtain the dimensionless distance (y^+) that represents the limit of boundary flow (Versteeg, 2007), one can estimate the skin friction C_f (equation 2.6) from the Reynolds number R_e (equation 2.7), hence the wall shear stress τ_w (equation 2.8), the friction velocity u^* (equation 2.9).

$$R_e = \frac{\rho}{\mu} U_{freestream} L_{boundary\,layer} \tag{2.7}$$

$$C_f = \left(2\log_{10}(R_e)\right)^{-2.3} for\ R_e < 10^9 \tag{2.6}$$

$$R_e = \frac{\rho}{\mu} U_{freestream} L_{boundary\,layer} \tag{2.7}$$

$$\tau_w = C_f \frac{1}{2} \rho U^2_{freestream} \tag{2.8}$$

$$u^* = \sqrt{\frac{\tau_w}{\rho}} \tag{2.9}$$

$$\frac{y}{y^+} = \frac{\mu}{\rho u^*} \tag{2.10}$$

For the low Reynolds number turbulence scheme employed i.e. kω-SST, we require y^+ to be less or equal to the order of 1.

The small passage ways between the combs and the hive (5 mm) necessitate cell widths of 1mm and smaller to satisfy a minimum feature cell count requirement. Using the equation above it shows that when combined with comb heights of 0.2m and air velocities between 0.2 and 10^{-4} ms^{-1}, we can expect that y^+ is in range 1.0 to 10^{-2}.

To confirm this, results from the y^+ post processing function object are logged to the database for each run. They indicate the largest y^+ values are on the surface of the hive and roof and only exceed 1.0 at ambient air velocities over 0.4 ms^{-1}, the maximum of 3.17 observed at ambient air velocities of $1ms^{-1}$. At the air velocities used for the investigation ($0.05ms^{-1}$), y^+ has a maximum value of 0.17.

2.1.5 Geometry capture

This is the process of taking the basic dimensions of the elements in the problem space and converting them in to a form suitable for the discretization/meshing software to process. This is usually done via a computer aided design program, often part of the complete CFD software suite. Open source CAD software includes FreeCAD, (Riegel and Mayer, 2019) and Salome (Ribes and Caremoli, 2007). In this study we will make use of FreeCAD, integrated with a SQL database via Python to provide automation and referential integrity between input geometry, run parameters and results.

2.1.6 Numerical solution of equations -solvers

The solver is the software that seeks the iterative solution to the discretised form of the governing differential equations. There are many classifications of solvers covering a wide range of problem spaces. Many of these are aimed at showing transient effects. However the problems considered in this research are essentially those on a much longer time scale than those usually related to fluid flows (e.g. days or weeks compared to milliseconds), so they are for all practical purposes, steady state (Sudarsan et al., 2012). The problem space is that of conjugate heat transfer i.e. thermal energy is being exchanged between different fluid and solid regions. The need to take account of buoyant convection flows requires either a compressible fluid solver, or one that uses the Boussinesq approximation (equation 2.11), where the relative change in density of the fluid is equal to the relative change in temperature (Incropera et al., 2007).

$$\frac{\rho_0-\rho_1}{\rho_{average}}=\frac{T_0-T_1}{T_{average}} \tag{2.11}$$

Thus a suitable solver in OpenFOAM V4.1 is compressible "ChtMultiRegionSimpleFoam" as described by (Välikanga, 2016).

2.1.7 Discretization and mesh generation

Discretization usually means taking a 3D computer aided design (CAD) drawing (figure 2.2) and breaking it up into enough, well formed, pieces (figure 2.3) to allow the iterative, approximate solving of the governing partial differential equations to converge on a solution in the requisite detail, but few enough for the computation to take place in a reasonable time for the computation resources available (Oberkampf and Trucano, 2002; Versteeg, 2007). The pieces or cells form a mesh which spans the problem space. The shape of these cells and the rate at which they change shape present the extra constraint of mesh quality (Knupp, 2002). Poor quality meshes, e.g cells changing size too quickly, too few cells or cells of the wrong shape, may prevent convergence of the solution, or give erroneous answers. In the early days of mesh generation this might have been done by hand. Now, despite that automated mesh generation dominates, it still requires intelligent input to create a useful mesh (Baker, 2005).

For a steady state problem, discretization in the dimension of time becomes one of iteration in sufficient detail to proceed to the correct solution. In this study the mesh generation is performed by the OpenFOAM meshing utility snappyHexMesh (Kortelainen, Juha, 2009).

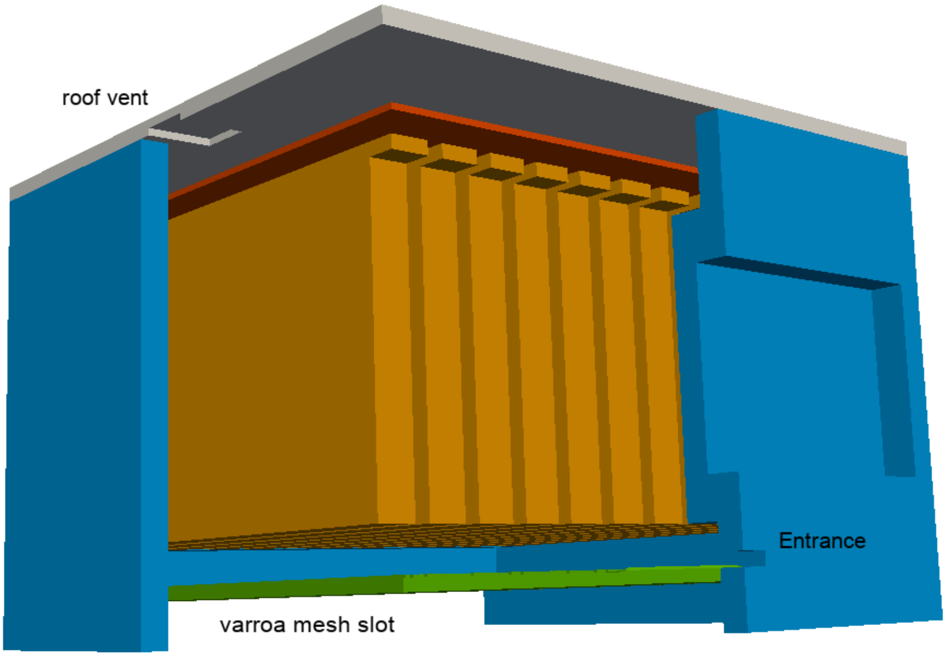

Figure 2.2: Hive cutaway: blue hive body, yellow combs, red crown board, green varroa mesh, grey roof.

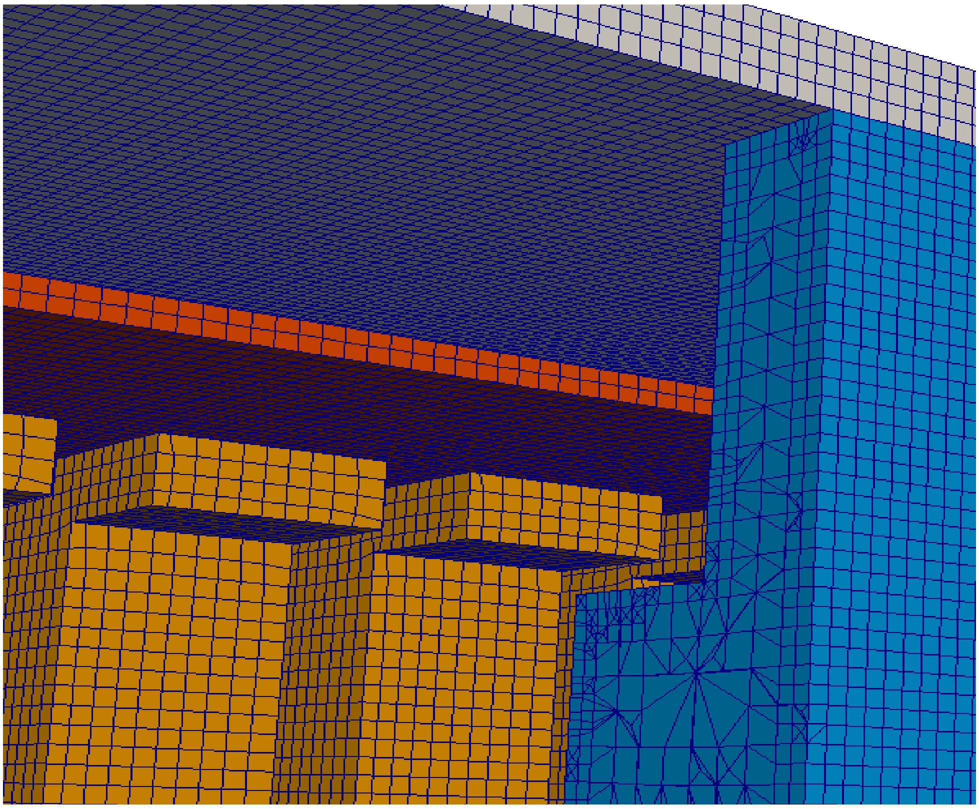

Figure 2.3: Hive cutaway with discretization.

2.1.8 CFD visualisation and post-processing

CFD produces large volumes of data that relate to often complex 3D problems. Being able to absorb the implication of the results has been its own challenge from the beginning, and finding ways to convey flows of various fields to an audience has led to its own areas of development and research (Mallinson, 2008). In this research we will make use of one of the well known open source tools, Paraview, which started its development in 2000 as a collaborative project between Kitware Inc and Los Alamos laboratory (Ayachit, 2015), MATLAB (MATLAB, 2018) and the tools built into OpenFOAM V4.1.

2.2 Biological background

Honey bees are one of the most intensively researched insects and their behaviour as a super organism and individually has been shown to be complex, with thousands of papers and books written on the subject. This review will only cover a tiny fraction of the subject.

Honey bee colonies have a single fertile female (queen) and many thousands ($4\text{x}10^3$ to $6\text{x}10^4$) of infertile females (workers), plus in spring and summer, a relatively small (15%) number of males (drones) (Boes, 2010). In a non man-made landscape they inhabit cavities (average dimensions 1.5m high by 0.2m diameter) in woodland trees (usually deciduous) located in temperate climates (from -40°C to +35°C) and maintain an active state all year. They feed on flower nectar and pollen when it is available and store this in the wax comb structure that they construct in their nests. In the case of nectar they concentrate this from a typically 20% to an 80% sugar concentration (honey), to conserve space and prevent deterioration (Seeley, 1985).

2.2.1 Nest internal structures

The typical natural nest dimensions and internal constructions found in a natural tree nest have been described by (Seeley and Morse, 1976). These structures consist of a number of honeycombs attached to the roof and sides of the nest, where the honey bees leave a number of passages (peripheral galleries) at the edge of the comb (figure 2.4).

Figure 2.4: Peripheral galleries (donated by T.D. Seeley).

The combs are arrays of almost horizontal (~13 degrees), wax, hexagonal tubes (cells) (Zhang et al., 2010) on both sides of a wax central spine. The wax is secreted in scales from glands on the underside of the honey bee abdomen. The cell walls are between 100 µm to 300 µm thick. The usage is organised primarily with honey storage at the top of the cavity and the brood nest (larvae and pupae) below, with pollen storage in between. While the behaviours associated with cell storage have been researched and modelled (Camazine et al., 1990; Camazine, 1991; Yang et al., 2005; Johnson, 2009; Montovan et al., 2013; Eyer et al., 2016), the peripheral galleries have not been described quantitatively nor their effect on air flow investigated.

2.2.2 Nest seeking behaviours

The honey bee colony fissions (Rangel and Seeley, 2012; Rangel et al., 2013; Loftus et al., 2016) by a significant proportion of the inhabitants leaving with a queen and then forming a dense ball of bees on a nearby structure or plant, while they determine the location of the new nest. The honey bee has a sophisticated method of finding, then selecting a nest that matches an optimum balance of several criteria, by what is essentially a voting methodology between those individuals of the colony that search for a new nest (scouts). The methodology selects the best nest out of those available. (Seeley and Visscher, 2003; Seeley and Kirk Visscher, 2004; Seeley, 2010). The known criteria include cavity volume (0.045m$^{3)}$, entrance area (5 to 25×10^{-4}m^{2}), entrance position relative to the cavity (at the bottom), entrance aspect (southerly) and shading (shaded), all of which are certainly relevant to heat transfer. These behaviours, combined with a known distribution of tree cavities (Seeley and Morse, 1976) can be used to form a model of a prototypical tree nest for study (Mitchell, 2017b).

2.2.3 Clustering

One of the behavioural adaptations of the honey bee is that rather than hibernating, it forms a distinct shell of individuals, usually around the queen and/or brood, to reduce heat loss and allow temperature regulation to occur. This may occur when the colony is in transit to a new nest, to survive in winter or to enable temperature regulation around brood when nest heat losses are high (Seeley, 1985). The cluster appears to take two forms one with an external surface temperature of ~18°C (Heinrich, 1981) and the other with an external surface temperature of ~10°C. The latter having a very dense shell of radially arranged, very low heat producing bees (mantle) about a lower density core of heat producing bees with a boundary interface at around 20°C (Stabentheiner et al., 2003). This behaviour has been the subject of numerous numerical studies, but these have either been without considering nest combs or enclosure (Watmough and Camazine, 1995; Humphrey and Dykes, 2008; Ocko and Mahadevan, 2014), or have not considered the conjugate heat problem of the enclosure or the combs (Sudarsan et al., 2012).

2.2.4 Honey ripening

Honey ripening is the term for the evaporation of water from the nectar (15% to 50% sugars), to honey (> 80% sugars). The nectar concentration being dependent on the flower source (Wykes, 1953; Garbuzov and Ratnieks, 2014). Honey is effectively a concentrated energy store for the colony that enables survival and growth to be decoupled from the nectar source variability or flying conditions e.g. long winter periods, low light levels, rain, or low temperatures. As the amount of honey involved is of the order of tens to hundreds of kilogrammes, the energy requirement of evaporating the considerable quantities of water (typically 2 to 4 times the weight of the honey), is significant given the high latent heat of vaporization of water (2.2MJKg^{-1}). The nectar required to fuel the ripening process may exceed the volume of nectar being ripened.

Therefore the efficiency of the thermal envelope of the colony is of importance not only during winter but during the nectar gathering seasons (Schmid-Hempel, 1987). Unfortunately this very large energy requirement (10^8~10^9 joules per year, per colony), and therefore its need for thermal efficiency, is not considered in population models which involve the energetics of nectar collection and survival (Becher et al., 2014).

2.2.5 Comfort diagram

In the built environment paradigm, the concept of a comfort diagram is considered relevant for designing and evaluating habitation (Moss, 2007). We will now construct one for honey bees (figure 2.5). For this, one has to consider that:

1. Coma death of individual bees occurs at 8°C (Seeley, 1985).
2. Temperature forced clustering of a colony is complete at a nest temperature 10°C (Southwick, 1982).
3. Individual bees require a temperature above 18°C so that they then can use their thorax muscles to produce the heat necessary to reach flying temperature. (Seeley, 1985).
4. Clustering is unlikely above a nest temperature of 20°C (Southwick, 1982).
5. Chalkbrood disease is easily induced below 26°C (Flores et al., 1996).
6. Brood temperature is required to be kept closely at 34°C for correct development and adult performance (Tautz et al., 2003).
7. Individual bees can survive temperatures close to 50°C for short periods and can use this together with heat production in the thorax to kill other insects (e.g. predators) that threaten the colony (Hosono et al., 2017).
8. Humidity levels need to be 75% RH for larvae development (Schmehl et al., 2016).
9. Humidity levels need to be 90% RH for egg development (Doull, 1976).

10. Humidity levels need to be above 80% RH to impede varroa parasite breeding (Kraus and Velthuis, 1997).

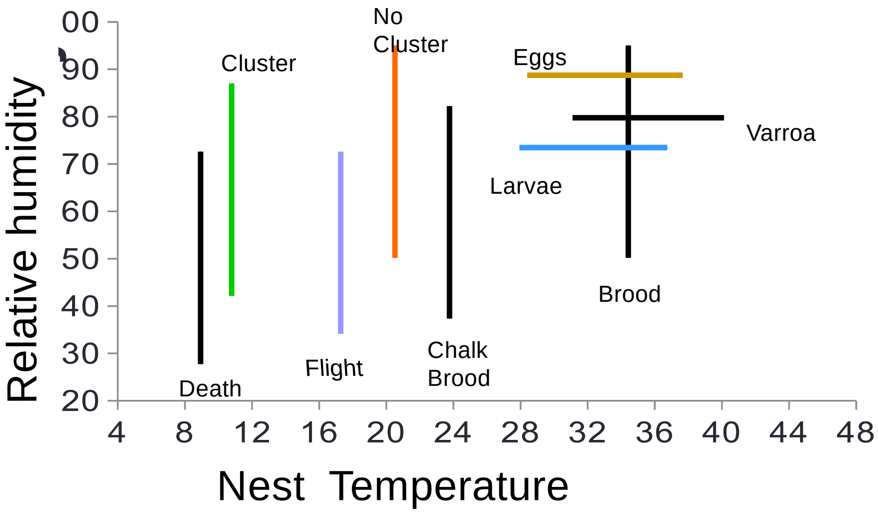

Figure 2.5: Honey bee comfort diagram RH vs Temperature °C.

2.2.6 Metabolism and temperature and temperature regulation of honey bee colonies

Honey bees, individually and as a colony, react to temperature changes in the surrounding environment with changes in their rate of heat output (W) i.e. metabolic rate. This has been described extensively in literature (Corkins and Gilbert, 1932; Heinrich, 1981; Southwick, 1982; Southwick and Heldmaier, 1987; Southwick, 1991). These studies have been done exclusively in isothermal environments. The results of Southwick are of particular note as shown in figure 2.6. This shows rising metabolic rate as the temperature in the not-clustered colony falls from above 30°C until 20°C, when it enters an area of instability from 10°C to 20°C, where the colony may transition into and out of cluster. Below 10°C, the metabolic rate stabilises in the clustered state, and then rises slowly as the temperature falls.

This reduction in metabolic rate has been the reasoning behind some bee farmers placing their honey bees in refrigerated storage at 5°C for the winter months (Currie and Spivak, 2015).

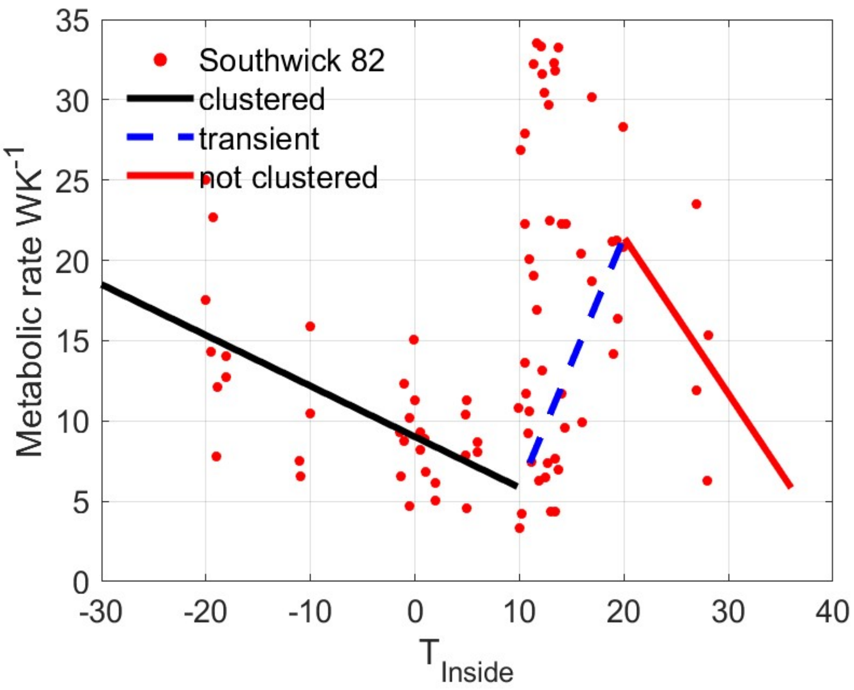

Figure 2.6: Metabolic rate Wkg^{-1} vs nest temperature °C (Southwick, 1982) red not-clustered state, black clustered state, blue transient state.

2.3 Heat and temperature studies on honey bees and their nests.

These aspects of honey bees have received considerable attention over the last 160 years but without a definitive outcome. This is discussed below.

2.3.1 The history

From the advent of framed hives, there has been speculation about the efficacy of insulation. Thus it is not surprising that the inventor of the framed hive, Langstroth, who effectively created modern beekeeping, was extremely concerned that his invention would result in high heat loss hives (Langstroth, 1853).

Over the next 160 years, in addition to the speculation there were experiments which compared the survival, growth and honey production in various modes of insulation or lack there of, with various modes of ventilation (Anderson, 1943; Anderson, 1948; Geiger and Braun, 1955; Owens, 1971; Bornus and Nowakowski, 1974; Vesterinen, 1974; Adam, 1975; Mobus, 1998b; Mobus, 1998a; Dodologlu et al., 2004; Erdogan et al., 2009). Some made detailed measurements of the temperatures developed by the bees inside (Phillips and Demuth, 1914; Owens, 1971) of these Phillips influentially expounded that the honey bees made an insulating shell in the cluster. However, they were almost completely uniform in not measuring the effect of hive insulation or the ventilation on heat loss. Prior to the 1940's, and especially prior to 1918 (Phillips, 1915; Clark, 1918), it was in vogue to insulate hives, however during the 1940's the economic pressures of wood shortages (Hansard, 1940; Huey, 1951) and the wartime demand for woodworkers and woodworking machinery for general war work, and projects like the De Havilland Mosquito, facilitated a change to thin walled high heat loss hives. This required a larger heat transfer rate from metabolism, which required high levels of respiration, which in turn required ventilation at the top of the hive to protect the hive structure and the adverse effect of condensation chilling the honey bees. This change to high heat loss hives was heavily promoted by C.L. Farrar in the U.SA. using the works of Anderson and Corkin as evidence (Corkins and Gilbert, 1932; Farrar, 1943; Anderson, 1943; Farrar, 1947; Anderson, 1948; Farrar, 1952). In Great Britain C.G. Butler broadcast on the BBC Home service numerous times to great effect (Butler and Gamble, 1941; Butler and Gamble, 1942). The change was adopted with such vigour that by 1945 bee keeping author's were stating “a well insulated hive in the dormant season may be dangerous...” (Hamilton, 1945). By 1948, heat loss by this ventilation, was related as a concern that “beginners may be caught by the superficial plausibility of this nonsense” (Manley, 1948). This combination of hive vents/entrances, applied to a building, would later be described by P.F. Linden as “natural ventilation” (Linden et al., 1990). In the 21st century the practice has continued with the use of thin walled wooden hives, despite the advent of polystyrene hives, which for the most part are constructed for strength, lightness and low cost and not low conductance (Mitchell, 2016) and research on honey bees is still conducted almost exclusively in thin walled wooden hives.

The results of all of the years of academic and agricultural research have been contradictory. Some showing significant gains (Villumstad, 1974; Alburaki and Corona, 2022) and some losses (Dodologlu et al., 2004) in survival and growth with reduced nest heat loss. However, with the exception of (Villumstad, 1974), the quantity of heat loss reduction was unknown. Equally unknown is the amount of water removed from nests by the ventilation added by researchers such as (Farrar, 1952; Owens, 1971; Dodologlu et al., 2004).

2.3.2 Why heat transfer in honey bee nests has not been considered

Since honey bees collect energy to expend in times of shortage, we must question why was the lumped thermal conductance not measured or compared to that of the tree cavities for which they evolved? This is not idle speculation, since an integral part of research is to promote its findings to the wider audience.

To an engineer or physicist, it seems obvious that this would be the first thing to do. From the workings of building, or for a star about to explode, thermal energy and how it is conserved and how it moves is one of the first, if not *the first thing*, to be considered. So, if engineers were to consider honey bees and their homes, then heat transfer from the insects through the nest walls would be studied at the beginning and studied in detail and with accuracy. However, engineers and physicists are adepts in the concepts of heat, energy and fluids. For heat transfer; from the insects to the air, to the hive walls, and so to the outside air, to be considered important, then those concepts need to be familiar to those involved and receiving the research. Thus we should look at how much of those concepts are understood by the entomologists and honey bee interested world.

To illustrate the problem, the term “endothermic” has very different meanings in biology and physical sciences. In biology it relates to temperature, and in the physical sciences energy.

The comprehension of the concepts of heat and temperature in education has been widely studied by education researchers. Here are only three of the many tens of papers found (Thomaz et al., 1995; Carlton, 2000; Wong et al., 2016). What is clear from the studies is that the common word usage of terms, the lack of clarity, and lack of uniformity in terminology in basic science education does not help the majority to apply what was taught to novel areas outside the class room (Carlton, 2000).

This is apparent even at the academic research level, where equations are quoted which directly equate energy to temperature and fail dimensional analysis (Fehler et al., 2007; Becher, 2010); or omit substantial phase change energies in their models and calculations (Cox and Myerscough, 2003; Schmickl and Crailsheim, 2007; Becher et al., 2014; Baveco et al., 2016).

2.4 Heat transfer of similar structures to honey bee nests

The honey bee nest, both man-made and natural, can be considered a built environment. As such, there are many elements in common with human structures and thus existing research into such structures are relevant, though often on a different scale. In this section we will review those elements and the literature available.

2.4.1 Natural convection with apertures

An occupied honey bee nest with vents/entrances both at the top and the bottom, is clearly an instance of natural convection or stacked convection, with the honey bees providing the buoyancy source through their metabolism generating heat, water vapour and carbon dioxide (Mitchell, 2017a).

This field of natural convection has been treated analytically for point heat sources at the bottom of a cavity in both the adiabatic (Linden et al., 1990) and non adiabatic cases (Lane-Serff et al., 2012) and also for a variety of other configurations that have relevance to the honey bee nest problem i.e. heat sources at different levels (Lin and Xu, 2013) and vertically distributed (Cooper and Hunt, 2010). These have for the most part considered the heat source forming a plume, which then merges into a buoyant, warm layer above a cooler layer. They then derive formulae for determining the temperature and depths of the layers, given the heat input, losses and sizes of the apertures. The results of the analysis are then compared to small scale experiments conducted using saline water, for visualisation purposes. This has then been extended to consider boxes filled with porous media (Roes et al., 2014).

When considering the above research one must be aware that the differences in scale, low temperature differences ~10°C, high content occupancy of the honey bee nest, with R_a and R_e in the bulk of the system $10^7 \sim 10^9$, and $10^2 \sim 10^3$ respectively, need to be taken into account (Partridge and Linden, 2013). This is especially true when the basic assumption is that the plume is narrow compared to the cavity and far from either one, or both of the cavity walls (Mullarney et al., 2004).

2.4.2 Natural convection within man-made honey comb structures

Honeycombs i.e. arrays of closely packed hexagonal tubes that share walls, have fascinated engineers with their strength and economy of material and have been incorporated in a wide variety of structures from aircraft components to racing cars. The heat transfer properties of honeycomb structures have been researched in various configurations for purposes such as transparent insulation (Suehrcke et al., 2004; Hum et al., 2004; Sun et al., 2011) and for enhanced heat dissipation (Yang et al., 2014).

The anisotropy of the honeycomb means that the heat transfer characteristics are very dependant on orientation and whether the comb is enclosed or filled in any way. Thus if we consider only the orientations that are close to the honey bee nest i.e. near horizontal cell axes and closed at one end, this limits the scope we need to consider.

(Scozia and Frederick, 1991; Lakhal et al., 1995; Kasbioui et al., 2003) analysed micro-cavities attached to a heated wall or cooled wall. Although geometrically similar (in 2D) to natural honeycomb, the minimum cavity aspect ratio considered was 0.25, compared to 0.21 for natural honeycomb. These papers considered putting the complete system (comb and surrounding air passages) at an angle to the direction of gravity, which is in contrast to the individual cells axes being at a small angle to the horizontal and the inter-comb passage being vertical in nature. These researchers results indicate that empty cells will be expected to transfer heat primarily by conduction rather than convection, but as the cells are filled, with either honey or larvae, then convection will increase inside the cells.

2.4.3 Convection within porous media and packed beds

Honey bees, on the comb tending the brood or clustering to retain heat, obstruct the convective air flow in a non regular pattern and may therefore be treated as aggregates that are similar to a porous material or a packed bed of particles (Sudarsan et al., 2012). This approach uses the Darcy-Forchheimer model of pressure difference per unit length across a porous material sometimes known as the Irgun equation (equation 2.12).

$$\Delta P = -\alpha \vec{U} - \beta \left| \vec{U} \right| \vec{U} \tag{2.12}$$

The first term relates to the viscous drag and is the dominant term below Reynolds numbers of 10. The second term relates to the obstruction effects of the particles. The first term coefficient is normally related as the ratio of viscosity and the permeability (equation 2.13).

$$\alpha = \frac{\mu}{K} \tag{2.13}$$

The formulation and determination of *K* the permeability and second term coefficient β in terms of the physical properties of the porous solid form the discussion for various scenarios of porous materials subject to convection.

Using the Carman-Kozeny equation *K* has been formulated in equations 2.14 and 2.15 (Nield and Bejan, 2006).

$$K = \frac{D_{P2}^2 \varphi^3}{180\left(1-\varphi^2\right)} \tag{2.14}$$

$$\beta = C_f K^{-1/2} \rho_f \tag{2.15}$$

Where φ is the porosity and D_{P2} is the effective average particle diameter, ρ_f the density of the fluid and C_f is factor based on the nature of the particles.

But this is not valid for particles that deviate strongly from a spherical shape or have large size distributions. Given that a honey bee fits within a cylinder 11mm in length a diameter of 3mm, other solutions should be considered.

Experimental work on fibres (Rahli et al., 1997) in the $R_e<1$ region has shown that the aspect ratio of the particle can have a profound effect on the permeability, with the greatest change being for an aspect ratio region of 1 to 20. This study used metal fibres 150 µm in diameter with varying lengths.

One experimental study (Li and Ma, 2011) is closer to the honey bee in terms of scale and aspect ratio used i.e. cylinders 6mm long and 3mm diameter. This compared its results to the following formulations (equations 2.16 and 2.17) of α and β in equation 2.12:

$$\alpha = 150 \frac{(1-\varphi)^2 \mu}{d_{eq}^2 \varphi^3} \tag{2.16}$$

$$\beta = 1.75 \frac{(1-\varphi)\rho}{d_{eq} \varphi^3} \tag{2.17}$$

where d_{eq} is equivalent diameter of the particles defined by equation 2.18 and V_p and A_p are the volume and the areas of the individual particles

$$d_{eq}=\frac{\pi^{\frac{1}{3}}(6\,V_p)^{\frac{5}{3}}}{A_p^2} \tag{2.18}$$

In OpenFOAM this is most easily implemented via *fvOptions*, using an explicit porosity source in the momentum equations of the form in equation 2.19,

$$S=(\mu\,D+\rho\,F|U|)\vec{U} \tag{2.19}$$

where the term D and F are related to the coefficients in equation 2.12 by equations 2.20 and 2.21:

$$\alpha=\mu\,D \tag{2.20}$$

$$\beta=\rho\,F \tag{2.21}$$

2.4.4 Convection through a wire mesh

In Europe, common hive designs contain a floor with a mesh open to a void below. To model this we need a structure that is more easily modelled in CFD than explicitly considering each apperture and wire. An approach to this is modelling the mesh as a porosity (Teitel et al., 2009). To realise this we then require to synthesise the α and β terms (equation (2.12)) from the properties of a mesh at the low flow velocities likely to be encountered in the area of the mesh i.e. $R_e < 50$. (Idelchik, 2006) gives a means of determining the fluid coefficient of resistance ζ at $R_e < 50$ for metal round wire screens (equation 2.22).

$$\zeta=\frac{\Delta p}{2\rho U^2}=\frac{22}{R_e}+1.3(1-\varphi)+\left(\frac{1}{\varphi}-1\right)^2 \tag{2.22}$$

which gives, when modelled as a porosity length L (Idelchik, 2006) equations 2.23 and 2.24. others have found for higher R_e e.g. (Miguel, 1998) in equations 2.25 and 2.26 (Valera et al., 2005) and in equation 2.27 and 2.28.

$$\alpha=\frac{44\,\mu}{d_{orifice}\,L} \tag{2.23}$$

$$\beta=\frac{2\rho}{L}\left(1.3(1-\varphi)+\left(\frac{1}{\varphi}-1\right)^2\right) \tag{2.24}$$

$$\alpha=\frac{\mu}{3.44\,10^{-8}\,\varphi^{1.6}\,L} \tag{2.25}$$

$$\alpha=\frac{44\mu}{d_{orifice}L} \tag{2.23}$$

$$\beta=\frac{\rho}{L}\frac{4.3.10^{-2}\varphi^{-2.13}}{\left(3.44.10^{-8}\varphi^{1.6}\right)^{1/2}} \tag{2.26}$$

$$\alpha=\frac{\mu}{5.68.10^{-8}\varphi^{3.68}L} \tag{2.27}$$

$$\beta=\frac{\rho}{L}\frac{5.67.10^{-2}\varphi^{-1.1604}}{\left(5.68.10^{-8}\varphi^{3.68}\right)^{1/2}} \tag{2.28}$$

2.4.5 Convection through orifices modelled as a porosity

At low *Re* (*Re* <50) Idelchik gives the resistance coefficient as equation 2.29

$$\zeta=\frac{\Delta p}{2\rho U^2}=\frac{33}{R_e} \tag{2.29}$$

Hence when simulated as porosity of depth L in equation 2.30

$$\alpha=\mu\frac{66}{d_{eff}L} \tag{2.30}$$

where $d_{eff}=\frac{2ab}{(a+b)}$

2.4.6 Radiation within packed beds

In a similar fashion to the above, the presence of honey bees between the comb, generating and receiving thermal radiation is similar to that of packed beds of particulates, where the media participates in the radiation processes.

Suitable CFD framework radiation models exist in OpenFOAM to utilise such results and are reviewed by (Vdovin, 2009) namely *P1* (Sazhin et al., 1996) and finite volume discrete ordinates method (*fvDOM*) which are described in more detail by (Sazhin et al., 1996; Kim and Huh, 1999; Krishnamoorthy, 2017).

2.5 Heat transfer of honey bee structures

In this section,we will review the research that has looked into the heat transfer of honey bee nests and structures, as distinct from honey bee performance while in occupation.

These will be grouped as:

1. CFD.

2. Other numerical methods.
3. Experimental.

2.5.1 CFD

Nine CFD studies into insects and their nests have been found. In summary:

1. Three related to insects other than *Apis mellifera* (Hozumi and Inagaki, 2010; Abou-Houly, 2010; Hozumi et al., 2011).
2. Six *Apis mellifera* CFD studies (Sudarsan et al., 2012; Thompson, 2013; Oskin and Ovsyannikov, 2019; Oskin et al., 2020; Oskin et al., 2022; Tapia Brito, 2022). Of these:
    1. Four utilised conjugate heat transfer (Oskin and Ovsyannikov, 2019; Oskin et al., 2020; Oskin et al., 2022; Tapia Brito, 2022).
    2. Three used a bee metabolic rate (W) based on a polynomial of temperature outside of the nest enclosure (Oskin and Ovsyannikov, 2019; Oskin et al., 2020; Oskin et al., 2022).
    3. Three used a bee metabolic rate (W) linear with respect to bee temperature (Sudarsan et al., 2012; Thompson, 2013; Tapia Brito, 2022) derived from earlier work (Humphrey and Dykes, 2008).
    4. Two employed additional non-bee heat generation and not the honey bee heating alone (Oskin et al., 2022; Tapia Brito, 2022).
    5. Two considered carbon dioxide generation (Sudarsan et al., 2012; Thompson, 2013).
    6. Three considered humidity (Oskin and Ovsyannikov, 2019; Oskin et al., 2020; Oskin et al., 2022).
    7. Three considered *Apis mellifera* as a porosity that effect the momentum equation (Sudarsan et al., 2012; Thompson, 2013; Tapia Brito, 2022).
    8. All six used thin wooden hives as the enclosure and not the natural nest of *Apis mellifera*.

9. One was compared to an experiment with honey bees and an in-vitro experiment (Tapia Brito, 2022).
10. None of these simulated *Apis mellifera* as a thermoregulating colony to a fixed temperature or varied the honey bee density. None of these considered radiation.

2.5.2 Other Numerical methods and studies

The thermal properties of honey bee clusters have received considerable attention and modelling but without participation of the comb and almost exclusively outside of, or disregarding any enclosure. (Omholt and Lonvik, 1986; Lemke and Lamprecht, 1990; Myerscough, 1993; Watmough and Camazine, 1995; Sumpter and Broomhead, 2000; Eskov and Toboev, 2009; Ocko and Mahadevan, 2014).

There has been a numerical study that considers a cluster between combs, but without thermal participation of the comb. (Sumpter and Broomhead, 2000). Two studies undertake thermal modelling of honey bees on comb, with the comb participating but without a participating enclosure (Fehler et al., 2007; Humphrey and Dykes, 2008). Of these, Humphreys uses a finite element method using Matlab. The approach used assumes that all significant heat transfer is conduction and that the comb has constant isothermal boundaries. It also assumes that the brood occupied cells are in relatively good thermal contact with the pollen and honey containing cells. Relying on conduction contradicts the evidence of the comb being suspended from the enclosure by thin, relatively low conductance, low melting point, attachments (Hepburn et al., 2014) which could not take the thermal loading (3 to 5W) implied by the assumption. Also the isothermal boundary condition contradicts known thermal stratification present in such cavities (Mitchell, 2016). Brood surrounded by empty cells which commonly occurs, would not be solvable with such assumptions as there would be insufficient heat dissipation to balance the residual heat generation.

Fehler's model (Fehler et al., 2007) is a multi-agent behavioural model that does not consider radiation, convection or conductance directly, but rather a set of coefficients that are manipulated to fit empirically to experimental data in a process of calibration, in order to determine the effect of and the optimum number of empty cells. There appears to be an implicit assumption that empty cells do not conduct.

2.5.3 Experimental methods in heat transfer of honey bee structures

The earliest experiments in trying to measure or compare heat loss were by Anderson in 1943, where he used a light bulb and a thermometer and two hives, one with a vent and one without (figure 2.7). He observed no difference in temperature between the hives.

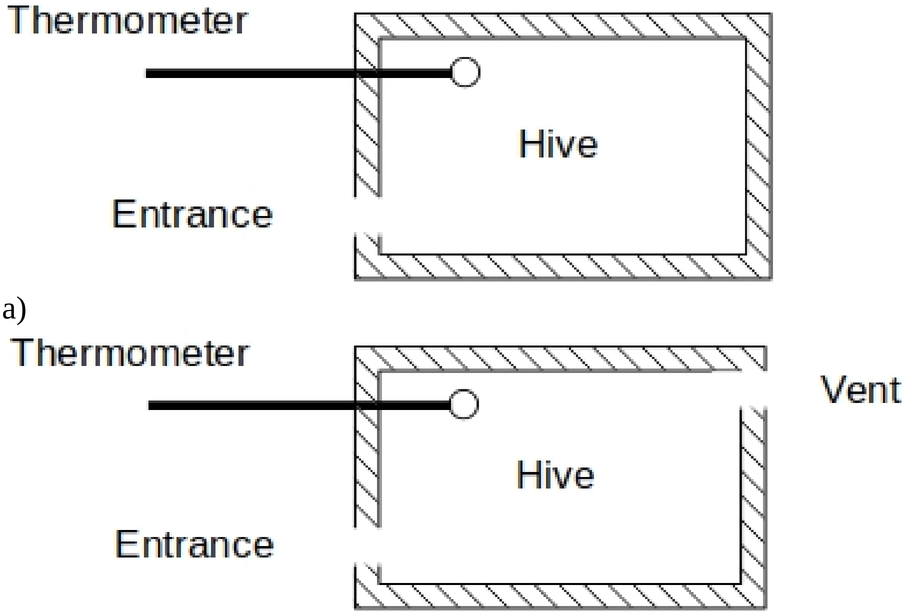

a)

b)

Figure 2.7: Anderson's experiment (Anderson, 1943; Mitchell, 2017a).

Since 1943 to as recently as 2015, this has been interpreted that no significant heat is lost through the vent (Anderson, 1943; Currie and Spivak, 2015). How this early study relates to current engineering understanding of natural ventilation (Lane-Serff et al., 2012) was explained in non-mathematical terms by the author (Mitchell, 2017a). Quantitative hive conductance measurements formed part of Villumstad’s work in the 1970’s (Villumstad, 1974) on honey production and colony survival and he quoted lumped conductances of between 3 for a standard hive and 0.75 WK^{-1} for the best insulated hive in his tests, which concurs with the author’s own values of hives lying between 2.65 WK^{-1} (wood) and 0.9 WK^{-1} (polystyrene).

To date there has only been the author’s own study (Mitchell, 2016) quantitatively comparing the conductance of tree nests and man made hives. This looked at the winter occupancy configuration, which yielded a lumped conductance of below 0.5 WK^{-1} for trees. Part of the physical cause of the dramatic difference in conductance is easily seen in the photograph in the introduction of a wooden hive and a cut open tree nest. The tree nest being of average size when compared to Seeley's nest survey (Seeley and Morse, 1976).

The method used, by the author, in both the tree and the hive models was to use a distributed electric heater and an array of temperature sensors to capture the internal air temperature. The difficulties in performing the experiment on a thermally massive tree were overcome by using a foam model which had the same radial thermal conductance of the average tree of Seeley's 1976 survey (Seeley and Morse, 1976). This was accomplished using the known properties of the foam and the shape factor for the hexagonal tube construction. The study then assessed the effect that the resulting colony mass conductance ratios would have on the upper and lower bound of the clustering temperatures found in Southwick's work (Southwick, 1982) by utilising the corresponding metabolic rates. The author concludes that with the non-clustering boundary for a colony in an average tree nest being well below -30°C, that forced clustering is not necessary (figure 2.8).

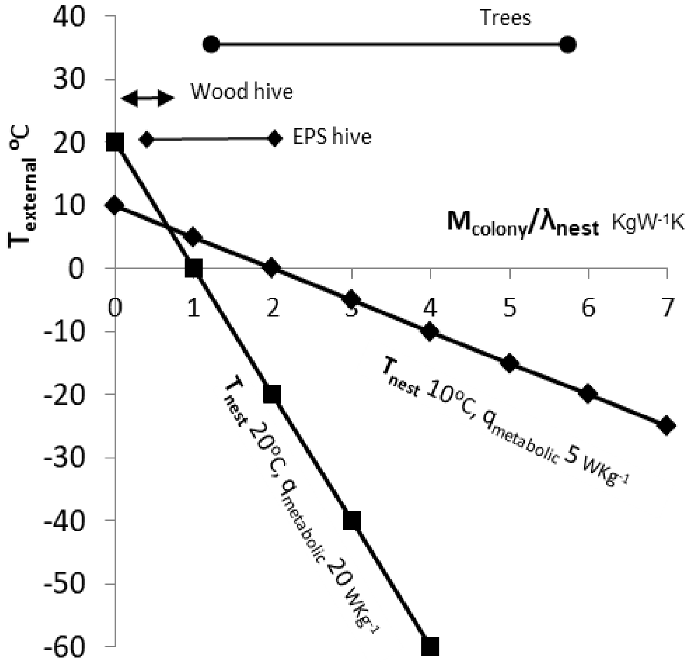

Figure 2.8: MCR versus external temperature (Mitchell, 2016).

Experimental work on the thermal conductance of honey bee made honeycomb seems to be limited to a single study by Southwick (Southwick, 1985) which gave a value of 0.15 WK^{-1} m^{-1} (converted from $0.36*10^{-3}$ cal $s^{-1}cm^{-1}$) which contrasts with (Humphrey and Dykes, 2008) who argue that the geometry of an empty comb approximates the conductivity of air (0.026 WK^{-1} m^{-1}). The reason for this discrepancy may be that Southwick conducted the measurement of the comb with the axes of cells orientated vertically. Given the anisotropy of the comb structure this approach does not give a valid value for the comb in its normal orientation in the nest.

2.6 Biological impact of heat transfer on honey bees

This section is largely reproduced from the author’s paper (Mitchell, 2016).

In almost all studies of honey bees that use insulated enclosures, the conductance has not been measured and in all cases are estimated (from material thickness, additional vents or onset of clustering) to be considerably less insulated than in tree enclosures. (Owens, 1971; Ptáček and Čermák, 2000; Olszewski, 2007; Villa et al., 2009; Erdogan et al., 2009). Some researchers have studied the thermal properties of tree cavities in relation to other animals, but many have not quantified the temperature rise in relation to heat input (Buttemer, 1985; Coombs et al., 2010; Maziarz and Wesołowski, 2013). Two studies of heat transfer in tree cavities tie their models to animals in conductive contact at the bottom of the nest (Thorkelson and Maxwell, 1974; Fornito et al., 1982). While there has been some speculation on the difference in the conductance between man-made hives and tree enclosures (Erickson, 1990), no attempts have been found of a measurement based comparison of heat transfer rate of the various types of honey bee enclosures apart from the author’s study (Mitchell, 2016).

To maintain temperature homoeostasis in a cool environment, energy lost through the nest enclosure must be made up by more honey bee activity and stress, either to generate more heat or to cluster. This can affect nest humidity, colony survival, spring development and honey production (Villumstad, 1974). Higher nest temperatures and humidity have been linked to reductions in disease and parasites (Flores et al., 1996; Kraus and Velthuis, 1997; Flores et al., 2004; Tahmasbi, 2009; Chen et al., 2012; Abou-Shaara et al., 2012)

In enclosures, with entrances only in the lower part, the buoyancy of water vapour in dry air and the generation of heat and water vapour from honey bee metabolism ensures that the nest humidity is limited by the temperature and vapour permeability of the enclosure walls. The honey bees coat the inside of the enclosure with propolis derived from tree resins (Seeley, 1985) which have very low water vapour permeability (Hagenmaier and Shaw, 2019) and form a vapour barrier. This implies an accumulation of water vapour in the top of the nest limited only by the enclosure wall temperature. For example, wall temperatures of 30°C would enable a nest relative humidity (RH) of 90% at 34°C. Previous workers in this field, with *A. m. scutellata (Human et al., 2006),* have overlooked the dehumidification effect of the condensing, cool surface of the high conductance walls. Their low results of typically 40% RH may be explained by air with water vapour at 34°C, condensing on a hive wall at its dew point temperature of circa 19 °C (Lawrence, 2005).

To overcome this dehumidification effect requires continual expenditure of considerable energy (2.2 $MJkg^{-1}$) in evaporating the water to replace the vapour condensing on the walls, and/or preventing air circulation close to the enclosure walls. This high energy cost may explain the weak humidity regulation observed by researchers (Human et al. 2006). Contrast this with the energy required to regulate humidity in a nest with low conductance walls where the wall temperature rises to 30 °C near the brood nest and is lower in other parts of the nest. As described above, the humidity in the air surrounding the nest will rise to circa 90% RH. Regulation to lower humidity can then be achieved by circulation of the air into the parts of the nest where the walls are cooler. In this case the latent heat released by condensation is contained within the nest. The net energy required is only that necessary to heat air from the required RH and dew point, back to 34 °C, less the latent heat released by condensation. Low lumped thermal conductance enclosures, by reducing the energy expenditure in humidity control and enabling other humidity control mechanisms, may reveal more honey bee humidity control behaviours.

2.6.1 Implications for Varroa (*Varroa destructor)*

Varroa mites are a major parasite on honey bees and are considered to be the dominant vectors of virulent strains of dwarf wing viruses (Nordström, 2003; Rosenkranz et al.,

2010) which can eliminate honey bee colonies. Thus, if a consequence of heat transfer impacts varroa then it is of importance to the honey bee.

(Kraus and Velthuis, 1997), investigating the causes for lower varroa breeding success in the tropics (de Jong et al. 1984), described that in three test series with a total of 127 brood cells kept at 79–85% RH on average only 2% of the mites produced offspring, whereas 174 brood cells kept at 59–68% RH on average 53% of the mites produced offspring. This demonstrated that high nest humidity results in very poor varroa breeding success. In contrast, higher humidity has been shown to improve survival in *A. m. carnica* and *A. m. jemenitica* (Abou-Shaara et al., 2012) and improves egg viability (Doull, 1976). It has been shown to be only a minor factor in chalkbrood disease (*Ascophaera apis),* with an effect an order of magnitude less than lowered temperature (Flores et al. 2010), indicating a highly insulated nest with high humidity would result in a markedly reduced chalkbrood incidence, but not its elimination.

2.7 Conclusion

This literature review has shown that this avenue of research is novel, in that:

- No other study has simulated:
    - The heat transfer, complete with contents and bees, of the natural nest of *Apis mellifera* and compared it to a similar simulation of man made nests.
    - *Apis mellifera* as a thermoregulating colony to a fixed temperature as opposed to heat generation as a function of temperature.
- No other study has investigated the variation of heat transfer with honey bee density while inside any nest enclosure.
- No other study has measured the gaps between the comb and the enclosure in natural nests (peripheral galleries) or modelled the convection through them.
- No other study has quantified the impact on heat transfer of:
    - Bee space above the combs.
    - The height of the thermoregulated region within the enclosure.
    - Honey bee size within nest.

- No other study has quantified the impact of the thermal efficiency of the nest on:
  - Foraging range and variety.
  - Humidity regulation within the nest.

2.8 References

Abou-Houly, H.E. 2010. Investigation of flow through and around the Macrotermes michaelseni termite mound skin. , p.273.

Abou-Shaara, H.F., Al-Ghamdi, A. a. and Mohamed, A. a. 2012. Tolerance of two honey bee races to various temperature and relative humidity gradients. *Environmental and Experimental Biology*. **10**, pp.133–138.

Adam, B. 1975. Beekeeping At Buckfast Abbey Autumn & Winter *In*: *Beekeeping At Buckfast Abbey*. Northern Bee Books, pp.55–58.

Aksouh, M., Mataoui, A., Seghouani, N. and Haddad, Z. 2010. Assessment of performance of low Reynolds turbulence models in predicting natural. *Fluid Dynamics*. (June), pp.14–17.

Alburaki, M. and Corona, M. 2022. Polyurethane honey bee hives provide better winter insulation than wooden hives. *Journal of Apicultural Research*. **61**(2), pp.190–196.

Anderson, E.J. 1948. Hive Humidity and Its Effect Upon Wintering of Bees1. *Journal of Economic Entomology*. **41**(4), pp.608–616.

Anderson, E.J. 1943. Some Research on the Wintering of Bees. *Gleanings in Bee Culture*. **71**, pp.681–683.

Anderson, J.D. 1995a. *Computational Fluid Dynamics: The basics with applications*. New York.

Anderson, J.D. 1995b. Forms of governing equations particulary suited for CFD *In*: *Computational Fluid Dynamics: The basics with applications*. New York, pp.83–85.

Aounallah, M., Addad, Y., Benhamadouche, S., Imine, O., Adjlout, L. and Laurence, D. 2007. Numerical investigation of turbulent natural convection in an inclined square cavity with a hot wavy wall. *International Journal of Heat and Mass Transfer*. **50**(9–10), pp.1683–1693.

Ayachit, U. 2015. *The ParaView Guide: A Parallel Visualization Application*. Kitware, Incorporated.

Baker, T.J. 2005. Mesh generation: Art or science? *Progress in Aerospace Sciences*. **41**(1), pp.29–63.

Baveco, J.M., Focks, A., Belgers, D., van der Steen, J.J.M., Boesten, J.J.T.I. and Roessink, I. 2016. An energetics-based honeybee nectar-foraging model used to assess the potential for landscape-level pesticide exposure dilution. *PeerJ*. **2016**(8), pp.1–25.

Becher, M.A. 2010. The influence of developmental temperatures on division of labour in honeybee colonies. , p.85.

Becher, M.A., Grimm, V., Thorbek, P., Horn, J., Kennedy, P.J. and Osborne, J.L. 2014. BEEHAVE: A systems model of honeybee colony dynamics and foraging to explore multifactorial causes of colony failure. *Journal of Applied Ecology*. **51**(2), pp.470–482.

Bergman, T.L. and Lavine, A.S. 2017. *Fundamentals of Heat and Mass Transfer 8th Edition*. Wiley.

Boes, K.E. 2010. Honeybee colony drone production and maintenance in accordance with environmental factors: An interplay of queen and worker decisions. *Insectes Sociaux*. **57**(1), pp.1–9.

Bornus, L. and Nowakowski, J. 1974. Wintering of Bees in Single Walled Hives in Cold Climate. *Apiacta*. **3**, pp.105–106.

Butler, C. and Gamble, R. 1941. Backs to the Land:Wintering cut your losses. *BBC Home Service*.

Butler, C.G. and Gamble, R. 1942. Backs to the Land: Successful Wintering. *BBC Home Service*.

Buttemer, W.A. 1985. Energy relations of winter roost-site utilization by American goldfinches (Carduelis tristis). *Oecologia*. **68**(1), pp.126–132.

Cable, M. 2009. An Evaluation of Turbulence Models for the Numerical Study of Forced and Natural Convective Flow in Atria. . (May), pp.1–136.

Camazine, S. 1991. Self-Organizing Pattern Formation on the Combs of Honey Bee Colonies. *Behavioral Ecology and Sociobiology*. **28**(1), pp.61–76.

Camazine, S., Sneyd, J., Jenkins, M.J. and Murray, J.D. 1990. A mathematical model of self-organized pattern formation on the combs of honeybee colonies. *Journal of Theoretical Biology*. **147**(4), pp.553–571.

Carlton, K. 2000. Teaching about heat and temperature. *Physics Education*. **35**(2), pp.101–105.

Chen, Y.W., Chung, W.P., Wang, C.H., Solter, L.F. and Huang, W.F. 2012. Nosema ceranae infection intensity highly correlates with temperature. *Journal of Invertebrate Pathology*. **111**(3), pp.264–267.

Clark, E.H. 1918. Constructive beekeeping.

Coombs, A.B., Bowman, J. and Garroway, C.J. 2010. Thermal Properties of Tree Cavities During Winter in a Northern Hardwood Forest. *Journal of Wildlife Management*. **74**(8), pp.1875–1881.

Cooper, P. and Hunt, G.R. 2010. The ventilated filling box containing a vertically distributed source of buoyancy. *Journal of Fluid Mechanics*. **646**(2010), pp.39–58.

Corkins, C.L. and Gilbert, C.S. 1932. The metabolism of honeybees in winter cluster. *Bull. Wyo. Agric. Exp. Sta.* **187**(187), pp.1–30.

Cox, M.D. and Myerscough, M.R. 2003. A flexible model of foraging by a honey bee colony: The effects of individual behaviour on foraging success. *Journal of Theoretical Biology*. **223**(2), pp.179–197.

Currie, R.W. and Spivak, M. 2015. Winter Management of HoneyBee Colonies *In*: J. Graham, ed. *Hive and the Honey bee*. Hamilton IL USA: Dadant.

Dodologlu, A., DÜLGER, C. and Genc, F. 2004. Colony condition and bee behaviour in honey bees (Apis mellifera) housed in wooden or polystyrene hives and fed ‘ bee cake ’ or syrup. *Journal Of Apicultural Research*. **43**(1), pp.3–8.

Doull, K.M. 1976. the Effects of Different Humidities on the Hatching of the Eggs of Honeybees. *Apidologie*. **7**(1), pp.61–66.

Erdogan, Y., Dodologlu, A. and Emsen, B. 2009. Some physiological characteristics of honeybee (Apis mellifera L.) housed in heated, fan wooden and insulated beehives. *Journal of Animal and Veterinary Advances*. **8**(8), pp.1516–1519.

Erickson, E.H. 1990. Stress and Honey Bees. *Gleanings in Bee Culture*. **118**(11).

Eskov, E.K. and Toboev, V.A. 2009. Mathematical modeling of the temperature field distribution in insect winter clusters. *Biophysics*. **54**(1), pp.85–89.

Eyer, M., Neumann, P. and Dietemann, V. 2016. A look into the cell: Honey storage in honey bees, Apis mellifera. *PLoS ONE*. **11**(8).

Farrar, C.L. 1943. An interpretation of the problems of wintering the honeybee colony. *Gleanings in Bee Culture*. **9**(1), pp.513–518.

Farrar, C.L. 1952. Ecological Studies on Overwintered Honey Bee Colonies. *Journal of Economic Entomology*. **45**(3), pp.445–449.

Farrar, C.L. 1947. The overwintering of productive colonies *In*: R. A. Grout, ed. *Hive and the honey bee*. Chicago: Dadant and sons, pp.425–451.

Fehler, M., Kleinhenz, M., Klügl, F., Puppe, F. and Tautz, J. 2007. Caps and gaps: A computer model for studies on brood incubation strategies in honeybees (Apis mellifera carnica). *Naturwissenschaften*. **94**(8), pp.675–680.

Flores, J.M., Gutierrez, I. and Puerta, F. 2004. A comparison of methods to experimentally induce chalk brood disease in honey bees. *Spanish journal of agricultural research*. **2**(1), pp.79–83.

Flores, J.M., Ruiz, J.A., Ruz, J.M., Puerta, F., Bustos, M., Padilla, F. and Campano, F. 1996. Effect of temperature and humidity of sealed brood on chalkbrood development under controlled conditions. *Apidologie*. **27**(4), pp.185–192.

Fornito, L., Lee, R. and Tajchman, S.J. 1982. Heat transfer models for nesting cavities. *Archives for Meteorology, Geophysics, and Bioclimatology Series B*. **30**(3), pp.271–282.

Garbuzov, M. and Ratnieks, F.L.W. 2014. Ivy: An underappreciated key resource to flower-visiting insects in autumn. *Insect Conservation and Diversity*. **7**(1), pp.91–102.

Geiger, J.E. and Braun, E. 1955. Comparison of Methods for wintering bees for the prairie provinces. . **4**(1), pp.23–34.

Hagenmaier, R.D. and Shaw, P.E. 2019. Gas Permeability of Fruit Coating Waxes. *Journal of the American Society for Horticultural Science*. **117**(1), pp.105–109.

Hamilton, W. 1945. The Art of Bee Keeping. , p.200.

Hansard 1940. House of Commons Debate: Timber control. *Hansard*.

Heinrich, B. 1981. The Mechanisms and Energetics of Honeybee Swarm Temperature Regulation. *J. Exp. Biol.* **91**(1).

Hepburn, H.R., Pirk, C.W.W. and Duangphakdee, O. 2014. *Honeybee Nests*.

Höpken, J., Tomislav, M. and Kyle, M. 2014. *The OpenFOAM Technology primer*. Sourceflux.

Hosono, S., Nakamura, J. and Ono, M. 2017. European honeybee defense against Japanese yellow hornet using heat generation by bee-balling behavior. *Entomological Science*. **20**(1), pp.163–167.

Hozumi, S. and Inagaki, T. 2010. A long slit-like entrance promotes ventilation in the mud nesting social wasp, Polybia spinifex: Visualization of nest microclimates using computational fluid dynamics. *Journal of Insect Science*. **10**, pp.1–12.

Hozumi, S., Inagaki, T., Kudo, K., Mateus, S. and Zucchi, R. 2011. Thermal characteristics of polybia scutellaris nests (Hymenoptera: Vespidae) using computational fluid dynamics: A possible adaptation to tropical climates. *Sociobiology*. **57**(1), pp.123–141.

Huey, B.M. 1951. Problems of timber products procurement during World War II , 1941-1945. , pp.1941–1945.

Hum, J.E.Y., Hollands, K.G.T. and Wright, J.L. 2004. Analytical model for the thermal conductance of double-compound honeycomb transparent insulation, with validation. *Solar Energy*. **76**(1–3), pp.85–91.

Human, H., Nicolson, S.W. and Dietemann, V. 2006. Do honeybees, Apis mellifera scutellata, regulate humidity in their nest? *Naturwissenschaften*. **93**(8).

Humphrey, J.A.C. and Dykes, E.S. 2008. Thermal energy conduction in a honey bee comb due to cell-heating bees. *Journal of Theoretical Biology*. **250**(1), pp.194–208.

Idelchik, I.E. 2006. Handbook of hydraulic resistance (3rd edition). *Washington*.

Incropera, F.P., Dewitt, D.P., Bergman, T.L. and Lavine, A.S. 2007. Free Convection *In*: *Fundamentals of Heat and MassTransfer*., pp.560–618.

Johnson, B.R. 2009. Pattern formation on the combs of honeybees: Increasing fitness by coupling self-organization with templates. *Proceedings of the Royal Society B: Biological Sciences*. **276**(1655), pp.255–261.

Kasbioui, S., Lakhal, E.K. and Hasnaoui, M. 2003. Natural convection in rectangular enclosures with adiabatic fins attached on the heated wall. *Engineering Computations*. **20**(1/2), p.152.

Kim, S.H. and Huh, K.Y. 1999. Assessment of the finite-volume method and the discrete ordinate method for radiative heat transfer in a three-dimensional rectangular enclosure. *Numerical Heat Transfer, Part B: Fundamentals*. **35**(1), pp.85–112.

Knupp, P.M. 2002. Algebraic mesh quality metrics. *SIAM Journal on Scientific Computing*. **23**(1), pp.193–218.

Kortelainen, Juha 2009. *Meshing Tools for Open Source CFD: A Practical Point of View* [Online]. VTT Technical Research Centre of Finland. Available from: https://cris.vtt.fi/ws/portalfiles/portal/41830665/VTT_R_02440_09.pdf.

Kovac, H., Käfer, H., Stabentheiner, A. and Costa, C. 2014. Metabolism and upper thermal limits of Apis mellifera carnica and A. m. ligustica. *Apidologie*. **45**(6), pp.664–677.

Kraus, B. and Velthuis, H.H.W. 1997. High humidity in the honey bee (Apis mellifera L.) brood nest limits reproduction of the parasitic mite Varroa jacobsoni Oud. *Naturwissenschaften*. **84**(5), pp.217–218.

Krishnamoorthy, G. 2017. A computationally efficient P1 radiation model for modern combustion systems utilizing pre-conditioned conjugate gradient methods. *Applied Thermal Engineering*. **119**, pp.197–206.

Lakhal, E.K., Bilgen, E. and Vasseur, P. 1995. Natural convection and conduction in inclined enclosures bounded by a wall with honeycomb structure. *International Journal of Heat and Mass Transfer*. **38**(8), pp.1397–1407.

Lane-Serff, G.F., Sandbach, S.D., El Khoury, G.K., Andersson, H.I., Pettersen, B., Tammisola, O., Renzi, E., Dias, F., Bogey, C. and Marsden, O. 2012. Emptying non-adiabatic filling boxes: The effects of heat transfers on the fluid dynamics of natural ventilation. *Journal of Fluid Mechanics*. **701**(2012), pp.386–406.

Langstroth, L. 1853. *THE HIVE AND THE HONEY-BEE*. NORTHAMPTON: HOPKINS, BRIDGMAN & COMPANY.

Lawrence, M.G. 2005. The relationship between relative humidity and the dewpoint temperature in moist air: A simple conversion and applications. *Bulletin of the American Meteorological Society*. **86**(2), pp.225–233.

Lemke, M. and Lamprecht, I. 1990. A model for heat production and thermoregulation in winter clusters of honey bees using differential heat conduction equations. *Journal of Theoretical Biology*. **142**(2), pp.261–273.

Li, L. and Ma, W. 2011. Experimental Study on the Effective Particle Diameter of a Packed Bed with Non-Spherical Particles. *Transport in Porous Media*. **89**(1), pp.35–48.

Lin, Y.J.P. and Xu, Z.Y. 2013. Buoyancy-driven flows by a heat source at different levels. *International Journal of Heat and Mass Transfer*. **58**(1–2), pp.312–321.

Linden, P.F., Lane-Serff, G.F. and Smeed, D.A. 1990. Emptying filling boxes: The fluid mechanics of natural ventilation. *Journal of Fluid Mechanics*. **212**(1990), pp.309–335.

Loftus, J.C., Smith, M.L. and Seeley, T.D. 2016. How honey bee colonies survive in the wild: Testing the importance of small nests and frequent swarming. *PLoS ONE*. **11**(3), pp.1–11.

Mallinson, G. 2008. CFD visualisation: Challenges of complex 3D and 4D data fields. *International Journal of Computational Fluid Dynamics*. **22**(1–2), pp.49–59.

Manley, R.O.B. 1948. *Bee keeping in Britain*. London: Faber and Faber.

Mathur, A. and He, S. 2013. Performance and implementation of the Launder-Sharma low-Reynolds number turbulence model. *Computers and Fluids*. **79**, pp.134–139.

MATLAB 2018. *9.4.0.813654 (R2018a)*. Natick, Massachusetts: The MathWorks Inc.

Maziarz, M. and Wesołowski, T. 2013. Microclimate of tree cavities used by Great Tits (Parus major) in a primeval forest. *Avian Biology Research*. **6**(1), pp.47–56.

Miguel, A.F. 1998. Airflow through porous screens: From theory to practical considerations. *Energy and Buildings*. **28**(1), pp.63–69.

Mitchell, D. 2017a. Honey bee engineering: Top ventilation and top entrances. *American Bee Journal*. **157**(8), pp.887–889.

Mitchell, D. 2017b. Putting a Number on Natural. *Natural Bee Husbandry*. **1**(3).

Mitchell, D. 2016. Ratios of colony mass to thermal conductance of tree and man-made nest enclosures of Apis mellifera: implications for survival, clustering, humidity regulation and Varroa destructor. *International Journal of Biometeorology*. **60**(5), pp.629–638.

Mobus, B. 1998a. Brood rearing in the winter cluster. *American Bee Journal*., pp.511–514.

Mobus, B. 1998b. Rethinking Our Ideas About the Winter Cluster Part II. *American Bee Journal*. **8**, pp.587–591.

Montovan, K.J., Karst, N., Jones, L.E. and Seeley, T.D. 2013. Local behavioral rules sustain the cell allocation pattern in the combs of honey bee colonies (Apis mellifera). *Journal of Theoretical Biology*. **336**, pp.75–86.

Moss, K.J. 2007. *Heat and Mass transfer in Buildings*. London: Taylor & Francis.

Moukalled, F., Managai, L. and Dawish, M. 2016. *The Finite volume method in computational Fluid dynamics*. Heidelburg: Springer.

Mullarney, J.C., Griffiths, R.W. and Hughes, G.O. 2004. Convection driven by differential heating at a horizontal boundary. *Journal of Fluid Mechanics*. **516**(2004), pp.181–209.

Myerscough, M.R. 1993. A simple model for temperature regulation in honeybee swarms. *Journal of theoretical biology*. **162**, pp.381–393.

Nield, D.A. and Bejan, A. 2006. *Convection in Porous Media*. Springer.

Nordström, S. 2003. Distribution of deformed wing virus within honey bee (Apis mellifera) brood cells infested with the ectoparasitic mite Varroa destructor. *Experimental and Applied Acarology*. **29**(3–4), pp.293–302.

Oberkampf, W.L. and Trucano, T.G. 2002. Verification and validation in computational fluid dynamics. *Progress in Aerospace Sciences*. **38**(3), pp.209–272.

Ocko, S.A. and Mahadevan, L. 2014. Collective thermoregulation in bee clusters. *Journal of the Royal Society Interface*. **11**(91).

Olszewski, K. 2007. Winter-Hardiness of Buckfast Bees Under Specific Weather Conditions of Areas With Alternating Influences of Maritime and. *Journal of Apicultural Science*. **51**(1), pp.73–82.

Omholt, S.W. and Lonvik, K. 1986. Heat production in the winter cluster of the honeybee, Apis mellifera. A theoretical study. *Journal of Theoretical Biology*. **120**(4), pp.447–456.

Oskin, S.V. and Ovsyannikov, D.A. 2019. Modeling the Main Physical Processes in Beehives. *Biophysics (Russian Federation)*. **64**(1), pp.129–136.

Oskin, S.V., Ovsyannikov, D.A. and Shishigin, I.N. 2022. Modeling Beehive Microclimate at the End of Wintering. *Biophysics (Russian Federation)*. **67**(1), pp.85–91.

Oskin, S.V., Tsokur, D.S., Sultanov, G.A. and Kudryavtseva, A.A. 2020. The thermal model of winter aggregation of bees. *IOP Conference Series: Earth and Environmental Science*. **488**(1).

Owens, C.D. 1971. *The thermology of wintering honey bee colonies*.

Partridge, J.L. and Linden, P.F. 2013. Validity of thermally-driven small-scale ventilated filling box models. *Experiments in Fluids*. **54**(11).

Phillips, E.F. 1915. *Beekeeping*. Macmillan.

Phillips, E.F. and Demuth, G.S. 1914. *The temperature of the honeybee cluster in winter*. U.S. Dept. of Agriculture.

Ptáček, V. and Čermák, K. 2000. How many individuals survive winter in intact colonies of Apis mellifera L. *Pszczelnicze zeszyty naukowe*. **44**(2).

Rahli, O., Tadrist, L., Miscevic, M. and Santini, R. 1997. Fluid flow through randomly packed monodisperse fibers: The kozeny-carman parameter analysis. *Journal of Fluids Engineering, Transactions of the ASME*. **119**(1), pp.188–192.

Rangel, J., Reeve, H.K. and Seeley, T.D. 2013. Optimal colony fissioning in social insects: Testing an inclusive fitness model with honey bees. *Insectes Sociaux*. **60**(4), pp.445–452.

Rangel, J. and Seeley, T.D. 2012. Colony fissioning in honey bees: Size and significance of the swarm fraction. *Insectes Sociaux*. **59**(4), pp.453–462.

Ribes, A. and Caremoli, C. 2007. Salomé platform component model for numerical simulation *In*: *31st Annual International Computer Software and Applications Conference (COMPSAC 2007)* [Online]., pp.553–564. [Accessed 28 September 2023]. Available from: https://ieeexplore.ieee.org/document/4291178.

Riegel, J. and Mayer, W. 2019. FreeCAD (Version 0.18).

Roes, M.A., Bolster, D.T. and Flynn, M.R. 2014. Buoyant convection from a discrete source in a leaky porous medium. *Journal of Fluid Mechanics*. **755**(2014), pp.204–229.

Rosenkranz, P., Aumeier, P. and Ziegelmann, B. 2010. Biology and control of Varroa destructor. *Journal of Invertebrate Pathology*. **103**(SUPPL. 1), pp.S96–S119.

Sazhin, S.S., Sazhina, E.M., Faltsi-Saravelou, O. and Wild, P. 1996. The p-1 model for thermal radiation transfer: Advantages and limitations. *Fuel*. **75**(3), pp.289–294.

Schmehl, D.R., Tomé, H.V.V., Mortensen, A.N., Martins, G.F. and Ellis, J.D. 2016. Protocol for the in vitro rearing of honey bee (Apis mellifera L.) workers. *Journal of Apicultural Research*. **55**(2), pp.113–129.

Schmickl, T. and Crailsheim, K. 2007. HoPoMo: A model of honeybee intracolonial population dynamics and resource management. *Ecological Modelling*. **204**(1–2), pp.219–245.

Schmid-Hempel, P. 1987. Efficient Nectar-Collecting by Honeybees I. Economic Models. *Journal of Animal Ecology*. **56**(1), pp.209–218.

Scozia, R. and Frederick, R.L. 1991. Natural convection in slender cavities with multiple fins attached to an active wall. *Numerical Heat Transfer; Part A: Applications*. **20**(2), pp.127–158.

Seeley, T.D. 2010. *Honeybee Democracy*. Princeton University Press.

Seeley, T.D. 1985. *Honeybee Ecology: A Study of Adaptation in Social Life*. New Jersey, United States: Princeton University Press.

Seeley, T.D. and Kirk Visscher, P. 2004. Quorum sensing during nest-site selection by honeybee swarms. *Behavioral Ecology and Sociobiology*. **56**(6), pp.594–601.

Seeley, T.D. and Morse, R.A. 1976. The nest of the honey bee (Apis mellifera L.). *Insectes Sociaux*. **23**(4), pp.495–512.

Seeley, T.D. and Visscher, P.K. 2003. Choosing a home: How the scouts in a honey bee swarm perceive the completion of their group decision making. *Behavioral Ecology and Sociobiology*. **54**(5), pp.511–520.

Sodja, J. 2007. Turbulence models in CFD. *University of Ljubljana*. (March), pp.1–18.

Southwick, E.E. 1982. Metabolic energy of intact honey bee colonies. *Comparative Biochemistry and Physiology -- Part A: Physiology*. **71**(2), pp.277–281.

Southwick, E.E. 1991. The colony as a thermoregulating superorganism. *The behaviour and physiology of bees.*, pp.28–47.

Southwick, E.E. 1985. Thermal conductivity of wax comb and its effect on heat balance in colonial honey bees (Apis mellifera L.). *Experientia*. **41**(11), pp.1486–1487.

Southwick, E.E. and Heldmaier, G. 1987. Temperature Control in Honey Bee Colonies. *BioScience*. **37**(6), pp.395–399.

Stabentheiner, A., Pressl, H., Papst, T., Hrassnigg, N. and Crailsheim, K. 2003. Endothermic heat production in honeybee winter clusters. *Journal of Experimental Biology*. **206**(2), pp.353–358.

Sudarsan, R., Thompson, C., Kevan, P.G. and Eberl, H.J. 2012. Flow currents and ventilation in Langstroth beehives due to brood thermoregulation efforts of honeybees. *Journal of Theoretical Biology*. **295**, pp.168–193.

Suehrcke, H., Däldehög, D., Harris, J.A. and Lowe, R.W. 2004. Heat transfer across corrugated sheets and honeycomb transparent insulation. *Solar Energy*. **76**(1–3), pp.351–358.

Sumpter, D.J.T. and Broomhead, D.S. 2000. Shape and dynamics of thermoregulating honey bee clusters. *Journal of Theoretical Biology*. **204**(1), pp.1–14.

Sun, H., Lauriat, G. and Nicolas, X. 2011. Natural convection and wall condensation or evaporation in humid air-filled cavities subjected to wall temperature variations. *International Journal of Thermal Sciences*. **50**(5), pp.663–679.

Tahmasbi, G.H. 2009. The effect of temperature and humidity on grooming behaviour of honeybee , Apis mellifera (Hym .: Apidae) colonies against varroa mite , Varroa destructor (Acari : Varroidae). *Journal of Entomological Society of Iran*. **28**(2), pp.7–23.

Tapia Brito, E. 2022. Application of phase change material heat storage device for control of Varroa mites in beehives. [Accessed 10 September 2023]. Available from: https://eprints.nottingham.ac.uk/71611/.

Tautz, J., Maier, S., Groh, C., Rössler, W. and Brockmann, A. 2003. Behavioral performance in adult honey bees is influenced by the temperature experienced during their pupal development. *Proceedings of the National Academy of Sciences of the United States of America*. **100**(12), pp.7343–7347.

Teitel, M., Dvorkin, D., Haim, Y., Tanny, J. and Seginer, I. 2009. Comparison of measured and simulated flow through screens: Effects of screen inclination and porosity. *Biosystems Engineering*. **104**(3), pp.404–416.

Thomaz, M., Malaquis, I.M., Valente, M.C. and Antunes, M.J. 1995. An attempt to overcome aIternative conceptions related to heat and temperature. *Physics Education*. **30**(19).

Thompson, C. 2013. a Cfd Study Investigating the Influence of Bottom Board Geometry on Physical Processes Within a Standard Honeybee Hive. *Journal of Chemical Information and Modeling*. **53**(9), pp.1689–1699.

Thorkelson, J. and Maxwell, R.K. 1974. Design and Testing of a Heat Transfer Model of a Raccon (Procyon Lotor) in a Closed Tree Den. *Ecology*. **55**(1), pp.29–39.

Valera, D.L., Molina, F.D., Álvarez, A.J., López, J.A., Terrés-Nicoli, J.M. and Madueño, A. 2005. Contribution to characterisation of insect-proof screens: Experimental measurements in wind tunnel and CFD simulation. *Acta Horticulturae*. **691**(February), pp.441–448.

Välikanga, T. 2016. *Conjugate heat transfer in OpenFOAM*.

Vdovin, A. 2009. Radiation heat transfer in OpenFOAM. *Report*., p.17.

Versteeg, H.K. 2007. *An introduction to computational fluid dynamics: the finite volume method* 2nd ed. Harlow, England ; Pearson Education Ltd.

Vesterinen, F. 1974. Wintering of Bees in Finland. *Apiacta*. **3**.

Villa, J.D., Rinderer, T.E. and Bigalk, M. 2009. Overwintering of Russian honey bees in northeastern Iowa. *Science of Bee Culture*. **1**(2), pp.19–21.

Villumstad, E. 1974. Importance of hive insulation for wintering , development and honey Yield in Norway. *Apiacta*. **3**, pp.116–118.

Watmough, J. and Camazine, S. 1995. Self-organized thermoregulation of honeybee clusters. *Journal of Theoretical Biology*. **176**(3), pp.391–402.

Wong, C.L., Chu, H.E. and Yap, K.C. 2016. Are Alternative Conceptions Dependent on Researchers' Methodology and Definition?: a Review of Empirical Studies Related To Concepts of Heat. *International Journal of Science and Mathematics Education*. **14**(3), pp.499–526.

Wykes, G.R. 1953. The sugar content of nectars. *The Biochemical journal*. **53**(2), pp.294–296.

Yang, M.-X., Ken, T., Phiancharoen, M. and Hepburn, R. 2005. Comb construction in mixed-species colonies of honeybees, Apis cerana and Apis mellifera. *Fortune*. **151**(11), p.22.

Yang, X., Bai, J., Lu, T. and Kim, T. 2014. Experimental investigation of chimney-enhanced natural convection in hexagonal honeycombs. *Theoretical and Applied Mechanics Letters*. **4**(3), p.032005.

Zhang, K., Duana, H., Karihaloo, B.L. and Wanga, J. 2010. Hierarchical, multilayered cell walls reinforced by recycled silk cocoons enhance the structural integrity of honeybee combs. *Proceedings of the National Academy of Sciences of the United States of America*. **107**(21), pp.9502–9506.

Chapter 3 Thermal efficiency extends distance and variety for honey bee foragers

This is based on the authors published work:

Mitchell, D. 2019. Thermal efficiency extends distance and variety for honeybee foragers: Analysis of the energetics of nectar collection and desiccation by Apis mellifera. Journal of the Royal Society Interface. ***16****(150).*

3.1 Abstract

The dessication of nectar to produce honey by honey bees (*Apis mellifera* L.) is an energy intensive process, as it involves a quasi-isothermal change in the concentration of sugars from typically 20% to 80% by vaporisation (honey ripening). This analysis creates mathematical models for: the collected nectar to honey ratio; energy recovery ratio; honey energy margin; and the break even distance, which includes the factors of nectar concentration and the distance to the nectar from the nest; energetics of dessication; and a new factor, thermal energy efficiency of nectar dessication (TEE). These models show a significant proportion of delivered energy in the nectar must be used in dessication and that there is a strong connection between TEE and nest lumped thermal conductance with colony behaviour. They show the connection between TEE and honey bee colony success, or failure, in the rate of return, in terms of distance or quality of foraging. Consequently TEE is a key parameter in honey bee population and foraging modelling. For bee-keeping it quantifies the summer benefits of a key hive design parameter, hive thermal conductance and gives a sound theoretical basis for improving honey yields, as seen in expanded polystyrene hives.

Table 3.1: Chapter nomenclature.

Term	Description	Units
$A_{Entrance}$	Cross sectional area of entrance	m^2
C_{Nectar}	Concentration of nectar	$kgkg^{-1}$
C_{Honey}	Concentration of honey	$kgkg^{-1}$
d	Distance from the nest to the flower patch	m
$d_{Break\,Even}$	Distance from the nest to the flower patch the result in zero energy gain in honey stored	m

Term	**Description**	**Units**
E_{Base}	Energy in resultant honey	J
$E_{Collected}$	Energy in the collected nectar	J
$E_{Evaporate}$	Energy required for evaporation excluding losses	J
$\dot{E}_{Evaporate}$	Rate of energy (power) required for evaporation excluding losses	W
$\widetilde{E}_{Evaporate}$	Energy required for evaporation including losses	J
E_{Flight}	Energy required for transport	J
E_{Losses}	Energy lost from dessication process not employed in dessication	J
$E_{Sucrose}$	Metabolic energy of sucrose	J
F_x	Dimension set of an air flow x i.e. factors that effect heat transfer outside the at rest properties and bulk velocity	-
HEM	Honey energy margin	-
L_{Flight}	Energy per kilogram of nectar delivered required for flight from the nest to the nectar flower patch and back	Jkg^{-1}
L_{Honey}	Metabolic value of honey per unit weight	Jkg^{-1}
L_{Honey}^{Nectar}	Latent heat of vaporisation of nectar to honey	Jkg^{-1}
$L_{Sucrose}$	Metabolic energy of sucrose per unit weight	Jkg^{-1}
L_{Water}	Latent heat of vaporisation per unit weight of water	Jkg^{-1}
M	Honey energy margin from collection to honey	-
P_x	Property set of an air flow x	
$\dot{q}_{Advection}$	Rate of nest heat loss by conduction	W
$\dot{q}_{Bee}$	Rate of metabolic heat input by the honey bees	W
$\dot{q}_{Conduction}$	Rate of nest heat loss by advection though the entrance	W
T_{Inward}	Temperature of air fanned inward to nest	C
$T_{Outward}$	Temperature of air exhausted from the nest	C
TEE	Thermal energy efficiency of nectar dessication	-
$\vec{u}_x$	Air velocity of flow x	ms^{-1}
$u_{Entrance}$	Air velocity through entrance	ms^{-1}
W_{Honey}^{Base}	Weight of the resultant honey	kg
W_{Nectar}^{Base}	Weight of resultant base honey in the form of nectar before dessication	kg
$W_{Sucrose}^{Base}$	Weight of the sucrose within the resultant honey	kg

Term	**Description**	**Units**
$W_{Nectar}^{Collected}$	Weight of delivered nectar plus net nectar used in transport	kg
$W_{Nectar}^{Delivered}$	Weight of nectar delivered to nest	kg
$W_{Nectar}^{Evaporate}$	Weight of nectar required as fuel for the evaporation of nectar	kg
$W_{Sucrose}^{Evaporate}$	Weight of sucrose required to evaporate water content of nectar	kg
$W_{Water}^{Evaporate}$	Weight of water to be evaporated	kg
W_{Nectar}^{Flight}	Weight of nectar required as fuel for flight	kg
$\dot{W}_{Water}^{Evaporate}$	Rate of water evaporated in honey ripening	kgs^{-1}
$\dot{W}_{Honey}^{Base}$	Rate of honey ripening in terms of resultant honey	kgs^{-1}
$\Pi_{Base,Honey}^{Collected,Nectar}$	Ratio of the weights of nectar collected to the resulting honey	-
$\Gamma_{Recovery} \equiv \Gamma_{Collected}^{Base}$	Energy recovery ratio: energy in honey divided by energy in collected nectar	-
$\Gamma_{Transport} \equiv \Gamma_{Collected}^{Delivered}$	Transported energy ratio: energies of nectar delivered divided by nectar collected	-
$\Gamma_{Thermal} \equiv \Gamma_{\langle Evaporate \rangle}^{Evaporate}$	Thermal efficiency of dessication : ratio of $E_{Evaporate}$ divided by $E_{\langle evaporate \rangle}$	-
$\Gamma_{Dessicate}$	Dessicate energy fraction, the proportion of energy delivered used in nectar evaporation	-
$\xi = \Pi_{Base,Sucrose}^{Evaporate,Water}$	Reciprocal concentration of honey subtract from reciprocal concentration of nectar	-
$\zeta = \Pi_{Base,Sucrose}^{Delivered,Nectar}$	Ratio of weights of delivered nectar to base sucrose	-
φ	Energy for flight per unit weight and distance	$Jkg^{-1}m^{-1}$
κ_{Air}	Heat capacity of air	Jkg^{-1}
ρ_{Air}	Density of air	kgm^{-3}
Λ_{nest}	Lumped thermal conductance of the nest enclosure e.g. hive, tree etc	WK^{-1}
$\Lambda_{Advection}^{x}$	Convection conductance for flow x	WK^{-1}
$\Lambda_{Advection}^{External}$	External convection conductance	WK^{-1}
$\Lambda_{Advection}^{Internal}$	Internal convection conductance	WK^{-1}

3.2 Introduction

Honey, a high sugar concentration (>80%) fluid, is dessicated by honey bees from flower nectar, a lower sugar concentration liquid (10% - 50%) and modified by the secretion of enzymes. After collection from numerous flowers, sometimes at the considerable distance of 1 to 9 Km. This nectar is passed by the forager honey bee to another honey bee, an unloader /storer, which starts the dessication process by selectively heating and aerating the nectar with their mouth parts, while placing it in a honey comb cell, this partially desiccated nectar is then exposed to low humidity air, while the hive population engages in vigorous forced air movement within the nest by fanning their wings (Park, 1925; Park, 1932; Eyer et al., 2016). The first part of the process, lasting a few minutes, the second part, a few hours up to a few days. This activity takes place with considerable intensity during summer evenings, it is clearly audible (i.e. greater than 30db) from a distance of several metres, and can last into the small hours of the following morning. The efficiency of this process is vital for the honey bee colony to survive periods when no nectar is available, especially during winter. *A. mellifera* does not hibernate in winter, but uses the stored energy in the honey’s sugars to maintain temperatures above 18C for some of the colony, and above 10C for the remainder, when temperatures outside the nest enclosure can be as low as -40C (Seeley, 1984; Ocko and Mahadevan, 2014).

The amount of water evaporated can be more than 400kg per year. Considerable amounts of energy of the order of 1GJ are required to achieve this, given the very high latent heat of evaporation of water of 2.426MJkg^{-1} at 305K (Incropera et al., 2005; Heyd et al., 2014).

This is a normal, routine operation in the nest and hence a factor in the thermoregulation of the colony. In the numerous discussions on how water is collected and used for thermoregulation (Lindauer, 1955; Southwick and Moritz, 1987; Nicolson, 2009; Ostwald et al., 2016; Shackleton et al., 2016; Bordier et al., 2017), the only parallels drawn between water and nectar are in the use of the proboscis. The water content of the nectar is referenced as a resource of water for brood (Lindauer, 1955).

Studies of honey bees under heat stress using simulated heat waves (Bordier et al., 2017) have noted honey bee nectar collection behaviour changes to collect more dilute nectar. The authors attributed this as a means of providing more resources for collection of water for thermoregulation.

Thermoregulatory temperature transitions after feeding with nectar would be expected as dessication proceeds i.e. temperature increases to reduce relative humidity(RH) followed by rapid decreases towards the end of the evaporation phase. These have been observed (Simone-Finstrom et al., 2014) but, to date, not attributed to nectar dessication.

The literature on honey bee population, thermoregulation and foraging e.g. (Southwick and Pimentel, 1981; Schmid-Hempel et al., 1985; Schmid-Hempel, 1987; DeGrandi-Hoffman et al., 1989; Kühnholz et al., 1997; Germ et al., 1997; Cresswell et al., 2000; De Vries and Biesmeijer, 2002; Higginson and Gilbert, 2004; Schmickl and Crailsheim, 2004; Ion et al., 2006; Schmickl and Crailsheim, 2007; Beekman and Lew, 2008; Ocko and Mahadevan, 2013; Nedić et al., 2013; Becher et al., 2013; Russell et al., 2013; Simone-Finstrom et al., 2014; Schürch and Gruẗer, 2014; Becher et al., 2014; Naug, 2014a; Alqarni, 2015; Torres et al., 2015; Schmickl and Karsai, 2016; Baveco et al., 2016; Adgaba et al., 2017; Henry et al., 2017; M. Betti et al., 2017; M.I. Betti et al., 2017; Schmickl and Karsai, 2017) say nothing about the thermal efficiency or detail about the energy of nectar dessication, theoretical or experimental. An older source on honey ripening (Park, 1946) gives the weight of nectar required to ripen a pound of honey at 40% nectar concentration and opines that this energy is largely sourced from insolation and the ambient air. This is the only article found by the author that considers the magnitude of the energy requirement of dessication.

The literature includes works on:

- Energy efficiency of honey production (Southwick and Pimentel, 1981).
- Predicting honey yields from nectar sources (Ion et al., 2006; Nedić et al., 2013; Alqarni, 2015; Adgaba et al., 2017).
- Models of honey bee population (DeGrandi-Hoffman et al., 1989; Schmickl and Crailsheim, 2007; Becher et al., 2013; Russell et al., 2013; Becher et al., 2014; Torres et al., 2015; M. Betti et al., 2017; M.I. Betti et al., 2017; Henry et al., 2017).

- Honeybee foraging strategies and costs (Schmid-Hempel et al., 1985; Germ et al., 1997; Cresswell et al., 2000; De Vries and Biesmeijer, 2002; Higginson and Gilbert, 2004; Schmickl and Crailsheim, 2004; Beekman and Lew, 2008; Naug, 2014a; Schürch and Gruẗer, 2014; Baveco et al., 2016; Schmickl and Karsai, 2017).

Their assumptions, not always explicit, include:

1. **Population overhead –** The energy cost is dependant only on the number of insects assigned to the processing or the hive population in general (Cresswell et al., 2000; Schmickl and Crailsheim, 2007; Russell et al., 2013).
2. **Direct energy equivalence –** The value of the energy in the nectar is identical to that stored in the honey (Becher et al., 2014; Schürch and Gruẗer, 2014; M. Betti et al., 2017; Henry et al., 2017), or that conversion cost is not significant (De Vries and Biesmeijer, 2002; Baveco et al., 2016).
3. **Nectar not honey as stored energy** – “Stored nectar” rather than honey as the stored energy medium (Schmickl and Karsai, 2017).

For Northern European honey bees (e.g. *A.m.mellifera, A.m. Iberiensis, A.m.ligustica*) in a temperate climate, nectar concentration during flight does not occur (Park, 1932). This contrasts with *A.m.scutellata* in hot arid climates (Nicolson and Human, 2008), where energy is gained in flight from the air and insolation.

While insolation may input energy in high thermal conductance (2.6 WK^{-1}) man-made hives in full sun, *A.mellifera,* in nature, resides in shaded, very low thermal conductance nests (0.4WK^{-1}) (Mitchell, 2016) (Seeley, 2010). In both types of nest, in temperate climates, vigorous nectar evaporation takes place at night. Therefore we may rule out insolation as a necessity for dessication. Thus for honey bee metabolic heat, conduction and advection are on the right hand side of the heat balance equation below (equations 3.22 and 3.3), and the energy required to dessicate the nectar on the left.

$$\dot{E}_{Evaporate} = \dot{q}_{bee} + \left(\Lambda_{Nest} + \frac{1}{2} A_{Entrance}\, \kappa_{Air} \rho_{Air} u_{Entrance}\right)\left(T_{Outside} - T_{Inside}\right) \qquad (3.1)$$

Typical values for the lumped conductance range from 1WK^{-1} for tree nests, and ~ 3WK^{-1} for man made nests. Typical values for entrance size and fanned air velocity are

10 cm^2 (Seeley, 1984)) and $1ms^{-1}$ (Peters et al., 2017). These give an advection term of around $0.5WK^{-1}$, thus in hives heat loss through the hive wall is dominant.

In temperate climates, the nest temperatures are usually significantly higher than ambient (Seeley, 1984). Given the above analysis and observations, one may discount the outside environment as being a major contributor of energy to desiccation, and is instead more likely to be a potential loss. This scenario forms the focus in this analysis.

The energy released by the honey bees converting disaccharide sugars to monosaccharides has been postulated as a source of energy, but this amounts to only ~$15KJmol^{-1}$, or ~$43KJkg^{-1}$ (Goldberg et al., 1989) is insignificant compared to the energy required in the evaporation process.

The metric in the literature (Schmid-Hempel et al., 1985; Naug, 2014b; Baveco et al., 2016) for assessing the continuing survival of a honey bee colony is the margin of return on the energy spent by the honey bees foraging. It was defined as the energy recovered minus the total energy expended divided by the energy expended. Long term survival was considered only to be likely when this metric is greater than zero. This was concerned with how much of the energy available, in all of the reachable or visited flowers, is delivered to the hive entrance. This did not account for how energy is made available for consumption as honey, or consider that the nectar to honey processing occurs within minutes after the forager arrives back at the nest (Park, 1946).

This analysis provides the physics that constrains the biological behaviours of the honey bees providing the basis for new hypotheses, insights and understanding for those behaviours. The magnitude of the energy involved in the dessication process, and how the losses and efficiency impact the honey bee colony are the focus of this study.

3.3 Approach

3.3.1 System Boundary

A system boundary defines the scope of an energy transfer analysis. For example previous studies have taken this boundary as:

- Only the colony of honey bees (Ocko and Mahadevan, 2014).

- The Individual honey bees, from the hive entrance to all of the individual flowers and back again (Stabentheiner and Kovac, 2014).

Energy Analysis considers the energy inputs and outputs of the system i.e. across the system boundary, as well as any change of state of the system e.g. from a liquid to a vapour.

This analysis will consider the system to be bounded by the nest enclosure, which loses heat, determined by the lumped conductance of the nest, and the outside temperature and the journey to and from the flower patch from the nest in the absence of wind. This approach has been chosen to focus on the colony and nest impacts rather than impacts and dependencies of the flowers. This focus involves factors of nectar dessication and distance flown to forage areas as opposed to flower patch depletion or honeybee time spent. As a consequence it excludes the flower to flower transport energy which is assumed to be replaced at the flower patch.

The nest consumption of honey e.g. the up keep of the nest, brood etc. are considered as an energy drain after the dessication process and therefore fall outside of the analysis.

Water and pollen collection are significant activities for the honey bees involving expenditure outlay and return, however for this analysis, we assume that the nectar collection is the dominant energy input process which is born out by the relative quantities and calorific gains (Seeley, 1984).

3.3.2 Thermal energy efficiency of nectar dessication

Losses from a system and the useful work done are usually treated as an efficiency coefficient. Defined as the ratio of energy or work, that is useful to the goal, divided by the total energy input in trying to achieve that goal. In this application this quantity, $\Gamma_{thermal}$, is shown in equation 3.2.

$$\Gamma_{thermal}=\frac{E_{Evaporate}}{\left(E_{Evaporate}+E_{Losses}\right)}=\frac{E_{Evaporate}}{\tilde{E}_{Evaporate}} \qquad (3.2)$$

The losses in equation 3.2 are dominated by the lumped nest conductance. The thermal efficiency of nectar dessication is dependent on the lumped conductance of the nest, the averaged temperature difference between the inside and outside of the nest, and the rate of water being evaporated as shown in equation 3.3.

$$\Gamma_{Thermal} \approx \frac{1}{\left(1+\frac{\Lambda_{Nest}\left(T_{Inside}-T_{Outside}\right)}{\dot{E}_{Evaporate}}\right)} \tag{3.3}$$

Important:

- The lumped thermal conductance includes the internal and external convective heat transfers, as well as the conduction through the nest envelope, the first and second are dependant on flow velocity and local geometry (equation 3.22).
- If the outside temperature is above the internal temperature, then the thermal efficiency will be greater than 1, because there is heat gain rather than loss.

3.3.3 Metrics

In the current analysis, the honey energy margin (HEM) is the sum of the energy costs the honey bees cannot immediately replace in the field $\sum E_{costs}$, subtracted from energy of the honey ripened E_{Honey}, divided by the sum of the energy costs as shown as M in equation 3.4.

$$M = \frac{E_{Honey} - \sum E_{costs}}{\sum E_{costs}} \tag{3.4}$$

Break even distance occurs when the expenditure on transport and dessication consumes all of the energy collected by the honey bees i.e. when HEM is zero in equation 3.5, then honey bees can not accumulate the stores needed for times of dearth e.g. droughts, poor weather and winter.

$$\exists d \; where \; M\left(d, \Gamma_{Thermal}, C_{Nectar}, C_{Honey\ldots}\right) = 0 \tag{3.5}$$

The transported energy ratio $\Gamma_{transport}$, is the energy delivered to the entrance divided by the sum of the energy delivered $E_{Delivered}$, and the energy consumed in travelling to and from the flower patch $E_{Transport}$. This metric determines the impact of fetching the nectar from a distance. Similarly to HEM, we will exclude the flower to flower flight costs. However, some of the more complex models, as related in the literature, can be included as part of further study by using a modified transport efficiency ratio that takes those factors into account.

$$\Gamma_{transport}=\frac{E_{Delivered}}{E_{Delivered}+E_{Transport}} \tag{3.6}$$

Energy consumption on the flight to the flower patch and back depends on numerous factors such as: distance, take off weight (Wolf et al., 1989), crop content temperature (Kovac et al., 2010), ambient wind speed (Barron, 2006), ambient temperature (Woods et al., 2005; Stabentheiner and Kovac, 2016). To cater for this complexity, the formulae in the analysis use a single parameter φ with dimensions of $\mathrm{Wkg^{-1}m^{-1}}$. However, the results below, following other researchers (Baveco et al., 2016), use a simplified form. This is derived from the averaged flight metabolic rate and averaged flight speed.

Energy recovery ratio $\Gamma_{Recovery}$, is the energy in the honey accumulated E_{Base}, divided by the energy in the nectar collected from the flowers $E_{Collected}$, in equation 3.7. This gives the proportion of useable energy compared to the losses from dessication and transport. In prior studies this is effectively assumed to be a fixed value of 1.0 at zero nest to nectar distance.

$$\Gamma_{Recovery}=\frac{E_{Base}}{E_{Collected}} \tag{3.7}$$

Dessication energy fraction is the fraction of the energy delivered to the nest that is used in the dessication process. This can be derived from the energy recovery ratio evaluated for zero distance. Hence equation 3.8.

$$\Gamma_{Dessicate}=\frac{E_{Deivered}+E_{Base}}{E_{Delivered}}=1-\Gamma_{Recovery}(d=0) \tag{3.8}$$

The collected nectar to honey ratio $\Pi_{Base,Honey}^{Collected,Nectar}$, is the weight of nectar collected $W_{Nectar}^{Collected}$, divided by the weight of honey after dessication W_{Honey}^{Base}, shown in equation 3.9. This enumerates the increase in honey bee trips needed to allow for dessication and transport losses.

$$\Pi_{Base,Honey}^{Collected,Nectar} = \frac{W_{Nectar}^{Collected}}{W_{Honey}^{Base}} \tag{3.9}$$

3.4 Analysis

3.4.1 Assumptions

The assumptions in this analysis are:

1. The product of a TEE factor and energy required to be generated by the honey bees for evaporating the water from the nectar, including losses, equals the product of the latent heat of vaporisation and the mass of water vaporised.
2. The system boundary is as defined in section 3.3.1.
3. The system is in equilibrium i.e. steady state.
4. The honey bee can refuel at the nectar source and that the nectar concentration the honey bee uses as fuel is the same as the nectar source.
5. Nectar concentration does not change in flight i.e. temperate climate (Park, 1932; Nicolson and Human, 2008).
6. No variation in energy consumed due to in flight changes in insect weight or wind speed.
7. Enthalpy of evaporating water from nectar to honey is assumed to be constant for all of the starting nectar concentrations over the range 10% to 50% with a finishing honey concentration of 80% and to be approximately that of water (Heyd et al., 2014).
8. Calorific value of the sugars in the honey and nectar are taken to be that of sucrose (Goldberg et al., 1989).
9. The enthalpy of inverting sucrose to fructose and glucose and its use of water are negligible, compared to the volume of evaporated water and the energy needed to vaporise it (Goldberg et al., 1989).
10. Radiation or changes in external RH are not taken into account.

11. All advection and conduction heat losses are attributed to nectar dessication for the purposes of thermal efficiency estimation.
12. Dominant process of energy collection is that of nectar. Water and pollen collection are therefore not considered.
13. Nectar sources are considered to be effectively at a single distance (single value energy cost) and concentration (single value reward) and do not deplete.

3.4.2 Fundamentals

Basic relations and notations are shown below:

1. Notation (equation 3.10).

G_B^A attribute G of quantity A of substance B. e.g $W_{Nectar}^{Collected}$ is weight of collected nectar (3.10)

2. Ratio of weights notation (equation 3.11).

$\Pi_{X,Y}^{A,B}=\frac{W_B^A}{W_Y^X}, \forall X \forall Y \forall A \forall B$ where names A and X are quantities, B and Y substances (3.11)

3. Ratio of energies notation (equation 3.12).

$$\Gamma_X^A=\frac{E_A}{E_X}, \forall A \forall X \text{ where names A and X are quantities} \tag{3.12}$$

4. Concentration of substances referenced to sucrose (equation 3.13).

$$W_Y^X=\frac{W_{Sucrose}^X}{C_Y}, \forall X \forall Y \text{ i.e. for all quantities X, substances Y} \tag{3.13}$$

5. Mass, energy and latent heats of flight, vaporisation and metabolism (equation 3.14).

$$W_Y^X=\frac{E_X}{L_Y}, \forall X \forall Y \text{ e.g. Mass quantity X of substance Y with Latent Heat } L_Y \tag{3.14}$$

6. Sum of evaporation energy and losses (equation 3.15).

$$\widetilde{E}_{Evaporate}=E_{Evaporate}+E_{Losses} \tag{3.15}$$

7. Thermal efficiency definition (equation 3.16).

$$\Gamma_{Thermal}E_{\langle evaporate\rangle}=L_{water}W_{Water}^{Evaporate} \tag{3.16}$$

3.4.3 Thermal energy efficiency

Energy that can be released from the sucrose is given in equation 3.14. The water needed to be evaporated is the difference in mass between the honey and the nectar (equation 3.17).

$$W_{Water}^{Evaporate}=W_{Nectar}^{Base}-W_{Honey}^{Base} \tag{3.17}$$

Equations (3.13) and (3.17) which rearranged give equation 3.18, the mass of evaporated water.

$$W_{Water}^{Evaporate}=W_{Sucrose}^{Base}\left(\frac{1}{C_{Nectar}}-\frac{1}{C_{Honey}}\right)=W_{Sucrose}\Pi_{Base,Sucrose}^{Evaporate,Water}=W_{Sucrose}^{Base}\xi \tag{3.18}$$

Equations 3.14 and 3.18 give the energy for evaporation.

$$E_{Evaporate}=L_{Water}W_{Sucrose}^{Base}\xi \tag{3.19}$$

Equation (3.19) as a rate, in terms of honey ripened rate using 3.13 gives equation 3.20.

$$\dot{E}_{Evaporate}=\dot{W}_{honey}^{Base}L_{Water}C_{Honey}\xi \tag{3.20}$$

Equation (3.19) substituted in to equation 3.2 gives equation 3.21.

$$\Gamma_{Thermal}=\frac{1}{\left(1+\frac{\Lambda_{nest}\left(T_{Inside}-T_{Outside}\right)}{\dot{W}_{Honey}^{Base}L_{Water}C_{Honey}\xi}\right)} \tag{3.21}$$

Important: Λ_{Nest} is an aggregation of a series network, comprising the enclosure and air to enclosure heat transfers as defined in equation 3.22. From reference (Bejan, 2004), these heat transfers are functions of the property set of the air being moved, the air velocity vectors and the dimension set of the formation of the air flow (equation 3.23).

In this case the internal air flow is the result of honey bee behaviour and natural convection.

$$\frac{1}{\Lambda_{Nest}}=\frac{1}{\Lambda_{Enclosure}}+\frac{1}{\Lambda_{advect}^{External}}+\frac{1}{\Lambda_{advect}^{Internal}} \tag{3.22}$$

$$\vec{u}_x, F_x, P_x| \rightarrow \Lambda_{advect}^{x}\left(\vec{u}_x, F_x, P_x\right) \tag{3.23}$$

3.4.4 Nectar delivered to hive

The total nectar required is nectar to be made in to honey (base amount) plus the nectar used as fuel for the evaporation (equation 3.24).

$$W_{Nectar}^{Delivered}=W_{Nectar}^{Base}+W_{Nectar}^{Evaporate} \tag{3.24}$$

Combining equation 3.19 and 3.16, then energy required for evaporation, is shown in equation 3.25.

$$\widetilde{E}_{evaporate}=\frac{L_{Water}W_{Sucrose}^{Base}\xi}{\Gamma_{Thermal}} \tag{3.25}$$

The sucrose required, as fuel can be determined, (equation 3.26), then expressed as a nectar mass (equation 3.27).

$$W_{Sucrose}^{Evaporate}=\frac{L_{water}W_{Sucrose}^{Base}\xi}{L_{Sucrose}\Gamma_{Thermal}} \tag{3.26}$$

$$W_{Nectar}^{Evaporate}=\frac{L_{water}W_{Sucrose}^{Base}\xi}{C_{Nectar}L_{Sucrose}\Gamma_{Thermal}} \tag{3.27}$$

This nectar mass is then added to the base nectar amount,(equation 3.24), to give a total mass of nectar that needs to be delivered to the hive, and is then rearranged as equation 3.28.

$$W_{Nectar}^{Delivered}=W_{Sucrose}^{Base}\frac{1}{C_{Nectar}}\left(1+\frac{L_{Water}\xi}{L_{Sucrose}\Gamma_{Thermal}}\right)=W_{Sucrose}^{Base}\Pi_{Base,Sucrose}^{Delivered,Nectar}=W_{Sucrose}^{Base}\zeta \tag{3.28}$$

3.4.5 Collected nectar, nectar to honey ratio and transported energy ratio

If we take into account the efficiency of nectar collection, i.e. allow for the nectar consumed in transportation (a function of distance of nest from nectar source), using the transported energy ratio then we can create an expression for the nectar collection to honey factor, equation 3.29, using equation 3.28.

$$W_{Nectar}^{Collected}=\frac{W_{Nectar}^{Delivered}}{\Gamma_{Transport}}=\frac{W_{Sucrose}^{Base}\zeta}{\Gamma_{Transport}} \tag{3.29}$$

L_{Flight} is defined as the energy required to deliver payload per unit weight over d, the distance to the flower patch from the nest, and back again as defined in equation 3.30.

$$L_{Flight}=2\varphi d \tag{3.30}$$

Using equation 3.13 the flight energy is in equation 3.31.

$$E_{Flight}=L_{Flight}W_{nectar}^{Delivered} \tag{3.31}$$

Then re-expressed as nectar in equation 3.32 using equations 3.13 and 3.14.

$$W_{Nectar}^{Flight}=\frac{L_{Flight}W_{nectar}^{Delivered}}{C_{Nectar}L_{Sucrose}} \tag{3.32}$$

Total nectar needed is the sum of delivered and flight fuel in equation 3.33.

$$W_{Nectar}^{Collected}=W_{Nectar}^{Flight}+W_{Nectar}^{Delivered} \tag{3.33}$$

By combining equations 3.33 and 3.32 gives equation 3.34.

$$W_{Nectar}^{Collected}=W_{Nectar}^{Delivered}\left(1+\frac{L_{Flight}}{\left(C_{Nectar}L_{Sucrose}\right)}\right) \tag{3.34}$$

The ratios of the energies and the weights of quantities of the same substance are equal therefore from equation 3.34 we can derive equation 3.35.

$$\Gamma_{Transport}=\Gamma_{Collected}^{Delivered}=\Pi_{Collected,Nectar}^{Delivered,Nectar}=\frac{1}{\left(1+\frac{L_{Flight}}{\left(C_{Nectar}L_{Sucrose}\right)}\right)} \tag{3.35}$$

From equations 3.35, 3.28 and 3.13 we derive the nectar to honey ratio, the multiplying factor for collected nectar versus base honey weight (equation 3.36).

$$\Pi_{Base,Honey}^{Collected,Nectar}=\frac{C_{Honey}\,\zeta}{\Gamma_{Transport}} \tag{3.36}$$

3.4.6 Energy recovery ratio and dessication energy fraction

From equations 3.13 and 3.14 we can derive equation 3.37.

$$E_{Base}=W_{Sucrose}^{Base}L_{Sucrose} \tag{3.37}$$

Combining equations 3.14 and 3.29, we can derive equation *3.38*.

$$E_{Collected}=\frac{C_{nectar}\,L_{Sucrose}\,W_{Sucrose}^{Base}\,\zeta}{\Gamma_{Transport}} \tag{3.38}$$

Thus from equations 3.7, 3.37 and 3.38, energy recovery ratio is found in equation 3.39.

$$\Gamma_{Recovery}=\Gamma_{Collected}^{Base}=\frac{\Gamma_{Transport}}{C_{Nectar}\,\zeta} \tag{3.39}$$

Similarly dessication energy fraction (equation 3.40).

$$\Gamma_{Dessicate}=1-\Gamma_{Delivered}^{Base}=\frac{1}{C_{Nectar}\,\zeta} \tag{3.40}$$

3.4.7 Honey energy margin and break even distance

From the definition of HEM in equation (3.4) derive equation (3.41).

$$M=\frac{E_{Base}-\left(\tilde{E}_{evaporate}+E_{Flight}\right)}{\left(\tilde{E}_{evaporate}+E_{Flight}\right)} \tag{3.41}$$

Equation 3.41 is expanded from equations 3.30, 3.31, 3.25, and 3.37 to give equation 3.42.

$$M=\frac{L_{Sucrose}}{\frac{L_{Water}\,\xi}{\Gamma_{Thermal}}+2\,\varphi d\,\zeta}-1 \tag{3.42}$$

Rearranging equation 3.42, one obtains the distance at which $M=0$, i.e. the break even distance.

$$d_{BreakEven}=\frac{1}{2\varphi\zeta}\left(L_{Sucrose}-\frac{L_{Water}\,\xi}{\Gamma_{Thermal}}\right) \tag{3.43}$$

3.5 Results

3.5.1 General parameters

Table 3.2: General parameters needed in the analysis from sources.

Item	**Value**	**Source**
κ_{Air}	1.2 $kJK^{-1}kg^{-1}$	(Pitts and Sissom, 1998)
$L_{Sucrose}$	16.2$MJkg^{-1}$	(South African Sugar Technologists Association, 2009)
φ	162.5$Jkg^{-1}m^{-1}$	(Seeley, 1984)
$A_{Entranc}$	25×10^{-4} m^2	(Seeley, 1996)
C_{Honey}	0.8	(Seeley, 1984)
ρ_{Air}	1kgm^{-3}	(Pitts and Sissom, 1998)
$u_{Entranc}$	0.94ms^{-1}	(Peters et al., 2017)
L_{Water}	2.426$MJkg^{-1}$ @305K	(Incropera et al., 2005)

3.5.2 Estimated thermal efficiency

Using a rate of honey ripening $\dot{W}^{Base}_{Honey}$ of $5.3\times10^{-6}kgs^{-1}$ (Park, 1946) from equation (3.3), one can plot TEE contours versus nest conductance, temperature difference and nectar concentrations (figure 3.1). Note that negative temperature differences (ambient > nest) generate TEE greater than 1.

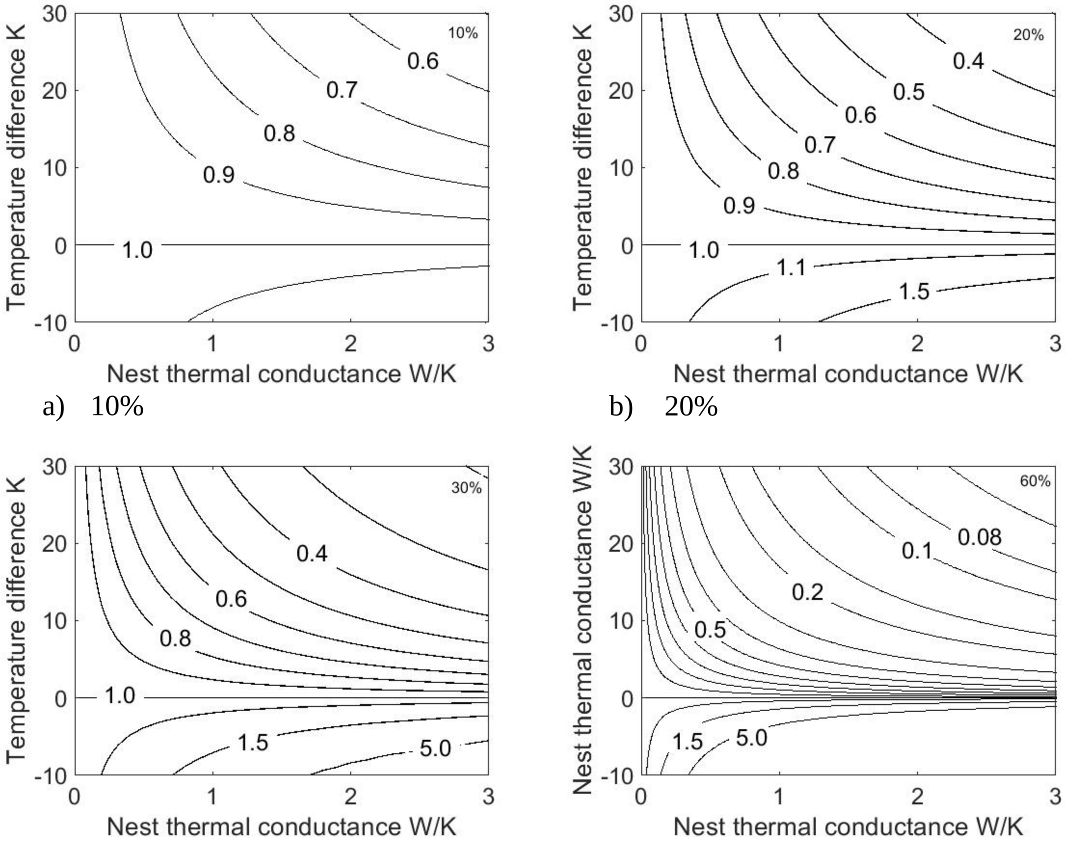

a) 10%

b) 20%

c) 30%

d) 60%

Figure 3.1: Thermal efficiency (TEE) contours versus nest conductance and internal to external temperature difference for various nectar concentrations (a-d).

3.5.3 Collected nectar to honey factor

From equation 3.36, one can produce a table of contour graphs at selected distances to the nectar source to produce contours of the factor versus thermal efficiency and nectar concentration in figure 3.2.

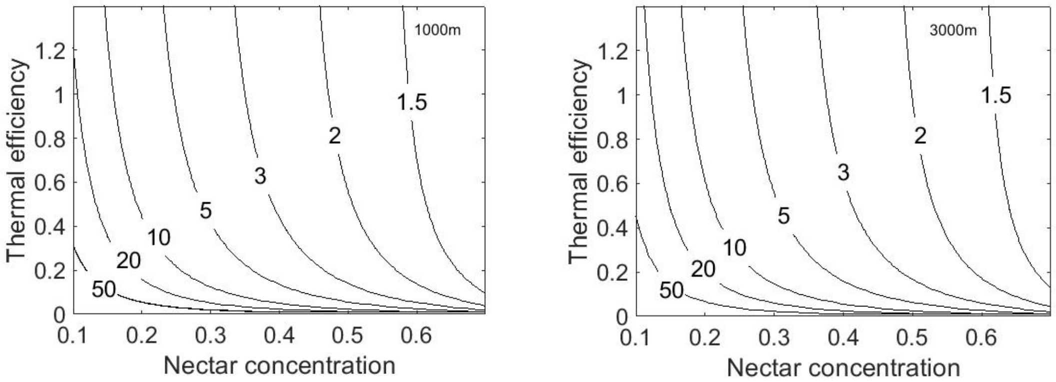

a) 1000m b) 3000m

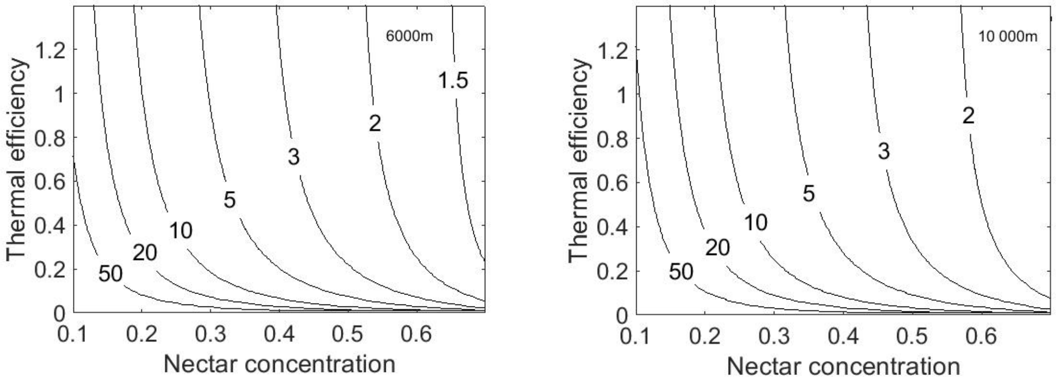

c) 6000m d) 10000m

Figure 3.2: Collected nectar to honey factor contours vs nectar concentration and thermal efficiency for various distances(a-d).

Note: Thermal efficiencies above 1 are included to allow for when temperatures outside greater than inside.

3.5.4 Energy recovery ratio

From equation(3.39) we can determine the energy recovery ratio of the process of fetching the honey and processing the nectar into honey. This is shown in contour graphs of for constant distance between nest and nectar source in figure 3.3.

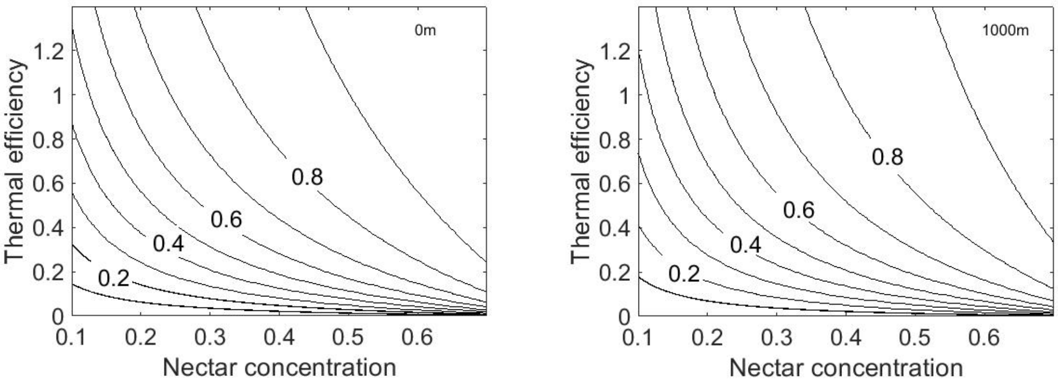

a) 0m　　b) 1000m

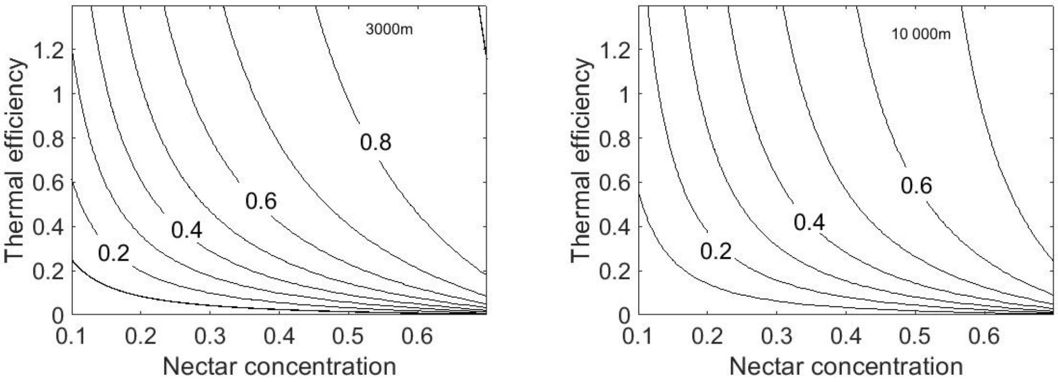

c) 3000m　　d) 10000m

Figure 3.3: Contours of energy recovery ratio vs nectar concentration and thermal efficiency.

3.5.5 Honey energy margin

From equation (3.42) one can plot contours of HEM in figure 3.4. Note this value is greater than zero when the energy is above break even.

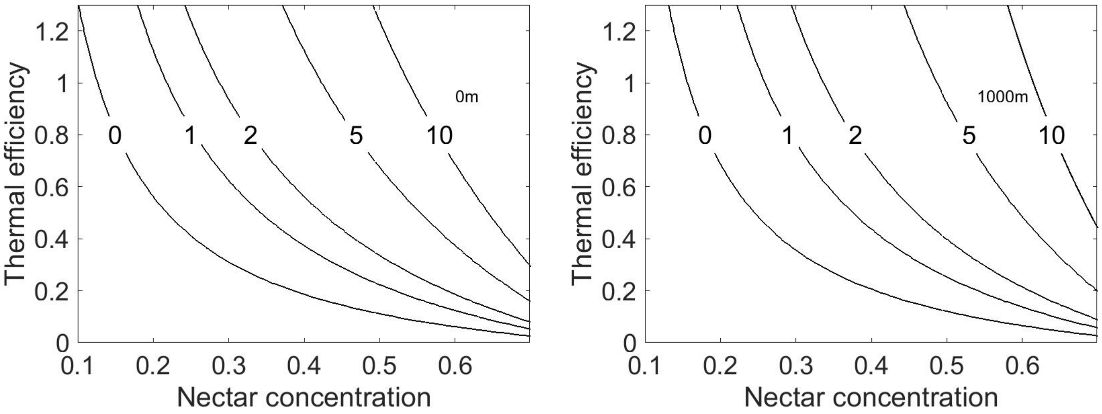

a) 0m

b) 1000m

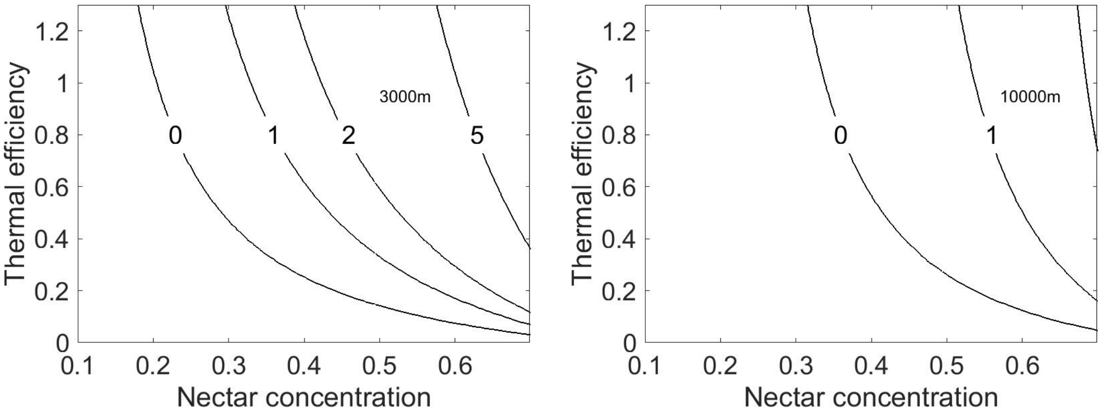

c) 3000m

d) 10000m

Figure 3.4: Honey energy margin contours vs nectar concentration and thermal efficiency at various distances to nectar (a-d).

3.5.6 Break even distance and dessication energy fraction

From equation 3.43, the break even point for foraging nectar for honey is shown in figure 3.5. Derived from equation 3.40, figure 3.6 gives the relative magnitude of the energy used in the process of honey ripening to that of energy delivered to the nest entrance.

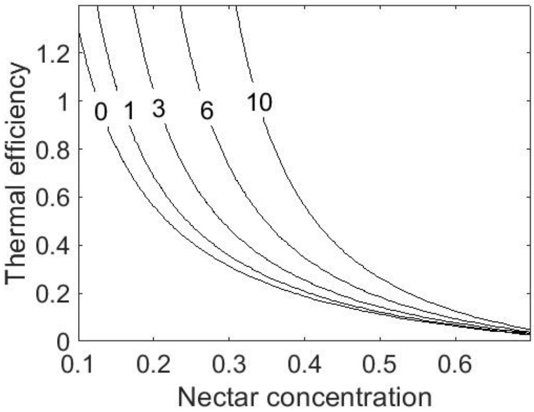

Figure 3.5: Contours of the Break even distance Km vs thermal efficiency and nectar concentration.

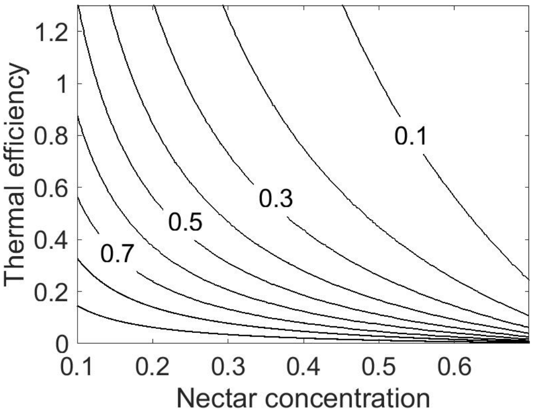

Figure 3.6: Contours of the fraction of delivered energy spent on nectar dessication vs thermal efficiency and nectar concentration.

3.5.7 Agreement with experimental data and observations

There are only isolated experimental data for the parameters that allow one to determine thermal efficiency i.e. honey ripening rate (Park, 1946) and the nest lumped conductance (Mitchell, 2016). The experimental lumped conductance values available do not take account of the contributions from nest internal structures, honey bee behaviours, seasonal variation or bee keepers adding boxes. However, there is sufficient data and dimensional parameters to determine valid ranges for these values. While it is clear that considerably more work is needed to add to the sparse data, there are experiments and data in the literature that are relevant to validating the model to some extent, as described in the following sections.

3.5.7.1 Higher ambient temperature allows lower viable nectar concentrations

One of the results of the model presented here is that higher ambient temperature with a constant honey ripening rate would give rise to a higher TEE. Consequently, the honey bees would be able to profitably forage on lower concentrations of nectar (provided the RH was not raised as well). One study (Bordier et al., 2017) has shown that by raising the external temperature of presumably a wooden hive in an internal apiary, the honey bees start collecting from lower nectar concentration flowers, yet collect the same amount of sucrose by increasing the total number of flights. Thus satisfying the models prediction.

3.5.7.2 Extreme range in unusual circumstances

Honeybee nectar foraging has been shown to extend beyond 9km (Beekman and Ratnieks, 2000) in infrequent, particular circumstances. The exceptional 9km foraging distance was recorded on a heather moor. Research has shown that, in the right circumstances, heather can yield up to 60% sugars (Enkegaard et al., 2016). This analysis shows the combination of 60% nectar concentration, a warm day of 25C and wooden hives of conductance 2.6WK^{-1} (Mitchell, 2016), would result in a TEE of 0.15 to 0.2 (figure 3.1). This TEE and nectar concentration would be within the break even distance even at 9km (figure 3.5) where 25% of energy is being used for nectar dessication (figure 3.6). However, it also shows that if the majority of the nectar sources are in the range of 20% to 30%, then we would expect most nectar foraging to be under 5km, which concurs with other studies in heather (Pierre et al., 1999; Danner et al., 2016) and those that include oil seed rape in Northern Europe.

3.5.7.3 Improvements in honey yield for insulated hives

In the models above, decreases in hive thermal conductance give rise to an improvement in thermal efficiency, which in turn gives rise to an improvement in HEM (figure 3.4), which allows more nectar to be desiccated to honey. Thus one would expect from the analysis that decreases in hive conductance improve honey yields. This has been shown to occur in practice, in both formal studies (Villumstad, 1974) and anecdotally, to give increases of up to 30% in yield (MacGregor, 2015). The latter were from expanded polystyrene hives. These have been measured at 1 WK^{-1} compared to 2.6 WK^{-1} for wooden hives and 0.4 WK^{-1} for tree nests (Mitchell, 2016). The graphs in figure 3.1 combined with the conductances from reference (Mitchell, 2016) show the improvement in thermal efficiency of expanded polystyrene hives compared to the common thin walled wooden hives.

3.5.7.4 Position of nectar deposition within the nest

As the temperature of the desiccating air is increased, its water carrying capacity (the mass of water/ unit mass of air at saturation) is increased (Lawrence, 2005). Thus less air needs to be moved to remove the same mass of liquid water. This temperature increase therefore improves TEE. If TEE was an evolutionary driver of honey bee behaviour, we may expect the nectar dessication process to take place in a part of the hive where it takes less energy to maintain a higher temperature. This is shown by honey bees preferentially depositing nectar in the upper portions of their nest i.e. above the brood nest (Johnson and Baker, 2007). The temperature stratification above the heat source (Mitchell, 2016) of the temperature controlled brood area, reduces the heat requirements and air movement energy for honey production. The insulating properties of empty comb (Humphrey and Dykes, 2008) enable losses to be reduced away from the walls of the nest which aligns with the observed behaviour of depositing nectar on combs not facing the outside walls (Johnson and Baker, 2007).

3.5.7.5 Seeking natural nests with low thermal conductance

The requirement to retain elevated temperatures, and hence reduced RH where the desiccation is taking place, shows an all year round advantage for nests with low thermal conductance. This would drive honey bees to seek out such nest sites i.e. tree hollows rather than ground crevices, with lower thermal conductance values (thick wooden walls, bottom entrances) (Seeley and Morse, 1976; Seeley and Morse, 1978) and modify, where possible, nest sites to further reduce the conductance value by for example closing up holes with propolis.

3.6 Discussion

3.6.1 Nectar dessication energy significance

In figure 3.6, at a TEE of 1.0, one can see that for a Northern European oil seed rape crop of 30% nectar sugars (Pierre et al., 1999), the nectar dessication process consumes

25% of the energy in the nectar delivered to the entrance. Similarly on clover with 20% (Wykes, 1953) sugars, it will consume 40% of the delivered energy.

At a TEE of 0.4, the situation is even more pronounced, dessication consumption rises to 40% and 60% for rape and clover respectively. Thus one can clearly see, that the process of nectar dessication into honey is a significant proportion of the energy collected, and that TEE, and consequently nest lumped thermal conductance are significant factors in the energy collection of *A. mellifera*.

3.6.2 Behaviour, lumped thermal conductance and TEE.

TEE as seen in equation 3.12 is a function of: honey ripening rate, which one expects honey bees to maximise; nectar concentration, which the honey bees try to maximise from what is available (Seeley, 1989; León et al., 2015); ambient temperature, which is out of the honey bees control, and finally the lumped thermal conductance. This is formed from a series network which includes the advective heat transfer of the internal air to the nest wall (equation 3.22). This is dependant on the air flow across the internal and external surfaces (equation 3.23) and therefore on the behaviours of the honey bee colony, and consequently so is the TEE. Armed with this knowledge, researchers can now interpret and quantify the benefit or otherwise of the details of fanning behaviour internal to the nest in conjunction with external factors, such as temperature and available nectar. For example, if behaviours were found that directed the air heated by honey bees, so that it is kept away from the walls of the nest until after it was laden with water vapour, this would dramatically reduce the lumped conductance and increase TEE.

3.6.3 Extended distance and variety

From inspection of figure 3.5, it is evident that an increase in TEE from perhaps an increase in the ambient temperature or a behaviourally lowered lumped nest conductance, allows the honey bees to profitably retrieve nectar and refine to honey from either a weaker nectar source or from a greater distance. For example: at a concentration of 30% (0.3), an increase in TEE of 0.4 to 0.6 increases the break even range from 1Km to 5Km. Similarly, at a range of 1Km, an increase in TEE from 0.3 to 0.6 enables a decrease in sugar concentration from 32% to 20% to be equally profitable in honey. A colony that collects nectar at distances, concentrations and TEE outside the break even line will not add to its honey reserves and risks extinction e.g. collecting 25% concentration at TEE of 0.5 at distance of 5Km.

3.6.4 Improved TEE reduces wing wear

Efficient usage of the limited wing lifetime of honey bees has been shown to be an important factor in colony success (Higginson and Gilbert, 2004; Higginson and Barnard, 2004; Higginson et al., 2011). This analysis has shown (figure 3.2), for the same amount of honey, improvements in TEE require less nectar and hence less foraging flights resulting in less flight wing beats and consequently less wing wear.

Further, improved efficiency in evaporation reduces the total amount of water that needs to be both evaporated and moved by fanning and hence reduces the wing beats and the wing damage that occurs from fanning activity (Peters et al., 2017).

3.6.5 Decreased thermal conductance increased profitability

Improved TEE results results in more energy being stored as honey, for a given colony size and forage area, which not only improves the chances of survival, but it can also improve the revenue for commercial honey bee farmers. This analysis points the way for bee farmers to increase yield and revenue by working synergistically with their honey bees to improve thermal efficiency by changing their hives to ones which lose less heat, and facilitating honey bee behaviours that have the same goal e.g. bottom entrances.

3.7 Conclusions

Honey bees are bound by the physics of water evaporation. In exploring the physics we can see that nectar dessication is a substantial part of the work done inside a honey bee nest even in the most favourable circumstances. The relations uncovered in this research have quantified those boundaries and have been validated by experimental work, but only as far as the current very sparse data allows. The magnitude of the energies devoted to nectar dessication show this area is worthy of more experimental research and detailed analysis.

The relations found show that:

- Dessication of honey takes a significant percentage of the energy delivered to the hive in the form of nectar for *A.mellifera*, particularly in the northern part of their range where nectar is lower in concentration. Typical values show that over 50% of the delivered energy may be used in the process of honey ripening and even in exceptionally favourable circumstances for temperate climates, do not use less than 25%.
- The relative magnitude of the energies involved and the ratios of nectar to honey show that thermal energy efficiency of nectar dessication should be considered as a key factor in the development and success or otherwise of honey bees in temperate climates where nectar sources are widely dispersed and of lower concentration.
- The lumped thermal conductance of hives, previously thought to be only a consideration for winter, has been shown to be a major factor during the nectar collecting periods of the year and is dependent on honey bee behaviour.
- The energy consumption of nectar dessication and hence TEE, limits the maximum foraging distance of honey bees. It also changes the energy return for a given nectar source and as a consequence which nectar sources are viable for the honey bee.

This appreciation of the importance of TEE improves our understanding of why honey bees moved into tree cavities and provides background into why they have developed their behaviours. It provides a new avenue for the research of honey bee behaviours and a firm theoretical foundation for improving the survival of colonies in the face of climate change. And improving the honey yield for bee keepers by reducing hive thermal conductances to be closer to those found in tree nests. Further work is required to investigate how honey bees interact with the bounds described by the models and expanding their scope to take account of the 3 dimensional heat and air flows within the nest.

3.8 References

Adgaba, N., Al-Ghamdi, A., Tadesse, Y., Getachew, A., Awad, A.M., Ansari, M.J., Owayss, A.A., Mohammed, S.E.A. and Alqarni, A.S. 2017. Nectar secretion dynamics and honey production potentials of some major honey plants in Saudi Arabia. *Saudi Journal of Biological Sciences*. **24**(1), pp.180–191.

Alqarni, A.S. 2015. Honeybee Foraging, Nectar Secretion, and Honey Potential of Wild Jujube Trees, Ziziphus nummularia. *Neotropical Entomology*. **44**(3), pp.232–241.

Barron, A. 2006. Visual regulation of ground speed and headwind compensation in freely flying honey bees (Apis mellifera L.). *Journal of Experimental Biology*. **209**(5), pp.978–984.

Baveco, J.M., Focks, A., Belgers, D., van der Steen, J.J.M., Boesten, J.J.T.I. and Roessink, I. 2016. An energetics-based honeybee nectar-foraging model used to assess the potential for landscape-level pesticide exposure dilution. *PeerJ*. **4**, p.e2293.

Becher, M.A., Grimm, V., Thorbek, P., Horn, J., Kennedy, P.J. and Osborne, J.L. 2014. BEEHAVE: A systems model of honeybee colony dynamics and foraging to explore multifactorial causes of colony failure. *Journal of Applied Ecology*. **51**(2), pp.470–482.

Becher, M.A., Osborne, J.L., Thorbek, P., Kennedy, P.J. and Grimm, V. 2013. Towards a systems approach for understanding honeybee decline: A stocktaking and synthesis of existing models. *Journal of Applied Ecology*. **50**(4), pp.868–880.

Beekman, M. and Lew, J. Bin 2008. Foraging in honeybees - When does it pay to dance? *Behavioral Ecology*. **19**(2), pp.255–262.

Beekman, M. and Ratnieks, F.L.W. 2000. Long-range foraging by the honey-bee, Apis melliera L. M. *Functional Ecology*. **14**(6), pp.490–496.

Bejan, A. 2004. *Convection Heat Transfer* 3rd ed. John Wiley and sons.

Betti, M., LeClair, J., Wahl, L.M. and Zamir, M. 2017. Bee++: An object-oriented, agent-based simulator for honey bee colonies. *Insects*. **8**(1), pp.20–23.

Betti, M.I., Wahl, L.M. and Zamir, M. 2017. Reproduction Number and Asymptotic Stability for the Dynamics of a Honey Bee Colony with Continuous Age Structure. *Bulletin of Mathematical Biology*. **79**(7), pp.1586–1611.

Bordier, C., Dechatre, H., Suchail, S., Peruzzi, M., Soubeyrand, S., Pioz, M., Pélissier, M., Crauser, Di., Conte, Y. Le and Alaux, C. 2017. Colony adaptive response to simulated heat waves and consequences at the individual level in honeybees (Apis mellifera). *Scientific Reports*. **7**(1), pp.1–11.

Cresswell, J.E., Osborne, J.L. and Goulson, D. 2000. An economic model of the limits to foraging range in the central-place foraging with numerical solutions for bumblebees. *Ecological Entomology*. **25**, pp.249–255.

Danner, N., Molitor, A.M., Schiele, S., Härtel, S. and Steffan-Dewenter, I. 2016. Season and landscape composition affect pollen foraging distances and habitat use of Honey bees. *Ecological Applications*. **26**(6), pp.1920–1929.

DeGrandi-Hoffman, G., Roth, S.A., Loper, G.L. and Erickson Jr., E.H. 1989. BEEPOP: A honeybee population dynamics simulation model. *Ecological Modelling*. **45**(2), pp.133–150.

Enkegaard, A., Kryger, P. and Boelt, B. 2016. Determinants of nectar production in heather. *Journal of Apicultural Research*. **8839**, pp.1–7.

Eyer, M., Neumann, P. and Dietemann, V. 2016. A Look into the Cell: Honey Storage in Honey Bees, Apis mellifera. *Plos One*. **11**(8), p.e0161059.

Germ, M., Stabentheiner, A. and Kastberger, G. 1997. Seasonal and daily variation of honeybee dancing temperature under constant feeding conditions. *Apidologie*. **28**(6), pp.385–398.

Goldberg, R.N., Tewari, Y.B. and Ahluwalia, J.C. 1989. Thermodynamics of the hydrolysis of sucrose. *Journal of Biological Chemistry*. **264**(17), pp.9901–9904.

Henry, M., Becher, M.A., Osborne, J.L., Kennedy, P.J., Aupinel, P., Bretagnolle, V., Brun, F., Grimm, V., Horn, J. and Requier, F. 2017. Predictive systems models can help elucidate bee declines driven by multiple combined stressors. *Apidologie*. **48**(3), pp.328–339.

Heyd, R., Rampino, A., Bellich, B., Elisei, E., Cesàro, A. and Saboungi, M.L. 2014. Isothermal dehydration of thin films of water and sugar solutions. *Journal of Chemical Physics*. **140**(12).

Higginson, A.D. and Barnard, C.J. 2004. Accumulating wing damage affects foraging decisions in honeybees (Apis mellifera L.). *Ecological Entomology*. **29**(1), pp.52–59.

Higginson, A.D., Barnard, C.J., Tofilski, A., Medina, L. and Ratnieks, F. 2011. Experimental wing damage affects foraging effort and foraging distance in honeybees Apis mellifera. *Psyche*. **2011**.

Higginson, A.D. and Gilbert, F. 2004. Paying for nectar with wingbeats: a new model of honeybee foraging. *Proceedings of the Royal Society B: Biological Sciences*. **271**(1557), pp.2595–2603.

Humphrey, J.A.C. and Dykes, E.S. 2008. Thermal energy conduction in a honey bee comb due to cell-heating bees. *Journal of Theoretical Biology*. **250**(1), pp.194–208.

Incropera, F.P., Dewitt, D.P., Bergman, T.L. and Lavine, A.S. 2005. Thermophysical properties of matter *In*: *Fundamentals of Heat and MassTransfer*. John Wiley and sons, pp.927–957.

Ion, N., Tefan, V.Ş., Ion, V., Fota, G. and Coman, R. 2006. Results concerning the melliferous characteristics of the sunflower hybrids cultivated in Romania. . **40**(figure 3), pp.1–9.

Johnson, B.R. and Baker, N. 2007. Adaptive spatial biases in nectar deposition in the nests of honey bees. *Insectes Sociaux*. **54**(4), pp.351–355.

Kovac, H., Stabentheiner, A. and Schmaranzer, S. 2010. Thermoregulation of water foraging honeybees-Balancing of endothermic activity with radiative heat gain and functional requirements. *Journal of Insect Physiology*. **56**(12), pp.1834–1845.

Kühnholz, S., Seeley, T.D., Kuhnholz, S. and Seeley, T.D. 1997. The control of water collection in honey bee colonies. *Behavioral Ecology and Sociobiology*. **41**(6), pp.407–422.

Lawrence, M.G. 2005. The relationship between relative humidity and the dewpoint temperature in moist air: A simple conversion and applications. *Bulletin of the American Meteorological Society*. **86**(2), pp.225–233.

León, A., Arias-Castro, C., Rodríguez-Mendiola, M.A., Meza-Gordillo, R., Gutiérrez-Miceli, F.A. and Nieh, J.C. 2015. Colony foraging allocation is finely tuned to food distance and sweetness even close to a bee colony. *Entomologia Experimentalis et Applicata*. **155**(1), pp.47–53.

Lindauer, M. 1955. The Water Economy and Temperature Regulation of the Honeybee Colony. *Bee World*. **36**(5), pp.81–92.

MacGregor, M. 2015. Online Conversation.

Mitchell, D. 2016. Ratios of colony mass to thermal conductance of tree and man-made nest enclosures of Apis mellifera: implications for survival, clustering, humidity regulation and Varroa destructor. *International Journal of Biometeorology*. **60**(5), pp.629–638.

Naug, D. 2014a. Infected honeybee foragers incur a higher loss in efficiency than in the rate of energetic gain. *Biology Letters*. **10**(11).

Naug, D. 2014b. Infected honeybee foragers incur a higher loss in efficiency than in the rate of energetic gain. *Biology Letters*. **10**(11).

Nedić, N., Mačukanović-Jocić, M., Rančić, D., Rørslett, B., Šoštarić, I., Stevanović, Z.D. and Mladenović, M. 2013. Melliferous potential of Brassica napus L. subsp. napus (Cruciferae). *Arthropod-Plant Interactions*. **7**(3), pp.323–333.

Nicolson, S.W. 2009. Water homeostasis in bees, with the emphasis on sociality. *The Journal of experimental biology*. **212**(Pt 3), pp.429–434.

Nicolson, S.W. and Human, H. 2008. Bees get a head start on honey production. *Biology letters*. **4**(3), pp.299–301.

Ocko, S. a and Mahadevan, L. 2014. Collective thermoregulation in bee clusters. *Journal of the Royal Society, Interface / the Royal Society*. **11**(91), p.20131033.

Ocko, S.A. and Mahadevan, L. 2013. Bees work together to keep cluster cool. . (December).

Ostwald, M.M., Smith, M.L. and Seeley, T.D. 2016. The behavioral regulation of thirst, water collection and water storage in honey bee colonies. *The Journal of Experimental Biology*. **219**(14), pp.2156–2165.

Park, O.W. 1946. Activities of Honeybees *In*: R. Grout, ed. *The Hive and the Honey bee*. Chicago: Dadant & Sons, pp.125–205.

Park, O.W. 1932. Studies on the changes in nectar concentration produced by the honeybee, Apis mellifera. Part I. Changes which occur between the flower and the hive. *Iowa Agriculture and Home Economics Experiment Station Research Bulletin*. **151**(151), pp.211–243.

Park, O.W. 1925. The Storing and Ripening of Honey by Honey Bees. *Journal of Economic Entomology*. **18**, pp.405–410.

Peters, J.M., Gravish, N. and Combes, S.A. 2017. Wings as impellers: honey bees co-opt flight system to induce nest ventilation and disperse pheromones. *The Journal of Experimental Biology*. **220**(12), pp.2203–2209.

Pierre, J., Mesquida, J., Marilleau, R., Pham-Delègue, M.H. and Renard, M. 1999. Nectar secretion in winter oilseed rape, Brassica napus quantitative and qualitative variability among 60 genotypes. *Plant Breeding*. **118**, pp.471–476.

Pitts, D.R. and Sissom, L.E. 1998. *Theory and Problems of Heat Transfer - Schaum's Outline*.

Russell, S., Barron, A.B. and Harris, D. 2013. Dynamic modelling of honey bee (Apis mellifera) colony growth and failure. *Ecological Modelling*. **265**, pp.158–169.

Schmickl, T. and Crailsheim, K. 2004. Costs of environmental fluctuations an benefits of dynamic foraging decisions in honey bees. *Adapitve Behavior*. **12**, pp.263–277.

Schmickl, T. and Crailsheim, K. 2007. HoPoMo: A model of honeybee intracolonial population dynamics and resource management. *Ecological Modelling*. **204**(1–2), pp.219–245.

Schmickl, T. and Karsai, I. 2016. How regulation based on a common stomach leads to economic optimization of honeybee foraging. *Journal of Theoretical Biology*. **389**, pp.274–286.

Schmickl, T. and Karsai, I. 2017. *Resilience of honeybee colonies via common stomach: A model of self-regulation of foraging*.

Schmid-Hempel, P. 1987. Efficient Nectar-Collecting by Honeybees I. Economic Models. *Journal of Animal Ecology*. **56**(1), pp.209–218.

Schmid-Hempel, P., Kacelnik, A. and Houston, A.I. 1985. Honeybees Maximize Efficiency by Not Filling Their Crop. *Behavioral Ecology and Sociobiology*. **17**(1), pp.61–66.

Schürch, R. and Gruïer, C. 2014. Dancing bees improve colony foraging success as long-term benefits outweigh short-term costs. *PLoS ONE*. **9**(8).

Seeley, T.D. 2010. *Honeybee Democracy*. Princeton University Press.

Seeley, T.D. 1984. *Honeybee Ecology*. Princeton University Press.

Seeley, T.D. 1989. Social Foraging in Honey Bees : How Nectar Foragers Assess Their Colony ' s Nutritional Status. *Behavioral Ecology and Sociobiology*. **24**(3), pp.181–199.

Seeley, T.D. 1996. *The Wisdom of the Hive: The Social Physiology of Honey Bee Colonies*. Cambridge, MA: Harvard University Press.

Seeley, T.D. and Morse, R.A. 1978. Nest site selection by the honey bee,Apis mellifera. *Insectes Sociaux*. **25**(4), pp.323–337.

Seeley, T.D. and Morse, R.A. 1976. The nest of the honey bee (Apis mellifera L.). *Insectes Sociaux*. **23**(4), pp.495–512.

Shackleton, K., Balfour, N.J., Al Toufailia, H., Gaioski, R., de Matos Barbosa, M., Silva, C.A. de S., Bento, J.M.S., Alves, D.A. and Ratnieks, F.L.W. 2016. Quality versus quantity: Foraging decisions in the honeybee (Apis mellifera scutellata) feeding on wildflower nectar and fruit juice. *Ecology and Evolution*. **6**(19), pp.7156–7165.

Simone-Finstrom, M., Foo, B., Tarpy, D.R. and Starks, P.T. 2014. Impact of Food Availability, Pathogen Exposure, and Genetic Diversity on Thermoregulation in Honey Bees (Apis mellifera). *Journal of Insect Behavior*. **27**, pp.527–539.

South African Sugar Technologists Association 2009. Method 2 . 3 – Bagasse : calorific value *In*: *SASTA Laboratory Manual*. Natal: South African Sugar Technologists Association, pp.2–5.

Southwick, E.E. and Moritz, R.F.A. 1987. Social control of air ventilation in colonies of honey bees, Apis mellifera. *Journal of Insect Physiology*. **33**(9), pp.623–626.

Southwick, E.E. and Pimentel, D. 1981. Energy Efficiency of Honey Production by Bees. *BioScience*. **31**(10), pp.730–732.

Stabentheiner, A. and Kovac, H. 2014. Energetic optimisation of foraging honeybees: Flexible change of strategies in response to environmental challenges. *PLoS ONE*. **9**(8).

Stabentheiner, A. and Kovac, H. 2016. Honeybee economics: Optimisation of foraging in a variable world. *Scientific Reports*. **6**(June), pp.1–7.

Torres, D.J., Ricoy, U.M. and Roybal, S. 2015. Modeling Honey Bee Populations. *PLoS ONE*. **10**(7).

Villumstad, E. 1974. Importance of hive insulation for wintering , development and honey Yield in Norway. *Apiacta*. **3**.

De Vries, H. and Biesmeijer, J.C. 2002. Self-organization in collective honeybee foraging: Emergence of symmetry breaking, cross inhibition and equal harvest-rate distribution. *Behavioral Ecology and Sociobiology*. **51**(6), pp.557–569.

Wolf, Th.J., Schmid-Hempel, P., Ellington, C.P. and Stevenson, R.D. 1989. Physiological Correlates of Foraging Efforts in Honey-Bees: Oxygen Consumption and Nectar Load. *Functional Ecology*. **3**(4), p.417.

Woods, W.A., Heinrich, B. and Stevenson, R.D. 2005. Honeybee flight metabolic rate: does it depend upon air temperature? *Journal of Experimental Biology*. **208**(6), pp.1161–1173.

Wykes, G.R. 1953. The Sugar Content of Nectars. *The Biochemical Journal*. **53**(2), pp.294–296.

Chapter 4 Nectar, humidity, honey bees (*Apis mellifera*) and varroa in summer

This chapter is based upon the authors published work:

Nectar, humidity, honey bees (Apis mellifera) and varroa in summer: A theoretical thermofluid analysis of the fate of water vapour from honey ripening and its implications on the control of Varroa destructor. Journal of the Royal Society Interface. ***16****(156).*

4.1 Abstract

This theoretical thermofluid analysis investigates the relationships between: honey production rate, nectar concentration, and the parameters of: entrance size, nest thermal conductance, brood nest humidity and the temperatures needed for nectar to honey conversion. It quantifies and shows that nest humidity is positively related to the amount, and water content of the nectar being desiccated into honey and negatively with respect to nest thermal conductance and entrance size. It is highly likely that honey bees, in temperate climates and in their natural home, with much smaller thermal conductance and entrance, can achieve higher humidities more easily and more frequently than in man-made hives. As a consequence it is possible that *Varroa destructor*, a parasite implicated in the spread of pathogenic viruses and colony collapse, which loses fecundity at absolute humidities of 4.3 kPa (~30 gm^{-3}) and above, is impacted by the more frequent occurrence of higher humidities in these low conductance, small entrance nests. This study provides the theoretical basis for new avenues of research into the control of varroa, via the modification of bee keeping practices to help maintain higher hive humidities.

Table 4.1: Chapter nomenclature.

Term	Value	Description	Units
A		Factor of coefficient α – vapour fraction of water content of nectar made into honey	-
B_0		Factor of coefficient β 0 - vapour fraction of water content of nectar used as fuel for nectar evaporation	-

Term	Value	Description	Units
B_1		Factor of coefficient β 1 - vapour fraction of water from oxidation of nectar used as fuel for nectar evaporation	-
$A_{Entrance}$		Cross sectional area of entrance	m^2
C_{Nectar}		Concentration of nectar	$kgkg^{-1}$
C_{Honey}	0.8	Typical concentration of sugars in honey (Seeley, 1985)	$kgkg^{-1}$
d_0	0.2	Diameter of tree cavity (Seeley and Morse, 1976)	m
d_1	0.5	External diameter of tree (Seeley and Morse, 1976)	m
$\dot{L}_{meta}$	10	Background colony metabolic rate (Southwick, 1982)	Wkg^{-1}
h_{Tree}	1.4	Height of tree cavity (Seeley and Morse, 1976)	m
h_{Hive}	0.825	Internal vertical dimension of hive with 4 shallows and one deep.(Cushman, 2011)	m
$L_{Sucrose}$	15.1	Latent heat of combustion of sucrose (lower heating value, water remains vapour).(South African Sugar Technologists Association, 2009)	$MJkg^{-1}$
L_{Water}	2.43	Latent heat of water vapourisation at 305K (32.8C). (Incropera et al., 2005)	$MJkg^{-1}$
r	58	Weight of metabolic water released per kilo of sucrose metabolised.	$kgkg^{-1}$
T_{Brood}	307.66	Brood temperature (Ellis et al., 2008)	K
T_D		Dew point temperature	K
T_i		Temperature instance i	K
T_{Out}	295.66	Temperature outside – For ZDUPSA average Pretoria spring summer (November – February) temperatures (Thorsen, 2018)	K
u_{Ent}		Air velocity through entrance	ms^{-1}
u_{EntMax}	0.94	Maximum entrance air velocity (Peters et al., 2017) due to fanning	ms^{-1}
$W_{Sucrose}^{Base}$		Weight of sucrose in resultant honey	kg
W_{Colony}	2	Background colony population those not involved in foraging or evaporations~20,000 honey bees (Seeley, 1985)	kg
$W_{Nectar}^{Delivered}$		Weight of nectar delivered to nest	kg
$W_{Nectar}^{Evaporate}$		Weight of nectar required as fuel for the evaporation of nectar	kg
$\dot{W}_{Water}^{Evaporate}$		Rate of water evaporated in honey ripening	kgs^{-1}

Term	**Value**	**Description**	**Units**
$\dot{W}_{Nest}^{Nectar}$		Rate of nectar consumption from other processes than honey evaporation	kgs^{-1}
$\dot{W}_{Honey}^{Base}$		Rate of honey ripening in terms of resultant honey	kgs^{-1}
$\dot{W}_{Vapour}^{Total}$		Rate of water vapour production from all sources inside the nest	kgs^{-1}
$\hat{\dot{W}}_{Vapour}^{Total}$		Rate of water vapour removal by all methods inside the nest	kgs^{-1}
x_0	0.440	Internal horizontal dimension of hive (Cushman, 2011)	m
x_1	0.478	External horizontal dimension of hive (Cushman, 2011)	m
α	1	Proportion of evaporate water emitted as vapour while in the nest	-
β_0	1	Proportion of water content of nectar consumed emitted as vapour while in the nest	-
β_1	1	Proportion of sugar content of nectar consumed emitted as vapour while in the nest	-
$\Gamma_{Thermal}$		TEE thermal efficiency of desiccation	-
ξ		Reciprocal concentration of honey subtract from reciprocal concentration of nectar	-
ρ_i		Density of water vapour in instance i	kgm^{-3}
ρ_{Inlet}		Density of water vapour entering entrance	kgm^{-3}
$\rho_{Exhaust}$		Density of water vapour exiting entrance	kgm^{-3}
Λ_{Evap}		Thermal conductance of the nest enclosure e.g. hive, tree etc. for evaporation processes	WK^{-1}
Λ_{Con}		Thermal conductance of the nest enclosure e.g. hive, tree etc..for condensation processes	WK^{-1}
λ_{Tree}	0.2	Thermal conductivity of tree wood (Mitchell, 2016)	$Wm^{-1}K^{-1}$
λ_{Hive}	0.12	Thermal conductivity of hive wood (Mitchell, 2016)	$Wm^{-1}K^{-1}$
χ_i		Relative humidity instance	-
χ_{Brood}		Relative humidity inside the brood zone	-
χ_{Out}	0.6	Outside relative humidity For ZDUPSA Pretoria summer spring relative humidity (Thorsen, 2018)	-
χ_{Honey}		Typical water activity of honey i.e. RH	-
θ_i		Water vapour pressure derived parameter	Pa
γ_i		RH derived dimensionless parameter	-
δ_i		Temperature derived dimensionless parameter	-

4.2 Introduction

The phenotype, the physical reflection of the gene, cannot be limited to purely the biological aspects of the organism itself because it directly causes change to the environment around it (Walsh, 2015), in accordance with the laws of thermodynamics and mass and energy conservation. For most organisms the realm of their influence extends only a very small distance from the biological tissue of the animal. However for those in which this goes beyond the usual, and their reach into the environment is significant, then it is termed an “extended phenotype”. The classic case cited is of beavers flooding areas with their dams (Dawkins, 1982). For honey bee colonies, perhaps because of the relationship with man, the extended nature of this super organism’s (Southwick, 1983) phenotype has been overlooked, and viewed as a simple shelter and container of honey and brood. In contrast to the beaver’s dam, which constrains a single visible fluid, some of the fluids involved in a honey bee colony’s nest: air, water vapour, water liquid and carbon dioxide are invisible to human eyes. These fluids are not passively restrained, but actively moved and changed in temperature and physical state within this extended phenotype. In addition: heat flux through the nest walls and entrance (Mitchell, 2016); condensation and evaporation of water; and desiccation of nectar into honey, literally sugar refining, some of which is metabolised/“burnt” (Seeley, 1985). Thermofluids is defined as the study of fluid flows, heat transfer including phase changes and the combustion of fluids (Massoud, 2005). Therefore, comprehensive analytical study of a honey bee’s extended phenotype must include analysis based on thermofluids and apply its relevant tools. That these are more commonly used to analyse sugar refineries, buildings or nuclear power plants should not be seen as a barrier (Walsh, 2015).

Research into honey bees is almost exclusively executed in man-made hives, and with only two exceptions (Villumstad, 1974; Mitchell, 2016), without any measurement of the hives physical characteristics. Unsurprisingly, there is very little quantitative research or analysis (Mitchell, 2016; Mitchell, 2019) into their thermofluid properties. It is from this low level that this analysis endeavours to understand the interplay of some of the thermofluid processes.

It is important to note that in this document the unqualified term, humidity, will be only used to refer to the absolute humidity expressed as the vapour pressure in kPa or as a tuple of the saturation ratio χ, and the absolute temperature T denoted as $\{\chi, T\}$. Thus the humidity of 80% saturation at 34 ^{o}C is shown as 4.3 kPa and/or {0.8, 307.2 K} from equation (4.3). The saturation ratio, (relative humidity), will be clearly denoted if used. The dew point temperature is the temperature TD, for that humidity, where the air is at complete saturation i.e. {1.0, TD}. Thus, because {0.8, 307.2 K} equals 4.3 kPa which equals {1.0, 303.2 K}, then one can say the dew point temperature of {0.8, 307.2 K} is 303.2 K.

Honey, a high sugar concentration (>0.8) fluid, is made by honey bees from flower nectar, a lower sugar concentration liquid (0.1 - 0.5), collected from numerous flowers, sometimes at considerable distance from the nest (up to 9 km) (Beekman and Ratnieks, 2000). This nectar is passed by the forager honey bee to another (Park, 1946) honey bee (unloader /storer), which then starts the desiccation process by selectively heating and aerating the nectar with their mouth parts, while placing it in a honey comb cell. This partially desiccated nectar is then exposed to low humidity air (Martin, 1958), while the hive population engages in vigorous forced air movement within the nest by fanning their wings (Park, 1925; Park, 1946; Eyer et al., 2016). This very energy intensive (Mitchell, 2019) process of nectar to honey conversion is placed above the brood nest in order to have less than 0.62 relative humidity (RH). After the desiccation process is completed, the cell may be capped with wax to prevent the reabsorption of water vapour. This RH value χ_{Honey}, when honey is in equilibrium with the vapour in the air, is termed the water activity of honey (Martin, 1958). It has been shown to range from 0.5 to 0.7 and has a linear relationship with the water content of the honey, equation(4.1) (Pérez et al., 2009) (See table 4.1 for term definitions and values).

$$\chi_{Honey} = 0.2686 + 1.756\left(1 - C_{Honey}\right) \qquad (4.1)$$

There are differences between subspecies as to when they begin the desiccation process, *A. m. scutellata* in dry hot climates, has been observed to reduce the water content by 50% in flight (Nicolson and Human, 2008), where as *A.m. mellifera* and *A.m ligustica* in cooler climates do not (Park, 1946).

In a nest with a single opening, all fluids from nectar desiccation and other processes must permeate through the walls or pass through the entrance. Water vapour and carbon dioxide can be removed by honey bees fanning at the entrance (Seeley, 1985), achieving a maximum entrance air velocity of approximately $1ms^{-1}$ (Southwick and Moritz, 1987; Peters et al., 2017). While bee keepers often, in addition to a mesh floor, provision multiple entrances in summer totalling over 80 cm^2 (Cushman, 2011); honey bee swarms prefer nests with single entrances of $12cm^2$ or smaller (Seeley, 1985). However, water vapour converts back to a liquid by condensation, a process which needs energy to be removed from the water vapour laden air. The principle of conservation of energy means that the rate of condensation is dependant on the lumped conductance of the nest walls, and the temperature difference between the dew point temperature of the humidity on the inside surface in the condensing zones and the outside air.

Values for the nest lumped conductance in a winter configuration have been experimentally measured (Mitchell, 2016) and represent a realistic estimate of the lower end of nest conductance. A realistic upper limit for nest conductance can be found analytically using standard shape factors (Incropera et al., 2007).

The permeability of the honey bee applied propolis lining (plant resins) is of the order of 10-13 $kgm^{-1}s^{-1}Pa^{-1}$ (Hagenmaier and Shaw, 1992). This results in a flow rate of the order of 2 mgs^{-1} at a water vapour pressure differential of 5 kPa and thickness of 0.25 mm. This is insignificant compared to water removal rates up to 100 mgs^{-1} for condensation and advection.

Research into the humidity relations of *A. mellifera*, while less extensive than for temperature, has found that honey bee eggs require 5.1 kPa {0.9, 308.2K} for development (Doull, 1976) and larvae require greater than 4.1kPa {0.75, 307.7 K} (Schmehl et al., 2016). The particularly high humidity for honey bee egg hatching should be taken in context that the eggs are laid at the far end of the cells, a microclimate separated from the general nest environment (Polat and Bilgen, 2002; Humphrey and Dykes, 2008). However fully grown larvae, which may then be infested with varroa, have conditions approaching that of the general nest environment.

Researchers have shown varroa fecundity falls significantly at humidities close to 4.3 kPa i.e. (Kraus and Velthuis, 1997) 4.3 kPa {0.8 307.2 K}, (Huang, 2012) 4.2 kPa

{0.75, 308.2 K}, (Le Conte et al., 1990) 4.3 kPa {0.7, 309.7 K}, (Egekwu et al., 2018) 4.2 kPa {0.872, 305.6 K}. Despite this, varroa has spread to honey bee colonies in a wide range of climates.

Condensate collection inside the hive or water disposal in the liquid phase by *A. mellifera* are not addressed in the literature. This absence has been noted by others (Ostwald et al., 2016).

The most recent and comprehensive studies into honey bee nest humidity have been undertaken by the Zoology department of the University of Pretoria in South Africa (ZDUPSA), and in a body of work related to humidity for *A.m. scutellata* have covered: the effects of external weather, winter clustering, differing nest types, hygropreference and honey bee fanning behaviour (Human et al., 2006; Ellis et al., 2008; Nicolson and Human, 2008; Ellis, 2008; Nicolson, 2009). This analysis, inspired by their work, seeks to provide the thermofluid theory to both explain and extend it, while using their climate and fanning data for input, and their results for experimental validation where possible.

4.3 Approach

This analysis will use a steady state, simple zoned temperature model of the nest cavity with a single bottom entrance, all at the same constant humidity, but at different average temperatures and consequently different average relative humidities consisting of :

- A honey/nectar zone below 0.6 RH at a temperature above 307.7 K (Ellis et al., 2008; Pérez et al., 2009).
- A brood zone at 307.7 K (34.5 °C) with a maximum humidity of 4.9 kPa {0.9, 307.7 K} (Seeley, 1985; Ellis et al., 2008).
- A condensing zone at the dew point temperature i.e. internal surface of the cavity.

In this model, which is a simplification of a complex system:

- Water vapour enters the system from nectar evaporation, nectar consumption and through entrance inlet air flow by forced convection.
- Water vapour leaves via condensation and entrance exhaust flow.

- Heat energy is produced by metabolising sugars.
- Heat energy exits via conduction through the nest walls. The heat flows of the entrance gases are insignificant in comparison (~10mW vs ~100W) (Mitchell, 2019) and ignored.
- The pollen to insect protein processes are considered as a constant rate metabolic energy overhead that consumes nectar, releasing water vapour from its water content and oxidation.

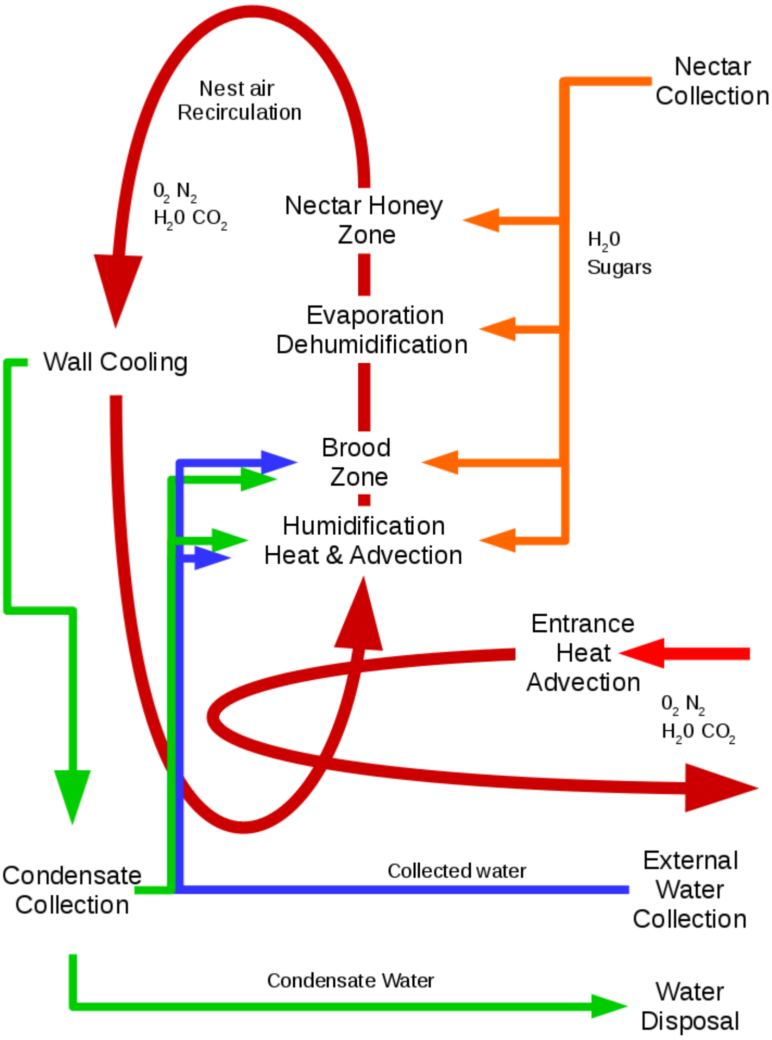

Figure 4.1: Nest fluid transfer and phase change processes.

In reality the honey bee nest is a set of complex interconnected processes as shown in Figure 4.1, involving the fluids: nectar (orange), externally collected water (blue), condensate water (green), and gases (red). The latter are a mixture of air, water vapour and CO_2. These are advected through the entrance and circulated between: a brood zone kept at constant temperature, a nectar zone at elevated temperature for evaporation, and a lower temperature condensation zone.

By using the standard thermofluid techniques of energy and mass balances across the system boundary to determine the ability of honey bees to dispose of the water vapour generated and therefore the resultant average humidity, this approach removes the necessity to analyse the internal detail while retaining validity.

To populate the model, the climatic and fanning behavioural data are from ZDUPSA (Ellis et al., 2008) and the results, generated using MATLAB (MATLAB, 2018) are correlated to their findings (Human et al., 2006; Ellis, 2008; Nicolson, 2009).

4.3.1 Water vapour production rate

For the purposes of this analysis, water vapour production consists of 5 components:

- Water evaporated from nectar, at honey production rates of 5 mgs^{-1} (1 lb/day) and may exceed 25 mgs^{-1} (5lb/day) (Park, 1925; Park, 1946).
- Water content from the nectar used as fuel for nectar evaporation.
- Metabolic water production from the nectar used as fuel for nectar evaporation.
- Water content from the nectar used for other processes in the nest.
- Metabolic water production from the nectar used for other processes in the nest.

The weight of water entering the vapour phase in the nest is defined in equation 4.2.

$$\dot{W}^{Total}_{Vapour} = \alpha \dot{W}^{Evaporate}_{Water} + [\dot{W}^{Nest}_{Nectar} + \dot{W}^{Evaporate}_{Nectar}][\beta_0 (1 - C_{Nectar}) + \beta_1 C_{Nectar} r] \qquad (4.2)$$

The coefficients α, β_0 and β_1 define the proportion resulting in water vapour (vapour fraction) inside the nest from 3 classes of water source:

- Water content of nectar that is “made” into honey α.
- Water content of the nectar consumed as metabolic fuel β_0.
- Water from the oxidation of the sugars from nectar consumed as fuel β_1.

Similarly, $1-\alpha$, $1-\beta_0$ and $1-\beta_1$ are the proportions that are excreted or do not arrive at the nest.

If one considers only the delivered nectar concentration, as opposed to the collected nectar concentration, then differences between races of honey bee desiccating the nectar in flight can be ignored (*A.m. mellifera* and *A.m. ligustica* (Park, 1932) versus *A.m. scutellata* (Nicolson and Human, 2008)). Then according to the behaviours described one may determine $\alpha \approx 1$ (Park, 1932). From the winter behaviour of not defecating for extended periods (Seeley, 198), one can deduce that β_1 can be close to unity and, from their consumption of honey with a ~0.2 water content during winter, that β_0 can be non zero. More precise values, or the validity in the nectar gathering season, are unknown. The analysis can assess the significance of these coefficients and consequently their importance for further research. For other purposes, assumptions may have to be made about these coefficients.

The amount of water to evaporate and the fuel required for evaporation $\dot{W}_{Water}^{Evaporate}$, $\dot{W}_{Nectar}^{Evaporate}$ are dependent on rate of honey production, nectar concentration and the thermal efficiency of the nectar evaporating process TEE or $\Gamma_{Thermal}$, as shown in the expressions in previous work (Mitchell, 2019). TEE is derived from the nest thermal conductance. However, depending on the nest configuration and the honey bee behaviours, the nest thermal conductances for evaporation and condensation may differ from each other, particularly in larger or higher aspect ratio nests that may give more space for stratification. Using the equation for the break-even energy margin from (Mitchell, 2019), an equation can be derived that gives maximum water vapour production at the minimum thermal efficiency for a specific nectar and honey concentration.

The rate of consumption of nectar for other metabolic processes $\dot{W}_{Nectar}^{Nest}$ is dependant on the honey bee colony mass and the metabolic rate, which is dependant on the nest internal temperature and hence the external temperature and the nest thermal conductance (Mitchell, 2016). However, as a simplification this rate of consumption will be assumed to be disjoint from the evaporation and condensation processes and a fixed value in this analysis, to concentrate on the effects of nectar condensation. Full integration into the analysis is left for future research.

4.3.2 Water removal rate

The total capacity for water removal is the sum of the water vapour that exits the entrance and that condensed inside the nest. The rate of condensation is defined by the latent heat lost through the nest walls as heat lost via entrance air flow is insignificant in comparison. The water vapour exhausted is characterised by the vapour density of the air and the total flow through the entrance. The maximum dew-point temperature and hence exhaust water vapour density and exhaust water mass are defined by the following constraints:

1. The brood area is not above 4.9 kPa {0.9, 307.7K} (Ellis et al., 2008). This defines the limit of the vapour pressure and vapour density for the gas exhausted by fanning and the dew point for condensation.
2. Honey can be ripened. This defines a vapour pressure that results in the maximum honey water activity (0.6) below a maximum achievable honey bee temperature of 318.2 K (Baracchi et al., 2010).
3. The maximum fanning air velocity (0.924 ms^{-1} (Peters et al., 2017)).

The fanning response to humidity is fitted, using a cubic polynomial (R-square 0.9934), to the ZDUPSA normalised data with the presence of brood (Ellis et al., 2008), as shown in figure 4.2, assuming the honey bees deliver air velocity proportional to this response up to their maximum.

Fanning responses to carbon dioxide levels can be ignored as they cannot exceed 20% of water vapour partial pressure during nectar evaporation (Seeley, 1974; Mitchell, 2019).

The climatic information i.e. ambient temperature and humidity used in analysis will be for the same location i.e. Pretoria South Africa averages for spring and summer (November to February) of 295.7K (22.5C) and 0.595 RH (Thorsen, 2018).

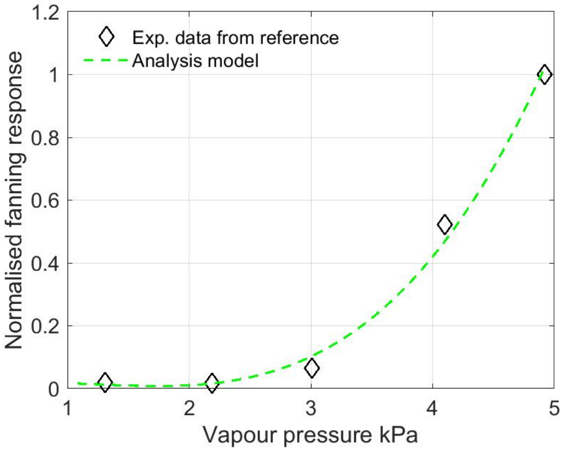

Figure 4.2: Fanning response versus vapour pressure kPa using data from (Ellis et al., 2008).

Honey bee constructions and behaviours, as well as the nest walls, define a lumped conductance for the condensation process. Limits of conductance of the nest walls for both tree and man-made nests are derived from standard shape factors and techniques (Incropera et al., 2007) using average dimensions from the literature (Seeley and Morse, 1976; Mitchell, 2016). For hives, the upper limit of one brood box and 4 shallows (Cushman, 2011) will be used.

The energy balance of wall heat conduction and the heat produced by condensation, produces an equation in terms of the dew point, which is then solved.

4.4 Analysis

4.4.1 Assumptions

The following assumptions in addition to those in section 4.3 are made:

1. System is in equilibrium i.e. steady state.
2. Entrance air velocity is proportional to fanning response and is independent of entrance size i.e. sufficient fanning honey bees will be recruited.
3. Water vapour losses or gains through permeation of the nest enclosure and its internal coating of propolis are insignificant.
4. Water vapour pressure is the same throughout the nest or hive.
5. There is only one entrance or vent and it is at the bottom of the nest or hive.
6. The energy changes due the thermal capacities of the fluids crossing the system boundaries are negligible compared to those involved in the state changes.

4.4.2 Fundamentals

The partial pressure of water vapour is given in equation 4.3 after (Tetens, 1930; Murray, 1967)

$$P_i = 610.78\,\chi_i\,\mathrm{e}^{\left[17.2694\frac{T_i - 273.16}{T_i - 35.86}\right]} \tag{4.3}$$

and the vapour density from equation 4.4.

$$\rho_i = 0.002166\,\frac{P_i}{T_i} \tag{4.4}$$

Let the following parameters be defined for instance *i* of temperature, relative humidity and vapour pressure in equation (4.5), then equation4.3 becomes equation 4.6 and at the dew point (equation4.7).

$$\delta_i=\frac{T_i-273.16}{T_i-35.86} \qquad \gamma_i=\frac{\log\chi_i}{17.2694} \qquad \theta_i=\frac{1}{17.2694}\log\left(\frac{P_i}{610.78}\right) \tag{4.5}$$

$$T_i=\frac{\delta_i 35.86-273.16}{\delta_i-1} \qquad \chi_i=\mathrm{e}^{[17.2694\,\gamma_i]} \qquad P_i=610.78\,\mathrm{e}^{[17.2694\,\theta_i]}$$

$$\theta_i=\gamma_i+\delta_i \tag{4.6}$$

$$\theta_D=\delta_D \tag{4.7}$$

If conditions change (RH, temperature) but the vapour pressure remains constant from instance *j* to *i* then equation 4.8.

$$\theta_j=\theta_i=\gamma_j+\delta_j=\gamma_i+\delta_i \tag{4.8}$$

Then equations 4.9, 4.10 and 4.11.

$$P_i=610.78\,\mathrm{e}^{[17.2694\,\theta_i]} \tag{4.9}$$

$$T_i=\frac{273.16-35.86\,\delta_i}{1-\delta_i}=\frac{273.16-35.86\,(\theta_j-\gamma_i)}{1-(\theta_j-\gamma_i)} \tag{4.10}$$

$$\chi_i=\mathrm{e}^{[17.2694\,\gamma_i]}=\mathrm{e}^{[17.2694(\theta_j-\delta_i)]} \tag{4.11}$$

The upper limits of conductance for condensation in tree nests and man-made hives are derived from the conductance being the sum of the products of conductivities and shape factors of the components forming the cavities. For the tree nest equation 4.12.

$$\Lambda_{Con}\approx\lambda_{Tree}\left[\frac{2\pi h_{Tree}}{\ln\left(\frac{d_1}{d_0}\right)}+2\frac{\pi d_0^2}{4}\frac{1}{\frac{1}{2}(d_1-d_0)}\right] \tag{4.12}$$

For man-made hives with roof thickness identical to the walls 4.13.

$$\Lambda_{Con}\approx\lambda_{Hive}\left[\frac{2\pi h_{hive}}{0.785\ln\left(\frac{x_1}{x_0}\right)}+2\frac{x_0^2}{\frac{1}{2}(x_1-x_0)}\right] \tag{4.13}$$

4.4.3 Water vapour generation

Taking from reference (Mitchell, 2019) the following:

The weight of evaporate (equation 4.14).

$$W_{Water}^{Evaporate}=W_{Sucrose}^{Base}\left(\frac{1}{C_{Nectar}}-\frac{1}{C_{Honey}}\right)=W_{Sucrose}^{Base}\,\xi \qquad (4.14)$$

In terms of the rate of production of honey (equation 4.15).

$$\dot{W}_{Water}^{Evaporate}=C_{Honey}\,\dot{W}_{honey}^{Base}\,\xi \qquad (4.15)$$

The weight of nectar metabolised in equation 4.16.

$$\dot{W}_{Nectar}^{Evaporate}=\frac{L_{water}\,\dot{W}_{Sucrose}^{Base}\,\xi}{C_{Nectar}\,L_{Sucrose}\,\Gamma_{Thermal}}=\frac{C_{Honey}\,L_{water}\,\dot{W}_{Honey}^{Base}\,\xi}{C_{Nectar}\,L_{Sucrose}\,\Gamma_{Thermal}} \qquad (4.16)$$

The volume of nest nectar consumed for other purposes is derived from the mass of the colony and the metabolic rate (equation 4.17).

$$\dot{W}_{Nectar}^{Nest}=\frac{\dot{L}_{meta}\,W_{colony}}{L_{Sucrose}\,C_{Nectar}} \qquad (4.17)$$

By substitution of equations 4.16 and 4.17 into 4.2 gives 4.18.

$$\dot{W}_{Vapour}^{Total}=\alpha C_{Honey}\,\dot{W}_{honey}^{Base}\,\xi$$

$$+\left[\frac{\dot{L}_{meta}\,W_{colony}}{L_{Sucrose}\,C_{Nectar}}+\frac{C_{Honey}\,L_{water}\,\dot{W}_{Honey}^{Base}\,\xi}{C_{Nectar}\,L_{Sucrose}\,\Gamma_{Thermal}}\right]\left[\beta_0\left(1-C_{Nectar}\right)+\beta_1 C_{Nectar}\,r\right] \qquad (4.18)$$

Nectar collection and ripening is subject to the break-even constraint for the energy margin M for nectar collection from reference (Mitchell, 2019) which is maximised when the nectar source is close to the nest, hence (4.19).

$$\frac{L_{Sucrose}}{L_{Water}}\geq\frac{\xi}{\Gamma_{Thermal}} \qquad (4.19)$$

Using equation 4.19 the water vapour rate for the value of TEE that breaks even in energy is given below in equation 4.20.

$$\dot{W}^{Total}_{Vapour} = \alpha C_{Honey} \dot{W}^{Base}_{honey} \xi + \left[\frac{\dot{L}_{meta} W_{colony}}{L_{Sucrose}} + C_{Honey} \dot{W}^{Base}_{Honey}\right]\left[\beta_0\left(\frac{1}{C_{Nectar}} - 1\right) + \beta_1 r\right] \tag{4.20}$$

For a colony to be successful then the power consumed by background metabolism must be insignificant compared to the rate at which energy is stored by the colony i.e. inequality (equation 4.21).

$$\dot{L}_{meta} W_{colony} \ll C_{Honey} \dot{W}^{Base}_{Honey} L_{Sucrose} \tag{4.21}$$

Then equation 4.20 becomes 4.22 the maximum possible water production, similarly at TEE =1 equation 4.23. Both equations are of form of equation 4.24.

$$\dot{W}^{Total}_{Vapour} \approx C_{Honey} \dot{W}^{Base}_{Honey}\left[\alpha \xi + \beta_0\left(\frac{1}{C_{Nectar}} - 1\right) + \beta_1 r\right] \tag{4.22}$$

$$\dot{W}^{Total}_{Vapour} \approx C_{Honey} \dot{W}^{Base}_{Honey}\left[\alpha \xi + \frac{L_{Water}\,\xi}{L_{Sucrose}}\left(\beta_0\left(\frac{1}{C_{Nectar}} - 1\right) + \beta_1 r\right)\right] \tag{4.23}$$

$$\dot{W}^{Total}_{Vapour} \approx C_{Honey} \dot{W}^{Base}_{Honey}\left(\alpha \mathrm{A} + \beta_0 \mathrm{B}_0 + \beta_1 \mathrm{B}_1\right) \tag{4.24}$$

4.4.4 Water removal capacity

Assuming the condensing region to be of uniform temperature in equilibrium, the gas volume in the cavity as incompressible, and the amount of energy dissipated via the entrance by advection is negligible (Mitchell, 2019), then latent heat of condensation is dissipated by the nest walls, giving the energy balance shown in equation 4.25.

$$\dot{W}_{Condensate} L_{water} \le \Lambda_{Con}\left(T_D - T_{Out}\right) where \left\{T_D \ge T_{Out}\right\} \tag{4.25}$$

The entrance velocity is described as the product of the maximum air velocity and cubic polynomial function with respect to RH at brood temperature 307.7 K. An RH at a known temperature is related to a dew point temperature T expressed as parameter δD by a function derived from equations 4.8, 4.9 and 4.10 to give equation 4.26.

$$\chi = \mathrm{e}^{\left[17.2694\left(\delta_D - \delta_{Brood}\right)\right]} \tag{4.26}$$

Substituting equation 4.26 into the polynomial gives equation 4.27.

$$u_{Ent}\left(T_D\right) = u_{Max}\left[a_3 \mathrm{e}^{3\left[17.27\left(\delta_D - \delta_{Brood}\right)\right]} + a_2 \mathrm{e}^{2\left[17.27\left(\delta_D - \delta_{Brood}\right)\right]} + a_1 \mathrm{e}^{\left[17.27\left(\delta_D - \delta_{Brood}\right)\right]} + a_0\right] \tag{4.27}$$

The total water removal capacity equals the sum of advection and condensation hence equation 4.28.

$$\hat{W}^{Total}_{Vapour} = \frac{\Lambda_{Con}}{L_{Water}}\left(T_D - T_{Out}\right) + \frac{A_{Ent}\, u_{Ent}\left(T_D\right)}{2}\left(\rho_{Exhaust} - \rho_{Inlet}\right) \tag{4.28}$$

Using equation 4.4 for the density of a vapour and equation 4.3 for the vapour pressure at the dew point T_D, gives equation 4.29.

$$\hat{W}^{Total}_{Vapour} = \frac{\Lambda_{Con}}{L_{Water}}\left(T_{Out} - T_D\right) + 0.6615\, A_{Ent} u_{Ent}\left(T_D\right)\left(\frac{\mathrm{e}^{\left[17.27\,\theta_D\right]}}{T_D} - \frac{\mathrm{e}^{\left[17.27\,\theta_{Out}\right]}}{T_{Out}}\right) \tag{4.29}$$

Λ_{Con} and u_{Ent} in equation (4.29) are expanded using equation 4.27, 4.12, 4.13 and 4.5 for the range of man-made hive and the tree nest cases, and then solved for TD. With TD known, one can determine the brood zone RH using equation 4.26.

Brood zone air at humidity $\{\chi_i, T_{Brood}\}$ is elevated to desiccating temperature, THoney, in the nectar/honey zone at the honey activity χ_{Honey} where $\{\chi_i, T_{Brood}\} = \{\chi_{Honey}, T_{Honey}\}$, as shown in equation 4.30, which is derived from equation (4.10).

$$T_{Honey} = \frac{273.16 - 35.86\left(\gamma_i + \delta_{Brood} - \gamma_{Honey}\right)}{1 - \left(\gamma_i + \delta_{Brood} - \gamma_{Honey}\right)} \tag{4.30}$$

4.5 Results

The honey bee fanning information is derived from honey bee colonies in Pretoria South Africa (Ellis et al., 2008). As a consequence the climatic data used is from that location.

4.5.1 Water vapour production

The break-even point values of TEE, where maximum water vapour production occurs, vary with nectar concentration as plotted in figure 4.5 from equation 4.19. This maximum water production was plotted in figure 4.4 and 4.7, using equations 4.29 and 4.25. This is compared as a ratio to the minimum water production (TEE =1.0) as shown in figure 4.3 using equation 4.18. The minimum water production is also shown in figure 4.6 Note: α, $\beta 0$, and $\beta 1$ are assumed to have a value of 1 in both figures 4.3 and 4.4.

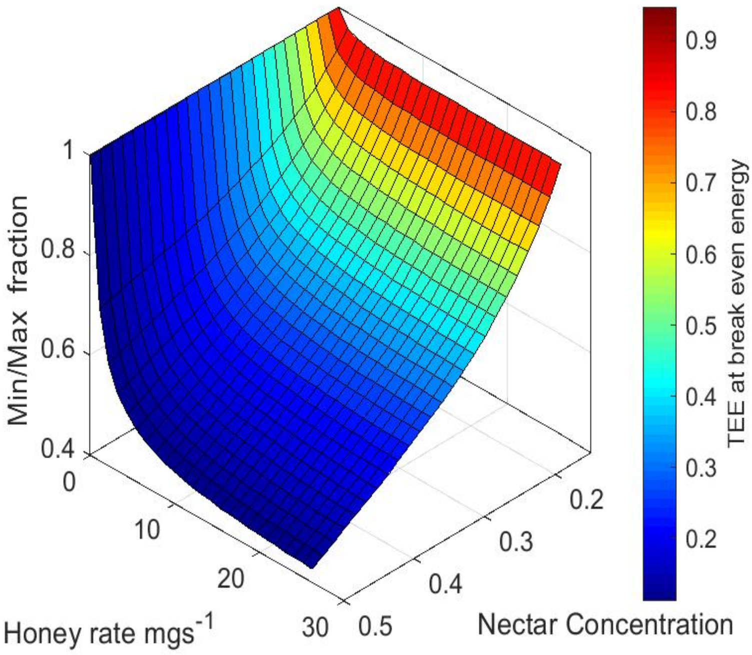

Figure 4.3: Ratio of minimum to maximum water product (Min: TEE=1, Max: TEE=break-even).

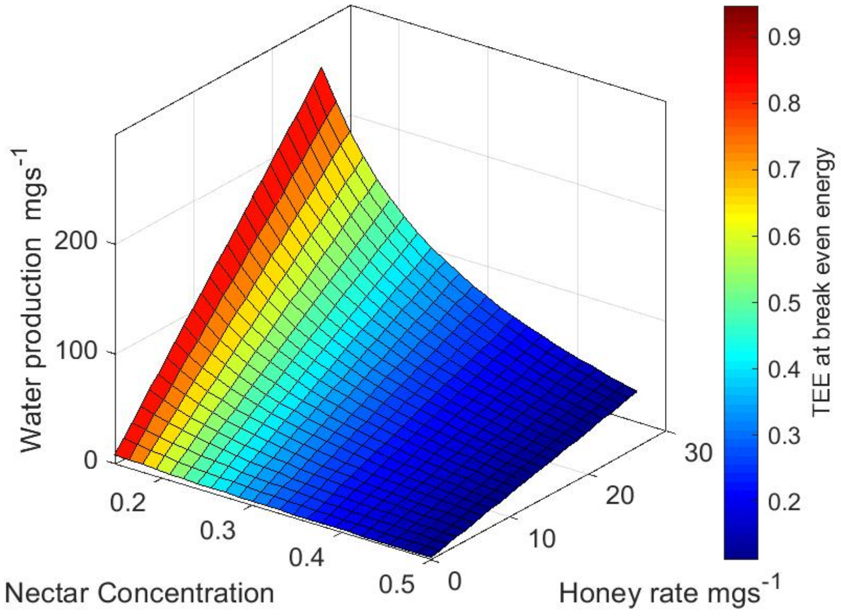

Figure 4.4: Maximum water product at break-even TEE.

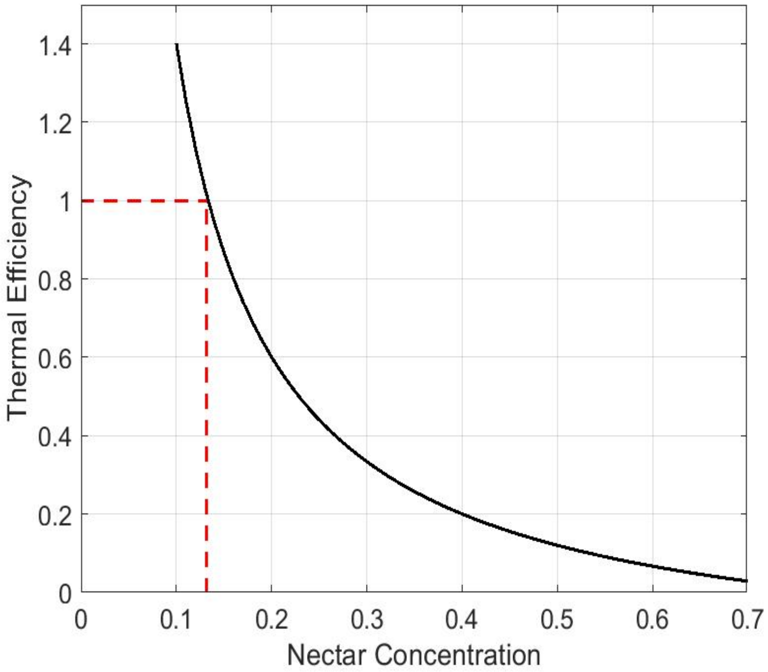

Figure 4.5: TEE to Nectar concentration at break-even point at zero nest to flower distance.

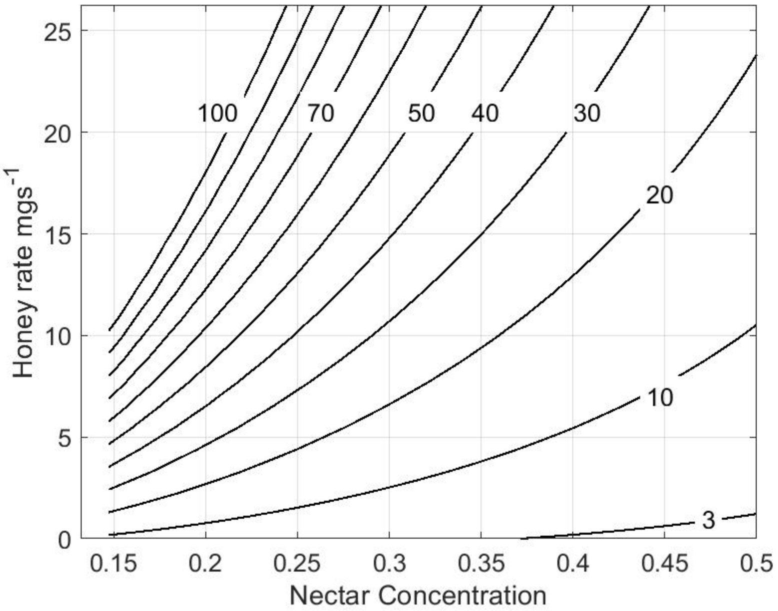

Figure 4.6: TEE=1 water production contours mgs^{-1} vs nectar concentration and honey rate.

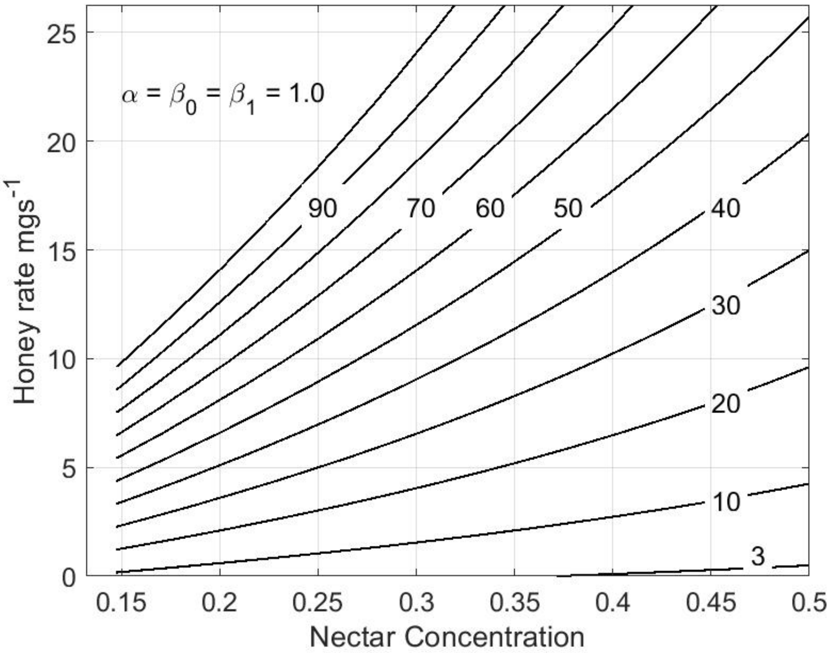

Figure 4.7: Break-even water production contours mgs^{-1} vs nectar concentration and honey rate.

Water production is dependant on 3 coefficients *α, β0,* and *β1*, which are multiplied by the terms *A*, *B0,* and *B1*. The relative magnitudes of these terms are plotted in: figure 4.8, for the case of TEE equal to one and fig 4.9 where TEE is at the break-even value using equations 4.22, 4.24 and 4.23.

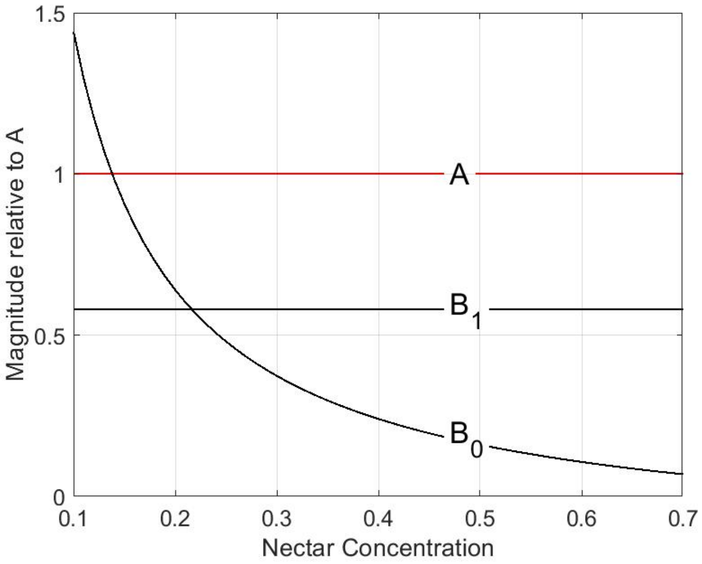

Figure 4.8: Water Product factors at TEE=1.

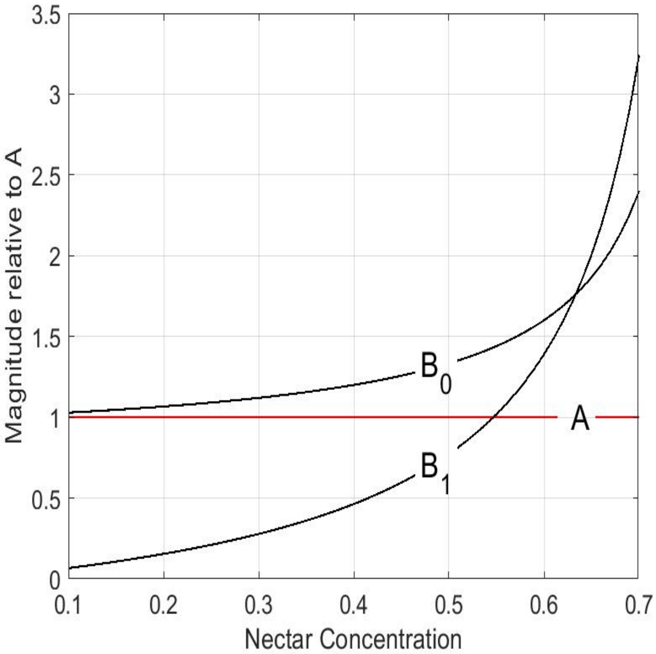

Figure 4.9: Water Product factors at TEE break-even.

4.5.2 Water vapour removal capacity

The scenarios studied are divided into two nest types; tree with a fixed height cavity and a man-made hive which can have variable height. Each nest type is divided into 4 combinations of high and low lumped thermal conductance, small and large entrances. The entrance and nest dimensions are taken from sources (Cushman, 2011; Mitchell, 2016). Equations 4.12 and 4.13 provide conductances as shown in table 4.2.

Using equation 4.29, one can then calculate the water vapour that can be removed by various combinations of entrance and condensation as shown in table 4.2 where A, B, C, & D represent the limits of conductance and entrance area for a tree nest and E, F, G, & H for man-made hives. The water removal capacity is tabulated at two levels of humidity 4.3 kPa and 4.9 kPa. The spread of conductance and entrance area is shown in figure 4.12 against the contours of water removal at 4.9 kPa. The brood zone humidity versus water removal capacity is plotted in the figures 4.10 and 4.11. The humidities of: optimal egg survival; the upper limit of varroa breeding success; Miami USA; summer Pretoria SA and winter Pretoria SA are shown for comparison.

The nectar desiccating temperature of the nectar/honey zone was plotted as contours against in the input RH at brood temperature (Pérez et al., 2009) and the resultant honey water content. This was calculated using equations 4.30 and 4.1, and shown in fig 4.13. The vertical dashed line indicates a typical long term storage water content of 0.2. The horizontal dashed line indicates 4.3 kPa, the upper limit of varroa breeding success.

4.5.3 Experimental Validation

The analysis indicates lower water vapour removal capacity in tree nests. Thus one may expect to find higher humidities observed compared to hives when nectar ripening activity is not intense. Unfortunately there are no studies available that give sufficient information to infer the rate of water vapour production, however, a ZDUPSA study (Ellis, 2008) does conduct a simultaneous measurement of humidity in both trees and man-made hives. It is reasonable to assume similar rates of water vapour production, and thus predict the humidity in one environment given the humidity of the other using the model with median conductances for both nests. The observed humidity in the trees in the study was~3.8 kPa {0.7, 307.7 K} which results from ~7 mgs-1 of water production according to the model in figure 4.11. Then using this water production in a median hive, it is predicted that this would produce ~3.0 kPa as shown in figure 4.10. This agrees with the ZDUPSA experimental values in the range 3.0 kPa to 3.3 kPa.

Further, the model determines that, if the nectar flow is zero or low and fanning is not taking place, the water vapour removal is primarily by condensation. Then the humidity is constrained by the internal nest surface temperature at saturation from equation (4.25) i.e. dew point. In the high conductance hives this will be within a few degrees of the outside air temperature i.e. { 1.0, ~T_{Out}}. ZDUPSA conducted two humidity studies in winter (Human et al., 2006; Ellis, 2008) in average ambient temperatures of 288 K. The elevation of inside temperature above ambient for wooden hives in cool winter configuration is around ~5 K (Mitchell, 2016) and less in warmer ambient temperatures. The model predicts then that the nest humidity will be about {1, 288+5} equal to {1, 293 K} or 2.3 kPa. The average observed humidity in the ZDUPSA experiment was between 1.9 kPa {0.35, 307.7 K} and 2.5 kPa {0.45, 307.7 K}. Another similar, earlier study in the UK (Simpson, 1950) showed the internal dew point 7 degrees higher than the external winter ambient temperature, which again concurs with the model.

Table 4.2: Water removal capacity of Nest limits of conductance and entrance area, at water vapour contents (a) 4.3 kPa (Kraus and Velthuis, 1997) and (b) 4.9 kPa (Schmehl et al., 2016).

				Water removal mgs^{-1}	
#	**Nest Description**	**A_{ent} cm^2**	**Λ_{Con} WK^{-1}**	**(a)**	**(b)**
A	Tree nest low conductance, small entrance	7.5	0.4	5.6	9.8
B	Tree nest low conductance, large entrance	15	0.4	9.8	17.9
C	Tree nest high conductance, small entrance	7.5	2	10.9	16.4
D	Tree nest high conductance, large entrance	15	2	15.1	24.5
E	Man-made hive, no shallows, small entrance	6.5	2.5	11.9	17.5
F	Man-made hive, no shallows large entrance	83	2.5	55.6	100.2
G	Man-made hive, 4 shallows small entrance	6.5	12	43.4	57.1
H	Man-made hive, 4 shallows large entrance	83	12	86.7	139.8

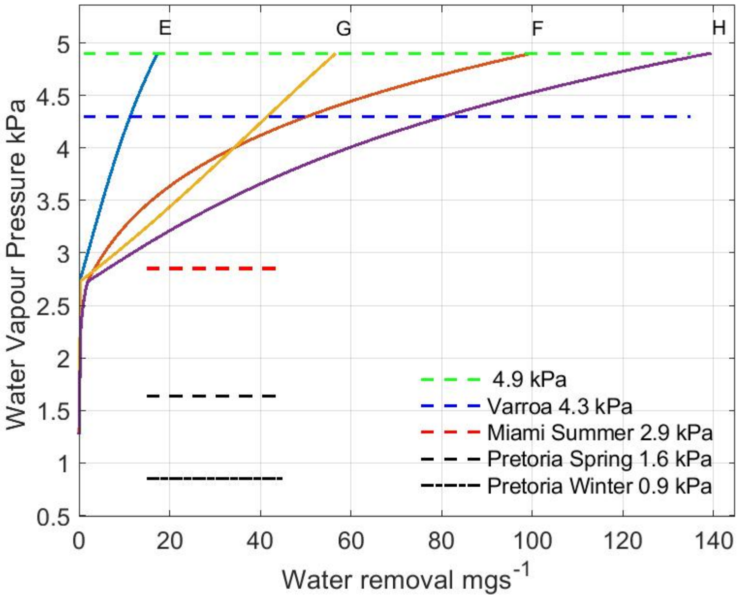

Figure 4.10: Man-made hive brood zone humidity.

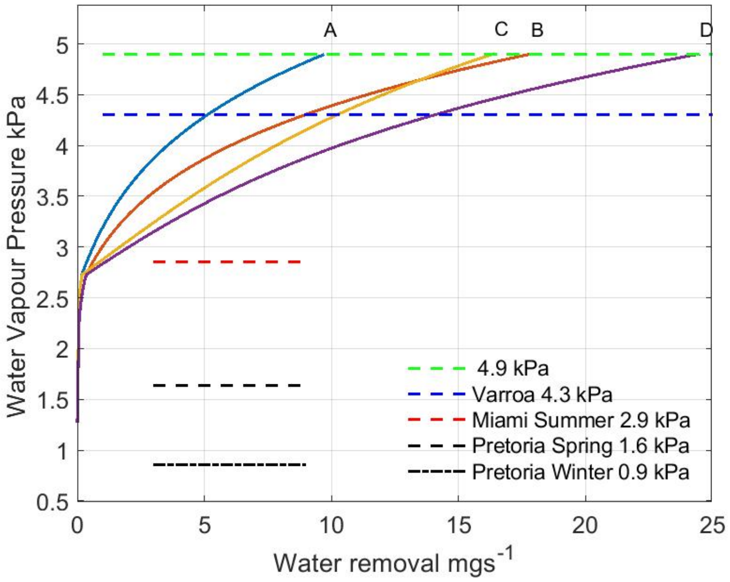

Figure 4.11: Tree nest brood zone humidity.

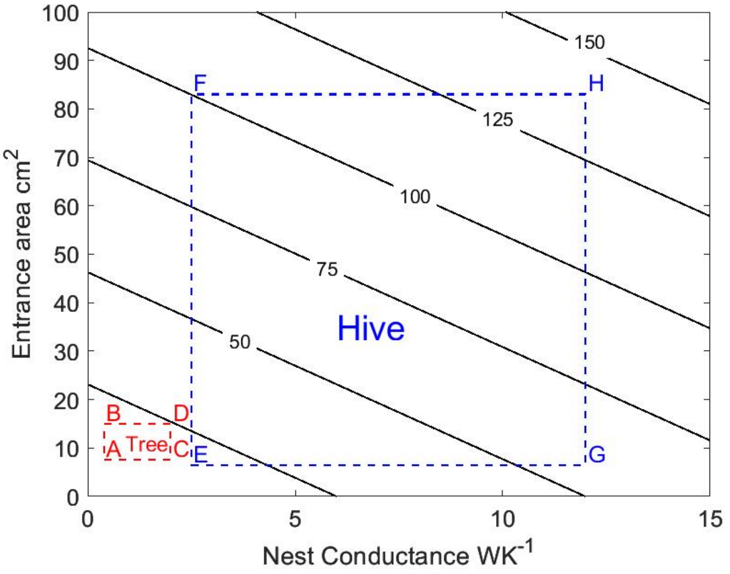

Figure 4.12: tree and man-made nest limits plotted onto contours of water removal vs nest conductance and entrance area.

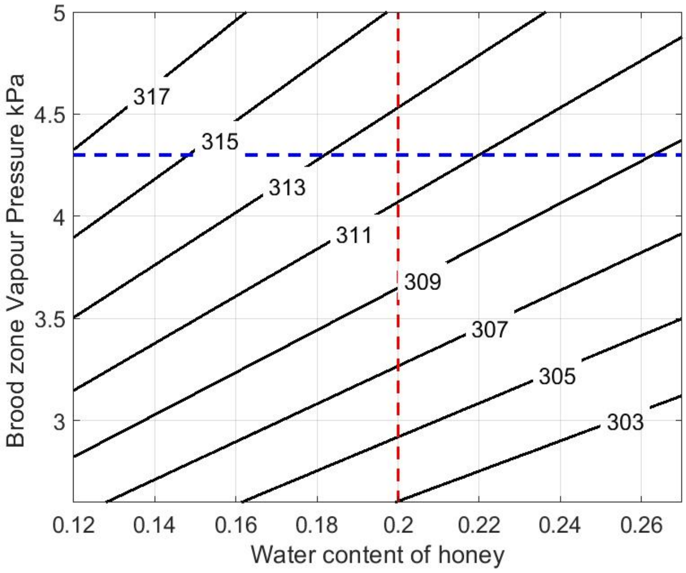

Figure 4.13: Contours of nectar/honey zone nectar desiccating temperature vs water content, $1-C_{Honey}$ *and brood zone vapour pressure.*

4.6 Discussion

This is a zoned steady state analysis of the averages of micro climates within the zones, thus extrapolating what occurs during the daily cycle is open to errors owing to thermal diffusivity, commonly known as thermal inertia. Thus internal humidity changes due to condensation will follow, but lag behind and be less severe than predicted from the external daily temperature changes depending on the construction, contents of the nest and amount of insolation. This lag and averaging out will be most pronounced in the high thermal capacity and low conductance of tree nests. Further, water production and removal is not completely synchronous, as average nest humidity increases following foraging activity and then decreases with time as nectar desiccation proceeds, often at night, after the cessation of foraging.

There is considerable further work in finding: data on thermal diffusivity and time-varying nectar gathering and desiccation rates, to populate a more accurate transient based analysis; factors governing microclimates within the zones, to determine their limits. However, this analysis should be sufficient to act as an aid to interpreting the daily rise and fall of hive humidity.

4.6.1 Factors in water Production

During nectar desiccation the overwhelming majority of the water vapour in the nest is a direct consequence of the nectar desiccation, the water vapour from the rest of the hives nectar consumption and metabolism becomes an insignificant factor, as can be seen in figures 4.7 and 4.6 from the values of contours that cross the zero honey rate-axis.

TEE has a profound effect on water production as can be seen in the degree of variation between maximum and minimum values shown in figure 4.3, where for typical concentration ranges (0.2 - 0.4) and honey ripening rates 5 mgs^{-1} to 15 mgs^{-1} the minimum to maximum ratio is 0.5 to 0.75. TEE also has a limiting effect on usable nectar concentration. If one looks at figure 4.5, for the value of TEE equal to 1, the corresponding nectar sugar concentration is 0.132 $KgKg^{-1}$. This value provides an indication of the lowest level of nectar resource that is of long term use to honey bees even in the most favourable conditions.

To understand the importance of the various sources of water within the nest, one needs to compare their relative magnitudes as shown in figures 4.8 and 4.9. These show the relative magnitudes of the terms (A, B_0, B_1) that are multiplied by the coefficients (α, β_0, β_1). When TEE is equal to one, see figure 4.8, it reflects a scenario where the external temperature is close to that inside the nest i.e. tropical. In contrast, figure 6 is a colder climate, high heat loss scenario at the break-even point, where the colony is at its most stressed. In the “tropical” scenario one can see that B_1 and B_0 both remain smaller than A except at very weak concentrations. The “colder” scenario however, has a high relative value for B_0 throughout the concentration range. This indicates the water content of nectar used as fuel to desiccate the honey is a significant contributor of water in the nest. The magnitude of B_0 means the coefficient β_0, the vapour fraction of nectar fuel water content, is an important value for the science related to honey bees in colder climates. Unlike α, β_0 can currently only be inferred and assumed.

4.6.2 Humid brood zone, dry nectar honey zone

Honey bees appear on first inspection to have conflicting requirements of a high temperature humid brood zone and dry air needed for nectar desiccation. If one looks at figure 4.13, one can see that if the humid air from the brood zone is heated it can desiccate nectar to low moisture levels. If air containing 4.3 kPa of water is than heated to 312 K then it will desiccate nectar to produce honey with only 20% water. This water content is low enough to prevent microbial growth in the honey and the vapour pressure is high enough to hinder the breeding of varroa. This fulfils both the need to have a long term food supply and to reduce the impact of this parasite.

In this model these zones are separated, however for honey bees this may not be easy to achieve, particularly in low aspect ratio man-made hives, where thermal stratification is not strong and is often disturbed by bee keepers.

4.6.3 High humidity required, low found in man-made hives

There is a marked contrast in humidity between in-vitro honey bee rearing 4.1 kPa (Schmehl et al., 2016) and man-made hives 2.2 kPa to 3.3 kPa (Simpson, 1950; Human et al., 2006). In the latter the humidity is measured outside the micro climates in the cells maintained by the nurse honey bees. If *A. mellifera* optimally evolved for tree dwelling then maintaining such difference between the general humidity and the micro climates must therefore represent a stress condition. The difference arises from the condition that unless there is very high water production rates then internal humidity in high conductance, large entrance hives is tied down to $\{1, T_{Out}\}$ (dew point ~ outside temperature) and when large top vent/entrances are added then it is tied to $\{\chi_{Out}, T_{Out}\}$

4.6.4 Hives good for Varroa, tree nests good for honey bees

That high humidities particularly in cooler climates require low thermal conductance enclosures has been discussed in relation to varroa in other work (Mitchell, 2016) and is an accepted thermofluid phenomenon (Mlakar and Štrancar, 2013). In addition, the possible impact of top vents or entrances, using recent thermofluid models (Lane-Serff et al., 2012), has also been discussed (Mitchell, 2017).

The common practice of man-made hives of thin walled wooden construction with many shallows on top is shown in the high conductance scenarios (limits E, F, G, & H) which result in much higher lumped thermal conductances than tree nests (limits A, B, C, & D) of 2.5 to 12 WK^{-1} vs 0.4 to 2.0 WK^{-1}. This and the very much larger entrances used in summer (limits F, H) tie the humidity close to $\{1, T_{Out}\}$ at low water production rates and increase the water production rate needed to reach 4.3 kPa, by a factor of five as can be seen in figures 4.10 and 4.11 (i.e. 50 mgs^{-1} vs 10 mgs^{-1}).

Taking nectar concentration of 0.33, typical of oil seed rape, a common European honey producing crop, one can see from figures 4.7 and 4.6 that these water production rates imply honey production rates of 12 to 25 mgs^{-1} for a man-made hive and 1 to 3 mgs^{-1} for a tree nest. This means honey bees, in man-made hives, need to forage and desiccate honey at 10 times the rate to obtain the 4.3 kPa humidity sufficient to affect varroa fecundity. The foraging conditions needed for these honey production rates will occur less frequently than those required by the modest rates needed by tree nests.

Counter-intuitively, a sub tropical climate, such as Florida, is not sufficient. The common practice of using high conductance, top vented hives (Phillips and Pett, 2014; Ratnieks, 2016), ties internal humidity to the outside, which in a Florida summer averages at 2.8 kPa $\{0.72, 301\ K\}$(NOAA, 2019). At low water production levels, in this climate and hives, but without top vents, humidity will only accumulate to circa 3.8 kPa, allowing varroa to proliferate.

However, with a sustained average outside temperature of above 303.2 K, e.g. warm dessert areas of southern Algeria, the analysis shows a high conductance hive, without top vents, can accumulate 4.3 kPa. This may account for the reported higher brood infestation in northern compared to southern Algeria (Adjlane et al., 2016) where, in the south, for large parts of the year, the average ambient temperature is above 303.2 K (MeteoStat, 2019); yet in the north, the average summer temperature is 298 K (Thorsen, 2018) with a corresponding hive humidity of 3.2 kPa.

In addition, better nectar sources and higher external temperatures, factors shown in this analysis to give higher nest humidity, have been positively correlated with reduced varroa infestation in an experimental research of Mediterranean apiaries (Leza et al., 2016).

Thus changes to bee keeping practice can improve the frequency of varroa disrupting high humidity for man-made hives: improved foraging, avoiding top vents, constructing hives from lower thermal conductivity materials, having fewer shallows on the hive, by more frequent harvesting and matching entrance size to water removal demand by changing the entrance size in response to changing internal humidity or ripening activity.

4.7 Conclusion

The thermofluid physics in the production and removal of water vapour bound the behaviours of the honey bee colony. Within the constraints of its steady state, averaging approach and assumptions, this theoretical analysis explores those boundaries and has found:

- Honey bees must produce and dispose of considerable quantities of water vapour in order to convert nectar into honey. Typically 4 to 7 times the weight of honey.
- Climate is a major factor especially when cooler climates are combined with high conductance hives. The fuel used in nectar desiccation then becomes the dominant source of water vapour in the nest.

- The thermal conductance of the nest and the dimensions of the entrance have a major impact on nest humidity. This makes high humidity a much more likely and frequent occurrence in tree nests and the low humidity found in man-made nests a likely stressor.
- Low humidities observed in some hives may be a direct result of their construction and thermal conductance.
- Hive thermal conductance and entrance size can potentially change the impact of varroa on honey bee colonies.
- Top vents can tie inside to outside humidity, which even in subtropical climates is substantially below the ideal for larval growth and the reduction of varroa fecundity. Therefore, they may increase the levels of honey bee stress and the likelihood of varroa infestation.

Finally, this study shows, through changing hive design and bee keeping practices, how to achieve the absolute humidity level of 4.3 kPa (~30 gm^{-3}), that makes varroa fecundity fall.

4.8 References

Adjlane, N., Dainat, B., Gauthier, L. and Dietemann, V. 2016. Atypical viral and parasitic pattern in Algerian honey bee subspecies Apis mellifera intermissa and A. m. sahariensis. *Apidologie*. **47**(5), pp.631–641.

Baracchi, D., Cusseau, G., Pradella, D. and Turillazzi, S. 2010. Defence reactions of Apis mellifera ligustica against attacks from the European hornet Vespa crabro. *Ethology Ecology & Evolution*. **22**(919804495), pp.281–294.

Beekman, M. and Ratnieks, F.L.W. 2000. Long-range foraging by the honey-bee, Apis melliera L. M. *Functional Ecology*. **14**(6), pp.490–496.

Le Conte, Y., Arnold, G. and Desenfant, Ph. 1990. Influence of Brood Temperature and Hygrometry Variations on the Development of the Honey Bee Ectoparasite Varroa jacobsoni (Mesostigmata: Varroidae). *Environmental Entomology*. **19**(6), pp.1780–1785.

Cushman, D. 2011. Drawings of Hives and Hive Parts. *Dave Cushman's Beekeeping and Bee Breeding Website*. [Online]. Available from: http://www.dave-cushman.net/bee/britparts.html.

Dawkins, R. 1982. *The Extended Phenotype*. W. H. Freeman & Co, Oxford.

Doull, K.M. 1976. The effects of different humidities on the hatching of the eggs of honeybees. *Apidologie*. **7**(1), pp.61–66.

Egekwu, N.I., Posada, F., Sonenshine, D.E. and Cook, S. 2018. Using an in vitro system for maintaining Varroa destructor mites on Apis mellifera pupae as hosts: studies of mite longevity and feeding behavior. *Experimental and Applied Acarology*. **74**(3), pp.301–315.

Ellis, M.B. 2008. Homeostasis: Humidity and water relations in honeybee colonies (Apis mellifera). *MSc Thesis*. [Online]. (November), p.126. Available from: https://repository.up.ac.za/handle/2263/28357.

Ellis, M.B., Nicolson, S.W., Crewe, R.M. and Dietemann, V. 2008. Hygropreference and brood care in the honeybee (Apis mellifera). *Journal of Insect Physiology*. **54**(12), pp.1516–1521.

Eyer, M., Neumann, P. and Dietemann, V. 2016. A Look into the Cell: Honey Storage in Honey Bees, Apis mellifera. *Plos One*. **11**(8), p.e0161059.

Hagenmaier, R.D. and Shaw, P.E. 1992. Gas Permeability of Fruit Coating Waxes. *Journal of the American Society for Horticultural Science*. **117**(1), pp.105–109.

Huang, Z. 2012. Varroa Mite Reproductive Biology. *American Bee Journal*. **152**(10), pp.981–985.

Human, H., Nicolson, S.W. and Dietemann, V. 2006. Do honeybees, Apis mellifera scutellata, regulate humidity in their nest? *Naturwissenschaften*. **93**(8), pp.397–401.

Humphrey, J.A.C. and Dykes, E.S. 2008. Thermal energy conduction in a honey bee comb due to cell-heating bees. *Journal of Theoretical Biology*. **250**(1), pp.194–208.

Incropera, F.P., Dewitt, D.P., Bergman, T.L. and Lavine, A.S. 2007. The Conduction Shape Factor and Dimensionless Conduction Heat Rate *In*: F. P. Incropera, ed. *Fundamentals of Heat and MassTransfer*., pp.207–212.

Incropera, F.P., Dewitt, D.P., Bergman, T.L. and Lavine, A.S. 2005. Thermophysical properties of matter *In*: F. P. Incropera, ed. *Fundamentals of Heat and MassTransfer*. John Wiley and sons, pp.927–957.

Kraus, B. and Velthuis, H.H.W. 1997. High humidity in the honey bee (Apis mellifera L.) brood nest limits reproduction of the parasitic mite Varroa jacobsoni Oud. *Naturwissenschaften*. **84**(5), pp.217–218.

Lane-Serff, G.F., Sandbach, S.D., El Khoury, G.K., Andersson, H.I., Pettersen, B., Tammisola, O., Renzi, E., Dias, F., Bogey, C. and Marsden, O. 2012. Emptying non-adiabatic filling boxes: the effects of heat transfers on the fluid dynamics of natural ventilation. *Journal of Fluid Mechanics*. **701**(2012), pp.386–406.

Leza, M.M., Miranda-Chueca, M.A. and Purse, B. V. 2016. Patterns in Varroa destructor depend on bee host abundance, availability of natural resources, and climate in Mediterranean apiaries. *Ecological Entomology*. **41**(5), pp.542–553.

Martin, E.C. 1958. Some Aspects of Hygroscopic Properties and Fermentation of Honey. *Bee World*. **39**(7), pp.165–178.

Massoud, M. 2005. *Engineering Thermofluids*. Springer-Verlag Berlin Heidelberg.

MATLAB 2018. *9.4.0.813654 (R2018a)*. Natick, Massachusetts: The MathWorks Inc.

MeteoStat 2019. *Weather Statistics Adrar*.

Mitchell, D. 2017. Honey Bee Engineering: Top Ventilation and top Entrances. *American Bee Journal*. **157**(8), pp.887–889.

Mitchell, D. 2016. Ratios of colony mass to thermal conductance of tree and man-made nest enclosures of Apis mellifera: implications for survival, clustering, humidity regulation and Varroa destructor. *International Journal of Biometeorology*. **60**(5), pp.629–638.

Mitchell, D. 2019. Thermal efficiency extends distance and variety for honey bee foragers: Analysis of the energetics of nectar collection and dessication by Apis mellifera. *Journal of the Royal Society, Interface*. **16**(20180879).

Mlakar, J. and Štrancar, J. 2013. Temperature and humidity profiles in passive-house building blocks. *Building and Environment*. **60**, pp.185–193.

Murray, F.W. 1967. On the Computation of Saturation Vapor Pressure. *Journal of Applied Meteorology*. **6**(1), pp.203–204.

Nicolson, S.W. 2009. Water homeostasis in bees, with the emphasis on sociality. *The Journal of experimental biology*. **212**(Pt 3), pp.429–434.

Nicolson, S.W. and Human, H. 2008. Bees get a head start on honey production. *Biology letters*. **4**(3), pp.299–301.

NOAA 2019. *Comparative Climatic Data*.

Ostwald, M.M., Smith, M.L. and Seeley, T.D. 2016. The behavioral regulation of thirst, water collection and water storage in honey bee colonies. *The Journal of Experimental Biology*. **219**(14), pp.2156–2165.

Park, O.W. 1946. Activities of Honey bees *In*: R. Grout, ed. *The Hive and the Honey bee*. Chicago: Dadant & Sons, pp.125–205.

Park, O.W. 1932. Studies on the changes in nectar concentration produced by the honeybee, Apis mellifera. Part I. Changes which occur between the flower and the hive. *Iowa Agriculture and Home Economics Experiment Station Research Bulletin*. **151**(151), pp.211–243.

Park, O.W. 1925. The Storing and Ripening of Honey by Honey Bees. *Journal of Economic Entomology*. **18**, pp.405–410.

Pérez, A., Sánchez, V., Baeza, R., Zamora, M.C. and Chirife, J. 2009. Literature review on linear regression equations for relating water activity to moisture content in floral honeys: Development of a weighted average equation. *Food and Bioprocess Technology*. **2**(4), pp.437–440.

Peters, J.M., Gravish, N. and Combes, S.A. 2017. Wings as impellers: honey bees co-opt flight system to induce nest ventilation and disperse pheromones. *The Journal of Experimental Biology*. **220**(12), pp.2203–2209.

Phillips, B. and Pett, W. 2014. Ensuring hive success this July 2014. *Michigan State University*. [Online], p.1. Available from: https://www.canr.msu.edu/news/ensuring_hive_success_this_july_2014.

Polat, O. and Bilgen, E. 2002. Laminar natural convection in inclined open shallow cavities. *International Journal of Thermal Sciences*. **41**, pp.360–368.

Ratnieks, F. 2016. Autumn preparation of hives for winter. [Accessed 23 February 2019]. Available from: http://www.lasiqueenbees.com/how-to/autumn-preparation-of-hives-for-winter.

Schmehl, D.R., Tomé, H.V. V, Mortensen, A.N., Martins, G.F. and Ellis, J.D. 2016. Protocol for the in vitro rearing of honey bee (Apis mellifera L.) workers. *Journal of Apicultural Research*. **55**(2), pp.113–129.

Seeley, T.D. 1974. Atmospheric carbon dioxide regulation in honey-bee (Apis mellifera) colonies. *Journal of Insect Physiology*. **20**(11), pp.2301–2305.

Seeley, T.D. 1985. *Honeybee Ecology: A Study of Adaptation in Social Life*. New Jersey, United States: Princeton University Press.

Seeley, T.D. and Morse, R.A. 1976. The nest of the honey bee (Apis mellifera L.). *Insectes Sociaux*. **23**(4), pp.495–512.

Simpson, J. 1950. Humidity in the winter cluster of a colony of honeybees. *Bee World*. **31(6)**, pp.41–44.

South African Sugar Technologists Association 2009. Method 2 . 3 – Bagasse : calorific value *In*: *SASTA Laboratory Manual*. Natal: South African Sugar Technologists Association, pp.2–5.

Southwick, E.E. 1982. Metabolic energy of intact honey bee colonies. *Comparative Biochemistry and Physiology -- Part A: Physiology*. **71**(2), pp.277–281.

Southwick, E.E. 1983. The honey bee cluster as a homeothermic superorganism. *Comparative Biochemistry and Physiology -- Part A: Physiology*. **75**(4), pp.641–645.

Southwick, E.E. and Moritz, R.F.A. 1987. Social control of air ventilation in colonies of honey bees, Apis mellifera. *Journal of Insect Physiology*. **33**(9), pp.623–626.

Tetens, O. 1930. Uber einige meteorologische Begriffe. *Zeitschrift fur Geophysik*. **6**(7), p.297.

Thorsen, S. 2018. Annual Weather Averages in Algiers. *Time and Date AS*. [Online]. [Accessed 16 December 2018]. Available from: https://www.timeanddate.com/weather/south-africa/pretoria/climate.

Villumstad, E. 1974. Importance of hive insulation for wintering , development and honey Yield in Norway. *Apiacta*. **3**, pp.116–118.

Walsh, D.M. 2015. *Organisms, Agency, and Evolution*. Cambridge: Cambridge University Press.

Chapter 5 Honey bee *(Apis mellifera)* size determines colony heat transfer when brood covering or distributed.

This chapter is based upon the authors published work:

Honey bee (Apis mellifera) size determines colony heat transfer when brood covering or distributed. International Journal of Biometeorology. ***66****(8), pp.1653–1663.*

5.1 Abstract

Heat transfer is key to the survival of honey bee colonies (*Apis mellifera* L.) in the wide range of hot (e.g. sub-Saharan) and cool climates (e.g. maritime-temperate) in which they have evolved and adapted. Here, a validated computational fluid dynamics, conjugate heat transfer model was used to determine the heat transfer of honey bee colonies in simulated standard wooden hives, complete with combs and brood, for a broad range of honey bee sizes, from slender lowland African *A.m.scutellata*, to broader (larger diameter) Northern European *A.m.mellifera*, across the whole range of brood covering honey bee densities, as well as when evenly distributed throughout the hive. It shows that under cooling stress, brood covering, broad subspecies need less than a third of the number of bees per unit of brood area for thermal insulation compared to slender subspecies. Also, when distributed evenly around the nest, broad subspecies lose less brood heat than when brood covering. These simulations demonstrate that honey bee girth has climate based evolutionary advantages directly for the colony as well as via the survival of the individual. In addition, it shows non-clustering behavioural patterns of passive honey bees can make significant, subspecies distinctive changes to nest heat loss, and therefore honey production and climate change survival.

Table 5.1: Chapter nomenclature.

Symbol	**Units**	**Description**
∇P	N m^{-3}	Pressure differential per unit length
$\vec{U}$	ms^{-1}	Velocity
β	kgm^{-4}	2nd order velocity coefficient (impact)
α	$Nm^{-4}s$	1st order velocity coefficient (viscous drag)
μ	$Nm^{-2}s$	Dynamic viscosity
φ	-	Porosity
d_P	m	Particle diameter
ρ	kgm^{-3}	Density
$\bar{d}$	m	Generic effective diameter
d_F	m	Effective particle diameter after (Sudarsan et al., 2012)
V_P	m^3	Volume of particle
ψ	-	Shape factor
A_P	m^2	Surface area of particle
d_{SD}	m	Sauter mean value
d_{EQ}	m	Effective particle diameter after (Li and Ma, 2011)
$d_{oriface}$	m	Effective diameter of mesh opening
L	m	Depth of mesh in simulation
ρ_B	m^{-3}	Number of honey bees per unit volume
V_{Bee}	m^3	Average volume of individual Honey bee
l_{Bee}	m	Length of honey bee

5.2 Introduction

Computational Fluid Dynamics (CFD), through the simulation of honey bee nests, their environment and their occupants, can provide insights into multiple subspecies, across multiple climates, which would be difficult and costly, if not impossible, by other means. The goal of the study is to use CFD to simulate the impact of the differing body sizes of the honey bee subspecies on heat transfer from brood areas, in commercially available hives. This research uses the power of CFD to explore both the conventional (e.g. honey bees do not heat the hive (Farrar, 1952)) and alternative hypotheses (e.g. honey bee size is significant factor for hive convection) of temperature and heat transfer related honey bee behaviour by considering a much wider ranging combination of states, ambient temperatures, colony sizes and sub-species than are logistically possible with conventional animal experiments.

Chapter 5 Honey bee (Apis mellifera) size determines colony heat transfer when brood covering or distributed.

By simulating a very small subset of the possible honey bee behaviours (generation of heat in the brood region, and passive obstruction of air flow) in a wide range of condition combinations this research aims to show how the honey bee and its environment interact at a basic level and thus form the basis to understand the intent and results of their more complex behaviours.

This study simulates the different subspecies in identical volume nests/hives but using the bee number densities for the subspecies derived from the literature (Schneider and Blyther, 1988; McNally and Schneider, 1996; Saucy, 2014; Mulisa et al., 2018). This commercially important pollinator, has evolved several (circa 24) subspecies suited to diverse environments from tropical forests and semi-desert to temperate lands that have -40C winters. These subspecies vary in body diameter and body hair length (Ruttner, 1988) demonstrating an increase in both in colder climates. They have also evolved behaviours for selecting and manipulating (Seeley, 1985) their nest thermofluid environment including: nest selection for thermal performance, close temperature regulation in brood area via endothermy and advection, evaporation of large volumes of liquid (nectar to honey 200+kg per year) and the resulting water vapour transport (Mitchell, 2019), and clustering to reduce heat losses.

The ability to withstand changes in ambient temperature without resorting to torpor by clustering in colder climates, in winter inside the nest and in spring outside while swarming, has been related in extensive studies into the thermography (Kovac et al., 2009; Stabentheiner et al., 2021) and metabolic rates (Southwick, 1982). There have also been studies into: the theoretical heat transfer in a clustered state outside of the nest (Myerscough, 1993; Watmough and Camazine, 1995; Basak et al., 1996; Ocko and Mahadevan, 2014); a convective computational fluid dynamic (CFD) analysis of honey bees clustered in a hive (Sudarsan et al., 2012; Thompson, 2013); conductive heat transfer on individual combs (Humphrey and Dykes, 2008) and experimental studies on the lumped conductance of the nest enclosure (Mitchell, 2016). However, there has not been, to date, a study which takes account of: first, both the convective and conductive heat transfer of complete honey bee nests/hives; second, the contribution of those honey bees not clustered and ectothermic by passively resisting air movement; third, differences arising from honey bee size or differences arising from honey bee density.

In the most comprehensive CFD study of hive air flow to date, (Sudarsan et al., 2012), convective airflow through the honey bees was treated as flow through an inert porous material of small cylinders in a perfectly insulated hive. However, that CFD study considered a single fixed honey bee size (11mm length, 3mm dia) from an unpublished estimate, and then derived the narrow porosity range (0.4-0.5) from published known cluster sizes and populations (Heinrich, 1981). This makes the calculations extremely sensitive to the honey bee diameter used (eq. 5.1 and 5.2). In the current study this sensitivity is overcome by both the porosity and honey bee size being treated as independent variables over as wide a range as practicable. This allowed the study of the wide variety of *Apis mellifera* subspecies adapted to various climates in Africa and Europe which exhibit different physical characteristics in both their phenotype i.e. body size, and extended phenotype i.e. their nest.

The volume of the natural nest, and the number of honey bees in them, vary on a subspecies basis, but the number of honey bees per unit volume are within 10% of each other (table 5.2) (Schneider and Blyther, 1988; Saucy, 2014; Mulisa et al., 2018) at around 1.3×10^6 honey bees per m^3. The studies in honey bee taxonomy to date have not focused on body length and diameter, with or without body hair, so the exact dimensions are uncertain and are further complicated by anthropogenic size modification (Saucy, 2014), but the range can be implied from the comb cell size in which the honey bees naturally pupate, and enter to clean etc. The cell sizes are shown in table 5.2. The upper bound has been validated in this study by a limited photometric survey by the author of hybridised European bees located in the UK.

For a given nest volume, the volume surrounding the comb in which the adult honey bees reside (intercomb volume) is, from comb geometry, nearer 0.3 of the total and this is the volume used to calculate the porosity.

Table 5.2: Subspecies cell sizes, colony populations and volumes (Schneider and Blyther, 1988; Saucy, 2014; Mulisa et al., 2018).

	Parameter	**A.m.scutelata**	**European**
1	Nest volume $m^3 \times 10^{-3}$	17	45
2	Population 10^3	6.4	18.8
3	Cell diameter $m \times 10^{-3}$	2.5–4.3	4.4-5.5
4	Cell length $m \times 10^{-3}$	9.5-11.4	11-12
5	Inter-comb gap (bee space) $m \times 10^{-3}$	9-11	9-11
6	Total inter-comb volume $m^3 \times 10^{-3}$	5.1	13.5
7	Individual honey bee volume $m^3 \times 10^{-9}$	54-138	167-261
8	Distributed bee number density in inter-comb volume $m^{-3} \times 10^6$	1.25	1.39
9	Distributed bee volume density in inter-comb volume $m^3\,m^{-3}$	0.07-0.18	0.23-0.36
10	Distributed bee porosity of inter-comb volume	0.82-0.93	0.64-0.77
11	Brood area m^2	0.24	0.59
12	Bees per unit area of brood $m^{-2} \times 10^3$	17.3 - 40.2	24.1– 42.4

5.2.1 Thermofluid modelling

To understand the significance of these differences in heat transfer we need look into the fluid dynamic theory related to porous materials.

The pressure differential caused by porous media such as distributed insects is the Darcy Forchheimer model of pressure difference per unit length across a porous material (Nield and Bejan, 2006).

$$\nabla P = -\alpha \vec{U} - \beta |\vec{U}| \vec{U} \quad (5.1)$$

The first term in equation 5.1 relates to the viscous drag and is the dominant term below Reynolds numbers of 10. The second term relates to the obstruction effects of the particles.

Ergun’s equation formulates α and β as per equations 5.2 and 5.3. (Li and Ma, 2011).

$$\alpha = \mu\, 150 \frac{(1-\varphi)^2}{d_P^2 \varphi^3} \quad (5.2)$$

$$\beta = \frac{\rho}{2} \frac{3.5(1-\varphi)}{d_P \varphi^3} \quad (5.3)$$

But this is not valid for particles that deviate strongly from a spherical shape or have non-uniform size distributions. So d_P is replaced by an effective particle diameter $\bar{d}$ usually calculated from the relationship between the volume and area, equations 5.4 and 5.5.

$$\alpha=\mu\,150\frac{(1-\varphi)^2}{\bar{d}^2\varphi^3} \tag{5.4}$$

$$\beta=\frac{\rho}{2}\frac{3.5(1-\varphi)}{\bar{d}\,\varphi^3} \tag{5.5}$$

Previous workers (Basak et al., 1996; Sudarsan et al., 2012) have used an effective particle diameter d_F (equation 5.6) then apply a shape factor Ψ (equation 7) which gives a result equal to the Sauter mean value d_{SD} (equation 8).

$$d_F=(6V_P)^{\frac{1}{3}}\pi^{-\frac{1}{3}} \tag{5.6}$$

$$\psi=\frac{\pi d_F^2}{A_P}=\frac{\pi^{\frac{1}{3}}(6\,\mathrm{V}_P)^{\frac{2}{3}}}{A_P} \tag{5.7}$$

$$\bar{d}=\psi\,d_F \tag{5.8}$$

$$\bar{d}=d_{SD}=\frac{6\,\mathrm{V}_P}{A_P} \tag{5.9}$$

One experimental engineering study (Li and Ma, 2011) used cylinders quite close to the honey bee in terms of scale and aspect ratio i.e. cylinders 6mm long and 3mm diameter. They determined that a more accurate approximation was to use the product of the shape factor Ψ and the Sauter mean diameter d_{SD} (equation 5.10).

$$\bar{d}=d_{EQ}=\frac{\pi^{\frac{1}{3}}(6\,\mathrm{V}_P)^{\frac{5}{3}}}{A_P^2} \tag{5.10}$$

To use equation 5.10 we need to compute the porosity of the different honey bees in their respective nests when distributed evenly around the nest. From the geometry of the comb and inter-comb spaces we can determine the non comb, honey bee occupied volume of the nest, and hence the number density of the honey bees (ρ_B). This, with the volume of the individual honey bee (V_{bee}), can be used in equation 5.11 to give the porosity.

$$\varphi=1-\rho_B V_{Bee} \tag{5.11}$$

To understand the impact of species differences the variation of the α and β coefficients need to be known, and their consequent changes to the overall heat transfer determined.

5.3 Methods

In order to determine the significance of differences in air resistances to the heat lost from a hive, a CFD simulation of full conjugate heat transfer was conducted of *Apis mellifera* colonies in a standard hive, complete with combs and brood.

A computer aided design model (CAD) model of a standard British National Hive (Cushman, 2011) of approximately 35 litres capacity was constructed using FreeCAD (Riegel and Mayer, 2019). The dimensions taken from an example Western Red Cedar hive and combs supplied by Thornes Ltd. The model simulated 12 standard combs, empty of stores or brood (fig 5.1) except for the 6 central combs each of which had brood areas of approximately 214 by 100mm (fig5.2 a). This model contained: air surrounding the hive (1m by 1m by 2m), mesh floor, entrance, crown board, roof and ventilated roof cavity as well as the internal air volume occupied by honeybees while distributed about the nest. For the clustered data the brood covering volumes 304×140×10 mm were simulated (fig5.2b). This model was then loaded into the CFD tool OpenFOAM v4.1. (Jasak et al., 2007). The comb thickness and inter-comb space were fixed at 25mm and 10mm respectively.

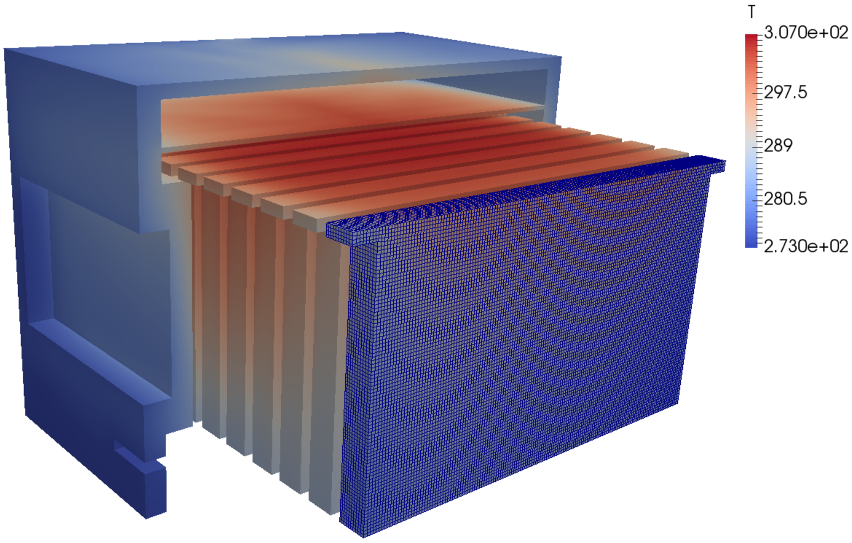

Figure 5.1: Cutaway of CFD model showing combs and typical temperature distribution and meshing.

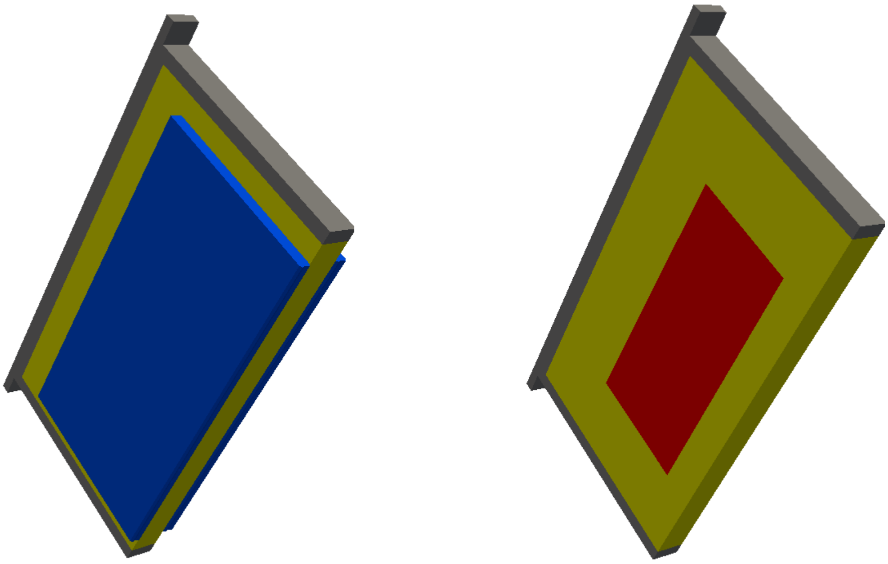

a)

b)

Figure 5.2: CFD Brood comb Frames, with covering honey bees a), and without b) Colour code: frame as grey,comb as yellow, brood covering honey bees as blue, brood cells as red.

5.3.1 Assumptions

The following assumptions were made in the CFD modelling:

3. The honey bee colony is in either one of two states: first, honey bees covering the thermoregulated honey bee brood (*brood covering*), second, evenly distributed around the hive (*distributed*). Conventionally, the *distributed* state can be thought to represent the summer day time or warm climate configuration and the *brood covering* state the colder climate or winter configuration.
4. The honey bees are approximated to cylinders 11mm long and diameters as specified.
5. The volume of brood on each of the six simulated brood containing combs is fixed, rectilinear and isothermally maintained at 307K and is the only heat source within the nest i.e. the contribution from endothermic bees is considered to be located either on the brood surface or within the brood (brood volume).
6. Radiation is ignored for the purposes of this simulation.
7. The flow is transitional from laminar to turbulent and thus amenable to a kwSST turbulence model.
8. Condensation and evaporation is ignored.
9. Thermal conductance of honey bee bodies is ignored.
10. A single fluid, air, is considered.
11. For the *distributed* state, all of the colony bees are simulated as evenly distributed into the space within 10mm of all the internal structures, i.e. a fixed volume of 10.5 litres.
12. In the *brood covering* state, all of the honey bees in the colony are simulated as evenly distributed in 7 fixed brood covering volumes 304×160×10 mm on each face of the 6 brood areas i.e a fixed volume of 3.4 litres. Thus varying porosity and number density values represent colonies with differing numbers of honey bees.

13. The lower limit of porosity, and the highest number density (e.g. when honey bees are clustered at extreme low temperatures), is the geometric limit of close packed cylinders i.e. 0.095.

The model was meshed using the standard OpenFOAM mesh utility *snappyHexMesh*. Care was taken to ensure the mesh was sufficiently fine in the boundary layers to enable valid lower Reynolds number turbulence modelling relevant to a kω-SST turbulence model (Menter et al., 2003; Moukalled et al., 2016) using the y^+ metric. The meshing gave values of $y^+ \sim 10^{-2}$ (CFD-Online, 2014a) inside and around the hive and 4 on the test cell walls. The meshed model was then used in the standard compressible flow, steady state conjugate multi-region heat transfer solver, *CHTmultiRegionSimpleFoam*, with *kω-SST* turbulence using the boundary condition *turbulentTemperatureCoupledBaffleMixed,* for coupling between the solid and fluid regions of the hive. The boundary conditions, at the walls of the volume under test, were set to fixed zero velocity gradient, with the inlet turbulent energy, turbulent dissipation rate and specific turbulent dissipation rate set to fixed values according to the literature *(CFD-Online, 2014b)*. The fixed parameters in table 5.3 were used in the simulation.

The empty comb conductance was selected to be close to that used by other workers (Humphrey and Dykes, 2008), and also suitable for later validation.

The ambient air velocity was chosen after sensitivity testing for a combination of rapid CFD solving and minimal impact on conductance i.e. less than 3%.

Table 5.3: CFD parameters.

	Parameter	**Value**	**Units**
1	Empty comb conductance	0.023	$WK^{-1}m^{-1}$
2	Ambient air velocity (inlet)	0.05	ms^{-1}
3	Inlet turbulent energy *k*	9.79 10-8	m^2s^{-2}
4	Inlet turbulent dissipation rate *ε*	9.94 10-11	m^2s^{-3}
5	Inlet specific turbulent dissipation rate ω	3.38 10-3	s^{-1}
6	Comb frame conductance	0.12	$WK^{-1}m^{-1}$
6	Hive conductance	0.12	$WK^{-1}m^{-1}$
8	Wire mesh pitch	4	mm
9	Wire mesh wire diameter	1	mm
10	Brood covering volume	3.4	litres
11	Model mesh size	3.2	Cells×10^6

5.3.2 Wire mesh and honey bee porosity modelling

in order to simulate the wire mesh, the industry standard formulae (Idelchik, 2006) were used to derive the α and β coefficients.

$$\alpha=\mu\frac{11\varphi}{d_{orifice}L} \tag{5.12}$$

$$\beta=\frac{\rho}{2}\frac{1}{L}\left(1.3(1-\varphi)+(\frac{1}{\varphi}-1)^2\right) \tag{5.13}$$

Both the honey bee volume and the wire mesh α and β coefficients were input into the model as parameters for porosity zones in the air region. This was accomplished using the explicit porosity *fvOption* facility within OpenFoam to modify the governing equations for momentum in the specified zones in order to implement equation 5.1. The thermoregulated brood was emulated as a zone of fixed temperature within the comb region using the explicit heat source *fvOption* facility to modify the governing equations for enthalpy in the specified zones.

The differing zones of thermal conductance within the comb regions were implemented by an enthalpy modification field to scale the conductance to an appropriate level from a generic comb value.

5.3.3 Execution

A separate CFD run was conducted for each combination of:

- Honey bee effective diameter.
- Honey bee porosity.
- *Brood covering* or *distributed* states.
- Ambient temperature.

The iteration steps were continued until the temperatures within the model reached equilibrium, typically after 3500 iterations.

5.3.4 Post processing

The heat flux from the frames into the surrounding air was computed from each of the runs using the wallHeatFlux (Venkatesh, 2016) post processing function. In addition Paraview (Ayachit, 2015), was used to derive visualisations of temperature and air flow. The results along with the key parameters were loaded into an open source SQL database (MariaDB (Widenius, 2020)) and then plotted using MATlab (MATLAB, 2018).

5.3.5 Validation

The CFD was validated by first, validating the CFD model convection/conduction resistance against a physical experiment, second, validating the porosity pressure differential against published results and third, a mesh sensitivity analysis.

The physical experiment used the hive that provided the dimensions for the model. The thermoregulated brood in each comb was emulated by 6 pairs of 12mm thick electrically heated, temperature monitored aluminium plates. The empty comb was emulated by 25mm thick Polyisocyanurate (PIR) insulation.

5.4 Results

5.4.1 Parameter analysis

Given the complexity of the problem it is useful to understand how key parameters interact before interpreting the CFD results. The resistance coefficients, α and β, to convective airflow are derived from the resistance of spheres, by using a conversion from the cylinder dimensions to the diameter of a sphere of the same effective resistance (see effective diameter in equation 5.10).

The variations of the α and β coefficients versus honey bee porosity for constant values of honey bee effective diameter as used in the CFD runs are plotted in figures 5.3a and 5.3b and versus actual honey bee diameter at values of constant number density and actual honey bee length in figures 5.3c and 5.3d.

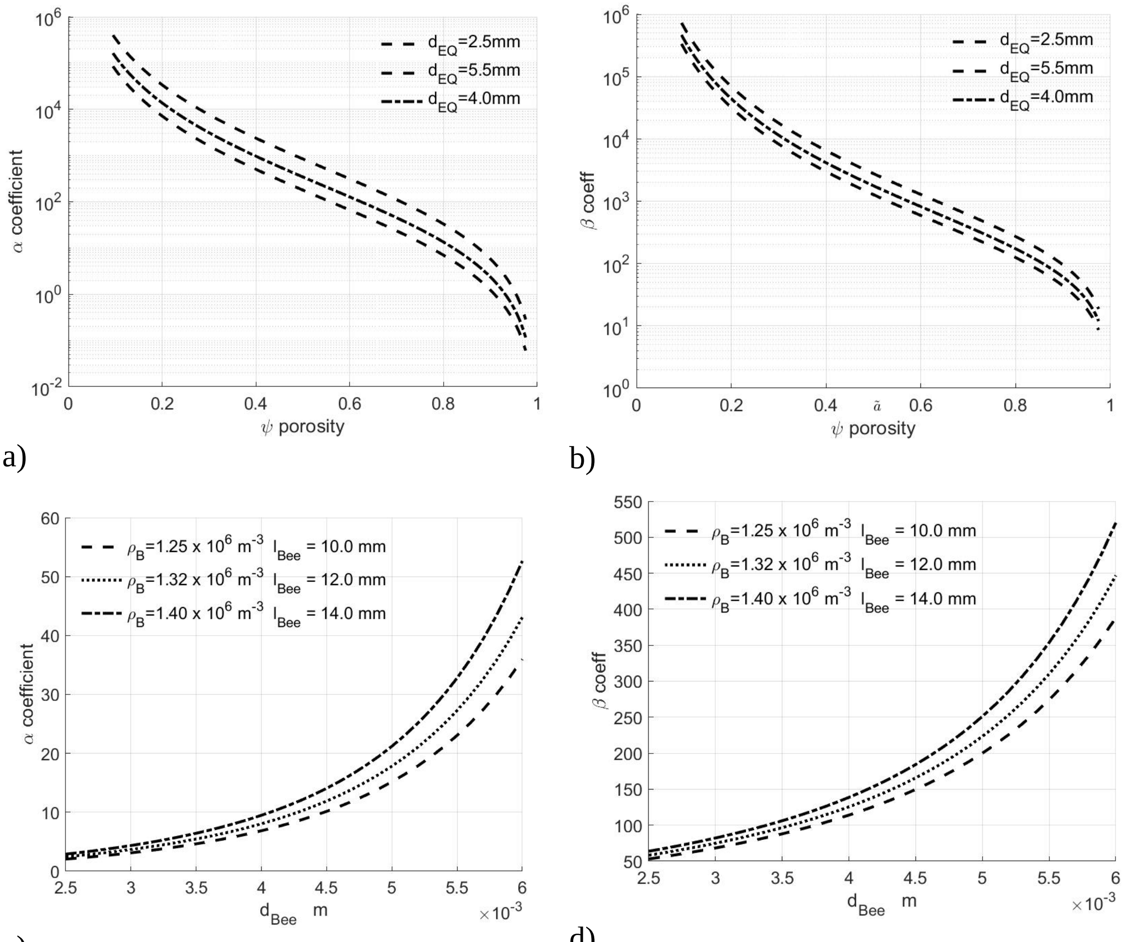

a)

b)

c)

d)

Fig 5.3 *α and β air flow resistance coefficients versus (a) & (b) porosity Ψ for varying effective diameters (d_{EQ}) and (c) & (d) actual bee diameters d_{Bee} at constant bee number densities ρ_B.*

5.4.2 CFD results

For the *brood covering* state, the CFD experiment used the porosity range 0.095 to 1.0 and the *distributed* state a range 0.2 to 1.0, both at temperatures of 273 and 293K. The plot of hive thermal resistance vs honey bee number density at constant ambient temperatures and effective diameter size for both *brood covering* & *distributed* is shown in figure 5.4. The plot of hive thermal resistance vs porosity at constant ambient temperatures and effective diameter size for both *brood covering* & *distributed* is shown in figure 5.5.

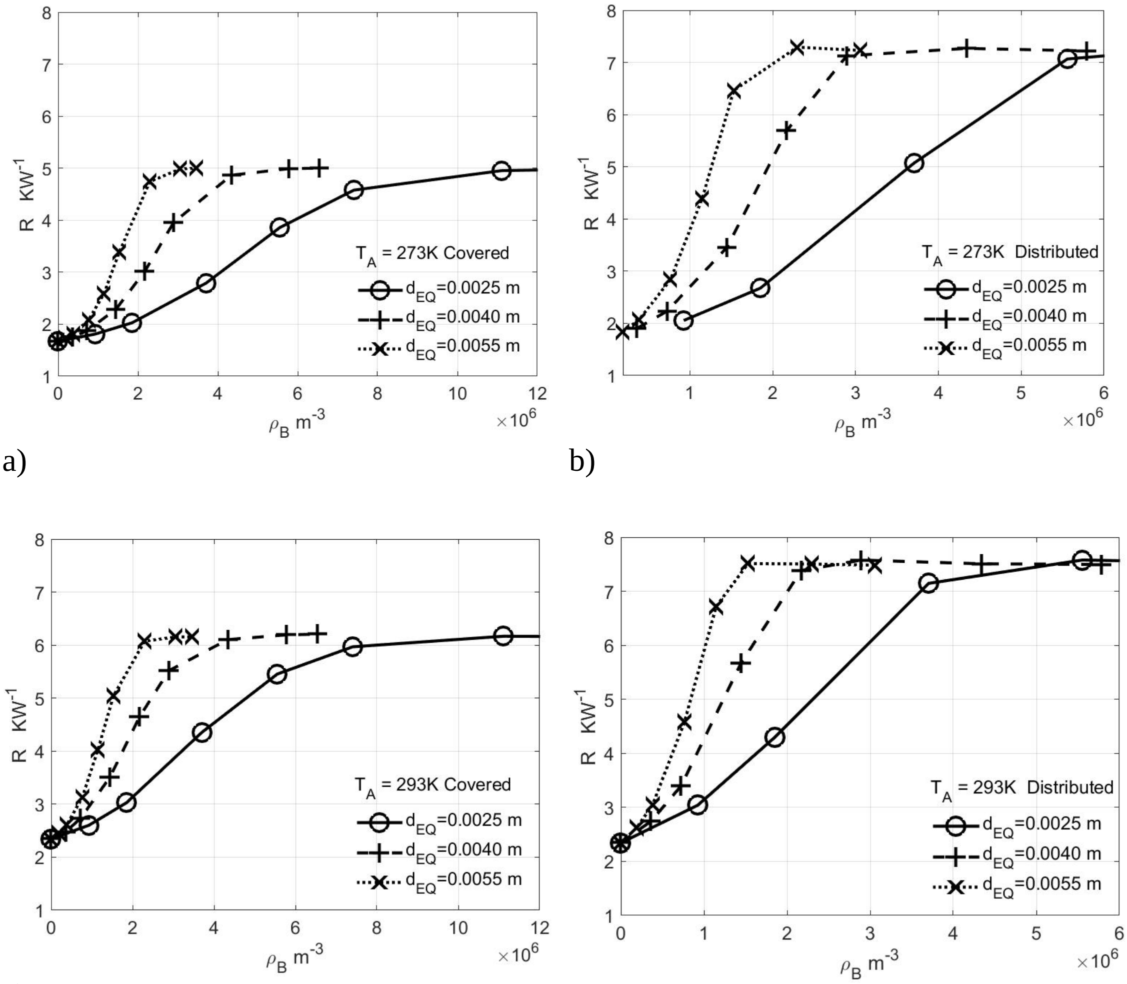

a)

b)

c)

d)

Fig 5.4 *Brood covering & distributed hive thermal resistance vs colony number density for effective diameters at constant ambient temperatures (a) 273K brood covering, (b)273K distributed, (c) 293K brood covering, (d) 293K distributed. The rightmost termination of the lines for distributed indicates the geometric packing limit with the exception of 2.5mm diameter.*

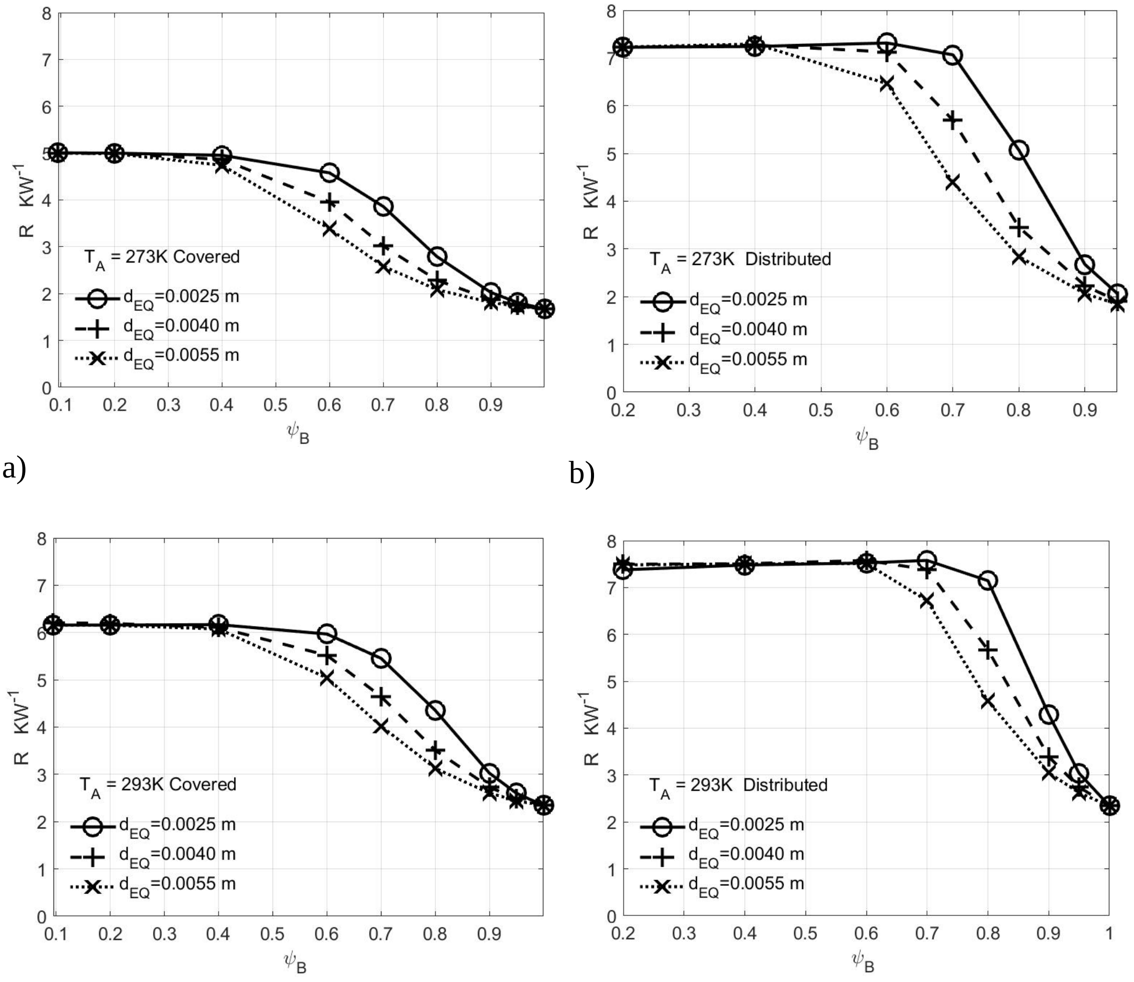

a)

b)

c)

d)

Fig 5.5 *Brood covering & distributed hive thermal resistance vs porosity for constant effective diameters at constant ambient temperatures (a) 273K brood covering, (b)273K distributed, (c) 293K brood covering, (d) 293K distributed.*

5.5 Discussion

From equations 5.1, 5.2 and 5.3, we can see that the key factors determining air resistance, and hence heat transfer are the porosity and the effective diameter of the honey bees. The length of the subspecies varies by about 10% and cause only minor changes in effective diameter. However the difference in diameter is in excess of a factor of two, and in volume by a factor of 5. In contrast the bee number density only changes by 10%. This leads to a difference in porosity when the honey bee are evenly distributed around the nest, with ~95% for low-land *A.m.scutellata* (effective diameter

~2.5mm) compared to ~70%, for European honey bees (effective diameter ~5mm, from table 5.2).

Previous studies (Sudarsan et al., 2012), which concentrated on porosities between 0.4 and 0.5 can now be shown to reside in the region where the thermal resistance is already at its maximum (figure 5.5).

From figures 5.3a and 5.3b, it can be clearly seen that such an apparently small difference in porosities will lead to a marked difference in air resistance coefficients α and β (factor of ~20) and hence thermal resistance. Similarly, at constant number densities changes in diameter of 2.5 to 5.0 mm lead to coefficient changes of a factor of 7 (figures 5.3c & 5.3d). This is borne out by the differences in thermal resistance (figure 5.4) between subspecies at the same number density in both *brood covering* and *distributed* CFD simulations across all temperatures, with the difference of approximately a factor of 2 in thermal resistance between the most extreme African and European subspecies (figures 5.4b 5.4c) at the observed distributed honey bee densities (1.25 and 1.39×10^{6} m^{-3} from table 5.2).

This higher thermal resistance of the colony for broad honey bees, might be seen as part of the adaptation of European honey bees to their colder climate by apparently conforming to Bergmann’s and Allen’s rules (Freckleton et al., 2003; Nudds and Oswald, 2007). These state body size and appendage width to length ratio of homeothermic animals increase inversely with climate temperature, because of the change in body surface area to volume ratio. While often reliable with mammals, it should be noted these rules are not suitable for Hymenoptera (Shelomi, 2012) or even social bees (Gérard et al., 2018). Given *Apis mellifera* are not homeotherms, can be either ectothermic or strongly endothermic, and spend 80%+ of their lifetime inside the nest, including the times of greatest seasonal or daily thermal stress, the individual’s body surface area to volume ratio is of diminished relevance and weakens Bergmann’s validity in honey bees. The heat loss causality for Allen’s rule is also weak for honey bees given that the heat source i.e. muscles, is in the thorax. Reduced limb length is observed in more northerly bees (Ruttner, 1988), and the resulting shortened gait may be interlinked with the higher number densities observed in northern honey bees. This is feasible if the honey bees were density regulated by the number of honey bee steps between honey bee to honey bee encounters, honey bee density sensitivity and step counting being known in other behaviours (Seeley, 1977; Smith et al., 2017). The resulting higher number densities can then combine with girth to increase airflow resistance (figures 5.3c, 5.3d).

The case for air flow resistance driving girth changes is further strengthened owing to the fact that the classic surface area to body ratio is a linear phenomenon, whereas resistance to nest airflow rises close to the cube of body diameter (figures 5.3c and 5.3d).

It has been observed that the length of body hair on honey bees has a correlation with latitude (Ruttner, 1988). The longer hair has been credited with giving greater heat retention when tightly clustered (Southwick, 1983), however, it can be seen that the upper limit of thermal resistance is reached well before cylinder packing limit (figure 5.4). Therefore the increase in hair length is not relevant to being tightly clustered, but is useful in reducing the individuals and colonies heat loss, not only by impeding air flow (Bejan, 1990) to the surface of the individual e.g. outside the hive, but also by reducing the colony's porosity via increasing the honey bees individual volume. Thus the very low porosity of winter clustering does not improve thermal resistance of the core endothermic honey bees, but instead improves thermal contact between the individuals and the core. However, if thermal contact with other honey bees was dominant for evolution, then maximisation of surface area would occur and a converse Bergmann relation would be observed in a similar manner to ectotherms needing surface area to gain heat from the sun.

The upper thermal resistance limit indicates the honey bee density at which the air stops moving under convection and heat transfer is by conduction through the air either in the brood cover volume or the space occupied by the distributed honey bees. Thus at the observed distributed number densities we can see that broad subspecies are close to the thermal resistance limit i.e. conduction only, while the slender subspecies are distant from the thermal resistance limit and thus the interior is strongly convective. This is indicative of a strong adaptation to climate for active colonies, with the slender subspecies able to dissipate heat in a warm climate, and the broad species retain it in a cool climate.

A surprising result is the thermal resistance of a *distributed* colony at the observed distributed number density is greater than thermal resistance limit for *brood covering* for the broad subspecies (figures 5.4a and 5.4c) and the reverse for slender subspecies. While for broad subspecies in cool climates, the *distributed* state reduces heat loss, for the slender subspecies, in the *distributed* state, at lower ambient temperatures, individual honey bees near the periphery would fail to stay above fatal temperatures.

This suggests that the driver for broad subspecies to brood cover is not directly for colony survival by reducing colony heat loss, but is driven by other behaviours and needs.

In the active season, this closeness in broad subspecies to the upper thermal limit when natural convection is close to being suppressed, implies that there are circumstances where honey bees will have to move to allow natural convection or forced convection to take place. Whereas studies of patterns of behaviour have previously been focused on action e.g. endothermy in the brood area or storing pollen and nectar, it can now be seen that the location of inactive ectothermic honey bees can have a significant impact on the thermofluid processes in the nest. Evidence of this is apparent when honey bees come out of the nest en-mass and wait around the entrance, called “bearding” (Hamdan, 2010). To date this has been labelled as “over heating” or “over crowding” but may in fact be behavioural movements to allow air flow based activity such as honey dessication.

The role of the male bees, a larger diameter minority (approximately 20% and cell size > 6mm) occupant of the nest, (Seeley, 1985), becomes of interest, particularly, since they have been observed to frequently congregate on outer frames of the nest, where their larger bodies, if at the same number density, would impart a stronger resistance to air flow down the cooler surfaces of the nest and hence present an effective thermal resistance. This is of relevance since male honey bees are present in the nest for large periods of the year when lower temperatures, e.g. at night, can be found. This is illustrated by *A.m. mellifera,* a large diameter subspecies, whose drones can be present from April to August and its external night time environment can be close to 0 C.

It is likely that there are other such behaviours that passively manipulate the airflow, not yet noted or studied.

For brood covering honey bees at ambient 293K (figure 5.5c), if we consider the bee densities, where the limit of thermal resistance is reached, we can see it is markedly different for 2.5mm and 5.5mm diameter bees i.e. ~11.5 and 3×10^6 m^{-3}. Thus if thermal stress resistance is a limiting factor for brood production, then the broad sub species can cover over 3 times the brood area compared to slender species for the same thermal stress. That both broad and slender have similar numbers of bees per unit area of brood (table 5.2) may indicate the differences of thermal stress caused by the climates of the sub species involved.

This study considers *brood covering* and *distributed* honey bee densities as isolated states, where as in reality they are a continuum bounded by the total colony population. Thus there is further work to be done e.g. using colony size and a *brood covering* to *distributed* blending function instead of honey bee number density.

5.6 Conclusion

This study has shown:

- Body hair has an impact on colony heat transfer but not when tightly clustered
- Body diameter halves brood heat loss for broad subspecies.
- Tight clustering is primarily for individual survival by thermal contact.
- “Doing nothing” ectothermic honey bees are reducing heat transfer especially when large diameter i.e. drones.
- Honey bees gathering outside the hive, for broad subspecies, is a necessary method of increasing heat transfer and internal air transport.
- The normally assumed causation of the apparent conformity to Bergmann's and Allen’s rules, where the ratio of individual surface area to individual volume determines size, is unreliable. Here it appears that it is the relation of colony number density to total colony body volume (i.e. individual girth) that is significant in determining the variation of body size with latitude.

These insights should influence how researchers and bee keepers interpret the acclimation and behaviour of the different subspecies of honey bees and consider patterns of distribution of relatively inactive honey bees as worthy of notice. It is clear that CFD can provide numerous new biological insights into multiple subspecies of honey bees across multiple climates, which would be difficult and costly, if not impossible, by other means, and provides a means of testing the physical validity of hypotheses of evolutionary pressure.

5.7 References

Ayachit, U. 2015. *The ParaView Guide: A Parallel Visualization Application*. Kitware, Incorporated.

Basak, T., Rao, K.K. and Bejan, A. 1996. A model for heat transfer in a honey bee swarm. *Chemical Engineering Science*. **51**(3), pp.387–400.

Bejan, A. 1990. Theory of heat transfer from a surface covered with hair. *Journal of Heat Transfer*. **112**(3), pp.662–667.

CFD-Online 2014a. Dimensionless wall distance (y plus). *CFD-Online*. [Online]. [Accessed 2 February 2022]. Available from: https://www.cfd-online.com/Wiki/Dimensionless_wall_distance_(y_plus).

CFD-Online 2014b. Turbulence free-stream boundary conditions. [Accessed 2 February 2022]. Available from: https://www.cfd-online.com/Wiki/Turbulence_free-stream_boundary_conditions.

Cushman, D. 2011. Drawings of Hives and Hive Parts. *Dave Cushman's Beekeeping and Bee Breeding Website*.

Farrar, C.L. 1952. Ecological Studies on Overwintered Honey Bee Colonies. *Journal of Economic Entomology*. **45**(3), pp.445–449.

Freckleton, R.P., Harvey, P.H. and Pagel, M. 2003. Bergmann's rule and body size in mammals. *American Naturalist*. **161**(5), pp.821–825.

Gérard, M., Vanderplanck, M., Franzen, M., Kuhlmann, M., Potts, S.G., Rasmont, P., Schweiger, O. and Michez, D. 2018. Patterns of size variation in bees at a continental scale: does Bergmann's rule apply? *Oikos*. **127**(8), pp.1095–1103.

Hamdan, K. 2010. The Phenomenon of Bees Bearding. *Bee World*. **87**(2), pp.22–23.

Heinrich, B. 1981. *The Mechanisms and Energetics of Honeybee Swarm Temperature Regulation*.

Humphrey, J.A.C. and Dykes, E.S. 2008. Thermal energy conduction in a honey bee comb due to cell-heating bees. *Journal of Theoretical Biology*. **250**(1), pp.194–208.

Idelchik, I.E. 2006. Handbook of hydraulic resistance (3rd edition). *Washington*.

Jasak, H., Jemcov, A. and Tukovic, Z. 2007. OpenFOAM : A C ++ Library for Complex Physics Simulations. *International Workshop on Coupled Methods in Numerical Dynamics*. **m**, pp.1–20.

Kovac, H., Stabentheiner, A. and Brodschneider, R. 2009. Contribution of honeybee drones of different age to colonial thermoregulation. *Apidologie*. **40**(1), pp.82–95.

Li, L. and Ma, W. 2011. Experimental Study on the Effective Particle Diameter of a Packed Bed with Non-Spherical Particles. *Transport in Porous Media*. **89**(1), pp.35–48.

MATLAB 2018. *9.4.0.813654 (R2018a)*. Natick, Massachusetts: The MathWorks Inc.

McNally, L.C. and Schneider, S.S. 1996. Spatial distribution and nesting biology of colonies of the African honey bee Apis mellifera scutellata (Hymenoptera: Apidae) in Botswana, Africa. *Environmental Entomology*. **25**(3), pp.643–652.

Menter, F.R., Ferreira, J.C. and Esch, T. 2003. The SST Turbulence Model with Improved Wall Treatment for Heat Transfer Predictions in Gas Turbines. *International Gas Turbine Congress 2003*. (1992), pp.1–7.

Mitchell, D. 2019. Nectar, humidity, honey bees (Apis mellifera) and varroa in summer: A theoretical thermofluid analysis of the fate of water vapour from honey ripening and its implications on the control of Varroa destructor. *Journal of the Royal Society Interface*. **16**(156).

Mitchell, D. 2016. Ratios of colony mass to thermal conductance of tree and man-made nest enclosures of Apis mellifera: implications for survival, clustering, humidity regulation and Varroa destructor. *International Journal of Biometeorology*. **60**(5), pp.629–638.

Moukalled, F., Managai, L. and Dawish, M. 2016. *The Finite volume method in computational Fluid dynamics*. Heidelburg: Springer.

Mulisa, F., Alemayehu, A., Diribi, M., Fekadu, B. and Alayu, T. 2018. Determination of bee spacing and comb cell dimensions for Apis mellifera Scutellata honeybee race in western Ethiopia. *International Journal of Livestock Production*. **9**(8), pp.206–210.

Myerscough, M.R. 1993. A simple model for temperature regulation in honeybee swarms. *Journal of Theoretical Biology*. **162**(3), pp.381–393.

Nield, D.A. and Bejan, A. 2006. *Convection in Porous Media*. Springer.

Nudds, R.L. and Oswald, S.A. 2007. An interspecific test of Allen’s rule: Evolutionary implications for endothermic species. *Evolution*. **61**(12), pp.2839–2848.

Ocko, S.A. and Mahadevan, L. 2014. Collective thermoregulation in bee clusters. *Journal of the Royal Society Interface*. **11**(91).

Riegel, J. and Mayer, W. 2019. FreeCAD (Version 0.18).

Ruttner, F. 1988. *Biogeography and Taxonomy of Honeybees*.

Saucy, F. 2014. On the natural cell size of European honey bees: A ‘fatal error’ or distortion of historical data? *Journal of Apicultural Research*. **53**(3), pp.327–336.

Schneider, S. and Blyther, R. 1988. The habitat and nesting biology of the African honey bee Apis mellifera scutellata in the Okavango River Delta, Botswana, Africa. *Insectes Sociaux*. **35**(2), pp.167–181.

Seeley, T.D. 1985. *Honeybee Ecology: A Study of Adaptation in Social Life*. New Jersey, United States: Princeton University Press.

Seeley, T.D. 1977. Measurement of nest cavity volume by the honey bee (Apis mellifera). *Behavioral Ecology and Sociobiology*. **2**(2), pp.201–227.

Shelomi, M. 2012. Where are we now? Bergmann’s rule Sensu Lato in insects. *American Naturalist*. **180**(4), pp.511–519.

Smith, M.L., Koenig, P.A. and Peters, J.M. 2017. The cues of colony size: How honey bees sense that their colony is large enough to begin to invest in reproduction. *Journal of Experimental Biology*. **220**(9), pp.1597–1605.

Southwick, E.E. 1982. Metabolic energy of intact honey bee colonies. *Comparative Biochemistry and Physiology -- Part A: Physiology*. **71**(2), pp.277–281.

Southwick, E.E. 1983. The honey bee cluster as a homeothermic superorganism. *Comparative Biochemistry and Physiology -- Part A: Physiology*. **75**(4), pp.641–645.

Stabentheiner, A., Kovac, H., Mandl, M. and Käfer, H. 2021. Coping with the cold and fighting the heat: thermal homeostasis of a superorganism, the honeybee colony. *Journal of Comparative Physiology A: Neuroethology, Sensory, Neural, and Behavioral Physiology*. **207**(3), pp.337–351.

Sudarsan, R., Thompson, C., Kevan, P.G. and Eberl, H.J. 2012. Flow currents and ventilation in Langstroth beehives due to brood thermoregulation efforts of honeybees. *Journal of Theoretical Biology*. **295**, pp.168–193.

Thompson, C. 2013. a Cfd Study Investigating the Influence of Bottom Board Geometry on Physical Processes Within a Standard Honeybee Hive. *Journal of Chemical Information and Modeling*. **53**(9), pp.1689–1699.

Venkatesh, V. 2016. CFD with OpenSource software Tutorial of convective heat transfer in a vertical slot. *Proceedings of CFD with OpenSource Software*.

Watmough, J. and Camazine, S. 1995. Self-organized thermoregulation of honeybee clusters. *Journal of Theoretical Biology*. **176**(3), pp.391–402.

Widenius, U.M. 2020. MariaDB version 10.2.36.

Chapter 6 Simulating the built environment for another globally distributed species

This chapter is based upon the authors published work:

Simulating the built environment for another globally distributed species In: Proceedings of BSO Conference 2022: 6th Conference of IBPSA-England [Online]. BSO Conference. Bath, UK: IBPSA-England. Available from: https://publications.ibpsa.org/conference/paper/?id=bso2022_40.

6.1 Abstract

Simulating the built environment for a globally distributed and diverse species e.g. to cope with climate change, has particular challenges. These are explored here using honey bees (*Apis Mellifera L*), a vital pollinator of food crops worldwide, consisting of 24 subspecies that maintain close temperature and humidity control in a self-constructed or partly human constructed built environment. Honey bee thermofluid characteristics and their requirements of the structure are largely unknown.

To address this an open source i.e. FreeCAD (Riegel and Mayer, 2019) and OpenFOAM (Jasak et al., 2007), computational fluid dynamics (CFD) conjugate heat model was developed.

Results from the model demonstrate the power of CFD in investigating the interactions with their built environment of another species by showing significant variation in convection flow with different honey bee subspecies in differing distributions within the nest.

6.2 Key Innovations

- Conjugate heat model of honey bee built environment including external and internal structures and occupants.
- Does not assume all honey bees are those from a single European subspecies.
- Enables the simulation of subspecies differences as well as hive design and climatic impacts.

6.3 Practical Implications

- This model enables refinement of the human contribution to hive design, to take into account subspecies and climate differences.
- It enables determination of evolutionary factors that have changed honey bee physical characteristics and behaviours. This is important for enabling the continuing efficiency and survival of this pollinator in the face of climate change.

Table 6.1 Chapter Nomenclature.

Symbol*	**Units**	**Description**
∇P	N m^{-3}	Pressure differential per unit length
$\vec{U}$	ms^{-1}	Velocity
β	kgm^{-4}	2nd order velocity coefficient (impact)
α	$Nm^{-4}s$	1st order velocity coefficient (viscous)
μ	$Nm^{-2}s$	Dynamic viscosity
φ	-	Porosity
ρ	kgm^{-3}	Density
$\bar{d}$	m	Generic effective diameter
V_P	m^3	Volume of particle
A_P	m^2	Surface area of particle
$\bar{d}$	m	Effective particle diameter
$d_{oriface}$	m	Effective diameter of mesh opening
L	m	Depth of mesh in simulation
ρ_B	m^{-3}	Honey bees per unit volume
V_{Bee}	m^3	Average volume of individual bee
A_S	m^2	Area of hive surface less the area of underfloor mesh
A_i	m^2	Area of inter-comb gap element (i) on Hive internal top surface
f_i	-	View factor of inter-comb gap element (i) on Hive internal top surface
$R_{CS(j)}$	$W^{-1}K$	Brood comb to hive surface lumped thermal resistance*
$R_{SA(j)}$	$W^{-1}K$	Hive external surface to ambient convective/conductive thermal resistance*
$R_{SAR(j)}$	$W^{-1}K$	Hive external surface to ambient radiative resistance*
$R_{CM(j)}$	$W^{-1}K$	Hive internal top surface mesh pass through radiative resistance*
$R_{CA(j)}$	$W^{-1}K$	Hive internal top surface mesh absorptive radiative resistance*
$\dot{q}_{E(j)}$	W	Brood comb heat flux*
$\dot{q}_{C(j)}$	W	Sum of radiated heat flux from brood comb downwards*

Symbol*	**Units**	**Description**
$\dot{q}_{CA(j)}$	W	Estimated downwards radiated heat flux brood comb to wire mesh absorbed*
$\dot{q}_{CM(j)}$	W	Downwards radiated heat flux brood comb to ambient*
$\dot{q}_{SA(j)}$	W	Convective/conductive heat flux hive top surface to ambient*
$\dot{q}_{SAR(j)}$	W	Radiated heat flux hive top surface to ambient*
$T_{S(j)}$	K	Hive surface temperature*
$T_{A(j)}$	K	Ambient temperature*
$T_{B(j)}$	K	Brood temperature*
$T_{M(j)}$	K	Temperature of wire mesh - physical experiment*
σ	$Wm^{-2}K^{-4}$	Stephan-Boltzmann constant 5.8×10^{-8}
ε_m	-	Emissivity of hive floor metal mesh 0.9
ε_S	-	Emissivity of hive external surface 0.9
φ	-	Porosity of hive floor mesh

Note :* j is one of *cfd, exp, lr, and lnr* models used in validation.

6.4 Introduction

Built environment simulation is almost completely focused on the relatively homogenous species *Homo sapiens*. However more diverse social species build structures that they inhabit.

The honey bee, a commercially important pollinator, has evolved several (circa 24) subspecies suited to diverse environments ranging from tropical forests and semi-desert to temperate lands that have 233K winters. These subspecies vary in body diameter and body hair length (Ruttner, 1988) showing an increase of both in colder climates. Behaviours have evolved for selecting and manipulating their nest thermofluid environment including: nest cavity selection (usually a tree hollow) for thermal performance (Seeley, 2019) (e.g. volume, entrance size, entrance location); close temperature regulation in brood area via endothermy and advection; evaporation of large volumes of liquid (nectar to honey 200+kg per year) and the resulting water vapour transport (Mitchell, 2019); and clustering to reduce heat losses. Their construction of comb in the cavity reduces the large void of the nest cavity into a series of vertical narrow slots approximately 10mm wide with total free volume of only 30%

of the original (Mitchell, 2022), the cell of the comb opening on to the slots with their long axis close to horizontal. In addition the honey bees coat the inside of the nest with a vapour retardant barrier made from plant resins propolis. They use the same material to close redundant openings in the cavity. They use this built environment to achieve both the temperature and humidity management for brood rearing i.e. 307K+/- 0.5, 80% RH and the low humidity (50%RH) required for the desiccation of low sugar concentration (20% to 40%) nectar in to high sugar concentration honey (82%+). The honey bees achieve this by self-organised zoned air conditioning via: sensitive temperature and humidity sensing on their antennae; heating using thorax muscles; ventilation through wing movements; and humidification by distributing water and dilute nectar throughout the nest. Further, the honey bees position themselves as obstructions to convective air currents as seen when they cluster in winter or when outside the nest (Heinrich, 1981).

Previous CFD research into honey bees inside their nest has not taken into account the global diversity in subspecies or climate, thermal properties of the hive walls or variation in honey bee distribution around the hive (Sudarsan et al., 2012). Similarly CFD research into other nest constructing species (*Macrotermes Michaelseni*, (Abou-Houly, 2010) *Polybia scutellaris,* (Hozumi et al., 2011)) have only concentrated on single subspecies and climate and not taken account of the effect of the occupants.

The biological implications of this research for this species have been discussed in detail elsewhere (Mitchell, 2022), while this paper will concentrate on the CFD modelling and verification.

Modelling an occupied structure necessitates not only knowledge of the environmental factor and the structure but also the key parameters of the inhabitants. Previous CFD research looked only at a single size of honey bee while treating it as a porous medium consisting of cylinders with a limited range of porosities located near the brood area. In order to address the global diversity in honey bees it was necessary in this research to include the full range of honey bee sizes and likely porosities.

Obtaining such information is challenging as often biological research has differing goals to building simulation and so in this case the dimensions have to be inferred indirectly from sizes of the cells in which the insects pupate. This is further complicated by subspecies having varying hair length which will change their effective dimensions (Ruttner, 1988), and human manipulation of body size by changing the cell size they use. The different subspecies have differing nest volumes and colony numbers in addition to body size. However from current research, it is possible to derive a range of honey bee diameters, lengths and number densities that cover all honey bee subspecies, see Table 6.2.

Table 6.2 Subspecies cell sizes, colony populations and volume (Schneider and Blyther, 1988; Saucy, 2014; Mulisa et al., 2018).

Parameter	**Tropical**	**Temperate**
Nest Volume $m^3 \times 10^{-3}$	17	45
Population 10^3	6.4	18.8
Cell diameter $m \times 10^{-3}$	2.5–4.3	4.4-5.5
Cell length $m \times 10^{-3}$	9.5-11.4	11-12
Distributed bee number density in inter-comb volume $m^{-3} \times 10^6$	1.25	1.39

Thus for given length and diameter and number density one can determine a porosity, equation 6.5, and hence an effective diameter in equation 6.4 (Li and Ma, 2011), which in turn can determine the coefficients that give the relationship between pressure differential per unit length and air velocity in equations 6.1, 6.2, 6.3, (Ergun and Orning, 1949).

$$\nabla P = -\alpha \vec{U} - \beta |\vec{U}| \vec{U} \tag{6.1}$$

$$\alpha = \mu\, 150 \frac{(1-\varphi)^2}{\bar{d}^2 \varphi^3} \tag{6.2}$$

$$\beta = \frac{\rho}{2} \frac{3.5(1-\varphi)}{\bar{d}\,\varphi^3} \tag{6.3}$$

$$\bar{d} = \frac{\pi^{\frac{1}{3}} (6 V_P)^{\frac{5}{3}}}{A_P^2} \tag{6.4}$$

$$\varphi = 1 - \rho_B V_{Bee} \tag{6.5}$$

Most modern designs of man-made honey bee hive follow a pattern of stacked thin walled (~ 19mm) open top and bottom wooden box sections (~470×470×300 mm). On the top of the box sections is a thin plywood cover surmounted by a more substantial roof.

These sections sit on stand via a low floor section (~19 mm high) incorporating an entrance (10×100mm) and a mesh covered opening beneath. So the same approach of modelling as porosity can be used to incorporate that feature in equations 6.6 and 6.7 (Idelchik, 2006).

$$\alpha=\mu\frac{11\varphi}{d_{orifice}L} \tag{6.6}$$

$$\beta=\frac{\rho}{2}\frac{1}{L}\left(1.3(1-\varphi)+\left(\frac{1}{\varphi}-1\right)^{2}\right) \tag{6.7}$$

The small scale and complexity of internal features and passages (<5mm) combined with the much larger enclosure (~0.5m) created a challenge to simulate efficiently and comprehensively.

6.5 Simulation Methods

The world-wide adoption of similar pattern hives enabled the use of a common model for the enclosure (British National hive (Cushman, 2011)) as depicted in partial cross section in figure 6.1. The CAD model was produced using FreeCAD with all of the construction parameters stored in MySQL.

The hive geometry provided particular challenges for meshing given a total volume of the simulation of 2 m^3 with the need to provide sufficient cells for solids and fluid details as small as 4mm. This was achieved using the OpenFOAM adaptive meshing tool snappyHexMesh layering feature as can be seen in figure 6.2. This enabled a high quality mesh with a minimum 4 cells in any dimension for any feature.

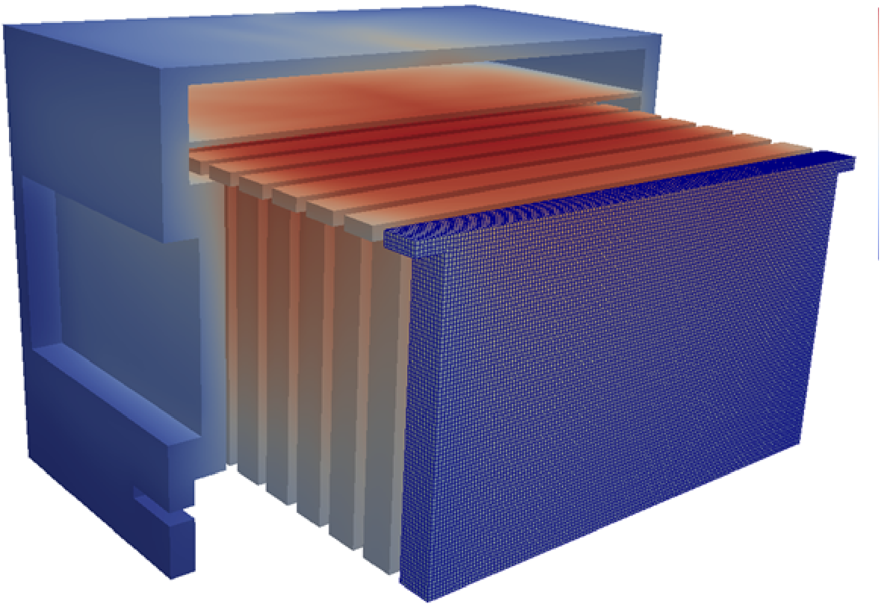

Figure 6.1: Cutaway of CFD model shows combs, cover board and roof.

The hive modelled was of 35 litres total capacity empty with 12 combs with centrally located constant temperature (307K) iso-thermal brood areas 214 × 100 mm in 6 of these combs. Two states of honey bee distribution were modelled, *"brood covering"* and "*distributed*". In the *distributed* state the bees were assumed to be at uniform number density in all of the free space within 10mm of the combs. In the *brood covering* state the honey bees were assumed to be solely located in 340×140×10mm volumes adjacent to each brood area. The only heat generation being the brood areas. Radiation was ignored. A standard compressible flow, steady state conjugate multi-region heat transfer solver, CHTmultiRegionSimpleFoam was used. As laminar flow was likely, but uncertain, a kω-SST turbulence model was selected with inlet turbulent energy, turbulent dissipation rate and specific turbulent dissipation rate set to fixed values according to the literature (CFD-Online, 2014b). The OpenFOAM feature fvOptions was used to generate the porosity zone simulating the honey bees and the floor wire mesh and the constant temperature zone simulating the brood within the comb. An enthalpy modifying field was used to give the varying conductivity zones within the comb regions to simulate the wooden frame (0.12 Wm^{-1}) the empty comb (0.023Wm^{-1}) and the brood (0.6Wm^{-1}) using values from the literature (Humphrey and Dykes, 2008) The hive cover board and roof were modelled as separate regions with a conductivity of 0.12Wm^{-1}. Condensation, evaporation and conductivity of the honey bees were not considered.

A separate CFD run was conducted for each combination of:

- Honey bee effective diameter, (2.5, 4.0, 5.5mm).
- Honey bee porosity 0.09 to 1.0.
- Brood covering or distributed states.
- Ambient temperature. (263, 273, 283, 293K).

The iteration steps were continued until the temperatures within the model reached equilibrium, typically after 3500 iterations. For post-processing, the heat flux from the frames into the surrounding air was computed from each of the runs using the wallHeatFlux (Venkatesh, 2016) post-processing function similarly for the y^+ (CFD-Online, 2014a) turbulence metric. In addition Paraview (Ayachit, 2015), was used to derive visualisations of temperature and air flow. The results along with the key parameters were loaded into an open source SQL databaseand then plotted using MATlab (MATLAB, 2018).

6.6 Sensitivity Analysis

6.6.1 Mesh sensitivity

Cell mesh sensitivity was tested using the same case parameters for 3 different numbers of cells per hive model. 3.2 million, 5.4 million and 9.2 million and the corresponding brood heat flux in table 6.3. 3.2 million being the normally used number for the hive cases. The magnitude of the deviation shows that the simulations are insensitive to cell numbers above 3.2 million. This is a result of the careful use of *snappyHexMesh* meshing utility features such as layering and taking care over mesh quality e.g. minimum numbers (>4) of cells in small features.(Knupp, 2002; Baker, 2005).

Table 6.3: Cell mesh sensitivity.

Initial number of Cells	**Refined number of Cells**	**Wall heat flux W**	**%Deviation**
31 250	3 219 444	-5.886	-0.01%
595 582	5 425 939	-5.919	+0.46%
1 118 638	9 215 215	-5.870	-0.37%

The differences between the 3.2 million cell mesh (figure 6.2a) and the 9.2 million cell meshes (figure 6.2b) are subtle and appear to be of marginal importance.

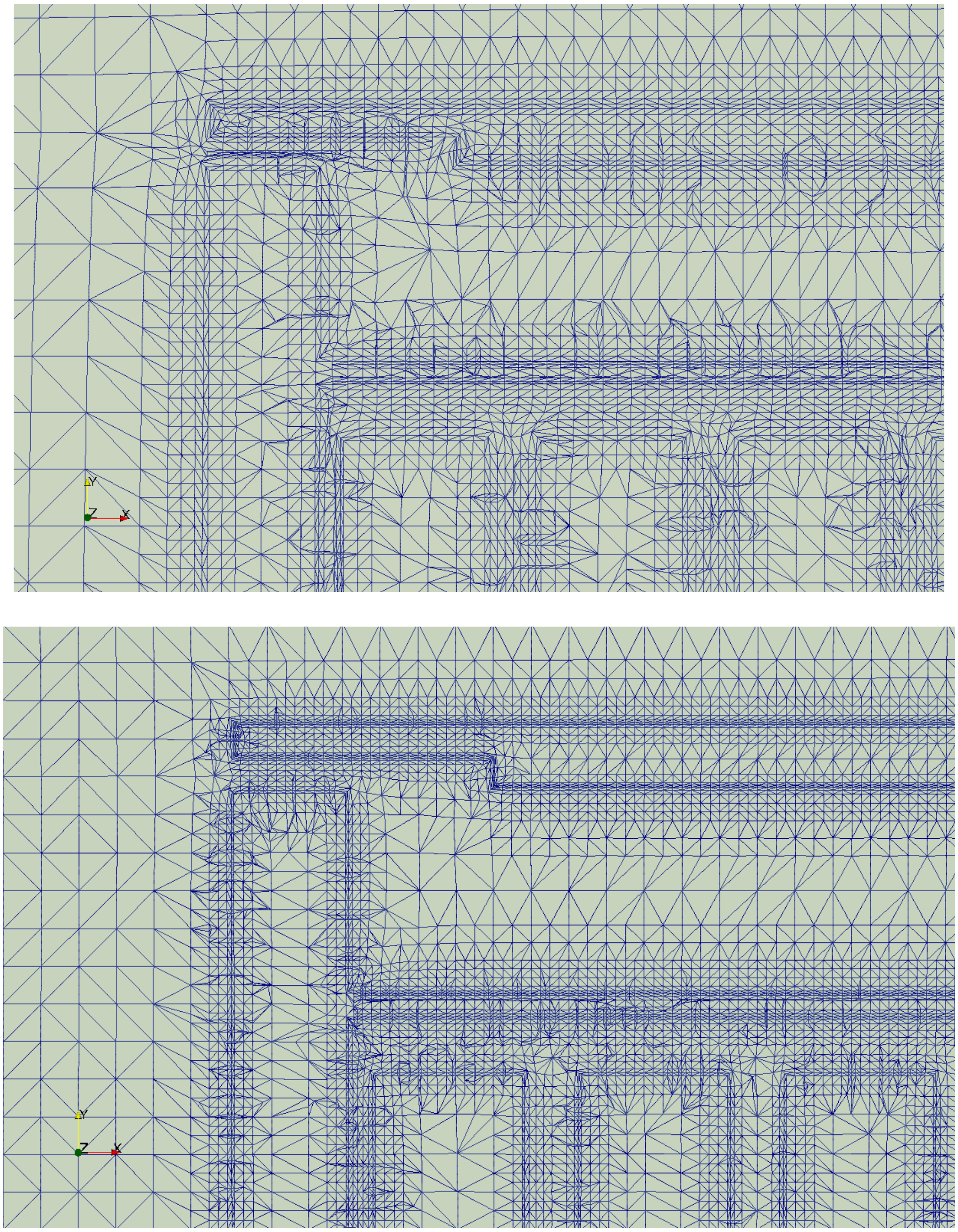

a)

b)

Figure 6.2: Meshing detail from: a) 3.2 million cell mesh, b) 9.2 million cell mesh.

6.6.2 Ambient air velocity sensitivity

A series of ambient air velocities i.e. air velocity across the test object, were tested to see if there was sensitivity to forced convection from the air velocities used. A value of zero ambient velocity in the test was avoided as this made the convergence of the model uncertain. This meant that a low enough velocity needed to be chosen as a base line for approximation to still air. To achieve this a series of CFD runs (N=84) was conducted with varying inlet velocity, honey bee covering and openings surrounding the comb, at constant ambient temperature and then measuring the nest thermal resistance. It became clear that there were two distinct velocity regions: One region above 0.2 ms^{-1} with fairly slow rise in resistance with decreasing velocity (-1.3 $KW^{-1}m^{-1}s$ figure 6.3a) another below 0.2 ms^{-1} where the resistance rose rapidly (-5 $KW^{-1}m^{-1}s$ figure 6.3b) with decreasing velocity.

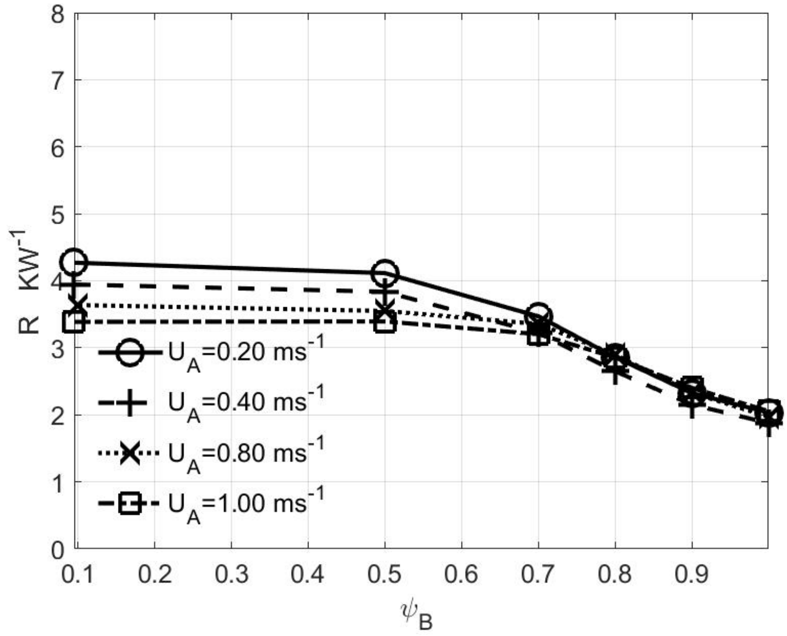

a)

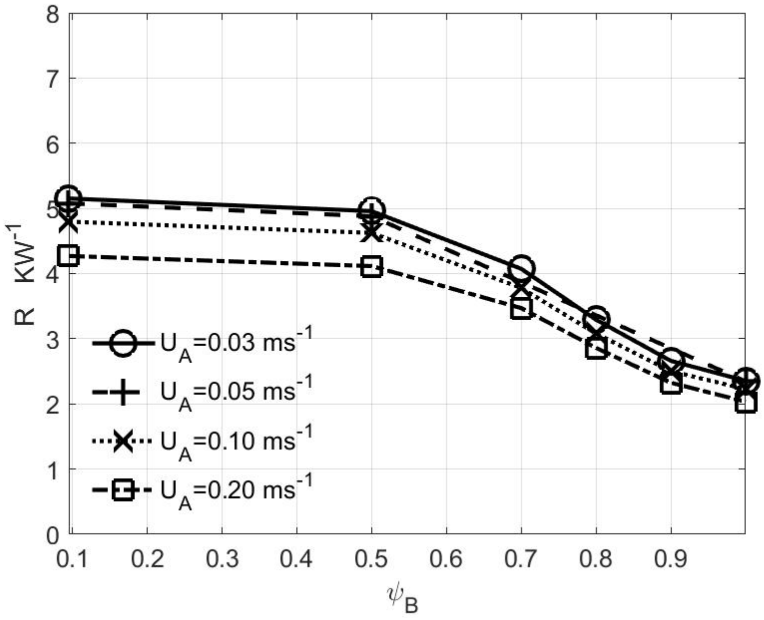

b)

Figure 6.3: a) Ambient velocity sensitivity high value region - hive thermal resistance R versus brood covering porosity b) ambient velocity sensitivity low velocity region - hive thermal resistance R versus brood covering porosity ψ_B .

This showed that in low velocity region air flow under the comb but above the floor mesh was not severely affected by the ambient air movement and was dominated by slow (0.025ms^{-1}) natural convection in both positive and negative x direction figure

6.4b, but in the high velocity region the under comb region is dominated by forced advection flows penetrating the mesh giving a strong negative x direction flow (0.17ms^{-1} figure 6.4a) . This clearly implies that the varroa mesh floor common in hive design may have a negative effect on honey bees by increasing heat loss.

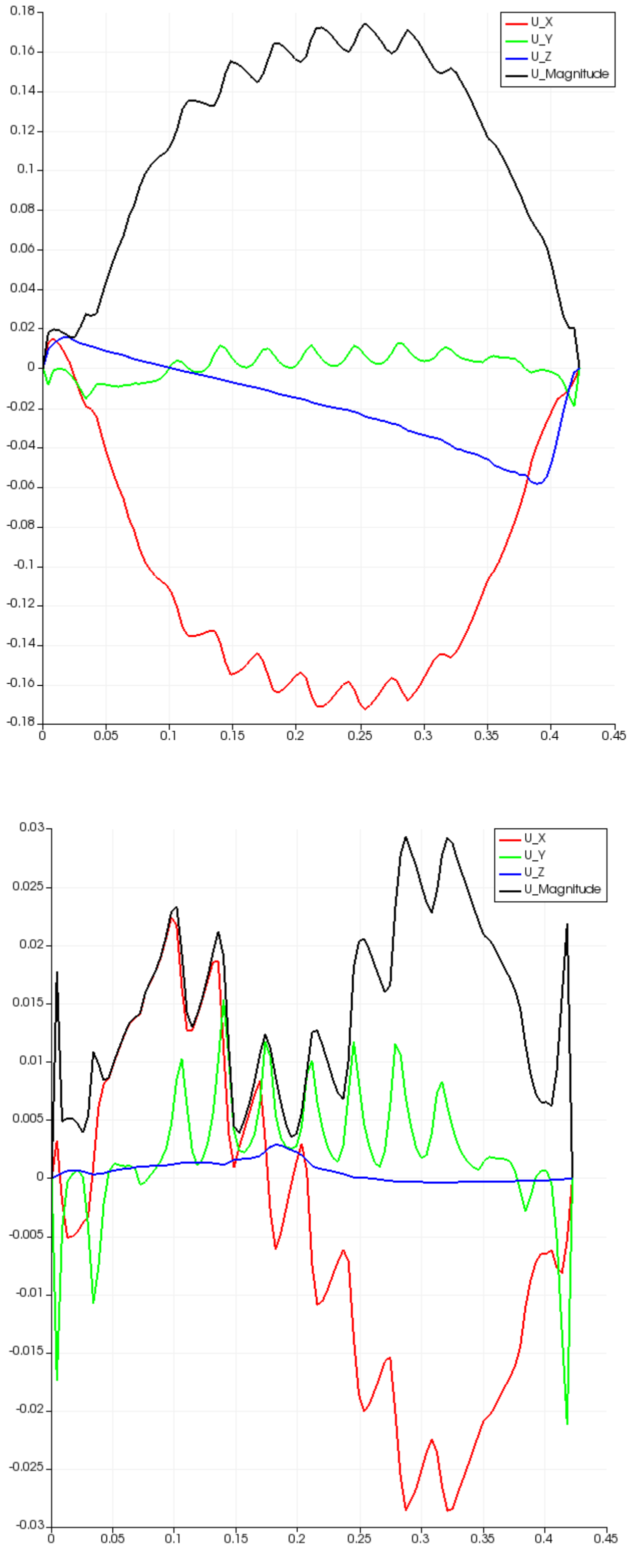

a)

b)

Figure 6.4: Centre line under comb over mesh air velocity, versus x distance at: a) ambient U=0.4 ms-1, b), ambient U=0.05 ms^{-1}.

6.7 Validation methods

6.7.1 Non homogenous conductivity validation

The CFD modelling makes use of an undocumented solver feature using a field called *betavSolid* to act as a conductivity multiplier. As this is fundamental to the models functionality it is important to validate its operation. This was done by simulating a two region bar as shown in figure 6.5.

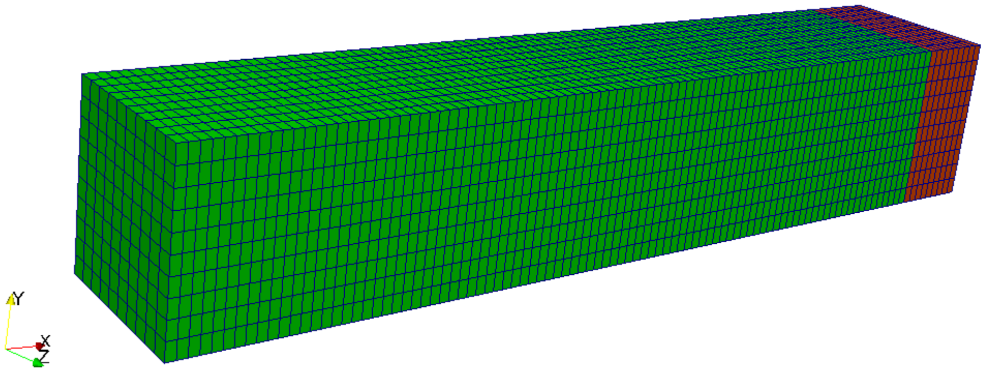

Figure 6.5: Conductivity validation meshing, "heater"region (green) "right" region (red).

The size of the bar is 1.1m in the x axis and 0.2 m in both y and Z axes. The "heater region" is 1m in the x-axis. The purpose of the "right" region is ensure a inter-region patch is included in the simulation. The conductivity of both regions was set to $k=1$. The leftmost x normal face of the heater region (i.e. $x= -0.5m$) was set to 500K the x normal on the rightmost face of the "right" region (i.e. $x= +0.6m$) was set to 300K. A cell zone "midheater" was created in the middle of "heater" (i.e. from $x= -0.1m$ to +0.1m). Using the *setFields* utility, the *betavSolid* parameter in "midheater" zone was set at one of 3 values for 3 CFD runs i.e. β_v = 0.1, 1.0, and 10. These CFD runs gave centre line temperature profiles as shown in figures 6.6, 6.7, and 6.8. These show the step in the profile when β_v has a value not equal to one.

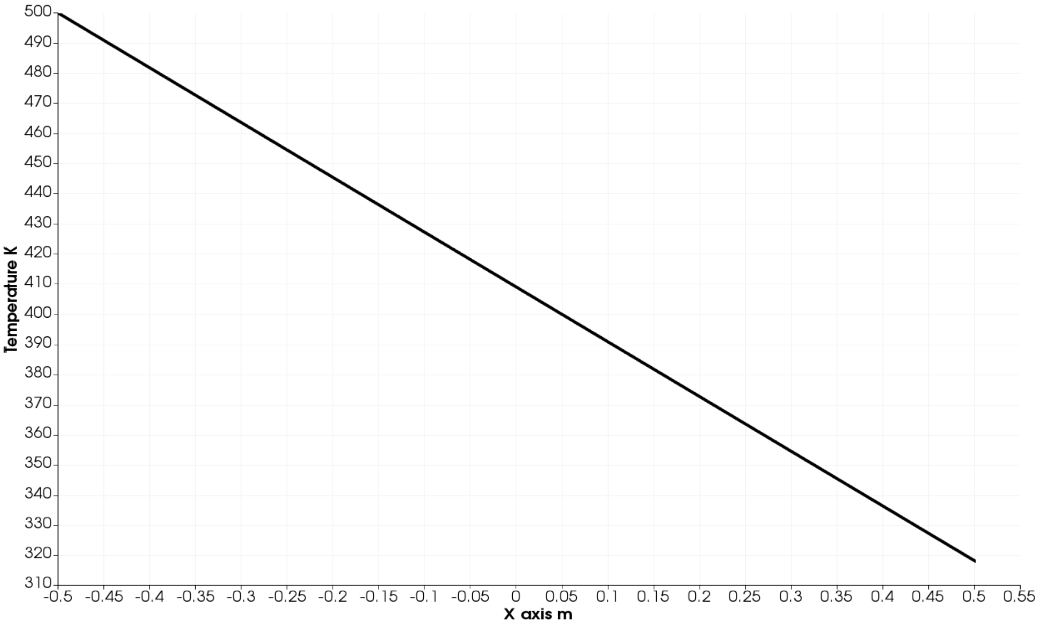

Figure 6.6: Temperature profile mid heater β_v*=1.0.*

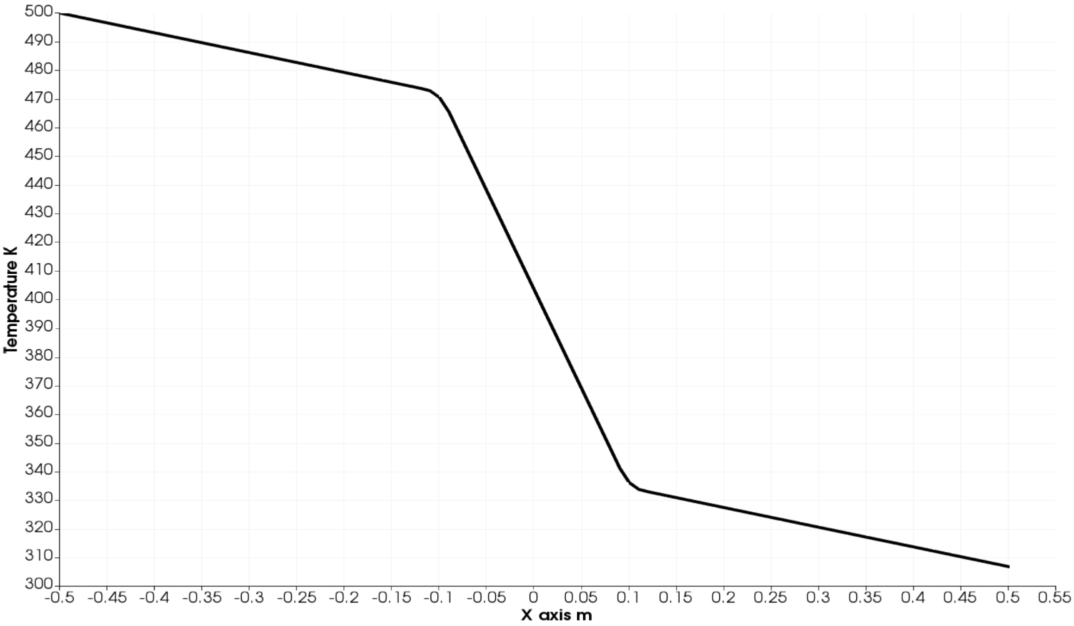

Figure 6.7: Temperature profile mid heater β_v*=0.1.*

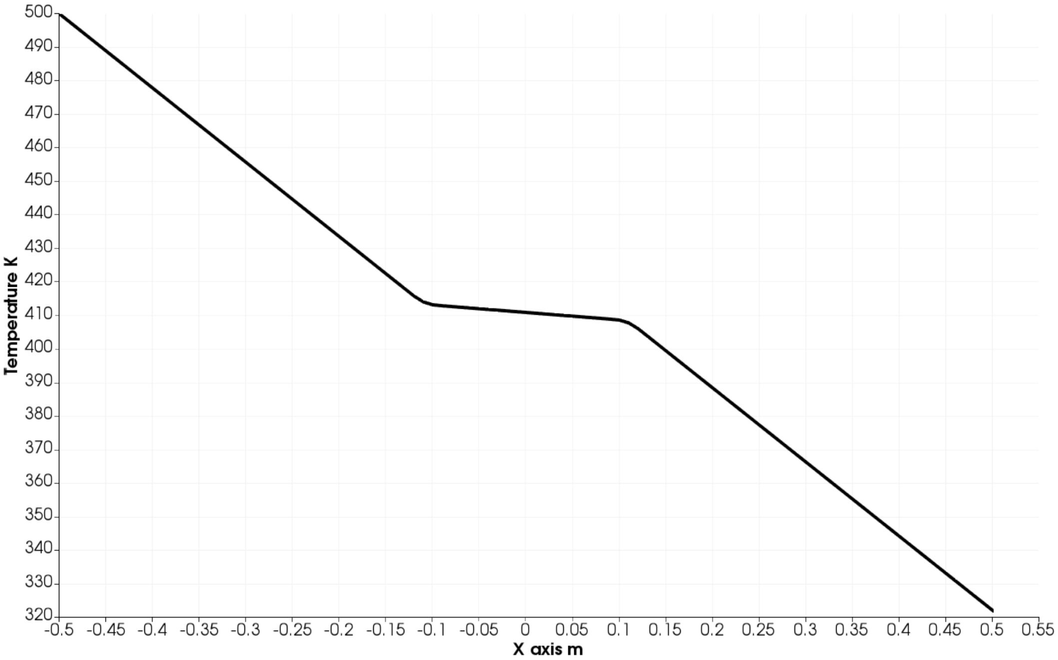

Figure 6.8: Temperature profile mid-heater β_v*=10.*

6.7.2 Porosity resistance validation

To understand the significance of these differences in heat transfer we need look into the fluid dynamic theory related to porous materials.

The pressure differential caused by porous media such as dispersed insects is the Darcy Forchheimer model of pressure difference per unit length across a porous material (Nield and Bejan, 2006).

$$\nabla P=-\alpha\vec{U}-\beta|\vec{U}|\vec{U} \tag{6.8}$$

$$\frac{\delta P}{\delta x}=-\alpha U_x-\beta U_x^2 \tag{6.9}$$

The first term in equation 6.8 relates to the viscous drag and is the dominant term below Reynolds numbers of 10. The second term relates to the obstruction effects of the particles. This is expressed in a single dimension in equation 6.9.

Ergun’s equation formulates α and β as per equations 6.10 and 6.11. (Li and Ma, 2011).

$$\alpha=\mu\,150\frac{(1-\varphi)^2}{d_P^2\varphi^3} \tag{6.10}$$

$$\beta=\frac{\rho}{2}\frac{3.5(1-\varphi)}{d_P\varphi^3} \tag{6.11}$$

As the porosity input parameters (D, F) to OpenFOAM are linearly derived from α and β (equations 6.12 and 6.13), we can use a single value of d_p in the mid range i.e. 0.004mm and validate solely over the ranges of φ and U.

$$D=\frac{\alpha}{\mu} \tag{6.12}$$

$$F=\frac{2\beta}{\rho} \tag{6.13}$$

To validate the implementation in OpenFOAM used in the study we can evaluate whether the equations hold by simulating a straight duct with a porosity and then determine the pressure differential for combinations of air velocity and porosity. The duct dimensions were 2.0×0.39×0.2 m. Underneath the duct was a solid region 2.0×0.01×0.2 m, to ensure that the solver was having to deal with multiple regions as per the simulations of the hive. The duct and its attached solid region were discretized into 500,000 equal hexahedrons. A porosity zone in the duct 1×0.39×0.2 m was created using the same methods as used in the hive simulation (figure 6.9).

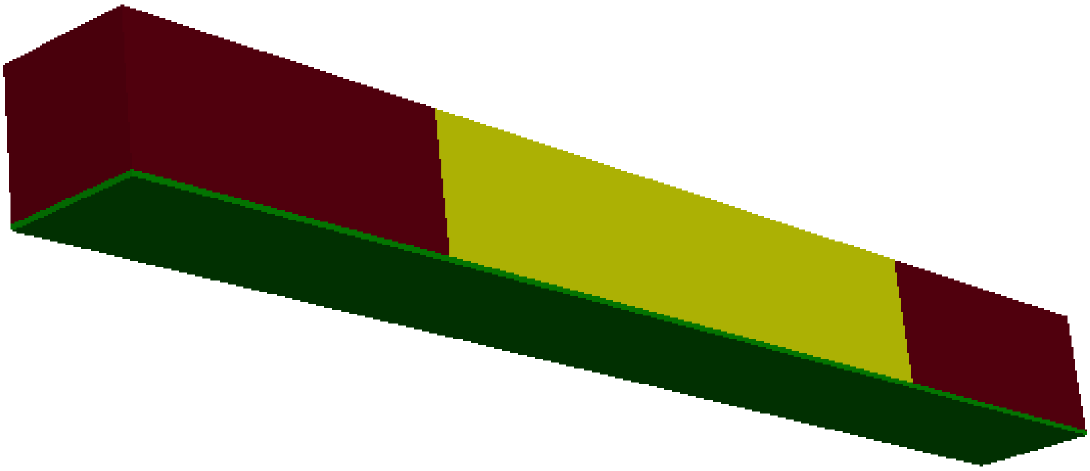

Figure 6.9: Porosity validation duct (brown, yellow) with attached solid region(green). and porosity zone (yellow).

The solver and all of the solver parameters including turbulence, tolerance, and relaxation factors were set to those of the hive simulations.

An optimised Latin hypercube (Morris and Mitchell, 1995) was used to select 50 points in each of the velocity ranges 0.1 to 0.01 and 0.01 to 0.001 ms^{-1}.

Each simulation was run for 4000 iterations to generate the pressure differential and post processed to obtain the pressures at the centres of both ends of the porosity. A typical pressure profile along the centreline of the duct is shown in figure 6.10a.

Each CFD pressure differential $\delta P'_{\varphi,U}$ at porosity φ and velocity U was compared with the predicted value $\delta P_{\varphi,U}$ by computing the absolute error ratio $E_{\varphi,U}$ using equation 6.14.

$$E_{\varphi,U}=\frac{|\delta P'_{\varphi,U}-\delta P_{\varphi,U}|}{\delta P_{\varphi,U}} \tag{6.14}$$

The absolute relative error $E_{\varphi,U}$ was plotted against the predicted pressure differential , velocity and the porosity as show in figures 6.10a, 6.11a, and 6.11b .

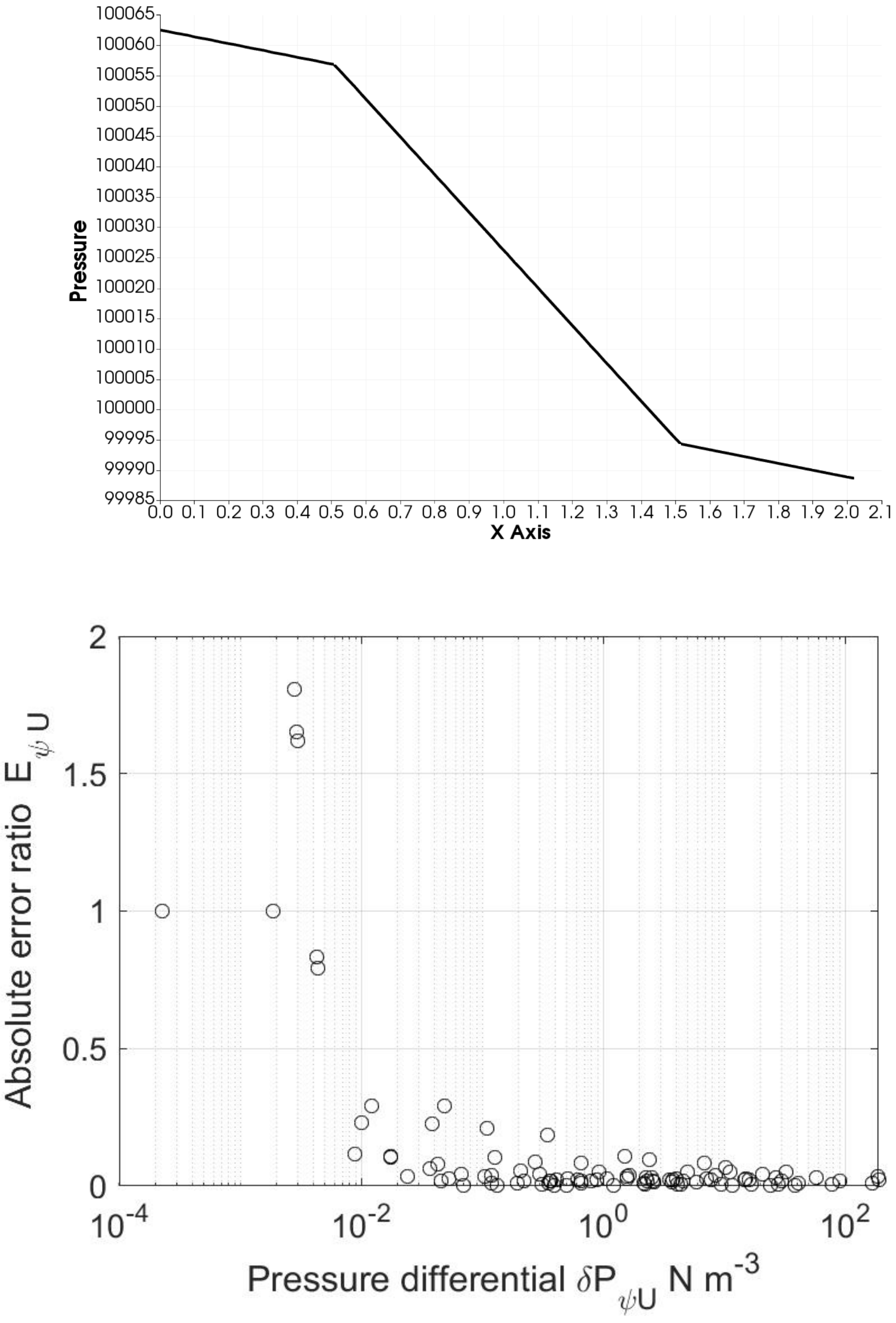

a)

b)

Figure 6.10: a) Typical pressure profile pressure versus distance along the duct centre line, b) absolute error ratio versus pressure differential (N=100).

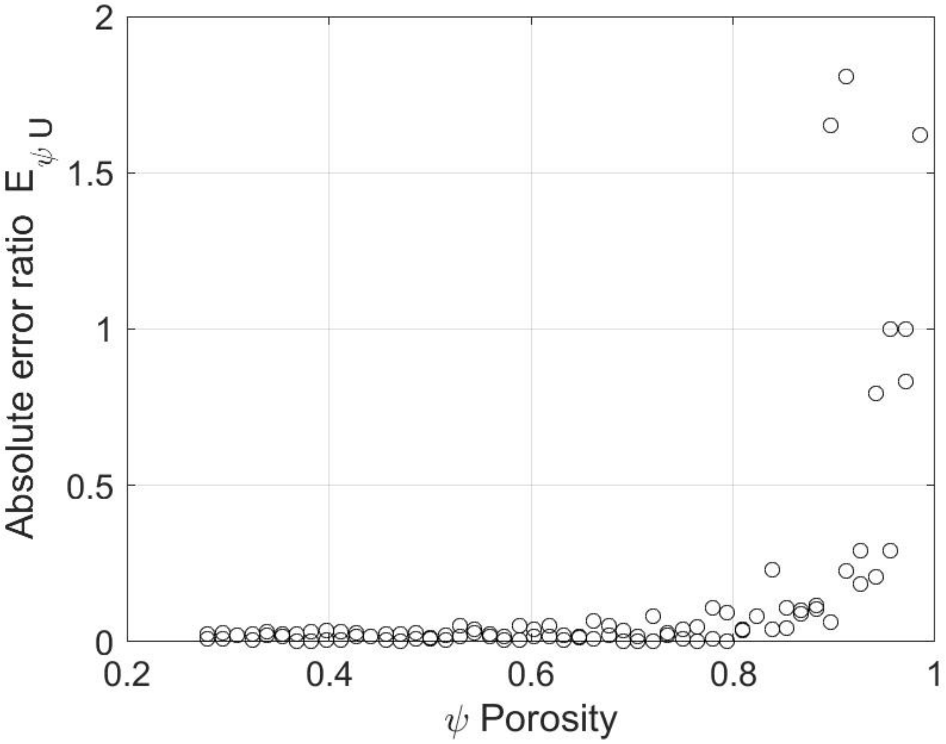

a)

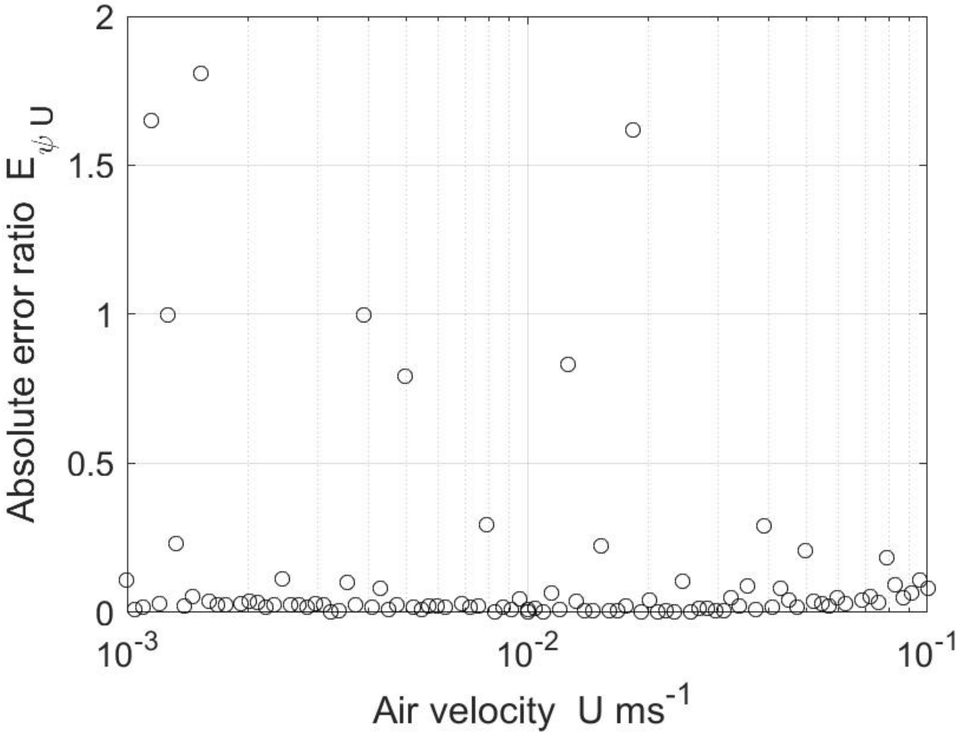

b)

Figure 6.11: a) Absolute error ratio versus porosity (N=100), b) absolute error ratio versus air velocity(c) N=100.

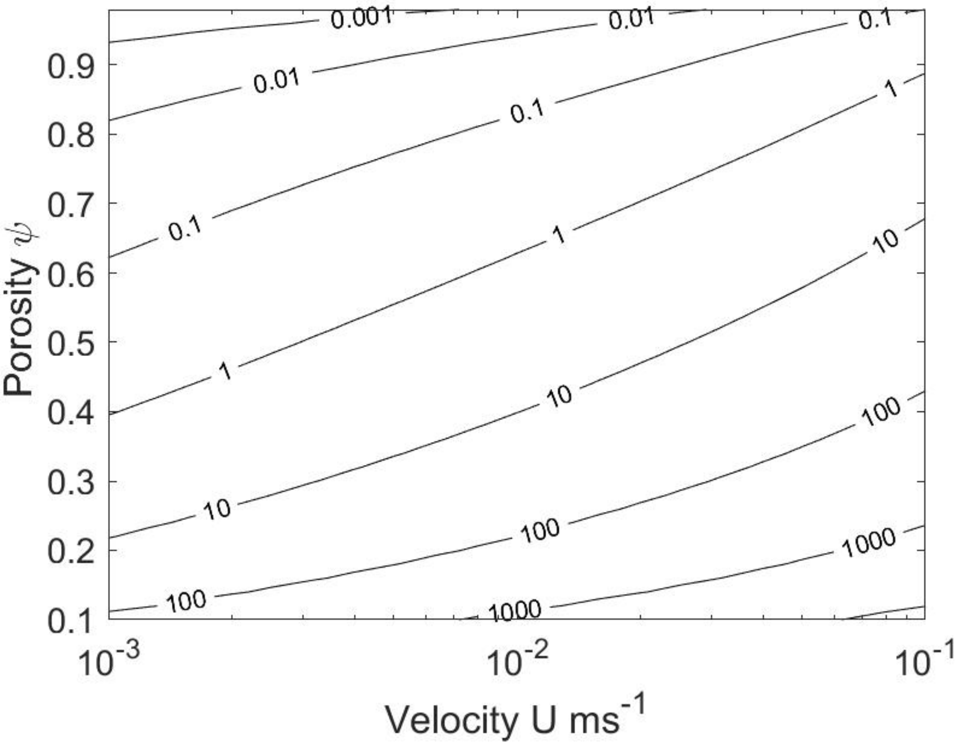

a)

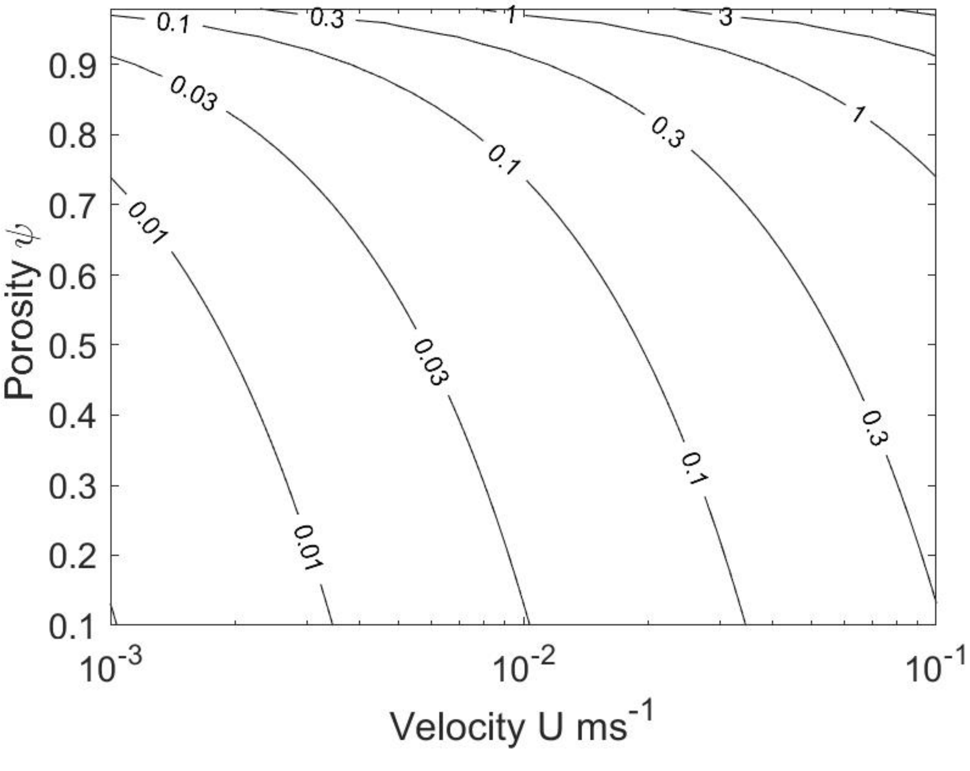

b)

Figure 6.12: a) Contours of $\frac{\delta P}{\delta x}$ *pressure gradient versus porosity and velocity b) contours of β/α ratio versus porosity and velocity.*

The velocities uncovered in the hive CFD experiments show natural convection velocities in the range 10^{-3} to 10^{-1} ms^{-1}. This, with the range of porosities considered 0.095 to 0.90, gives air resistances of 10^{-1} to 5×10^{-3} Nm^{-3}, (figure 6.12a) with the predominance of the α term over the β term in equation 6.8 (figure 6.12b)

From figure6.3 it can be clearly seen that the errors in the porosity resistance pressure per unit length $\frac{\delta P}{\delta x}$ are, for the intervals under consideration, independent of duct velocity, but dependent on the expected porosity resistance pressure and/or the porosity. The magnitude of the error is as expected given the tolerance in the CFD solver (10^{-6}), i.e. an average 3.3% +/- 3.5% over the ranges of concern i.e. velocity $10^{-1}>U>10^{-3}\, ms^{-1}$, porosity resistance pressure $\delta P_{\varphi,U}>10^{-2}N\,m^{-3}$ and porosity $0.2<\varphi<0.895$.

6.7.3 Physical/radiation free CFD validation

The method of using β_v is validated if the ratio of the temperature gradients equals the ratio of β_v values. The results are shown in table 6.4. The deviation from expected is less than 1% and therefore *betavSolid* is valid for this purpose.

Table 6.4: BetavSolid validation results.

β_v value set	**Temperature gradient β_v=value**	**Temperature gradient β_v=1**	**Temperature gradient ratio**	**%deviation**
0.1	-690.0000	-69.1111	0.10016	0.02%
10	-22.1333	-221.4722	10.0062	0.63%

Validation against a hive occupied with a live honey bee colony was impractical so an in-vitro analogue for the contents of the hive was substituted so that validation of the model of a hive with brood heating but without honey bees could be accomplished. A hive with comb frames were sourced from a commercial supplier and the combs made from foam with a similar thermal conductance (Humphrey and Dykes, 2008). The isothermal brood areas in the 6 combs were constructed from a sandwich of 2 aluminium plates and a serpentine resistance wire to which was attached a digital thermal sensor (MicroChip, 2005) see figure 6.13.

Figure 6.13: Brood frame analogue.

There is also a problem trying to map directly the CFD model results to experimental results, as the CFD model does not include the radiation from the hive surface and radiation passed through the floor mesh and absorbed re-radiated by the floor mesh.

The radiation is surprisingly significant in this problem owing to the large surface areas (~0.8 m^2) involved for such a relatively small heat input (~10W), where a 1K surface temperature above ambient gives rise to a net radiation of 4.5W (equation 21). This radiation is large enough to be used to locate the position and size of the honey bee cluster, in thin walled wooden hives, in winter, using infrared thermography (6.14) (Shaw et al., 2011).

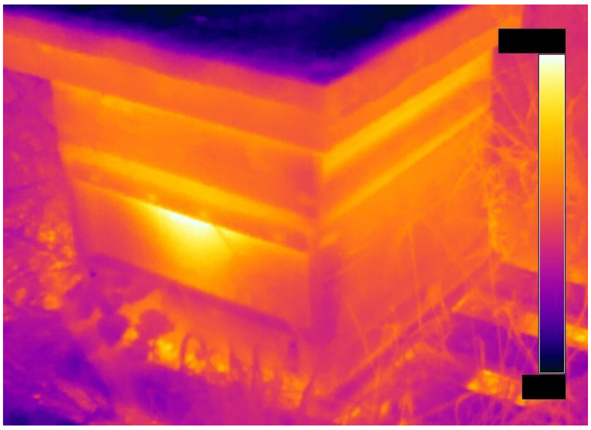

Figure 6.14: Infra-red thermograph of a hive (AIRSS Ltd).

Thus the validation experiment and analysis were fashioned to overcome this issue by considering the surface temperatures in both the validation analysis and the experiment.

For the experiment, the heater wattage was set to give heated plate/brood temperatures in the range of 14 to 20K above ambient after a period of 48 hours. At equilibrium, temperatures of the top surface of hive and the mesh underneath were measured for a period of 24 hours using 26 digital surface temperature sensors. The distribution of the individual sensors within a patch utilised an Optimised Latin Hypercube sampling method (Morris and Mitchell, 1995). By the use of symmetry, the cross-calibrated sensors were arranged in patches to achieve the same effect as 78 sensors distributed across the entire surface (figure 6.15).

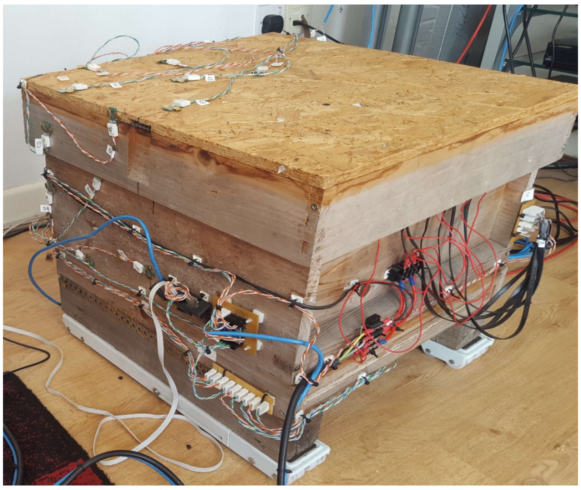

Figure 6.15: Hive with networked contact thermometers.

For analysis , the approach taken is to compare the CFD (*cfd*) model (figure 6.16a) of a hive with brood heating but without honey bees and the experiment (*exp*) (figure 6.16b) via two lumped thermal models, radiating (*lr*) (figure 6.16d), and non-radiating (*lnr*) (figure 6.16c), where the conductive and convective resistances are more easily analysed.

The following were set: identical conductive/convective resistances and input energies between CFD and lumped non-radiative (*lnr*), and between experimental and lumped radiative (*lr*) equations 15,16, and 21; The ambient and brood temperature are identical in all models equation 17 and 18; The *lr* mesh temperature equals the average experimental mesh temperature and thus the downward radiative energies equation 19.

$$R_{SA(lnr)}=R_{SA(cfd)},\ R_{SA(lr)}=R_{SA(\exp)} \tag{15}$$

$$R_{CS(lnr)}=R_{CS(cfd)},\ R_{CS(lr)}=R_{CS(\exp)} \tag{16}$$

$$T_{B(cfd)}=T_{B(lnr)}=T_{B(lr)}=T_{B(\exp)} \tag{17}$$

$$T_{A(cfd)}=T_{A(lnr)}=T_{A(lr)}=T_{A(\exp)} \tag{18}$$

$$T_{M(lr)}=T_{M(\exp)} \tag{19}$$

$$\dot{q}_{CA(lr)}=\dot{q}_{CA(\exp)},\dot{q}_{CM(lr)}=\dot{q}_{CM(\exp)} \tag{20}$$

$$\dot{q}_{E(lnr)}=\dot{q}_{E(cfd)}\dot{q}_{E(lr)}=\dot{q}_{E(\exp)} \tag{21}$$

From energy balance then if equation 22 is true then equations 23 and 24 are also true.

$$\dot{q}_{SAR(\exp)}=\dot{q}_{SAR(lr)} \tag{22}$$

$$R_{CS(cfd)}=R_{CS(lnr)}=R_{CS(lr)}=R_{CS(\exp)} \tag{23}$$

$$R_{SA(cfd)}=R_{SA(lnr)}=R_{SA(lr)}=R_{SA(\exp)} \tag{24}$$

Therefore, the goal is changed to one where we prove that the surface to ambient convective thermal resistance (R_{SA}) and the hive comb to surface convective thermal resistance (R_{CS}) are similar, in all four models for conduction convection, at the temperatures and energy fluxes involved.

We can analyse the lumped models via the thermal circuits in figures 6.17 and 6.18. Then *lnr* convective resistances in equations 25 and 26 can derived.

$$R_{CS(lnr)}=\frac{T_{B(cfd)}-T_{S(lnr)}}{\dot{q}_{E(cfd)}} \tag{25}$$

$$R_{SA(lnr)}=\frac{T_{S(lnr)}-T_{A(cfd)}}{\dot{q}_{E(cfd)}} \tag{26}$$

If the downward radiation is considered to be 7 slots at brood temperature using view factors we determine the downward radiations in equations 27 and 28.

$$\dot{q}_{CM(\exp)}=\sigma(1-\varphi)\Sigma A_i f_i\left(T^4_{B(\exp)}-T^4_{M(\exp)}\right) \tag{27}$$

$$\dot{q}_{CA(\exp)}=\epsilon_M\sigma\varphi\Sigma A_i f_i\left(T^4_{B(\exp)}-T^4_{A(\exp)}\right) \tag{28}$$

The *lr* surface temperature is given by equation 29.

$$T_{S(lr)}=T_{B(lr)}-\left(\dot{q}_{E(lr)}-\dot{q}_{CA(lr)}-\dot{q}_{CM(lr)}\right)R_{CS(lr)} \tag{29}$$

The *lr* surface radiative and convective energy fluxes equations 30 and 31.

$$\dot{q}_{SAR(lr)} = \sigma \epsilon_S A_S \left(T_{S(lr)}^4 - T_{A(\exp)}^4 \right) \tag{30}$$

$$\dot{q}_{SA(lr)} = \frac{T_{S(lr)} - T_{A(\exp)}}{R_{S(lr)}} \tag{31}$$

The energy balance is expressed as equation 32.

$$\dot{q}_{E(\exp)} - \dot{q}_{CM(\exp)} - \dot{q}_{CA(\exp)} - \dot{q}_{SA(lr)} - \dot{q}_{SAR(lr)} = 0 \tag{32}$$

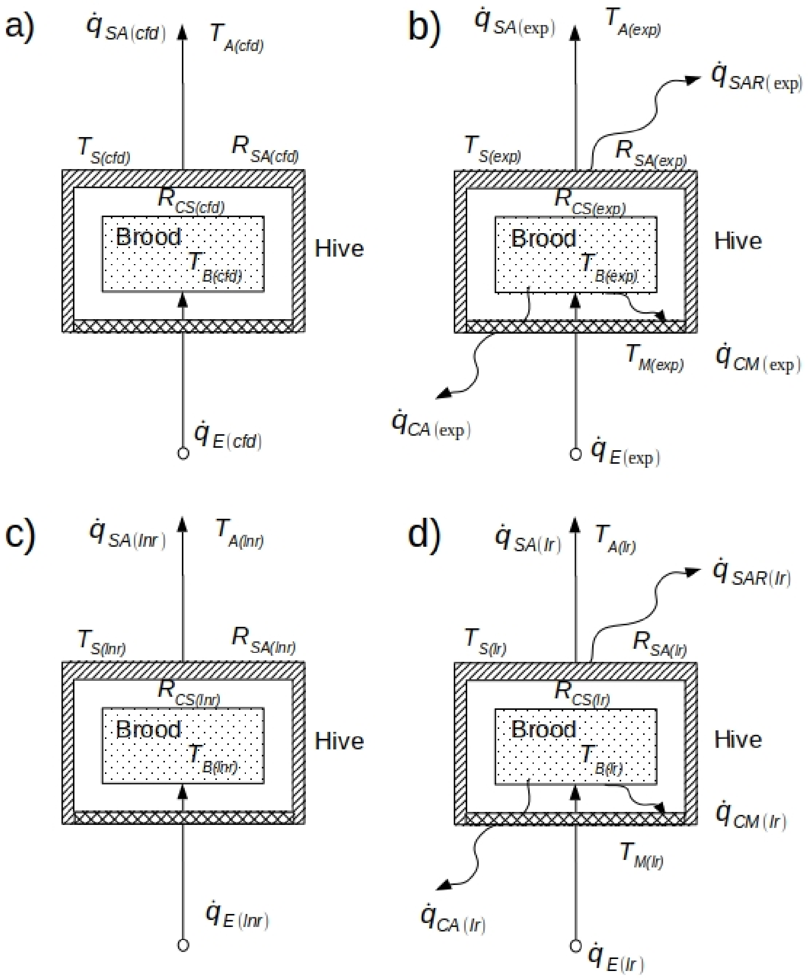

Figure 6.16: Schematic of thermal models a) CFD, b) experiment (exp), c) lumped non radiative (lnr), d) lumped radiative (lr)

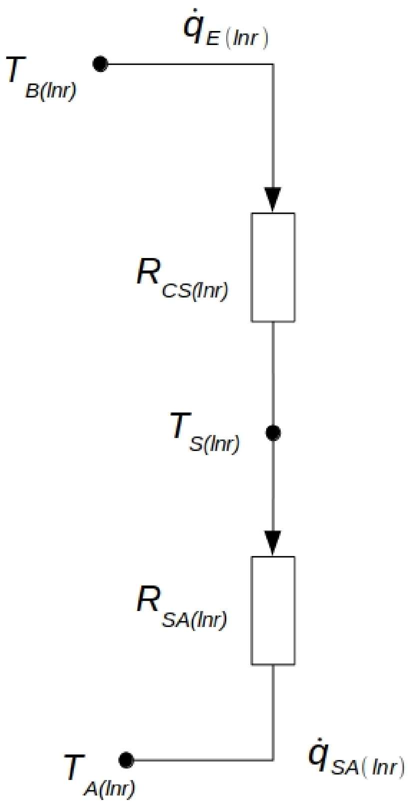

Figure 6.17: Lumped thermal models non-radiative (lnr).

If the convective resistances are equal then equation 32 can then be solved numerically to determine $T_{S(lr)}$.With solutions of $T_{S(lr)}$ known, the values of $\dot{q}_{SAR(lr)}$, can be determined for values of $\dot{q}_{E(\exp)}$.$\dot{q}_{E(lr)}$ and $\dot{q}_{CA(\exp)}$.

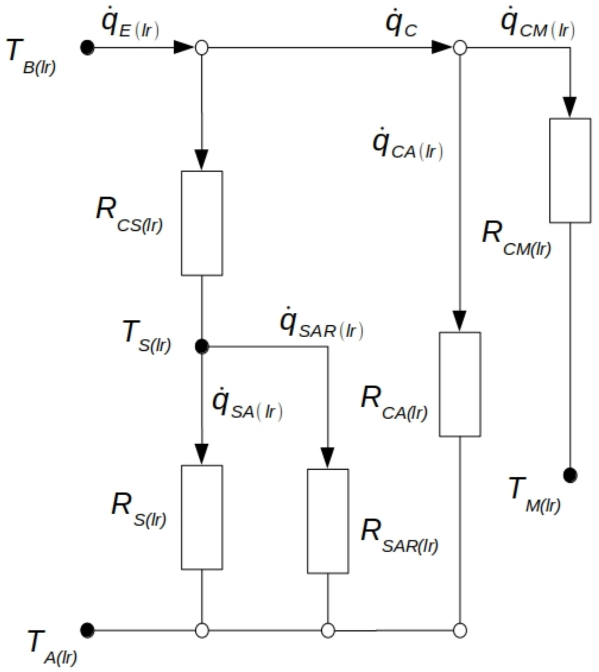

Figure 6.18: Lumped thermal model Radiative (lr).

6.8 Model Results

Given the complexity of the problem it is useful to understand how key parameters interact before interpreting the CFD results. The low velocity dominant coefficient α from equations 6.2 and 6.3 is plotted versus actual honey bee diameter at values of constant number density and actual honey bee length in figure 6.19.

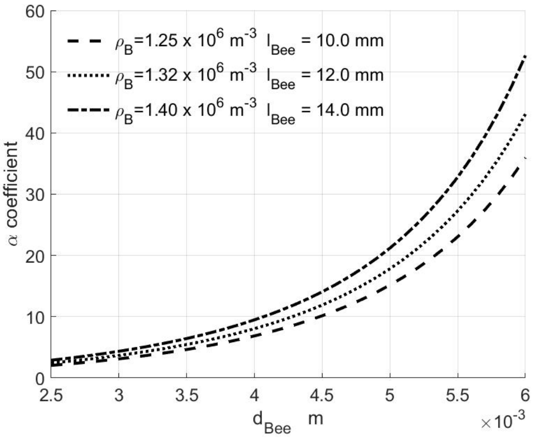

Figure 6.19: Flow resistance coefficient α versus actual bee diameters dBee at constant bee number densities ρB.

The plot of hive thermal resistance vs honey bee number density in the *distributed* state shown in figure 6.21. Similarly for the *brood covering* state, hive thermal resistance versus porosity in figure 6.20. Both plots are at constant ambient temperature 293K and effective diameter sizes.

6.9 Validation Results

Three experimental runs at approximately 10, 15 and 20W yielded the brood and ambient temperatures as shown in table 6.5. Matching CFD runs were completed at those temperatures. The values of $\dot{q}_{E(cfd)}$ were extracted from the CFD runs and the values of$\dot{q}_{E(\exp)}$, $\dot{q}_{C(\exp)}$ and $\dot{q}_{SAR(\exp)}$ extracted from the experiment. $\dot{q}_{SAR(lr)}$ was determined as described above and tabulated in table 6.5.

To check the sensitivity of this approach for a given $\dot{q}_{E(\exp)}$ values of $\dot{q}_{SAR(lr)}$ were plotted against values of $\dot{q}_{E(cfd)}$ and $\dot{q}_{C(\exp)}$. The plot for $\dot{q}_{E(\exp)}=20W$ is shown in figure 6.22.

Table 6.5: Physical Experiment Parameters and results for 10W 15W and 20W.

	CFD & experimental values		
Parameter	**10W**	**15W**	**20W**
$T_{B(exp)}$ K	308.71	314.66	319.69
$T_{A(exp)}$ K	293.96	294.52	294.44
$\dot{q}_{E(\exp)}$W	10.19 ± 1%	15.08 ± 1%	20.09 ± 1%
$\dot{q}_{SAR(\exp)}$W	6.08 ± 15%	8.61 ± 11%	10.51 ± 8%
$\dot{q}_{SAR(lr)}$W	5.32	7.85	10.19
$\dot{q}_{E(cfd)}$W	6.40	9.62	13.10
$\dot{q}_{C(\exp)}$W	2.45 ± 5%	3.44 ± 4%	4.44 ± 3%
Validation error	12%	9%	3%

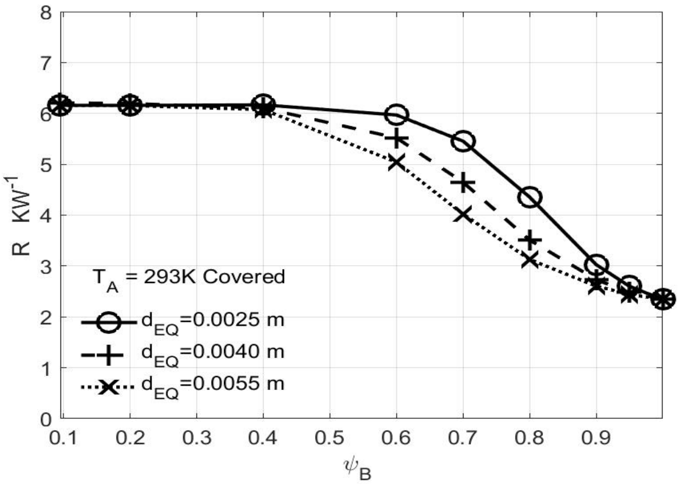

Figure 6.20: Brood covering hive thermal resistance vs porosity for constant effective diameters TA = 293K.

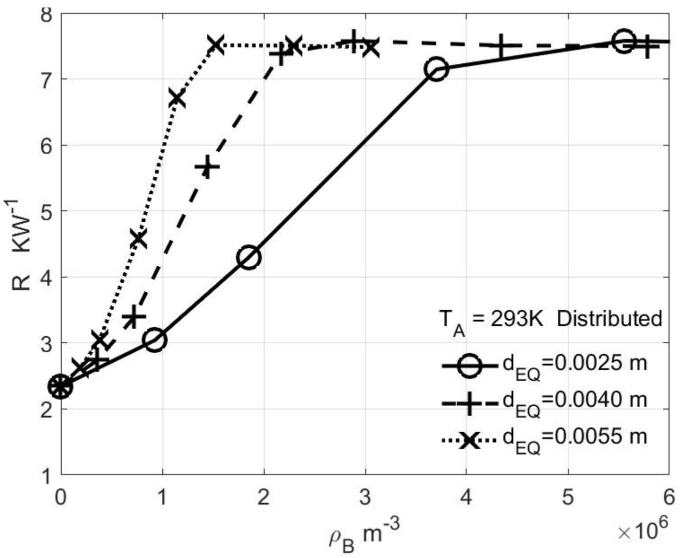

Figure 6.21: Distributed hive thermal resistance vs colony number density for effective diameters at constant ambient temperature 293K. The rightmost termination of the lines for distributed indicates the geometric packing limit with the exception of 2.5mm diameter.

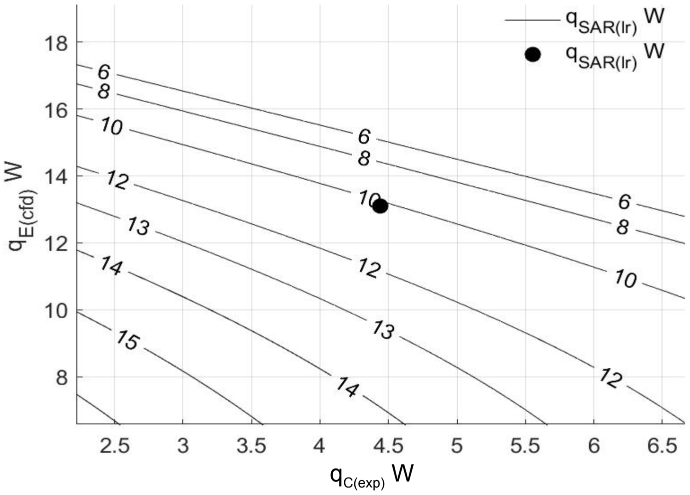

Figure 6.22: Plot of lumped hive surface radiation flux for CFD input power and mesh radiation flux where = 20W(c) with the experimental point value.

6.10 Discussion

Almost all building simulation is for human occupants from a single extant subspecies, so it is important to test our inbuilt assumptions. Honey bees have been used to test anthropogenic assumptions in others fields and have proved useful (Dyer et al., 2005) and as shown by this research. The most obvious difference is size and their lack of confinement to floors, however, if we use a dimensionless occupancy i.e. occupants per occupant volume (*Nr density** in table 6.6) other differences emerge. Thus we can see honey bees have a dimensionless occupancy of 1 to 2 orders of magnitude higher than humans and have an order of magnitude variation between subspecies.

The CFD simulation of the built environment likewise shows striking differences between the subspecies as can be seen in figure 6.21 where although the distributed number density for both subspecies is similar (1.3 to 1.4 $\times 10^6$) the effect on thermal resistance is dramatic, giving 7 to 3.5 i.e. a factor of two. This marked difference is based on the flow resistance physics shown in figure 6.19. Here we can clearly see for constant number density the diffusive coefficient, α, increases as the 3rd power of the honey bee diameter. This means that temperate honey bees are close to stopping convective heat transfer within their hive, yet the tropical subspecies will have considerable convective heat transfer. This shows that temperate honey bees need to create bee-less spaces in order to efficiently move air around their hive e.g. for removing water vapour from nectar desiccation. This behaviour has been observed in honey bee clusters (Heinrich, 1981).

The validation has shown radiation to be significant. Given the low temperatures involved this may be surprising to some. The validation technique used has shown that this simulated convection model has an accuracy within or close to the scope of the experimental error (see table 6.5).

Table 6.6: Dimensionless comparison of human and honey bee occupancy (Department for Communities and Local Government, 2016).

Parameter	**Humans**	**Temperate bee**	**Tropical bee**
length m	1.7	0.014	0.011
diameter m	0.6	0.0055	0.0025
occupant m^3	4.8E-01	3.3E-07	5.4E-08
dwelling m^3	300	0.014	0.0051
occupants	8	1.8E+04	6.4E+03
Nr density m^{-3}	2.7E-02	1.4E+06	1.3E+06
dwelling volume*	6.3E+02	4.1E+04	9.5E+04
Nr density*	1.3E-02	4.7E-01	6.8E-02

6.11 Conclusion

This research shows that when simulating unfamiliar constructions and occupants it is necessary to challenge assumptions. Here we have demonstrated that unlike anthropocentric experience, it possible for relatively small subspecies differences to have marked effects on the thermal performance of the built environment that can be as least significant as the change in the thermal performance of the individual animal. In this case , changing building performance by a factor of 2. Despite radiation being significant, the simulation results were successfully validated.

6.12 References

Abou-Houly, H.E. 2010. Investigation of flow through and around the Macrotermes michaelseni termite mound skin. , p.273.

Ayachit, U. 2015. *The ParaView Guide: A Parallel Visualization Application*. Kitware, Incorporated.

CFD-Online 2014a. Dimensionless wall distance (y plus). *CFD-Online*. [Online]. [Accessed 2 February 2022]. Available from: https://www.cfd-online.com/Wiki/Dimensionless_wall_distance_(y_plus).

CFD-Online 2014b. Turbulence freestream boundary conditions. *CFD-Online*. [Online], pp.3–5. [Accessed 2 February 2022]. Available from: https://www.cfd-online.com/Wiki/Turbulence_free-stream_boundary_conditions.

Cushman, D. 2011. Drawings of Hives and Hive Parts. *Dave Cushman's Beekeeping and Bee Breeding Website*.

Department for Communities and Local Government 2016. Technical housing standards – nationally described space standard.

Dyer, A.G., Neumeyer, C. and Chittka, L. 2005. Honeybee (Apis mellifera) vision can discriminate between and recognise images of human faces. *Journal of Experimental Biology*. **208**(24), pp.4709–4714.

Ergun, S. and Orning, A.A. 1949. Fluid Flow through Randomly Packed Columns and Fluidized Beds. *Industrial & Engineering Chemistry*. **41**(6), pp.1179–1184.

Heinrich, B. 1981. *The Mechanisms and Energetics of Honeybee Swarm Temperature Regulation*.

Hozumi, S., Inagaki, T., Kudo, K., Mateus, S. and Zucchi, R. 2011. Thermal characteristics of polybia scutellaris nests (Hymenoptera: Vespidae) using computational fluid dynamics: A possible adaptation to tropical climates. *Sociobiology*. **57**(1), pp.123–141.

Humphrey, J.A.C. and Dykes, E.S. 2008. Thermal energy conduction in a honey bee comb due to cell-heating bees. *Journal of Theoretical Biology*. **250**(1), pp.194–208.

Idelchik, I.E. 2006. Handbook of hydraulic resistance (3rd edition). *Washington*.

Jasak, H., Jemcov, A. and Tukovic, Z. 2007. OpenFOAM : A C ++ Library for Complex Physics Simulations. *International Workshop on Coupled Methods in Numerical Dynamics*. **m**, pp.1–20.

MATLAB 2018. *9.4.0.813654 (R2018a)*. Natick, Massachusetts: The MathWorks Inc.

MicroChip 2005. 2-Wire Serial Temperature Sensor TCN75A. , pp.1–30.

Mitchell, D.M. 2022. Honey bee (Apis mellifera) size determines colony heat transfer when brood covering or distributed. *International Journal of Biometeorology*. **66**(8), pp.1653–1663.

Morris, M.D. and Mitchell, T.J. 1995. Exploratory designs for computational experiments. *Journal of Statistical Planning and Inference*. **43**(3), pp.381–402.

Mulisa, F., Alemayehu, A., Diribi, M., Fekadu, B. and Alayu, T. 2018. Determination of bee spacing and comb cell dimensions for Apis mellifera Scutellata honeybee race in western Ethiopia. *International Journal of Livestock Production*. **9**(8), pp.206–210.

Riegel, J. and Mayer, W. 2019. FreeCAD (Version 0.18).

Ruttner, F. 1988. *Biogeography and Taxonomy of Honeybees*.

Saucy, F. 2014. On the natural cell size of European honey bees: A ‘fatal error’ or distortion of historical data? *Journal of Apicultural Research*. **53**(3), pp.327–336.

Schneider, S. and Blyther, R. 1988. The habitat and nesting biology of the African honey bee Apis mellifera scutellata in the Okavango River Delta, Botswana, Africa. *Insectes Sociaux*. **35**(2), pp.167–181.

Shaw, J.A., Nugent, P.W., Johnson, J., Bromenshenk, J.J., Henderson, C.B. and Debnam, S. 2011. Long-wave infrared imaging for non-invasive beehive population assessment. *Optics Express*. **19**(1), p.399.

Sudarsan, R., Thompson, C., Kevan, P.G. and Eberl, H.J. 2012. Flow currents and ventilation in Langstroth beehives due to brood thermoregulation efforts of honeybees. *Journal of Theoretical Biology*. **295**, pp.168–193.

Venkatesh, V. 2016. CFD with OpenSource software Tutorial of convective heat transfer in a vertical slot. *Proceedings of CFD with OpenSource Software*.

Chapter 7 Are Man-Made Hives Valid Thermal Surrogates for Natural Honey Bee nests?

This chapter is based upon the authors published work:

Are Man-Made Hives valid thermal surrogates for natural Honey Bee nests [in review] Journal of Thermal Biology

7.1 Abstract

Honey bees preferentially occupy thick walled tall narrow tree cavities and attach their combs directly to the nest wall, leaving periodic gaps. However, academic research and beekeeping are conducted in squat, thin walled man made hives, with a continuous gap between the combs and the walls and roof. Utilising a computational fluid dynamics (CFD) model of thermoregulating bees in complete nests in trees and thin walled man made hives, with the average size of tree comb gaps determined from honey bee occupied synthetic tree nests, this research compared the metabolic energy impacts of comb gaps and vertical movement of the thermoregulated brood area. This shows their heat transfer regimes are disparate, including: bee space above combs increases heat loss by up to ~70%; hives, compared to tree nests, require at least 150% the density of honey bees to arrest convection across the brood area. Tree cavities have a larger vertical freedom, a greater thermal resistance and can make dense clustering redundant. With the thermal environment being critical to honey bees, the magnitude and scope of these differences suggest that some hive based behavioural research needs extra validation to be considered non-anthropogenic, and some bee keeping practices are sub-optimal.

Table 7.1: Chapter nomenclature.

Symbol	Units	Description
d_p	m	Diameter of honey bee
h^*	-	Relative vertical position of the brood heating region
l_p	m	Length of honey bee
R	Km^2W^{-1}	R value i.e. ambient to brood temperature difference (K) divided by brood metabolic heat flux (Wm^{-2})
R_{max}	Km^2W^{-1}	Maximum R value
R_{min}	Km^2W^{-1}	Minimum R value
ρ_B	m^{-3}	Number of honey bees per unit volume
ψ	-	Porosity
ψ_B	-	Brood covering porosity
ψ_P	-	Peripheral comb-gap porosity
$\rho_{critical\,95}$	m^{-3}	95% critical honey bee number density
γ		Cylinder spacing relative to cylinder diameter
$\gamma_{critical\,95}$		95% critical honey bee relative spacing

7.2 Introduction

Honey bees (*Apis mellifera*) regulate their colony temperature through variable heat generation (Simpson, 1961; Southwick, 1985), variable colony conductance (i.e. clustering) and water evaporation. Their natural geographical range extends from cool temperate to hot arid regions and they are differentiated into subspecies to cope with the diverse climates (Ruttner, 1988). In cold climates they do not hibernate in winter, maintaining some part of the colony above 18 °C all year. The honey bees’ most preferred nest enclosure is a tree (Adedeji, 2014) with a tall, narrow and thick walled cavity, often tapered at the top (Seeley and Morse, 1976). They prefer entrances towards the bottom of the cavity (Seeley and Morse, 1978). They create their combs from body secretions of wax, starting at the top of the cavity, in vertical curtains that have a continuous wax attachment near the top of the cavity and with periodic gaps (peripheral galleries) on the walls (see fig 7.2). The peripheral galleries have been described (Seeley and Morse, 1976), but not measured nor their impact on the properties of the nest investigated.

Chapter 7 Are Man-Made Hives Valid Thermal Surrogates for Natural Honey Bee nests?

Most research and beekeeping is conducted in squat box-like (~200mm high) wide (~450mm x ~450mm) hives (Delaplane et al., 2013) with wooden walls typically 13mm to 19mm thick (Cushman, 2011). In these hives the honey bees are constrained to build their combs within wooden frames upon a manufactured beeswax template (foundation) that forms the central spine. The frames are suspended within the hive cavity so that they are between 5 and 10mm (bee space) from the main hive structure (i.e walls and roof) and each other, with the objective of preventing the honey bees fixing the frames to the hive structure with comb. This removable frame design is largely unchanged from the mid 19th century when it was devised (Langstroth, 1853). In trees, the brood cells on all combs extend close to the walls in the lower part of the nest (Seeley and Morse, 1976), whereas in man made hives the brood area is typically in an interrupted oblate ellipsoid shape (Sudarsan et al., 2012), with large spaces between the brood cell area and the walls and the outside combs are without brood cells. Honey bees will attempt to move the location of the thermoregulated brood area up and down the nest in response to available space and outside conditions (Currie and Spivak, 2015).

Computational Fluid Dynamics (CFD), through the simulation of honey bee nests, their environment and their occupants, can provide insights into multiple sub species, nest types and configurations, colony sizes and honey bee number densities across multiple climates which would be difficult, time consuming and costly, if not impossible, by other means. Experimental investigations of tree nests are especially difficult with the high mass and heat capacity of tree nest ~ $0.5 \times 10^{6}\,JK^{-1}$ and low heat input (~20W) requiring very long times to reach thermal equilibrium (Mitchell, 2016).

There have have been previous CFD investigations into thin walled man made honey bee hives (Sudarsan et al., 2012; Thompson, 2013; Oskin et al., 2020; Tapia Brito, 2022). However all of these have used non-thermoregulating fixed metabolic rate heat sources for the simulated honey bees, and investigated the resulting temperatures and fluid flows in only one or very restricted range of bee densities/porosities and none have investigated tree nests, or the effect of heat source height, or the effect of gaps around the comb. A feature by feature comparison of the studies is included in table 7.2. The results presented here are unique in that they are from a metabolic energy focused study based on a realistic thermoregulating heat source to simulate the bees allowing investigation into the metabolic energy needed to maintain that thermoregulation. It uses the same model to compare the energy related performance characteristics of nests in both trees and hives, across the full range of clustering bee densities/porosities with varying heat source height and changes in comb gaps. This is relevant as energy lost through the nest enclosure must be made up by more honey bee activity and stress, either to generate more heat or to cluster. This can affect nest humidity, colony survival, spring development and honey production (Villumstad, 1974). Higher nest temperatures and humidity have been linked to reductions in disease and parasites (Flores et al., 1996; Kraus and Velthuis, 1997; Tahmasbi, 2009; Chen et al., 2012; Abou-Shaara et al., 2012).

Table 7.2: CFD studies and features : A) (Sudarsan et al., 2012) , B) (Thompson, 2013), C) (Oskin et al., 2020), D) (Tapia Brito, 2022), E)Author's model results published in 1(Mitchell, 2022a) 2 (Mitchell, 2022b) 3 (this paper) and model files published in 4 (Mitchell, 2023)

	A	B	C	D	E
Model features					
Conjugate heat transfer			√	√	√
Radiation					
Turbulence				√	√
Mesh/grid size sensitivity tested					√$_{1,2}$
Published validation of model					√$_{2}$
Model files published					√$_{4}$
Carbon dioxide	√	√			
Water vapour*	√	√	√		
Variation of bee conductivity with outside temperature			√		
Bee metabolic rate locally fixed	√	√		√	
Bee metabolic rate determined by outside of nest temperature			√		
Thermoregulated bee temperature					√
Open floor mesh					√
Bees modelled as solid			√		
Bee air resistance as a porosity	√	√		√	√
Cell count millions of cells hive/tree	2.5/-	3.2/-	-	0.5/-	3.2$_{1,2,3}$/6.6$_{3}$
Model Input Variables					
Trees vs hives geometry					√$_{3}$

---

* This is only generation and diffusion. The other processes of condensation, evaporation, emission and dissolving are not included

	A	B	C	D	E
Cluster height in nest geometry			√		√$_3$
Comb gaps geometry					√$_3$
Bee size variation					√$_{1,2}$
Extensive Bee density/ Bee porosity					√
External temperature	√	√			√
Bottom board depth		√			
Additional heat sources			√	√	
Model result variables					
Metabolic Energy					√
Nest thermal resistance					√
Nest Temperature profiles			√	√	√
CO$_2$ concentration profiles	√	√			
Humidity profiles			√		
Gas Velocities	√	√	√		√$_3$

7.3 Approach

Because of the difficulty of validating a tree CFD model, an integrated open source automation approach (*FreeCAD, OpenFOAM 4.1*, *Paraview*, *Python 2.7*) was chosen, where a single CFD model was used for both trees and hives so that the validation for both could be achieved using a low heat capacity hive. The automated process was driven by a combined parameter and results database that generated the different nest geometries, with the same physical parameters, comb spacing, heating and area, then apply the same meshing algorithms (*snappyHexMesh with layering*) to produce the same meshing density within and near the hive cavity, solver code and run parameters. The running of the *OpenFOAM* solver (*CHTmultiRegionSimpleFoam*), post-processing (*wallHeatFlux*, *Paraview*) and storage of the results in the database were part of the same automated process.

This model was configured to compare the metabolic rate differences required for thermoregulation between trees and hives with a variable configuration of comb gaps, honey bee sizes, comb contents, clustering honey bee density, ambient air velocity and temperature. This involves heat transfer (conduction, convection) in and between air and the various solids involved by using a methodology called conjugate heat transfer to calculate heat passing from one medium to another. The nest, surrounding air and its contents are split into separate regions (7 for trees, 16 for hives) and the applicable equations solved for each region and the results of each iteration are passed from one region to an adjacent region through the cells that are in contact (patch) using appropriate boundary conditions (e.g. *turbulentTemperatureCoupledBaffleMixed*). The equations solved are the classic set of energy conservation, mass continuity, and momentum (*Navier-Stokes*). To simulate the air resistance of the clustering bees, the momentum equations are modified using a standard method in the solver (*fvOptions explicitPorositySource*) to conform to the properties of a porous solid using a similar approach to other studies (Sudarsan et al., 2012; Thompson, 2013). This is covered in more detail in an earlier publication of results where this process/model explored the differences between honey bee subspecies in conventional hives (Mitchell, 2022a) and in the published validation of the model (Mitchell, 2022b). Further CFD details to enable replication of results are located in the files of *OpenFOAM* case directories in the open data repository for this paper (Mitchell, 2023).The metric R value was chosen to allow comparison of metabolic heat output and therefore the performance of the nest enclosure to be independent of temperature and brood area. R value is the brood to ambient temperature difference divided by the metabolic heat flux (rate of metabolic heat divided by brood area).

7.4 Methods

The key objectives are using CFD to measure and compare the metabolic heating impact of brood heating relative height and comb gap/peripheral porosity. However in order to successfully compare with trees we require data on tree peripheral galleries, hence a requirement for an additional experiment and method i.e. Tree nest peripheral gallery measurement

7.4.1 Tree nest peripheral gallery measurement

To understand the role and impact of the presence of peripheral galleries in trees one needs to understand the magnitude of their impedance to convective flow and therefore their likely sizes and spacing. To find and destroy several tree nests and their trees to find that information is no longer practical or ethical as it was in the past (Seeley and Morse, 1978) with some calling for this practice to be made illegal (Adedeji, 2014). Thus several nests, that simulate the aspect ratio, volume and thermal conductance of tree nests (figure 7.1), were constructed from 35mm pine planks with a 20mm PIR foam cover to the internal dimensions (1.4m x 180mm x 180mm) and thermal conductance of that (Mitchell, 2016) for tree nests. Eight Honey bee colonies were then persuaded to occupy them for one year.

The nests were then dismantled, colonies rehoused and the mark-space measurements of the peripheral galleries noted (figure 7.2).

Figure 7.1: Artificial tree nest constructed from wood and foam

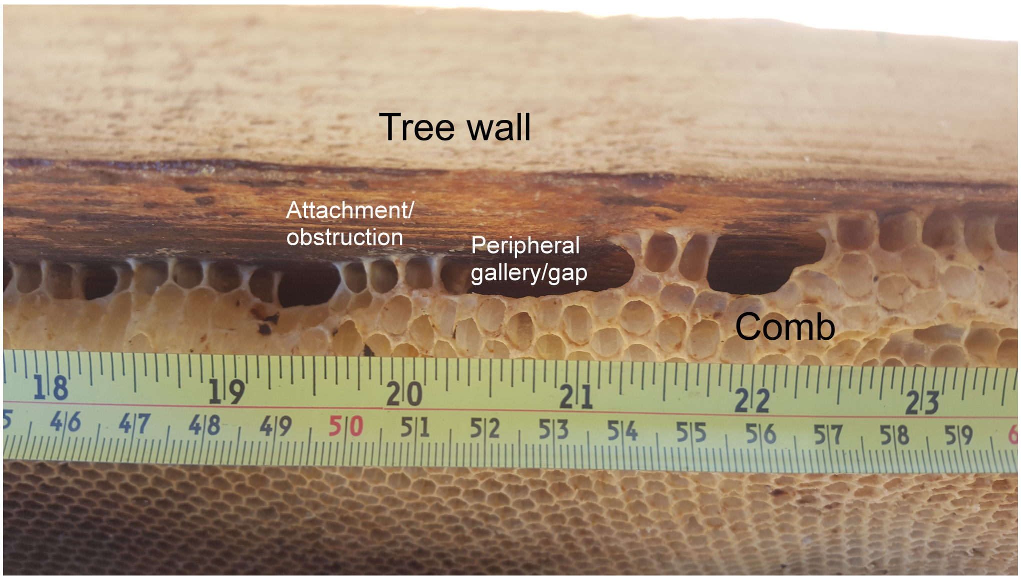

Figure 7.2: An example of peripheral galleries from the artificial tree showing the wax attachments of the comb to the nest walls.

7.4.2 CFD

The overall process consists of parameterization of the nest geometry for *FreeCAD* (Riegel and Mayer, 2019). to create 3D representations of the nests (figures 7.3a and 7.3b) and then to convert them into a format (STL) acceptable for the mesh generation of *OpenFOAM* (Jasak et al., 2007), with sufficient detail (y+ metric (Versteeg, 2007; Mitchell, 2022b)) to allow transitional laminar to turbulent modelling to cater for the abrupt changes in section (Ahmad et al., 2007) via the *kwSST* turbulence model. The *OpenFOAM* solver (*CHTmultiRegionSimpleFoam*) is then run for a series of non geometry related input parameters (e.g. cluster porosity, ambient temperature). The boundary conditions, at the walls of the volume under test, were set to fixed zero velocity gradient, with the inlet turbulent energy, turbulent dissipation rate and specific turbulent dissipation rate set to fixed values according to the literature *(CFD-Online, 2014)*. The fixed parameters in table 7.3 were used in the simulation. The solver results are then post processed to extract the metabolic rate via the *OpenFOAM wallHeatFlux* utility and various visualisations of temperature and air velocity of the nest using *Paraview* (Ayachit, 2015). After a sequence of runs from the above process the metabolic rates are analysed using *MATLAB* (MATLAB, 2018)

The non geometry parameters investigated here were ambient temperatures (T_A *Table 7.1*), brood cover porosities (ψ_B), the geometry related parameters were the comb-gap porosities (ψ_P) and relative vertical position (h^*) of the isothermal brood heat region with its associated brood covering honey bee porosity. The R value (ambient to brood temperature difference divided by the brood heat flux (Wm^{-2})) was used as the metric for the metabolic rate required for homeostasis.

For the geometry of the hive, a standard British National Hive (Cushman, 2011) of approximately 35 litres capacity was used (figure 7.3a).The dimensions taken from an example Western Red Cedar hive and combs supplied by Thornes Ltd. This comprises of hive body, floor with wire mesh, crown board and 12 standard combs, empty of stores or brood except for the 6 central combs each of which had brood areas of approximately 214 ×100mm (figure 7.4). These simulations included the air surrounding the hive (1 × 1 × 2m), wire mesh floor, entrance, crown board, roof and ventilated roof cavity as well as the internal air volume occupied by honey bees while distributed about the nest. For the clustered bees , the brood covering volumes 244 × 140 × 10 mm were simulated (fig 7.4b). The honey bee brood areas and hence the brood covering bees leave a space between themselves and the wall and roof (Sudarsan et al., 2012), thus all of the honey bees in the colony are simulated as evenly distributed in 7 fixed brood covering volumes on each face of the 6 brood areas i.e a fixed volume of 2.39 litres.

The tree dimensions were adapted from Seeley's (Seeley and Morse, 1976) tree nest survey (figure 7.3b) : external height 2.45m diameter 0.5m with a roughly cylindrical cavity shape positioned 0.2m from bottom of tree, internal height 1.2m, internal diameter 0.2m. The entrance of diameter 50mm, was positioned with its centre line 125 mm from of bottom of cavity. Both tree and hive conductivities were 0.12W $K^{-1}m^{-1}$,and the comb conductivity 0.023 W $K^{-1}m^{-1}$. From Seeley's observations and because of the smaller internal dimensions compared to the hive, the tree brood area is the full width less the 10mm periphery, stretching over the bottom 181mm. In trees an identical brood cover volume to the hives is distributed across all 5 combs for a height of 202mm. These simulations included the air surrounding the Tree (1 × 2 × 3.45m).

Extra care was taken to ensure the exposed surface areas of the honey bee brood areas, in both tree and hive, were similar i.e within a few percent. The comb thickness and inter-comb space were fixed at 25mm and 10mm respectively in both trees and hives. Note varying porosity and number density values changes the number of honey bees in a colony.

To investigate comb-gap porosities obstructions between frames (hives) or the comb and the nest interior were constructed in the geometries as shown in figures 7.4 and 7.5 to create the values of peripheral porosity (ψ_P). From both Seeley's and our own observations, honey bees do not normally have any porosity near the top of their nests. Thus in both nests the gap over the top bar is simulated as: a) Completely open i.e. $\psi_P = 0.0$ as per current hive practice (figures 7.3a, 7.4a and 7.5c); b) closed i.e. $\psi_P = 1.0$ figures 7.4b, 7.4c, 7.5a, and 7.5b; c) intermediate values including those found in tree cavities (i.e. $\psi_P = 0.17 \sim 0.24$) (figures 7.4c and 7.5b). To compare the effect of comb gaps, the relative height of the brood and cover for both trees and hives is set to zero ($h^*=0$) i.e. at the bottom of the comb.

To investigate the effect of the vertical position of the heat generation, the metric of relative height (h^*) was used for both nests (figure 7.5) with values of 0.0 (at the bottom of the nest figure 7.5a) 0.5 (mid point figure 7.5b) and 1.0 (at the top of the nest figure 7.5c). However, it became apparent that for the tree, additional measurement points were needed, so relative heights of 0.75, 0.88 and 0.98 were added. The peripheral porosities used for this were those normally encountered for each nest type i.e. for hives $\psi_P=1.0$ *and* for trees $\psi_P=0.18$ *(figures 7.4a and 7.5b)*

If all the honey bees obstructing the air flow are isothermal and in equilibrium with the heat source then the heat capacity of honey bee bodies can be ignored i.e. the honey bees are close to the heat producing brood area (Bergman and Lavine, 2017). The validity of this will be tested in the simulations. Investigating where there are bees further away from heat production, and the variation of thermal conductivity is significant, is left to future research.

Only a single man-made hive section is considered as: a) the application of additional height by beekeepers is almost always accompanied with practices that prevent the thermoregulated region of brood rearing occurring above the bottom section e.g. a wire mesh that confines the larger queen bee to the bottom section, and b) migratory pollination practice is almost always in a single section hives. Other key parameters for the CFD runs are shown in table 7.3.

The following assumptions were made in the CFD modelling: a) the honey bee colony is in brood covering state i.e. bees covering the thermoregulated brood; b) the bees are approximated to cylinders 11mm long and 4 mm diameter (Mitchell, 2022a); c) the volume of brood on each of the brood containing combs is fixed, rectilinear and isothermally maintained at 307K and is the only heat source within the nest i.e. the contribution from endothermic bees is considered to be located either on the brood surface or within the brood (brood volume) (Stabentheiner et al., 2003); d) radiation is ignored for the purposes of this simulation; e) condensation and evaporation are ignored; f) a single fluid, air, is considered i.e. not carbon dioxide or water vapour; g) the lower limit of porosity, and the highest number density (e.g. when honey bees are clustered at extreme low temperatures), is the geometric limit of close packed cylinders i.e. 0.095.

Table 7.3: CFD parameters

Parameter	**Value**	**Units**
Empty comb conductance	0.023	$WK^{-1}m^{-1}$
Ambient air velocity (inlet)	0.05	ms^{-1}
Inlet turbulent energy k	$9.79\ 10^{-8}$	m^2s^{-2}
Inlet turbulent dissipation rate ε	$9.94\ 10^{-11}$	m^2s^{-3}
Inlet specific turbulent dissipation rate ω	$3.38\ 10^{-3}$	s^{-1}
Comb frame conductance	0.12	$WK^{-1}m^{-1}$
Hive & tree conductance	0.12	$WK^{-1}m^{-1}$
Wire mesh pitch	4	mm
Wire mesh wire diameter	1	mm
Brood used t covering volume	3.4	litres
Mesh size hive	3.2	Cells x 10^6
Mesh size tree	6.2	Cells x 10^6

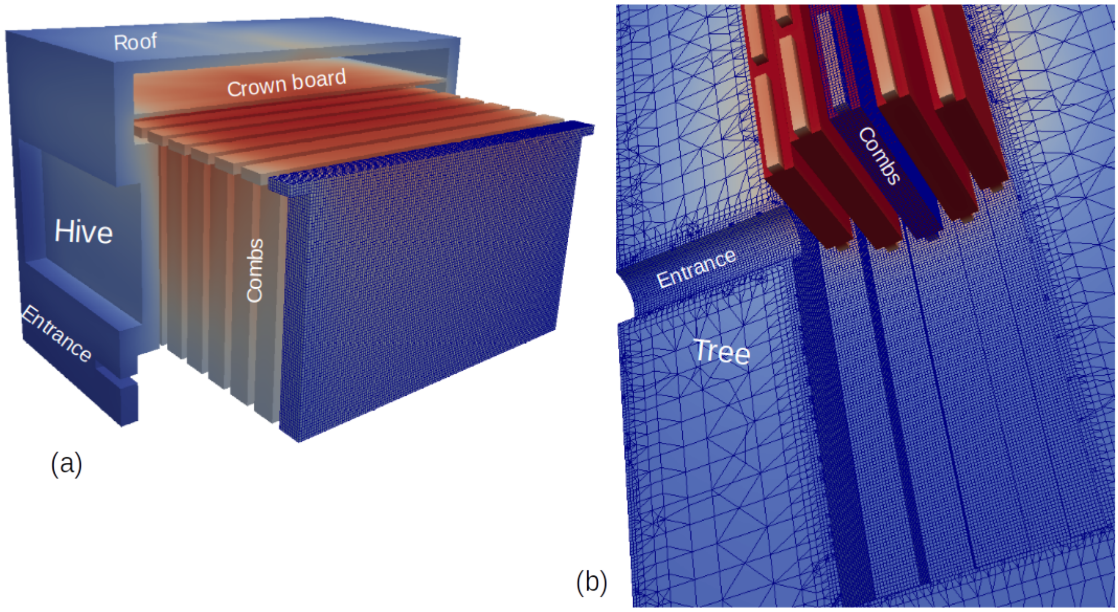

Figure 7.3: Cut away sections of CFD geometries a) hive from the side b) tree viewed obliquely from below showing the entrances combs, cavity and enclosure.

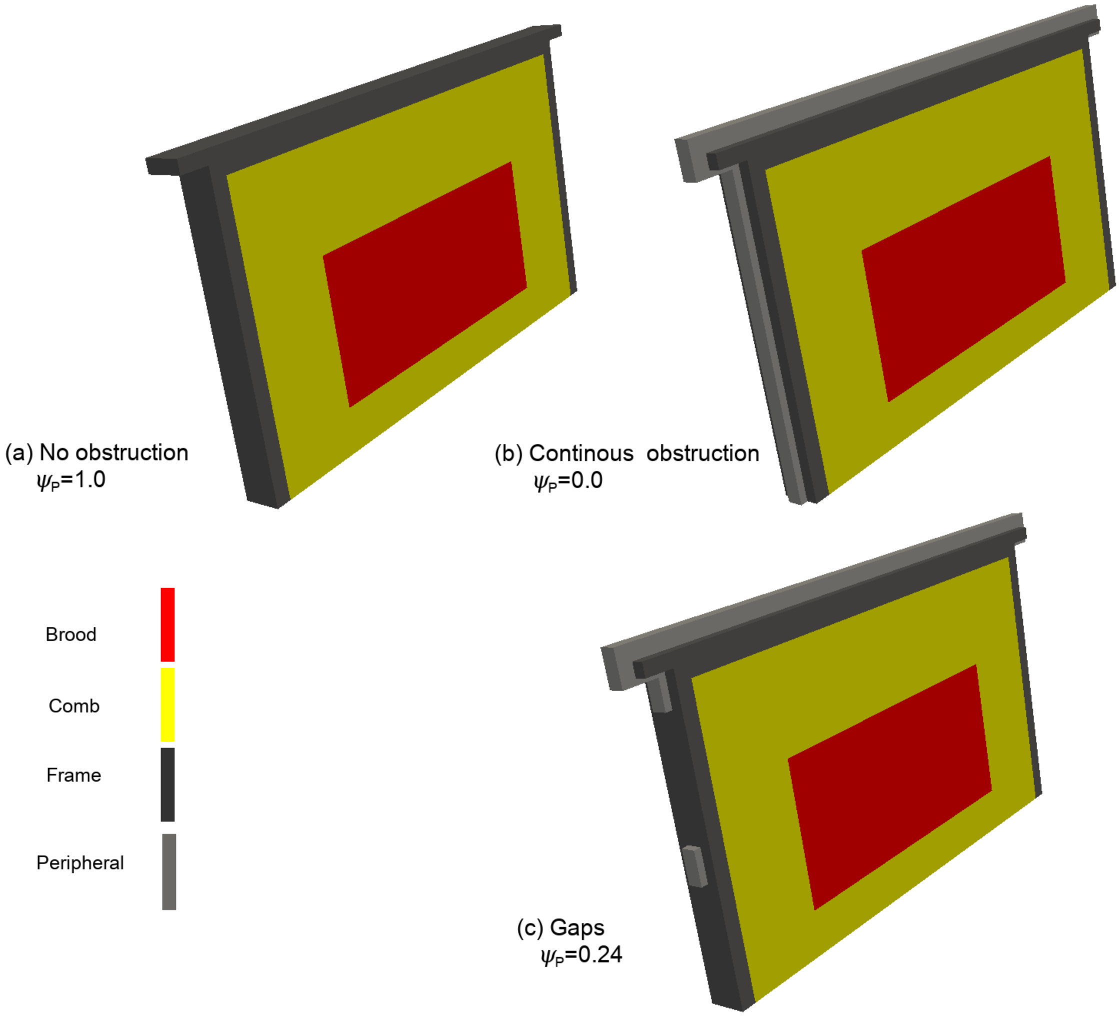

Figure 7.4:Central hive comb showing the frame, comb and heated brood area with varying peripheral porosity (ψ_P) made of gaps (bee space) and obstructions.

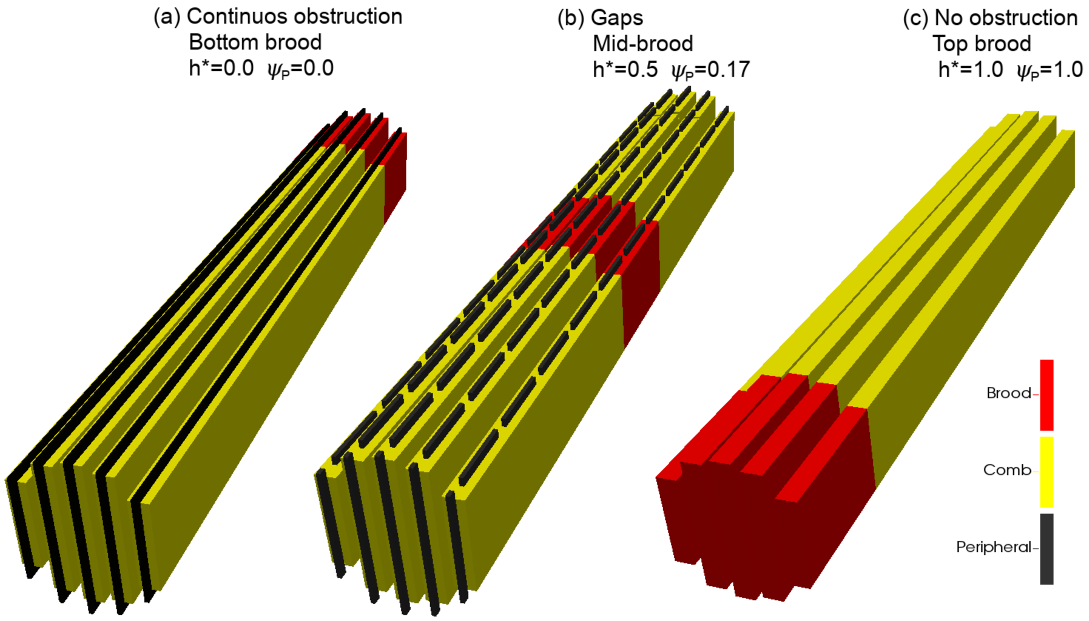

Figure 7.5: Tree combs (top nearest the viewer) showing varying peripheral porosity (ψ_P) *made from gaps (peripheral galleries) and obstructions and relative height (h*) of the heated brood area*

7.5 Results

7.5.1 Peripheral gallery honey bee experiments

Measurements were taken from 3 nests which successfully produced a total of 14 combs from the top of the tree nest. These gave the following: average gallery opening=22.9mm, standard deviation, 19.0, N=78; average interval between openings=89.7 mm, standard deviation=144.4, N=74. It should be noted that bees do not normally have any porosity near the top their nests.

7.5.2 CFD results

The focus of this study is the metabolic heat needed to maintain thermoregulation, the metric used is R value (R). As in the earlier work (Mitchell, 2022a), this and the brood covering porosity ψ_B (Table 7.1) form a sigmoid curve shown in figure 7.6. We can characterise this curve by the maximum and minimum values of R. The parameters which cause R to approach its upper bound describe the requirements upon the honey bee colony to achieve the maximum metabolic heat transfer impact of brood covering. As the curve is asymptotic, it is practical to describe a point where most of this impact is achieved. This is termed here as the critical point. The critical bee covering porosity $\psi_{critical95}$ is defined as the brood covering porosity below which the R value R is at or above 95% of the maximum R value (R_{max})

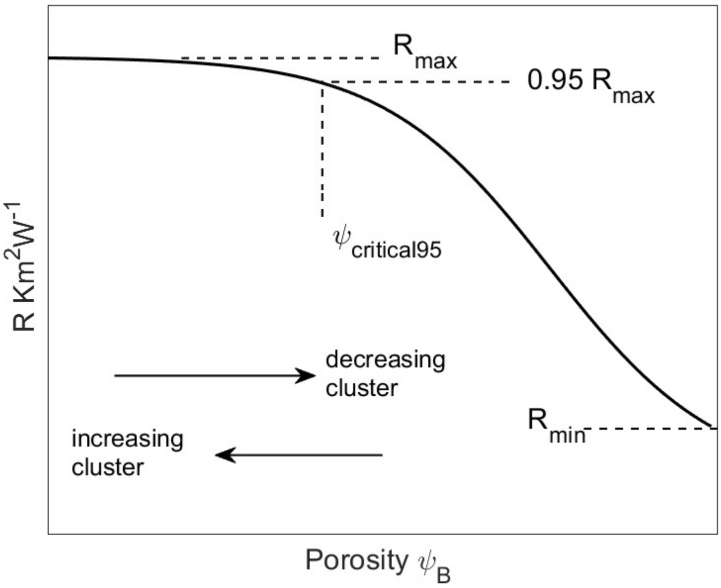

Figure 7.6: Definition of maximum R value (R_{max}), minimum R value (R_{min})and critical porosity ($\psi_{critical95}$) on a typical R value (R) versus porosity curve (ψ_B).

While porosity is used for the CFD modelling, for those considering the biological impact, the number density or the spacing relative to the size of the honey bee is more useful. The critical honey bee covering number density $\rho_{critical95}$ can be calculated directly from $\psi_{critical95}$ using the dimensions of the bee, however, calculating the relative spacing $\gamma_{critical95}$ is more involved.

If we consider the clustering of bees as the same as regular packing of cylinders with spacing between them expressed as a fraction of the honey bee cylinder diameter (γ) we can derive the relation for hexagonal packing as equation 7.1, which can be solved numerically for γ and therefore the spacing when R value (R) is at or above 95% of the maximum R value (R_{max}) can be determined i.e $\gamma_{critical95}$.

$$\varphi=1-\frac{\pi l_p}{2\sqrt{3}(\gamma+1)^2(\gamma d_p+l_p)} \tag{7.1}$$

Thus R_{max} gives the best thermal performance that can be achieved when clustered and R_{min} gives the base performance of the nest (i.e. without bees). $\rho_{critical95}$ tells us the number density needed to stop convection i.e. the maximum number of bees need to create an effective cluster, while $\gamma_{critical95}$ can tell us the size of the gaps between the bee we can expect when the cluster us effective

To illustrate the significance of the warm convective air flow spreading across the top of combs the it is visualised in figure 7.7. This shows a man made hive, as commonly found with no obstructions, and without bees to control the air flow, has velocities reaching ~0.07ms^{-1} across the top of the combs despite the low temperature difference driving the natural convection. To illustrate the differences in natural convection between trees and hives, stream lines from inter comb spaces are plotted in figure 7.8 with temperature plots of same comb spaces in figure 7.9. Note the innermost outlines denote the isothermally heated areas of comb simulating brood, the other outlines show the comb and hive bounding boxes. Attention is drawn to in figures 7.8e to 7.8f : a) the high velocity areas next to the walls, which clearly indicate areas of heat transfer and b) how the flow passes through brood areas. Figures 7.9b, 7.9d, 7.9f, 7.9h show the uniformity of the temperature in the space between the combs in the brood covering area when bees are present.

The results for investigating the effect of peripheral porosity are present in the R value for each combination of tree, hive, comb-gap porosity ψ_P, bee covering porosity ψ_B and ambient temperature T_A at zero brood heating relative height ($h^*=0$) are shown in the graphs within figure 7.10. The derived values of R_{max}, R_{min}, $\rho_{critical\ 95}$, $\gamma_{critical\ 95}$ versus ψ_P are shown the graphs within figure 7.11. Attention is drawn to difference in how R_{min} $\rho_{critical\ 95}$, $\gamma_{critical\ 95}$ differ in slope between hives and trees.

Th effects of brood heating height are shown in the R value for each combination of tree, hive, brood heating relative height h^*, honey bee covering porosity ψ_B and ambient temperature T_A at the normally found comb gap porosity (standard ψ_P) in the graphs contained in figure 7.12. Derived from these values of R_{max}, R_{min}, $\rho_{critical\ 95}$, $\gamma_{critical\ 95}$ versus h^* are shown in the graphs contained in figure 7.13. Attention is drawn to reduction in of dependance of porosity, and strong changes in critical distance and number density as the relative height approaches zero for trees.

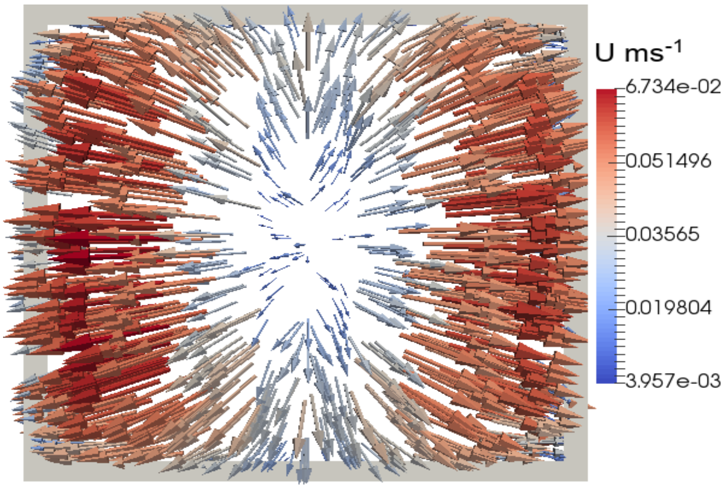

Figure 7.7: Effect of top bee space on air flow under crown board/inner cover- velocity of the air flow looking down in space between the top of the combs, below the crownboard, when: brood covering porosity ψ_B *=* *1.0, peripheral porosity* ψ_P *= 1.0, ambient temperature* T_A*=293K.*

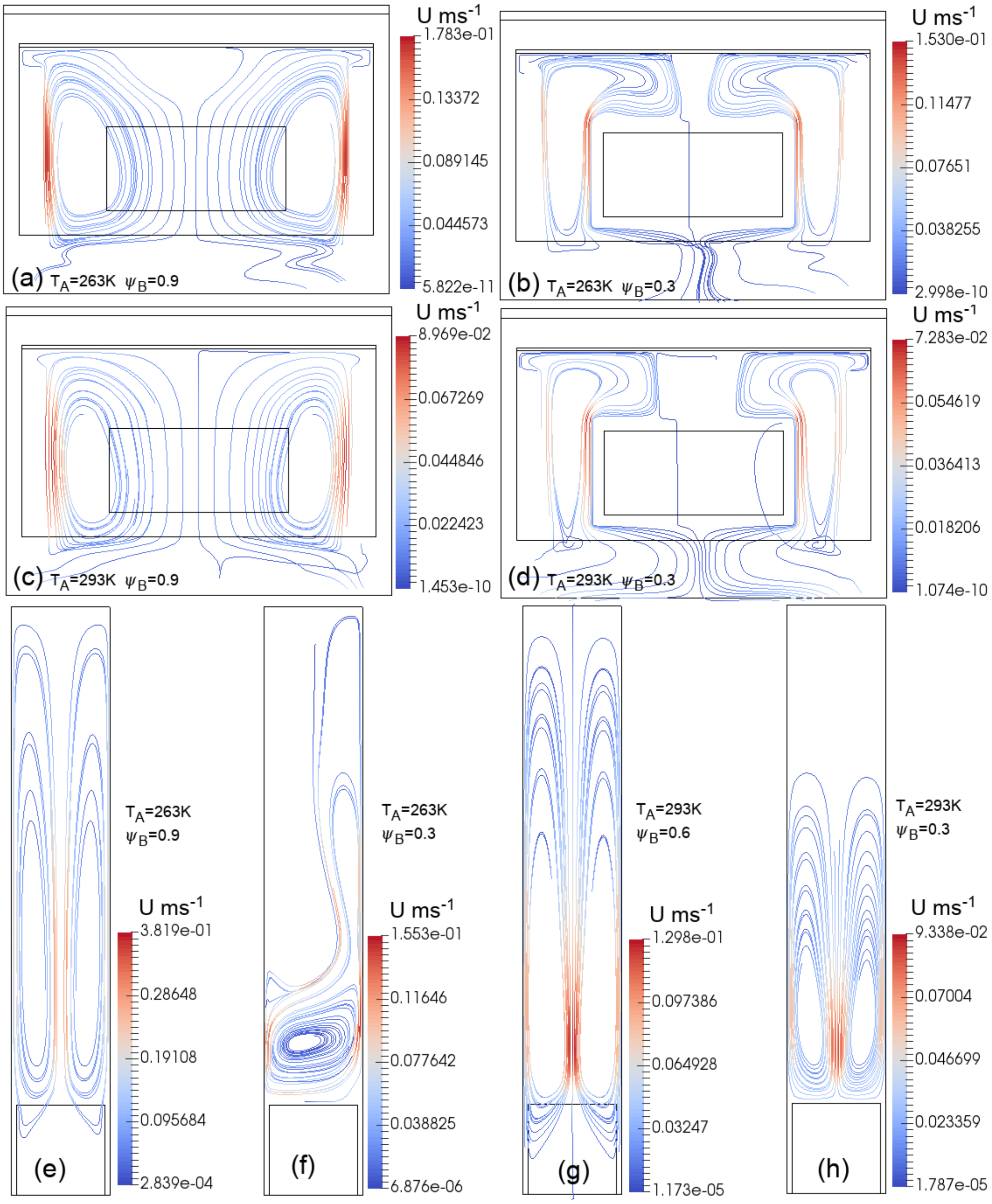

Figure 7.8: Heat transfer regime differences - stream lines of air flow between the central combs of hives (a-d) and trees (e-h) with the innermost rectangular outlines denoting the isothermally brood heated areas of comb with peripheral porosity $\psi_P = 0$; with varying ambient temperatures (T_A) and brood covering porosities (ψ_B).

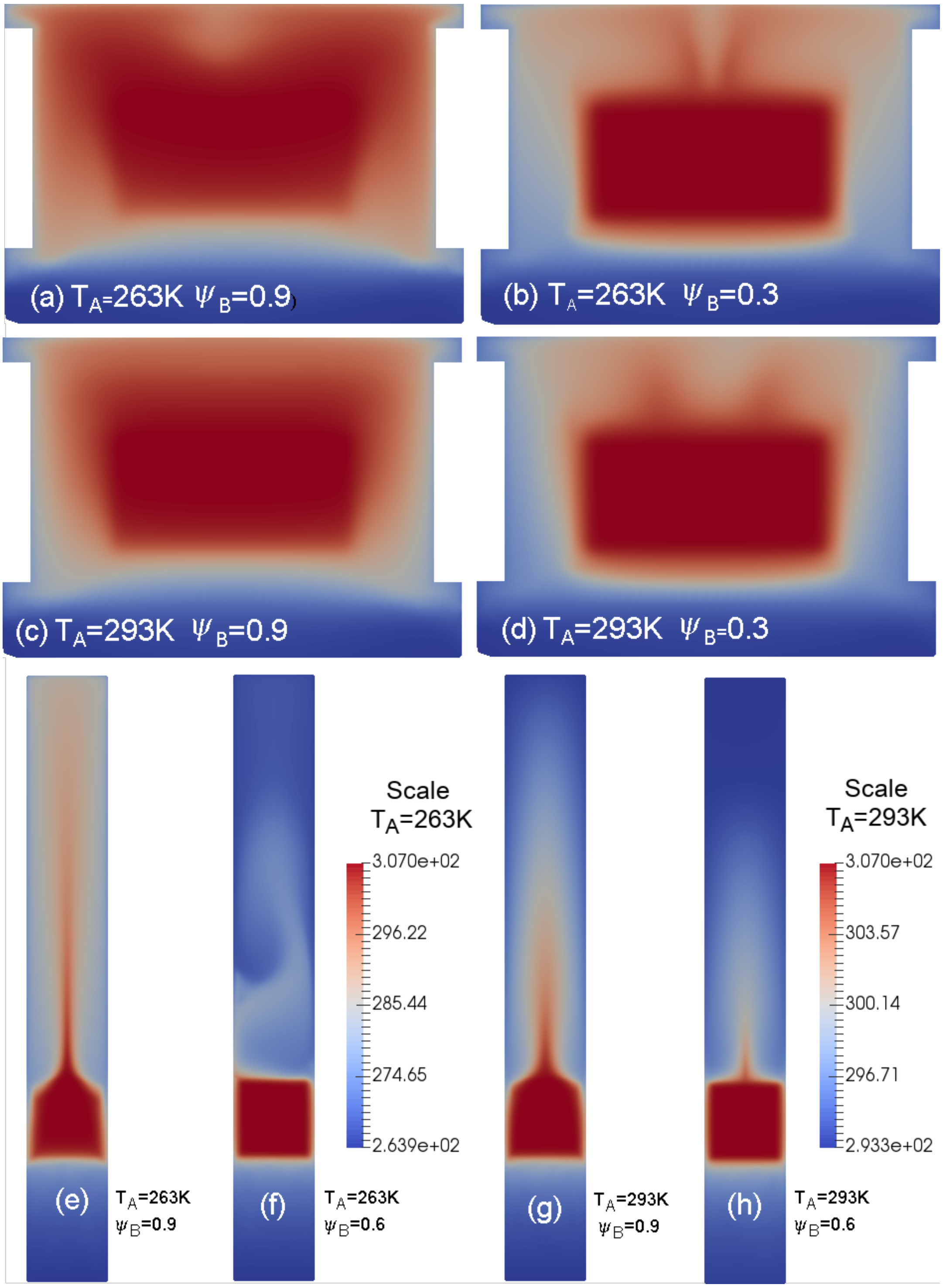

Figure 7.9: Heat transfer regime differences - temperature plots of the same inter comb spaces as shown in figure 7.8 : for hives and trees with peripheral porosity $\psi_P = 0$ *; with varying ambient temperatures* (T_A) *and brood covering porosities* (ψ_B)

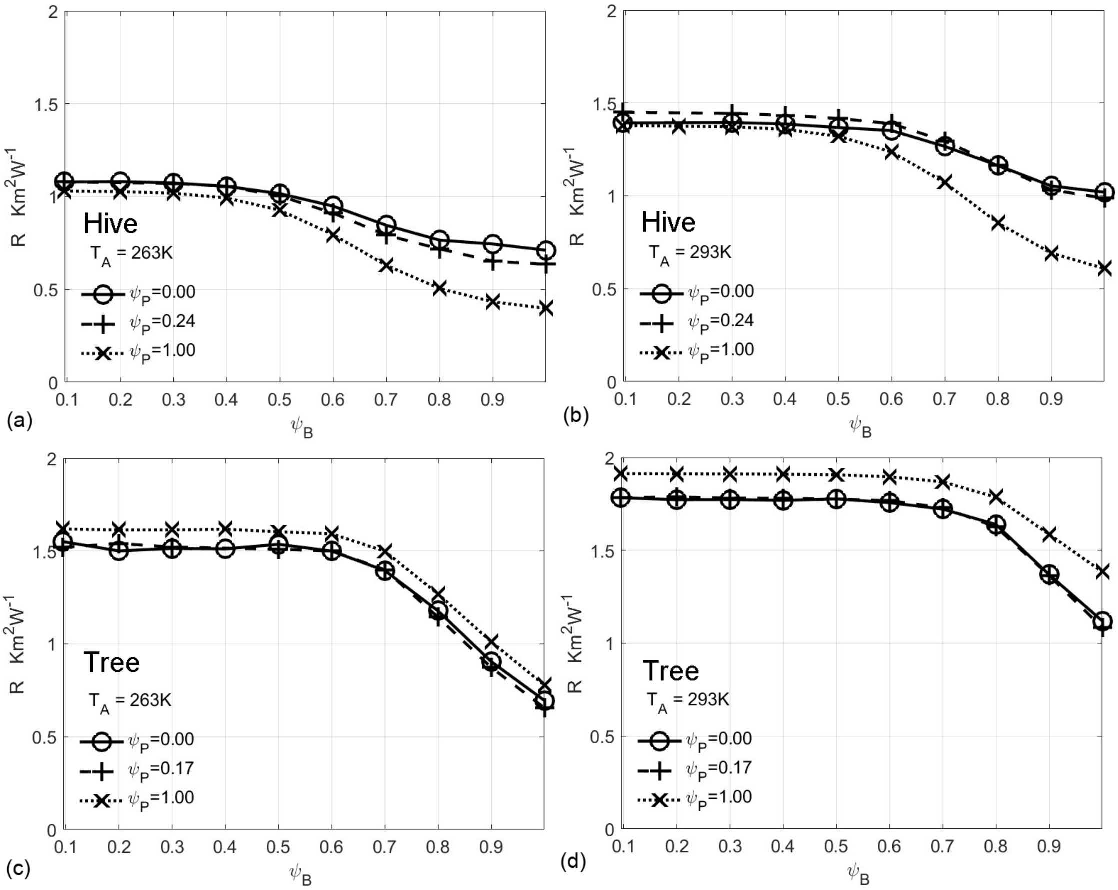

Figure 7.10: Effect of peripheral porosity on R value - R value (R) versus brood cover porosity (ψ_B) with the brood heating area at the bottom i.e. h=0 for various tree and hive peripheral porosities (ψ_P) for ambient temperatures (T_A) 263K and 293K.*

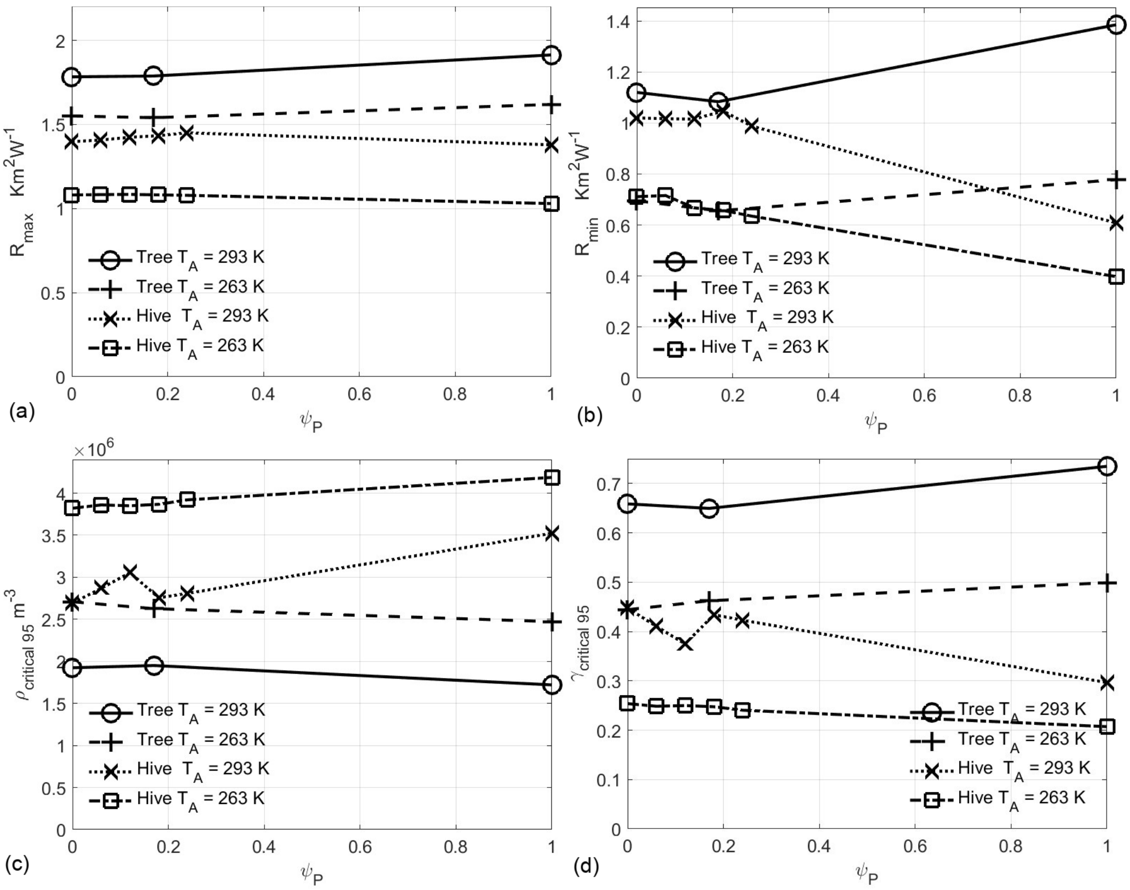

Figure 7.11: Effect of peripheral porosity on thermal performance - hives and trees at ambient temperatures (T_A) 263K and 293K peripheral porosity versus: a) Maximum R value R_{max} ; b) Minimum R value R_{min}; c) 95% critical bee density $\rho_{critical\ 95}$; d) 95% critical bee spacing $\gamma_{critical\ 95}$.

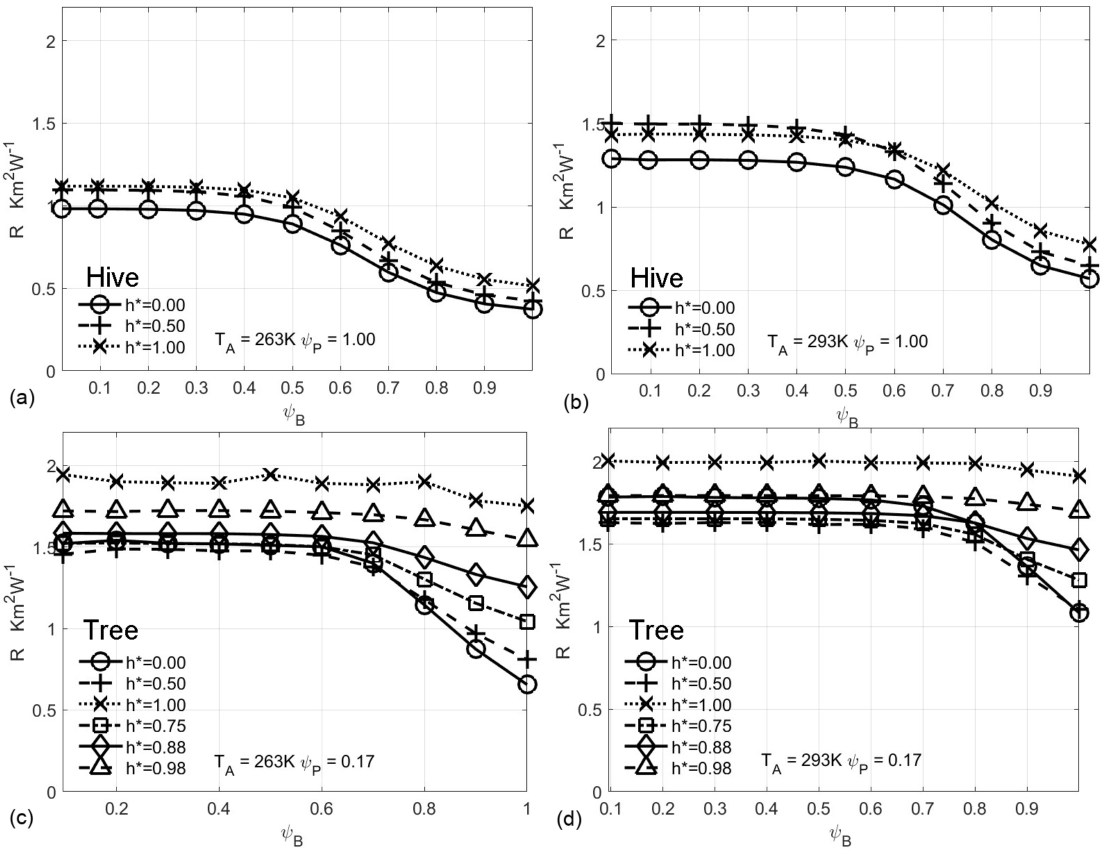

Figure 7.12: Effect of relative height on R value - R value (R) versus brood cover porosity (ψ_B): for hives and tree cavity relative brood heating heights h at ambient temperatures T_A = 293K and T_A = 263K;*

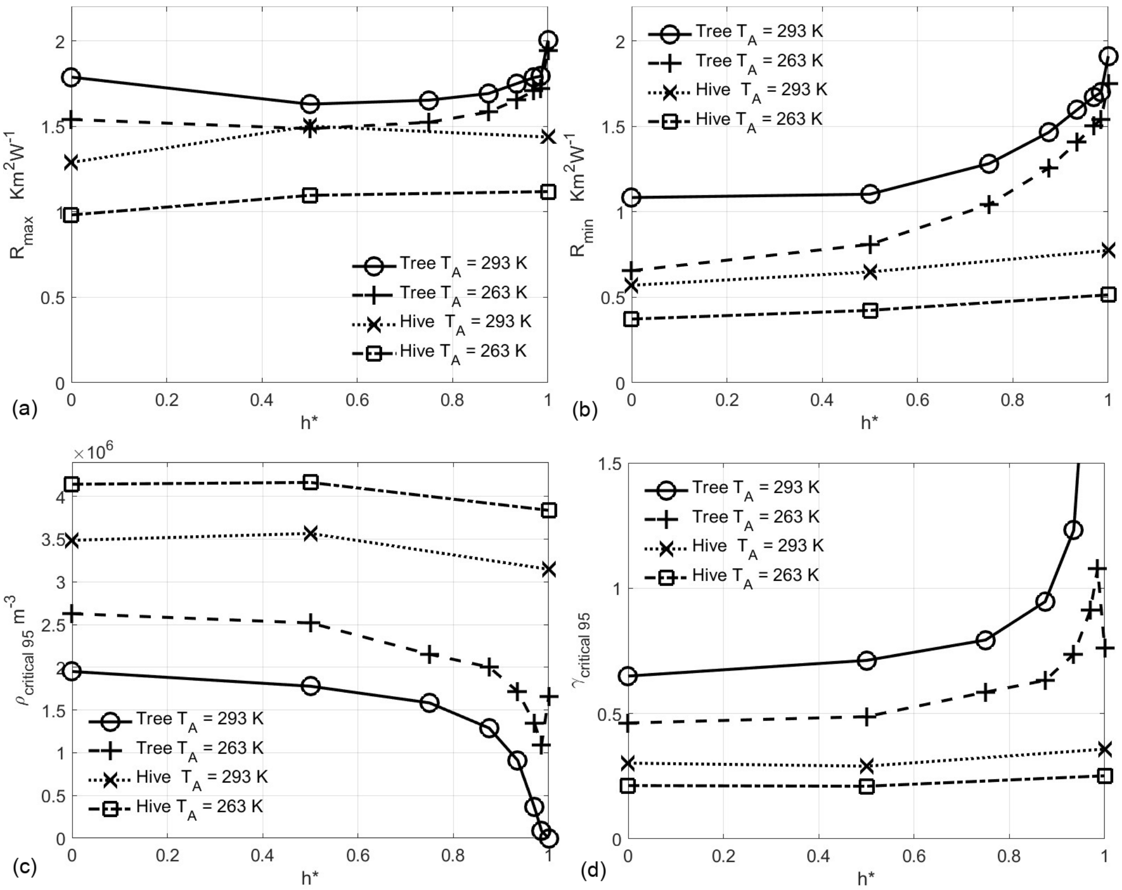

Figure 7.13: Effect of relative height on thermal performance - cavity relative brood heating height h versus: a) Maximum R value (R_{max}); b) Minimum R value (R_{min}); c) 95% critical honey bee number density $\rho_{critical\ 95}$; d) 95% critical honey bee spacing $\gamma_{critical\ 95}$.*

7.6 Discussion

The marked difference in convection flow between hives and trees is evident in the flow lines in figure 7.8 and temperature distributions in figure 7.9. This shows that in hives the circulation between the combs revolves around a centre to the side of the heated area regardless of brood cover porosity, whereas in the tree the circulation centre moves from inside the heated area to above it as the porosity decreases. In figures 7.8a, 7.8c, 7.8e, 7.8g, 7.8h we can clearly see the higher velocity (0.4 to 0.01 ms^{-1}) downward air flow in both trees and hives forming the cooling part of the air circulation. At the lower population extreme (i.e. zero honey bee density) the convection from the brood resembles that of heated plates in a partially insulated cavity. At finite high porosities/low bee densities these differences can be classified as a) vertical flow through convection and b) penetrative convection, in hives (figures 7.8a,7.8c) and tree nests(figures 7.8e, 7.8g) respectively (Nield and Bejan, 2017). Figures 7.9b, 7.9d, 7.9f, 7.9h also show that the temperatures of the air, bees and heated brood area are identical when the bees are present in significant density (lower porosity), enabling the conductivity of the bees to be ignored in this set of circumstances.

At low porosity/high bee densities, the convection around brood covering bees superficially resembles that around a heated solid with again significant differences between hives and tree cavities. In hives it becomes like a solid heated object between plates suspended in a larger 3 dimensional partially insulated box with the convection airflow passing over the entire surface of the objects and the interior containing box. In contrast, in tree nests, it resembles heated plates obstructing gaps in channels, with the convection mostly occurring above the plates.

This has an important consequence, that in tree nests, the cavity surface below the heat producing volume is not in the cooling part of convection circuit. Hives have the full area of the brood covered region available to lose heat by convection. This in contrast to tree nests, where only the top surface is exposed.

This is a result of the heating source extending to, or close to, the cavity walls in the case of trees, whereas in hives, there is a considerable gap. Increasing the level of insulation has been suggested by many researchers (Mitchell, 2016; Mitchell, 2019; Seeley, 2019) and deemed unnecessary by others (Farrar, 1947; Currie and Spivak, 2015; Milbrath, 2020), and reduction of comb length as been suggested as beneficial (Perichon, 2021). In this study we can see that the effects of both can make dramatic changes to the system of air movement within the nest and they also infer honey bees in trees are likely to have increased control of heat loss compared to hives, by adjusting their position vertically. This is a subject for further research.

The presence or absence of comb gaps (peripheral porosity) has a marked influence on the thermal resistance in nests. For hives normally with ψ_P=1 there is a significant component of air flow at right angles to the long axis of the combs, as shown in figure 7.7. This results in extra external surface area being involved in the heat transfer via convection.

In hives, convection through the gaps dominates over the conduction of the comb attachment as shown in figures 7.10a, 8b and figure 7.11a. As indicated by the marked decrease (between 68% and 79%) in values of R_{min} with increase in peripheral porosity (transitions from 0 to 1). In trees the reverse happens and the conduction of the comb attachments is the more significant, as shown by values of R_{min} increasing (between 19% and 28%) with increasing peripheral porosity (transitions from 0.17 to 1). The differences shown between T_A=263 and T_A=293 resulting from the changes in heat transfer coefficient from the differing temperature ranges involved.

This identifies a substantial improvement in thermal resistance that can be made easily in the hive design by eliminating or blocking the space above the combs (e.g. a sheet of plastic resting on the top of the combs). This would also reduce the bee density to achieve maximum covering effect (-9% to -24%) as shown in figure 7.11d.

As previously noted honey bees are known to move the thermoregulated area of the nest upwards as winter progresses. This is assumed in the literature (Owens, 1971) to be for access to honey stores. It has been shown that the man made hive has only a small advantage in moving the brood area upwards, as the convection continues to be effective between the brood area and the hive sides, which is evident in the R_{max} variation (10-12%) $\rho_{critical\ 95}$ (-7% to -10%) while R_{min} is a little larger at 26% to 28%, see figures 7.12 and 7.13. However, in trees there is very different picture with R_{max} increasing 12% to 26%, R_{min} 76% to 167% and $\rho_{critical\ 95}$ changing -37% to -100%. In addition the differences between T_A=263K and T_A=293K dissipate. This is a result of the convection above the brood being suppressed and the remaining convection underneath being small in magnitude and the external surface to air temperature differences changing little. Thus in trees the R value increases and effectively becomes a constant regardless of the density of bees covering the heat source and the external temperature. This implies that when at the very top of the cavity in trees, dense clustering no longer has any significant metabolic heat transfer impact under these conditions.

The density of bees needed to achieve the maximum benefit in reducing heat loss via covering the brood is of great consequence to bees to achieve winter survival and summer efficiency, as it determines the population needed to achieve maximum control of their internal environment. From figures 7.11c and 7.13c we can see that hives and trees have very different critical bee densities, with hives requiring at least 1.58 times the density for trees indicating that smaller colonies will have better survival in trees compared to hives of the same volume. Note the anomalous values for $\rho_{critical\ 95}$ and $\gamma_{critical\ 95}$ at h*=0 and T_A=263K in figures7.13c, 7.13d are a result of the scattering of R values in a flat distribution seen in figure 7.12c creating uncertainty.

The thermal resistance measurements R_{max} and R_{min} show temperature, peripheral porosity and nest type dependence. They both demonstrate the markedly superior heat transfer performance of the tree,particularly R_{min} when h*=1. Even though the distance to the top of the nest cavity is much greater in the tree nest (~1m vs ~0.1m) the values of R_{max} and R_{min} are higher in the tree nest when the brood is at the bottom and for their normal peripheral porosities by a factor of 1.29 to 1.49 for R_{max} and 1.78 to 1.64 for R_{min}. This can be attributed to the much higher levels of insulation afforded by the much thicker walls of the tree nest (0.2m vs 0.019m) and the differing convection regime. When comparing the current study to the only existing experimental metabolic energy comparison of hives and trees (Mitchell, 2016), the differences between trees and hives are reduced from a range of 4-7 times to one of a factor of 3. This is probably due to the air resistance of the combs in the present study being absent in the earlier one.

The spacing below which natural convection stops is in the range of 0.2 to 0.45 bee widths for hives and 0.5 to greater than 1 for natural nests. Such spacing does not appear to be the tightly packed arrangement related in literature, especially in tree nests, and confirms that the honey bees may be modelled as a solid over the range of density from pre-cluster/less dense cluster, through to cluster.

7.7 Conclusions

This study is unique in comparing the metabolic energy requirements for colony thermoregulation between hives and trees complete with combs and bees. It has shown that tree nests have a completely different regime of natural convection compared to man made hives i.e. penetrative convection vs vertical flow through. The space above the frames in a man-made hive creates an avoidable significant extra heat loss because of the extra convection paths across the tops of the frames, which increases the number of bees required to achieve maximum thermal resistance. The evolution of the known behaviour of moving the brood volume to the top of the nest is probably due the major changes in heat transfer found in tree cavities reducing both heat loss and the number of honey bees required to stop convection. This is unlike the minimal effects found in man-made hives. The effect of moving to the very top of the nest in trees makes dense clustering redundant. This suggests, originally, in natural nests, clustering is a behaviour developed to cope with exceptions and when the nest is first inhabited, and not the norm that it is in man made hives. Regardless of vertical position, clustering in tree cavities results in higher thermal resistance for the application of less bees than man-made made hives. The heat transfer differences between natural nests and man made hives are broad in scope and significant enough in magnitude to have dramatic impacts on honey bee behaviour. This calls into doubt whether some past research conducted in man-made hives reflects the behaviour of honey bees generally or just their reaction to human constructions.

Thus new research into honey bees now needs to: first, carefully validate whether the conclusions they arrive at are innate honey bee behaviours that would occur in their natural nests or are anthropogenic i.e. artefacts of the conditions in man-made environments; second, have a clear understanding of heat transfer and the heat transfer implications of their experimental treatments and controls i.e. beyond previous simplistic temperature concepts (Anderson, 1943; Owens, 1971).

7.8 References

Abou-Shaara, H.F., Al-Ghamdi, A. a. and Mohamed, A. a. 2012. Tolerance of two honey bee races to various temperature and relative humidity gradients. *Environmental and Experimental Biology*. **10**, pp.133–138.

Adedeji, G. 2014. Preliminary Survey of Wood Species Cavities Preferred by Honeybees in Nigeria. *International Journal of Scientific and Engineering Research*. **5**, pp.1313–1320.

Ahmad, F., Yamada, S. and Chaudhry, S.R. 2007. Assessment of Turbulence Models for Turbulent Flow over Backward Facing Step.

Anderson, E.J. 1943. Some Research on the Wintering of Bees. *Gleanings in Bee Culture*. **71**, pp.681–683.

Ayachit, U. 2015. *The ParaView Guide: A Parallel Visualization Application*. Kitware, Incorporated.

Bergman, T.L. and Lavine, A.S. 2017. *Fundamentals of Heat and Mass Transfer 8th Edition*. Wiley.

CFD-Online 2014. Turbulence free-stream boundary conditions. [Accessed 2 February 2022]. Available from: https://www.cfd-online.com/Wiki/Turbulence_free-stream_boundary_conditions.

Chen, Y.W., Chung, W.P., Wang, C.H., Solter, L.F. and Huang, W.F. 2012. Nosema ceranae infection intensity highly correlates with temperature. *Journal of Invertebrate Pathology*. **111**(3), pp.264–267.

Currie, R.W. and Spivak, M. 2015. Winter Management of HoneyBee Colonies *In*: J. Graham, ed. *Hive and the Honey bee*. Hamilton IL USA: Dadant.

Cushman, D. 2011. Drawings of Hives and Hive Parts. *Dave Cushman's Beekeeping and Bee Breeding Website*.

Delaplane, K.S., Van Der Steen, J. and Guzman-Novoa, E. 2013. Standard methods for estimating strength parameters of Apis mellifera colonies. *Journal of Apicultural Research*. **52**(1), pp.1–12.

Farrar, C.L. 1947. The overwintering of productive colonies *In*: R. A. Grout, ed. *Hive and the honey bee*. Chicago: Dadant and sons, pp.425–451.

Flores, J.M., Ruiz, J.A., Ruz, J.M., Puerta, F., Bustos, M., Padilla, F. and Campano, F. 1996. Effect of temperature and humidity of sealed brood on chalkbrood development under controlled conditions. *Apidologie*. **27**(4), pp.185–192.

Jasak, H., Jemcov, A. and Tukovic, Z. 2007. OpenFOAM : A C ++ Library for Complex Physics Simulations. *International Workshop on Coupled Methods in Numerical Dynamics*. **m**, pp.1–20.

Kraus, B. and Velthuis, H.H.W. 1997. High humidity in the honey bee (Apis mellifera L.) brood nest limits reproduction of the parasitic mite Varroa jacobsoni Oud. *Naturwissenschaften*. **84**(5), pp.217–218.

Langstroth, L.L. 1853. *LANGSTROTH ON THE HIVE AND THE HONEY-BEE, A BEE KEEPER'S MANUAL*. NORTHAMPTON HOPKINS, BRIDGMAN & COMPANY.

MATLAB 2018. *9.4.0.813654 (R2018a)*. Natick, Massachusetts: The MathWorks Inc.

Milbrath, M. 2020. The Greatest Generation : Winter Bees. *American Bee Journal*. **160**(1), pp.33–36.

Mitchell, D.M. 2023. Data associated with 'Are Man-Made Hives valid thermal surrogates for natural Honey Bee nests (Apis mellifera)?' [Accessed 16 December 2023]. Available from: https://archive.researchdata.leeds.ac.uk/1159/.

Mitchell, D.M. 2022a. Honey bee (Apis mellifera) size determines colony heat transfer when brood covering or distributed. *International Journal of Biometeorology*. **66**(8), pp.1653–1663.

Mitchell, D.M. 2019. Nectar, humidity, honey bees (Apis mellifera) and varroa in summer: A theoretical thermofluid analysis of the fate of water vapour from honey ripening and its implications on the control of Varroa destructor. *Journal of the Royal Society Interface*. **16**(156).

Mitchell, D.M. 2016. Ratios of colony mass to thermal conductance of tree and man-made nest enclosures of Apis mellifera: implications for survival, clustering, humidity regulation and Varroa destructor. *International Journal of Biometeorology*. **60**(5), pp.629–638.

Mitchell, D.M. 2022b. Simulating the built environment for another globally distributed species *In*: *Proceedings of BSO Conference 2022: 6th Conference of IBPSA-England* [Online]. BSO Conference. Bath, UK: IBPSA-England. Available from: https://publications.ibpsa.org/conference/paper/?id=bso2022_40.

Nield, D.A. and Bejan, A. 2017. *Convection in porous media*.

Oskin, S.V., Tsokur, D.S., Sultanov, G.A. and Kudryavtseva, A.A. 2020. The thermal model of winter aggregation of bees. *IOP Conference Series: Earth and Environmental Science*. **488**(1).

Owens, C.D. 1971. *The thermology of the wintering honey bee*. U.S. Agricultural Research Service.

Perichon, S. 2021. Feedback from beekeepers that use the Warré (People’s) Hive Questionnaire online survey both in Europe and other parts of the world. *Journal of Apicultural Research*. **0**(0), pp.1–16.

Riegel, J. and Mayer, W. 2019. FreeCAD (Version 0.18).

Ruttner, F. 1988. *Biogeography and Taxonomy of Honeybees*.

Seeley, T.D. 2019. Darwinian Beekeeping. *The Lives of Bees*. (March), pp.277–292.

Seeley, T.D. and Morse, R.A. 1978. Nest site selection by the honey bee, Apis mellifera. *Insectes Sociaux*. **25**(4), pp.323–337.

Seeley, T.D. and Morse, R.A. 1976. The nest of the honey bee (Apis mellifera L.). *Insectes Sociaux*. **23**(4), pp.495–512.

Simpson, J. 1961. Nest Climate Regulation in Honey Bee Colonies. *Science*. **133**(3461), pp.1327–1333.

Southwick, E.E. 1985. Allometric relations, metabolism and heat conductance in clusters of honey bees at cool temperatures. *Journal of Comparative Physiology B*. **156**(1), pp.143–149.

Stabentheiner, A., Pressl, H., Papst, T., Hrassnigg, N. and Crailsheim, K. 2003. Endothermic heat production in honeybee winter clusters. *Journal of Experimental Biology*. **206**(2), pp.353–358.

Sudarsan, R., Thompson, C., Kevan, P.G. and Eberl, H.J. 2012. Flow currents and ventilation in Langstroth beehives due to brood thermoregulation efforts of honeybees. *Journal of Theoretical Biology*. **295**, pp.168–193.

Tahmasbi, G. 2009. The effect of temperature and humidity on grooming behaviour of honeybee, Apis mellifera (Hym.: Apidae) colonies against varroa mite, Varroa destructor (Acari: Varroidae). (2)28 .نامه انجمن حشره شناسی ایران, pp.7–23.

Tapia Brito, E. 2022. *Application of phase change material heat storage device for control of Varroa mites in beehives*.[Online] Thesis (University of Nottingham only), Nottingham UK: University of Nottingham. [Accessed 10 September 2023]. Available from: https://eprints.nottingham.ac.uk/71611/.

Thompson, C. 2013. a Cfd Study Investigating the Influence of Bottom Board Geometry on Physical Processes Within a Standard Honeybee Hive. *Journal of Chemical Information and Modeling*. **53**(9), pp.1689–1699.

Versteeg, H.K. 2007. *An introduction to computational fluid dynamics: the finite volume method* 2nd ed. Harlow, England ; Pearson Education Ltd.

Villumstad, E. 1974. Importance of hive insulation for wintering , development and honey Yield in Norway. *Apiacta*. **3**, pp.116–118.

Chapter 8 Honey bee cluster – not insulation but stressful heat sink

This chapter is based upon the authors published work:

Mitchell, D.M. 2023. Honeybee cluster—not insulation but stressful heat sink. Journal of the Royal Society Interface.

8.1 Abstract

Since the early 20th century, the outer layer (mantle) of honey bees (*Apis mellifera*) in the winter cluster has been said to insulate the cluster core. This has encouraged enforced clustering, by the beekeepers' dominant use of inadequately insulated hives and in North America, refrigeration. This is often seen as a benign or even a necessary process, with beekeeping, and academic research considering these conditions of extreme heat loss, compared to the honey bee’s natural habitat, as natural and normal. By using porous material correlations, analysis of previous findings and a model of a cluster within a hive in a landscape, that implements convection, conduction and radiation, we show that a honey bee colony increases in thermal conductivity, on transition from pre-cluster to dense mantle, by a factor of ~2, insulation R-value can decrease by more than 11. These results show that the mantle does not act like insulation and that clustering is not benign, but instead is an evolutionary behavioural reaction to an existential threat that results in increased cold and exertion stress. Thus the attitude to forced clustering, i.e. deliberately provoking a stressful survival behaviour, needs revision as avoidable forced stress upon animals may be regarded as cruel.

Table 8.1: Chapter nomenclature.

Symbol	Units	Description
c_1 to c_4	-	Constants for sphere- cube convection correlation (Warrington and Powe, 1985)
d_B, d_{BH}, d_h	m	Diameters of individual honey bee body, body and hair envelope and hair
$\bar{d}_B, \bar{d}_{BH}$	m	Sauter mean diameters of individual bee body, body and hair envelope
f_{ground}	-	View factor radiated hive outer to ground
f_{sky}	-	View factor hive to sky

Symbol	Units	Description
$\bar{h}_{a(conv)}$	$Wm^{-2}K^{-1}$	Average heat transfer coefficient of total hive outer surface
$\bar{h}_{bottom}$	$Wm^{-2}K^{-1}$	Average heat transfer coefficient of hive outer bottom surface
$\bar{h}_{Li}$	$Wm^{-2}K^{-1}$	Average heat transfer coefficient of gap between mantle and hive interior
$\bar{h}_{side}$	$Wm^{-2}K^{-1}$	Average heat transfer coefficient of hive outer side surface
$\bar{h}_{top}$	$Wm^{-2}K^{-1}$	Average heat transfer coefficient of hive outer top surface
g	ms^{-2}	Acceleration of gravity 9.81 ms-2
k_{air}	$Wm^{-1}K^{-1}$	Thermal conductivity of air
k_{hive}	$Wm^{-1}K^{-1}$	Thermal conductivity for hive
k_{eff}	$Wm^{-1}K^{-1}$	Effective thermal conductivity of honey bees in cluster mantle
k_B	$Wm^{-1}K^{-1}$	Effective thermal conductivity of a honey bee body
l_B, l_{BH}, l_h	m	Length of individual honey bee body, body and hair envelope and hair
m_B	kg	Mass of individual honey bee
p_h	-	Plumosity of honey bee hair
$\dot{q}_{g(rad)}$	W	Heat transfer rate radiated from hive outer to ground
$\dot{q}_{inner(conv)}$	W	Heat transfer rate hive inner convection
$\dot{q}_{hive(conduct)}$	W	Heat transfer rate between hive inner and outer surfaces by conduction
$\dot{q}_{mantle}$	W	Total heat transfer rate from mantle
$\dot{q}_{thermal}$	W	Sky downward heat flux
$\dot{q}_{sky(rad)}$	W	Heat flux radiated from hive outer to sky
$\dot{q}_{inner(rad)}$	W	Heat transfer rate outer radiation
$\dot{q}_{air(conv)}$	W	Heat transfer rate outer convection
r_{eff}	m	Effective radius of hive cavity
r_{mantle}	m	Radius of mantle
x_a, y_a, z_a	m	Dimension of hive a=inner or outer
A_B, A_{BH}, A_h	m^2	Surface areas of individual honey bee body, body and hair envelope and hair
A_{side}	m^2	Total area of hive outer vertical sides
A_{bottom}	m^2	Area of hive outer bottom surface
A_{top}	m^2	Area of hive outer top surface
A_{outer}	m^2	Total area of hive outer surfaces
A_{inner}	m^2	Total area of hive inner surfaces
A_{mantle}	m^2	Area of mantle outer surface
C	-	Cloud cover coefficient
Cp_{air}, Cp_B	$Jkg^{-1}K^{-1}$	Heat capacities of air and honey bees
H	m	Vertical dimension of the core
L_x	m	Characteristic length of x
L_{bottom}	m	Characteristic length of hive outer bottom surface
L_i	m	Characteristic length of gap between mantle and hive interior
L_{side}	m	Characteristic length of hive outer vertical side surfaces
$\bar{L}$	m	Characteristic length of honey bees between combs
K	-	Cloud height coefficient

Symbol	**Units**	**Description**
$\overline{Nu}_{bottom}$	-	Average Nusselt number of hive outer bottom surface
$\overline{Nu}_{Li}$	-	Average Nusselt number of hive mantle gap
$\overline{Nu}_{side}$	-	Average Nusselt number of hive outer side surface
$\overline{Nu}_{top}$	-	Average Nusselt number of hive outer top surface
Pr	-	Prandtl number of air
Ra_{Li}	-	Rayleigh number of hive mantle gap
Ra_{Lx}	-	Rayleigh number at characteristic length Lx
Ra_{Ltop}	-	Rayleigh number of hive top surface
$Ra_{Lbottom}$	-	Rayleigh number of hive bottom surface
Ra_{Lside}	-	Rayleigh number of hive side surfaces
Ra_{L}	-	Rayleigh number of honey bees between combs
Ra_{C}	-	Critical Rayleigh number typically ~40 for porous materials
R_{value}	Km^2W^{-1}	R-value thermal insulance (Thermal Engineering, 2019)
R_{H}	-	Relative humidity of air (0-1)
S^{*}	-	Total conduction shape factor for hive (Bergman and Lavine, 2017b)
T_{air}	K	Temperature of air
T_{film}	K	Temperature to calculate air properties
T_{ground}	K	Temperature of ground
$T_{hive(inner)}$	K	Temperature of hive inner surface
$T_{hive(outer)}$	K	Temperature of hive outer surface
T_{mantle}	K	Temperature of mantle outer surface
T_{core}	K	Temperature of core-mantle boundary
T_{sky}	K	Effective temperature of sky
V_{B}, V_{BH}, V_{h}	m^3	Volumes of individual honey bee body, body and hair envelope and hair
α_{T}, α_{B}	m^2s^{-1}	Thermal diffusivity at temperature T_{film} and honey bee bodies
β_{T}	K^{-1}	Thermal expansion coefficient at temperature T_{film}
ϵ_{ground}	-	Emissivity of ground typically 0.9
ϵ_{inner}	-	Emissivity of hive inner surface typically 0.9
ϵ_{outer}	-	Emissivity of hive outer surface typically 0.9
ϵ_{mantle}	-	Emissivity of mantle 0.9
ϵ_{sky}	-	Emissivity of sky 0.75
$\varphi_{B}, \varphi_{BH}$	-	Porosity of honey bees in mantle i.e. fraction of air
φ_{0}, φ_{P}	-	porosity of honey bee when tightly packed in mantle, and pre clustered
ν_{T}	m^2s^{-1}	Kinematic viscosity at temperature T_{film}
ρ_{Ah}	m^{-2}	Surface density of hairs on honey bee
ρ_{B}	kgm^{-3}	Density of honey bee
τ	m	Hive wall thickness
χ_{Vh}	-	Volume ratio of hair on a honey bee
σ	$kgs^{-3}K^{-4}$	Steffan-Boltzmann constant
Γ	-	Degree of clustering

8.2 Introduction

Honey bee colonies (*Apis mellifera*), overwinter in cavities keeping at least some of their number above 18°C (Seeley, 1985) throughout the year in a wide range of climates that include -40°C winters. Human experience of their overwintering behaviour is almost exclusively by observation in thin walled (19mm) wooden hives of very different thermal properties (Seeley, 2019b) to their preferred natural habitat of tree hollows e.g. thermal conductance of these hives can be up to 7 times higher than tree hollows (Mitchell, 2016). In these hives, on warm days the honey bees are observed distributed about the hive engaged in various activities. On very cold days they form a cluster (figure 8.2), a series of dense disks of honey bees between the combs, the outline of the disks conforming to a rough spheroid (figure 8.6). The centres of these disks (core) are less dense and at a higher temperature (20°C to 34°C), producing almost all of the cluster heat (Stabentheiner et al., 2003). The outer layers of the cluster (mantle) that fall below 18°C generate little metabolic heat. Those honey bees on the periphery of the cluster that fall below 10°C must move inwards or will eventually die and fall from the cluster. This gives the surface temperature of the cluster a lower limit of ~ 10°C.

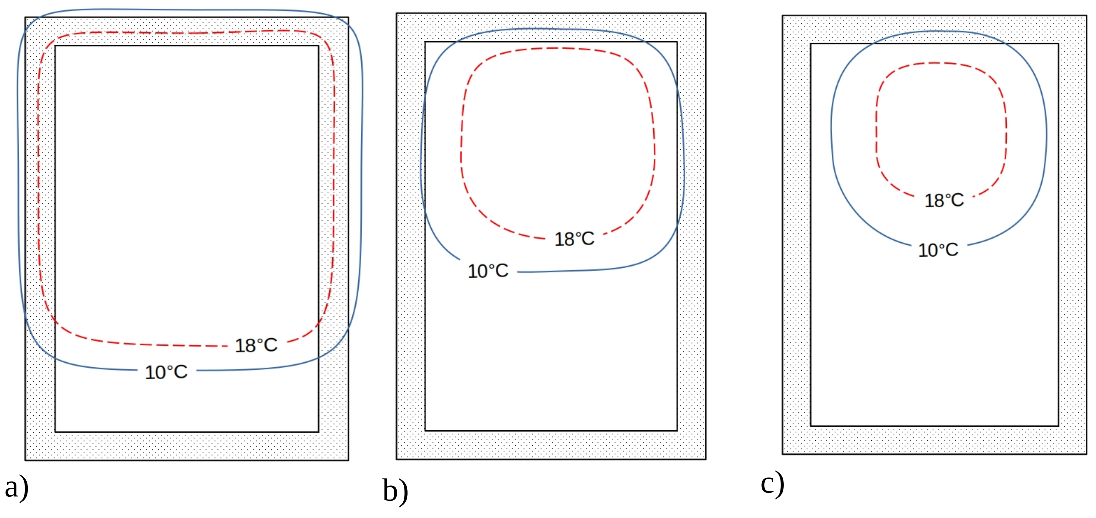

Figure 8.1: Clustering process from Owens 1971 (Owens, 1971; Stabentheiner et al., 2003) a) pre-cluster, b) low density cluster, c) dense cluster.

Research into the heat transfer of the honey bees within their nests has been limited to applying insulation to hives. These have been conducted:

1. Without quantitatively measuring its heat transfer impact (apart from sometimes quoting the R-value of the sheet stock used, which is insufficient on its own see paragraph 2).
2. With the absence of realistic consideration of the heat transfer impact of apertures (Mitchell, 2017), including a) not mentioning their presence or dimensions, b) quoting inadequate experiments (Anderson, 1943).
3. By omitting quantitative comparison to the honey bees evolutionary preferred abode.
4. Failing to determine if the treatment has heat transfer significance compared to the control.

There are a few exceptions e.g. Villumstad (Villumstad, 1974) measuring the thermal conductance of the hives.

The lack of heat transfer experimental rigour, and lack of application of heat transfer knowledge has unsurprisingly led to ambiguous or contradictory results (Dodologlu et al., 2004; Alburaki and Corona, 2022). When these results are combined with mixed support from academics (Currie and Spivak, 2015; Seeley, 2019a) and the classification of the mantle as insulation (Phillips and Demuth, 1914; Stabentheiner et al., 2003), it has enabled poor uptake of permanently or intermittently insulated hives. This is despite many acknowledging the stress it causes. In addition it has enabled the academic practice of employing high heat loss hives as surrogates for honey bee preferred abodes. As research into honey bees and their behaviour inside cavities that have heat transfer similar to their natural abode is extremely rare (Seeley, 2019b), the validity of using hives as surrogates is uncertain.

From 1914, the mantle has been described as insulation (Phillips and Demuth, 1914; Farrar, 1943; Winston, 1987; Southwick, 1991; Becher et al., 2010; Currie and Spivak, 2015; Jarimi et al., 2020; Milbrath, 2020; Norrström et al., 2021). This "insulation" has been part of the rationale behind using high conductance hives, in both peer reviewed academic research and bee keeping (Currie and Spivak, 2015; Milbrath, 2020) and the increasing North American practice (currently Southern California US to Canada (Hopkins et al., 2023)) of refrigeration. This applies an ambient temperature of ~4°C to colonies for winter and to force brood breaks (DeGrandi-Hoffman et al., 2023; Meikle et al., 2023) originally for economic reasons, and recently for varroa control. The survival of the colony in these circumstances is reliant on having large honey bee numbers and considerable metabolic heating, consuming up to 60 kg of honey in the most adverse conditions (Farrar, 1947). The low temperature differential between the internal space near the hive surface and the outside environment being attributed to the "honey bee heats the cluster not the hive" rather than the high conductance of the hive compared to the rest of the system. This has led to high heat loss being seen as benign and/or beneficial (Farrar, 1947; Currie and Spivak, 2015; Milbrath, 2020) and use of alternatives as an illogical or emotional response (Milbrath, 2020).

In the apicultural literature, some questions remain open:

- **What constitutes insulation?** Any material causing a temperature difference, reductions in surface area and reductions in metabolism have all been termed "insulation" (Heinrich, 1981; Southwick, 1991; Currie and Spivak, 2015). This and other qualitative usages differ from the more precise quantitative definition of insulation i.e. thermal insulance factor or R-value; the ratio of temperature difference to rate of heat transfer per unit area (heat flux) (Thermal Engineering, 2019).
- **Convection or conduction?** The conduction or convection of pre-cluster state (i.e. not closely gathered into discs), mantle and core have been, with one exception (Mitchell, 2022), assumed rather than analysed, measured or modelled. The most frequent assumption being: in all situations convection is dominant.
- **Where is the metabolic heat coming from?** The heat has been variously assumed to be coming from the mantle (Watmough and Camazine, 1995) and the core, with later infrared studies (Stabentheiner et al., 2003; Stabentheiner et al., 2010) placing source as the regions of the cluster above 18°C i.e. the core, where individual bees, metabolising sugars from honey, undergo a limited period of vigorous exertion of their thorax flight muscles before eventually becoming ectothermic and returning to the mantle and temperatures close to 10°C.

- **If and how does the hive body conductance, the air in the cavity and surrounding landscape contribute?** This has been largely ignored with the exception of one experimental (Mitchell, 2016) and one CFD study (Mitchell, 2022), neither of which used a radiative landscape model.
- **If and how do honey bee bodies and hair contribute?** The quantitative thermal properties of the honey bee bodies and hair have either been ignored, used unrealistically (Watmough and Camazine, 1995) and/or ad hoc honey bee density to thermal conductivity (Basak et al., 1996; Ocko and Mahadevan, 2014) relations used rather than published engineering models.

8.3 Approach

We will proceed by :

- Establishing criteria for the mantle being insulation or heat sink.
- Determining the roles of conduction or convection or radiation in the core, mantle and pre-cluster heat transfer.
- Evaluating whether the above criteria are met, including the contributions from the hive, landscape, honey bee bodies and hair.

8.3.1 Insulation Criteria

First, in colloquial speech, “insulation” occurs when insulation substance is added, it results in reduced heat loss rate, and the opposite with “heat sink”. In other words: attach a bigger heat sink it will increase heat flow, if wrapped in thicker insulation material the object will have reduced heat flow. This qualitative criteria for being an insulator or heat sink can be expressed quantitatively as the sign of the slope $\left(\frac{\delta \dot{q}}{\delta r}\right)$ of the graph of heat transfer rate $(\dot{q})$ versus cluster size (r) e.g. equation 8.1.

$$\frac{\delta \dot{q}}{\delta r} > 0 \Rightarrow insulator \qquad \frac{\delta \dot{q}}{\delta r} < 0 \Rightarrow heatsink \quad \text{Criteria 1} \tag{8.1}$$

Second, insulation can refer to a “more insulating material ” i.e. a decrease in thermal conductivity of the substance e.g. interlocking hairs on honey bee bodies have been described as “increasing the insulation” as the bees get closer. For clustering to be termed insulation in this definition the effective conductivity k_{eff} of the bee air mixture should decrease as the clustering progresses. The degree of clustering Γ (equation 8.2)is related to the porosity of the mantle φ i.e, zero clustering $(\Gamma=0)$ when the mantle has the pre-cluster porosity φ_P and maximum clustering $(\Gamma=1)$ when the bees are tightly packed together (porosity= φ_0) i.e. maximum clustering should accompany minimum mantle conductivity k_{mantle} if the mantel is insulation (equation 8.3) and minimum clustering if a heat sink as per equation 8.3.

$$\Gamma=\frac{\varphi_P-\varphi}{\varphi_P-\varphi_0} \tag{8.2}$$

$$\frac{\delta k_{mantle}}{\delta\Gamma}<0\Rightarrow insulator \qquad \frac{\delta k_{mantle}}{\delta\Gamma}>0\Rightarrow heatsink \quad \text{Criteria 2} \tag{8.3}$$

Third, insulation can mean the application of material with lower thermal conductivity than that of the item being insulated. In this case we need to compare the thermal conductivity of the core and the mantle i.e. equation 8.4.

$$k_{mantle}<k_{core}\Rightarrow insulator \qquad k_{mantle}>k_{core}\Rightarrow heatsink \quad \text{Criteria 3} \tag{8.4}$$

Fourth, using the definition of thermal insulance (R-value), temperature difference per unit of heat flux in equation 8.5, we can then test if R_{value} increases with clustering i.e. the gradient of R_{value} with respect to clustering (equation 8.6).

$$R_{value}=\frac{T_{Core}-T_{Mantle}}{\frac{\dot{q}}{A}} \tag{8.5}$$

$$\frac{\delta R_{value}}{\delta\Gamma}>0\Rightarrow insulator \quad \text{Criteria 4} \tag{8.6}$$

8.3.2 Conduction or convection or radiation

Common building insulation (styrofoam, rock wool) and cold climate clothing rely on gases to perform the actual insulation, but they need to keep the gases still or nearly still to prevent a high rate of heat transfer via convection. When this is achieved we get thermal conductivities (0.025 $Wm^{-1}K^{-1}$) an order of magnitude lower (better) than the best non-metallic solid (e.g. plastics (0.12-0.5, wool fibre 0.5 $Wm^{-1}K^{-1}$) (Xue et al., 2019) and the body of a honey bee (0.5 $Wm^{-1}K^{-1}$ See methods). The thermal resistance of a collection of objects with gaps between them is dependent on the distance between the objects, their effective diameter and the thickness of the object collection (Carson et al., 2005).

When the distance between the objects is relatively large (porosity close to 1) then convection currents, set up within the air between the objects, dominate the heat transfer. These currents decrease as the porosity decreases. When the porosity falls below a particular value (dependant on the gas properties, temperature differences, geometry etc.), the convection currents stop, then heat transfer takes place by conduction only, both though the air and importantly, the objects. As the porosity decreases further, the thermal conductivity becomes more like the object and less like that of air. If the objects have a high conductivity compared to air, it results in a variation of thermal resistance to porosity like that shown in figure 1, where the thermal resistance peaks near the cessation of convection currents, and falls on either side, at lower porosities due to conduction, at higher porosities due to convection. The porosity has a lower limit determined by geometry of the objects. For a mixture of cylinders of two different sizes e.g. k_{mantle} honey bees and hair, this is between 0.1 and 0.01 depending on the mixture.

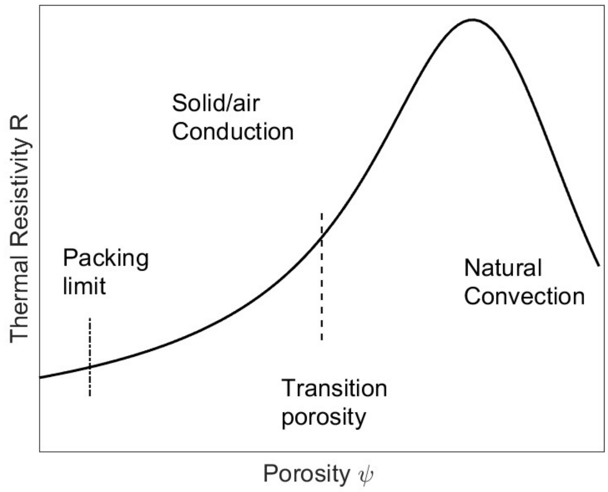

Figure 8.2: Typical thermal resistance versus porosity.

This transition porosity can be determined by experiment, computational fluid dynamics (CFD) or by analysis. The latter is where a dimensionless number (Rayleigh Number) is evaluated for a porous system or part system and if above a threshold indicates natural convection will start. One CFD analysis has shown that the average initial winter population of *Apis mellifera mellifera* (Free and Racey, 1968) in a British National hive complete with combs may be sufficient to suppress natural convection (Mitchell, 2022). One can visualise this as when the honey bees are evenly distributed throughout the nest, the resistance of the circulation path of convecting air is equivalent to a 0.8m long, 20mm wide tube, half filled with small objects, with circulation propelled only by the tiny amount of buoyancy created by a few degrees of temperature difference.

If we can treat the mixtures of honey bees and air, both pre-cluster and cluster as solids then we can estimate the effective conductivity(k_{eff}) of any bee/air mixture given the conductivity of bee bodies (k_{body}) and air (k_{air}) using the Effective Medium Theory (EMT) correlation described by Carson (Carson et al., 2005) and not the unrealistic models employed by others i.e non-conducting honey bees (Southwick, 1985) and negative density conductivity coefficients (Watmough and Camazine, 1995)

The literature on porous solid heat transfer (Carson et al., 2005) shows that determining the effective conductivity of the combination of the gas and solid is complex even when convection is eliminated. It has been shown that variation of conductivity with porosity is likely to be the Effective Medium Theory (EMT) (equation 8.7).

$$\begin{gathered} k_{eff}=\frac{1}{4}\Big\{(3\varphi-1)k_{air}+\left[3(1-\varphi)-1\right]k_B \\ +\sqrt{\left\{(3\varphi-1)k_{air}+\left[3(1-\varphi)-1\right]k_B\right\}^2+8k_{air}k_B}\Big\} \end{gathered} \tag{8.7}$$

For the known conductivities of air and honey bee bodies, this gives the relationship between effective conductivity and porosity.

The thermal system of a honey bee cluster within a hive in a realistic landscape is a complex one in which factors such as radiation and effective sky temperature, not often considered, can be significant, however we can readily produce a reasonably detailed approximation. This is where we consider the cluster to be a solid sphere inside a box set above ground in a cold bare landscape with a clear sky at low humidity e.g. figures 8.3 and 8.4. In this scenario, it is sufficiently cold for the sphere of honey bees to have a surface temperature of 10°C regardless of size, as observed by various researchers (Stabentheiner et al., 2003).

Figure 8.3 Hives in a bare cold landscape (Scott Hall).

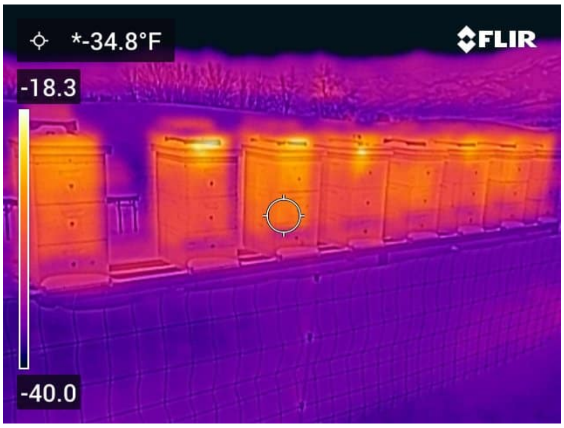

Figure 8.4 Hives in a bare landscape via infrared (FLIR C5, Scott Hall).

8.3.3 Alternative hive constructions

To understand the impact of assuming the mantle insulates, we simulate the usage of 4 additional hive constructions. Thus, we can better assess the basis of statements that consider the hive construction irrelevant to honey bee winter homeostasis. The alternative constructions considered (all with the same internal dimensions as (Owens, 1971)) are as follows:

1. Aluminium with 1mm walls.

2. Stainless steel 1mm walls.
3. Expanded polystyrene 30mm.
4. Polyisocyanurate (PIR) 50mm.

8.4 Methods

8.4.1 Convection-conduction transition.

The critical Rayleigh number in a natural convection system determines whether natural convection can occur. If the Rayleigh number is above the critical number, convection starts in addition to conduction, below this number only conduction occurs. This involves calculation of both permeability and diffusivity of the bee/air mixtures. When the honey bees are far apart the total permeability K_T is made up of the permeability around the space enveloped by bee bodies and hair K_{BH} . As honey bees come together it changes into permeability through hair with bee bodies in it K_B . The changeover is governed by porosity around bee and hair envelopes φ_{BH} as shown in equation 8.8.

$$K_T = K_{BH} + (1 - \varphi_{BH}) K_B \tag{8.8}$$

We can derive the terms in equation 8.8 by considering bee plus hair as a combined particle with length and diameter l_{BH}, d_{BH} from the bee body and hair dimensions l_B, d_B, l_h, d_h .

We can then define the volumes and areas of the bee bodies, the combined particle of bee bodies plus hair V_{BH}, A_{BH} and hairs V_h, A_h as per equations 8.9,8.10 and 8.11.

$$l_{BH} = l_B + 2 l_h \qquad d_{BH} = d_B + 2 l_h \tag{8.9}$$

$$V_{BH} = \frac{\pi}{4} l_{BH} d_{BH}^2 \qquad V_B = \frac{\pi}{4} l_B d_B^2 \qquad V_h = \frac{\pi}{4} l_h d_h^2 \tag{8.10}$$

$$A_{BH} = \pi l_{BH} d_{BH} + \frac{\pi}{2} d_{BH}^2 \qquad A_B = \pi l_B d_B + \frac{\pi}{2} d_B^2 \qquad A_h = \pi l_h d_h + \frac{\pi}{2} d_h^2 \tag{8.11}$$

φ_{BH} can then be derived from the porosity around bee bodies φ_B and V_{BH}, V_B equation 8.12.

$$\varphi_{BH} = 1 - \frac{(1 - \varphi_B) V_{BH}}{V_B} \quad \text{where} \quad \varphi_{BH} \geq 0 \tag{8.12}$$

Using the volume fraction in equation 8.12, we can then derive the effective particles diameters using the Sauter mean and the cubic average as used by Glover (Glover and Luo, 2020) in equation 8.13 and equation 8.14.

$$\chi_{Vh}=\frac{A_B p_h \rho_{Ah} V_h}{V_B+A_B p_h \rho_{Ah} V_h} \tag{8.13}$$

$$\bar{d}_{BH}=\frac{6V_{BH}}{A_{BH}} \qquad \bar{d}_B=6\left(\frac{V_B}{A_B}-\left(\frac{V_B}{A_B}-\frac{V_h}{A_h}\right)\chi_{Vh}^{1/3}\right) \tag{8.14}$$

The different effective size for the permeabilities is shown in equation 8.15.

$$K_{BH}=\bar{d}_{BH}^2\frac{\varphi_{BH}^3}{180(1-\varphi_{BH})^2} \qquad K_B=\bar{d}_B^2\frac{\varphi_B^3}{180(1-\varphi_B)^2} \tag{8.15}$$

In equation 8.16 the diffusivity is derived according to Carson (Carson et al., 2005) from the hairless size and porosity. The effective conductivity is calculated using the EMT from equation 8.7.

$$\alpha_B=\frac{k_B}{\rho_B Cp_B(1-\varphi_B)+\rho_{air} Cp_{air}\varphi_B} \quad \text{where} \quad \rho_B=\frac{m_B}{V_B} \tag{8.16}$$

In equation 8.15 the permeability is derived according to Bejan (Nield and Bejan, 2006) from the size and porosity including the honey bee hair.

The mantle can be treated as a porous volume heated allowing the Rayleigh number to be calculated using the permeability and diffusivity, the temperature difference and the characteristic length. Given the gap between the combs is significantly less than the size of the sum of the two boundary layers, the characteristic length may be interpreted as the gap. For this Rayleigh number, convection occurs when it exceeds a value of ~40.

$$Ra_{\bar{L}}=\frac{g\beta K_T(T_0-T_1)\bar{L}}{\nu\alpha_B} \tag{8.17}$$

8.4.2 Honey bee body, pre–cluster, core and mantle thermal conductivity

Table 8.2: Honey bee body thermal conductivity.

Experimenter/s	**Experimental conductivity $Wm^{-1}K^{-1}$**	**Experimental porosity**	**Honey bee body conductivity $Wm^{-1}K^{-1}$**
Basak, Heinrich, Abre	0.2	0.45	0.5012
Ocko, Southwick	0.17	0.5	0.5008

Ocko and L. Mahadevan (Ocko and Mahadevan, 2014) derived a conductivity (0.17 $Wm^{-1}K^{-1}$) at a known porosity (0.5) from an experiment by Southwick (Southwick, 1982). Basak (Basak et al., 1996) derived a conductivity (0.2 $Wm^{-1}K^{-1}$) from Heinrich (Heinrich, 1981) for a disordered packing of honey bees.

By using these experiments in bee/air mixture thermal conductivity (Heinrich, 1981; Southwick, 1985; Basak et al., 1996; Ocko and Mahadevan, 2014) (table 8.2), equation 8.7, and approximating honey bees to sphero-cylinders of aspect ratio 3 (length 14mm, diameter 5mm),we can determine a bee body conductivity and use that to determine the conductivity of the bee/air mixtures from pre-clustered state to the densest possible mantle.

Using these pairs of values for conductivity and porosity and iteratively solving equation 8.7 (MATLAB, 2018), we can determine two values for honey bee body thermal conductivity. These values are within the range of experimental results for other types of solid flesh (Elansari and Hobani, 2009).

The porosity of the mantle when tightly clustered is made up of both bees and hair which can be approximated to cylinders and sphero-cylinders respectively. The limiting porosity therefore lies some where between 0.09 and 0.09^2 i.e. 0.008 (Li et al., 2010; Glover and Luo, 2020). The pre-clustered porosity is derived from CFD investigations into hive convection (0.5) (Mitchell, 2022).

From the above determined honey bee body conductivity, the conductivity of air, pre-cluster and mantle porosities we can determine the thermal conductivity of the mantle and pre-cluster honey bees from equation 8.7.

8.4.3 Heat loss, mantle size ratio determination

This considers the honey bee winter cluster as a sphere with its surface at a constant temperature inside, but not in contact with, a completely closed box above the ground, in a bare landscape with radiation convection and conduction (figure 8.5). The ground, air and sky are at potentially different temperatures. The energy of the cluster is transmitted to the hive interior surface via convection and radiation. It moves from the interior surface of the hive to the exterior surface by conduction. This is then convected into the air and radiated to the ground and sky. As the outside temperatures decrease the energy output of the colony increases and the surface area of the colony decreases as the colony contracts.

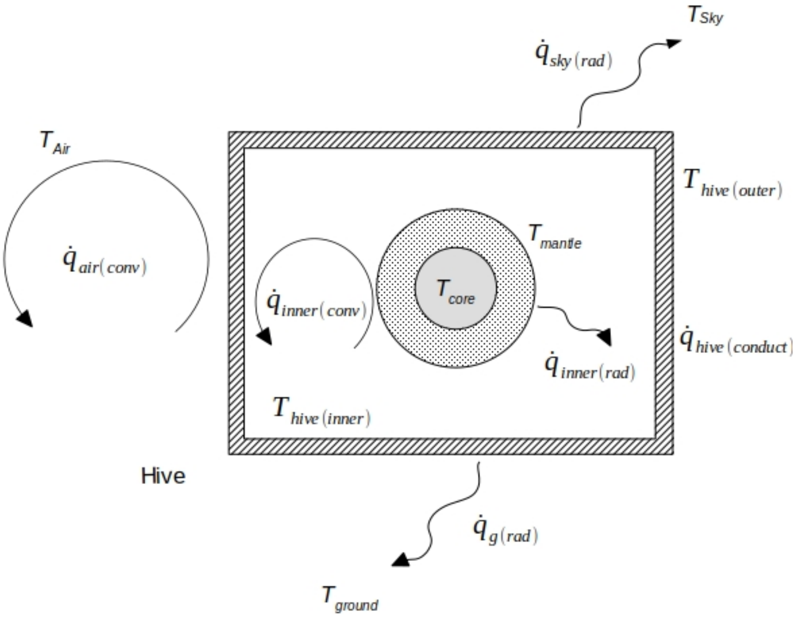

Figure 8.5: Cluster hive landscape schematic.

Conservation of energy implies the following:

convection and radiation from hive outer surface to environment (equation 8.18),

$$\dot{q}_{mantle}+\left(\dot{q}_{air(conv)}+\dot{q}_{g(rad)}+\dot{q}_{sky(rad)}\right)=0 \qquad (8.18)$$

conduction through hive from hive inner surface to hive outer surface (equation 8.19),

$$\dot{q}_{mantle}+\dot{q}_{hive(conduct)}=0 \qquad (8.19)$$

convection and radiation from mantle surface to hive inner surface (equation 8.20),

$$\dot{q}_{mantle}+\left(\dot{q}_{inner(conv)}+\dot{q}_{inner(rad)}\right)=0 \quad . \tag{8.20}$$

This involves the iterative simultaneous solution of 3 equations (8.18, 8.19, 8.20) (MATLAB, 2018) for $\dot{q}_{mantle}, T_{hive(outer)}, T_{hive(inner)}$ for values of T_{air}, r_{mantle} when T_{ground}, T_{sky} can be derived from T_{air}.

The determination of the terms $\dot{q}_{air(conv)}, \dot{q}_{g(rad)}, \dot{q}_{sky(rad)}, \dot{q}_{hive(conduct)}, \dot{q}_{inner(conv)}, \dot{q}_{inner(rad)}$ are described below.

Hive outer surface to environment by convection heat flux $\dot{q}_{air(conv)}$ is calculated for the sides, top and bottom separately assuming uniform surface temperature via calculation of the Rayleigh and Nusselt numbers in equations 8.21 to 8.34 using air properties α, β, ν, Pr at average temperature (equation 8.25) and the hive dimensions (Cushman, 2011) ($x_{inner}=0.44, y_{inner}=0.3, z_{inner}=0.44, \tau=0.012$).

$$x_{outer}=x_{inner}+\tau \qquad y_{outer}=y_{inner}+\tau \qquad z_{outer}=z_{inner}+\tau \tag{8.21}$$

$$A_{side}=2z_{outer}\,y_{outer}+2x_{outer}\,y_{outer} \qquad A_{bottom}=A_{top}=y_{outer}\,x_{outer} \tag{8.22}$$

$$A_{outer}=A_{top}+A_{bottom}+A_{side} \tag{8.23}$$

$$A_{inner}=2x_{inner}\,y_{inner}+2x_{inner}\,z_{inner}+2y_{inner}\,z_{inner} \tag{8.24}$$

$$T_{film}=\frac{T_{hive(outer)}+T_{air}}{2} \tag{8.25}$$

$$Ra_{Lx}=\frac{g\beta_T\left(T_{hive(outer)}-T_{air}\right)L_x^3}{\alpha_T\,\nu} \tag{8.26}$$

$$L_{top}=L_{bottom}=\frac{A_{top}}{2x_{outer}+2z_{outer}} \tag{8.27}$$

$$L_{side}=z_{outer} \qquad L_{top}=L_{bottom}=\frac{A_{top}}{2x_{outer}+2y_{outer}} \tag{8.28}$$

$$\overline{Nu}_{top}=0.27\,Ra_{Ltop}{}^{1/4} \tag{8.29}$$

$$\overline{Nu}_{bottom}=0.15\,Ra_{Lbottom}{}^{1/3} \tag{8.30}$$

$$\overline{Nu}_{side}=0.68+\frac{0.670\,Ra_{Lside}{}^{1/4}}{\left[1+\left(0.492/Pr\right)^{9/16}\right]^{4/9}} \tag{8.31}$$

$$\bar{h}_{top}=\frac{\overline{Nu}_{top}\,k_{air}}{L_{top}} \qquad \bar{h}_{bottom}=\frac{\overline{Nu}_{bottom}\,k_{air}}{L_{bottom}} \qquad \bar{h}_{side}=\frac{\overline{Nu}_{side}\,k_{air}}{L_{side}} \tag{8.32}$$

$$\bar{h}_{a(conv)}=\frac{4\bar{h}_{side}A_{side}+\bar{h}_{top}A_{top}+\bar{h}_{bottom}A_{bottom}}{4A_{side}+A_{top}+A_{bottom}} \tag{8.33}$$

$$\dot{q}_{air(conv)}=\bar{h}_{a(conv)}A_{outer}\left(T_{hive(outer)}-T_{air}\right) \tag{8.34}$$

Hive outer surface to environment by radiation to sky $\dot{q}_{sky(rad)}$ and ground $\dot{q}_{g(rad)}$ heat fluxes are derived via equations 8.37,8.38. Sky temperature is computed (Goforth et al., 2002) for high (K=0.06) cloudless (C=0) and relative humidity of 1% (RH=0.01) (equations 8.35, 8.36) with little or no shade ($f_{sky}=f_{ground}=0.5$).

$$\dot{q}_{thermal}=\left(1+KC^2\right)8.78\times10^{-13}T_{air}^{5.852}\left(100\times R_H\right)^{0.07195} \tag{8.35}$$

$$T_{sky}=\left(\frac{\dot{q}_{thermal}}{\epsilon_{sky}\,\sigma}\right)^{1/4} \tag{8.36}$$

$$\dot{q}_{sky(rad)}=f_{sky}\,\epsilon_{outer}\,\sigma A_{outer}\left(T_{hive(outer)}^4-T_{sky}^4\right) \tag{8.37}$$

$$\dot{q}_{g(rad)}=f_{ground}\,\epsilon_{outer}\,\sigma A_{outer}\left(T_{hive(outer)}^4-T_{ground}^4\right) \tag{8.38}$$

Hive inner surface to hive outer surface by conduction $\dot{q}_{hive(conduct)}$ heat flux is derived using shape factors for a cuboid.(Bergman and Lavine, 2017b) in equation 8.39.

$$S^*=\frac{A_{inner}}{\tau}+2.16\left(x_{inner}+y_{inner}+z_{inner}\right)+1.22\,\tau \tag{8.39}$$

$$\dot{q}_{hive(conduct)}=S^*k_{hive}\left(T_{hive(outer)}-T_{hive(inner)}\right) \tag{8.40}$$

Mantle to hive interior surface by convection heat flux $\dot{q}_{inner(conv)}$ is computed using the correlations (Warrington and Powe, 1985) in equations 8.41 to 8.48 using air properties α,β,ν,Pr at average temperature (equation 8.44).

$$A_{mantle}=4\pi r_{mantle}^2 \tag{8.41}$$

$$r_{eff}=\left(\frac{x_{inner}\,y_{inner}\,z_{inner}}{4\pi/3}\right)^{1/3} \tag{8.42}$$

$$L_i=r_{eff}-r_{mantle} \tag{8.43}$$

$$T_{film}=\frac{T_{hive(inner)}+T_{mantle}}{2} \tag{8.44}$$

$$Ra_{Li}=\frac{g\beta\left(T_{mantle}-T_{hive(inner)}\right)L_i^3}{\alpha_T\,\nu_T} \tag{8.45}$$

$$\overline{Nu}_{Li}=c_1 Ra_{Li}^{c_2}\left(\frac{L_i}{r_{mantle}}\right)^{c_3}Pr^{c_4} \tag{8.46}$$

$$A_{mantle} = 4\pi r^2_{mantle} \tag{8.41}$$

$$\bar{h}_{Li} = \frac{k_{air}\overline{Nu}_{Li}}{L_i} \tag{8.47}$$

$$\dot{q}_{inner(conv)} = \bar{h}_{Li} A_{mantle}\left(T_{mantle} - T_{hive(inner)}\right) \tag{8.48}$$

Mantle to hive interior by radiation heat flux $\dot{q}_{inner(rad)}$ is computed using the equation for concentric spheres(Bergman and Lavine, 2017a) in equation 8.49.

$$\dot{q}_{inner(rad)} = \frac{\sigma A_{mantle}\left(T^4_{mantle} - T^4_{hive(inner)}\right)}{\frac{1}{\epsilon_{mantle}} + \frac{1-\epsilon_{inner}}{\epsilon_{inner}}\left(\frac{r_{mantle}}{r_{eff}}\right)^2} \tag{8.49}$$

8.4.4 R-value analysis

In the published results of (Owens, 1971), the temperature contours inside a hive are shown for a colony clustering during falling external temperatures (figures 8.2 and 8.6). From the width of the 10°C contour one can estimate the external diameter of that colony mantle in that hive at varying external ambient temperatures. Using hive dimensions given in the publication and the model in section 8.4.3 then one can calculate the metabolic heat production for a shaded hive. From the definition of thermal insulance or R-value in equation 8.5, and the known temperatures for the mantle external surface and core of brood-less clusters (10°C, 20°C), one can then determine the change in R-value. Also from the model we can determine how much of the core to ambient temperature difference is a result of the mantle, air gap between the mantle and the hive, the hive body and external surface heat transfer.

8.4.5 Alternative constructions

The model from section 8.4.3 is used with parameters in table 8.3 and the dimensions from (Owens, 1971).

Table 8.3: Model parameters for hive construction.

Material	**Wall thickness mm**	**Conductivity $Wm^{-1}K^{-1}$**	**Emissivity**
Wood	19	0.1	0.9
Aluminium	1	200	0.1
Stainless Steel	1	20	0.8
Expanded polystrene	30	0.03	0.9
PIR	50	0.023	0.3

8.5 Results

8.5.1 Convection conduction transition.

Using the parameters in table 8.3, mantle Rayleigh numbers were calculated for the temperatures found in the cluster mantle inner to mantle outer, T_0=283K (10°C), $T_{1=}$291K (18°C) as shown in figure 8.6.

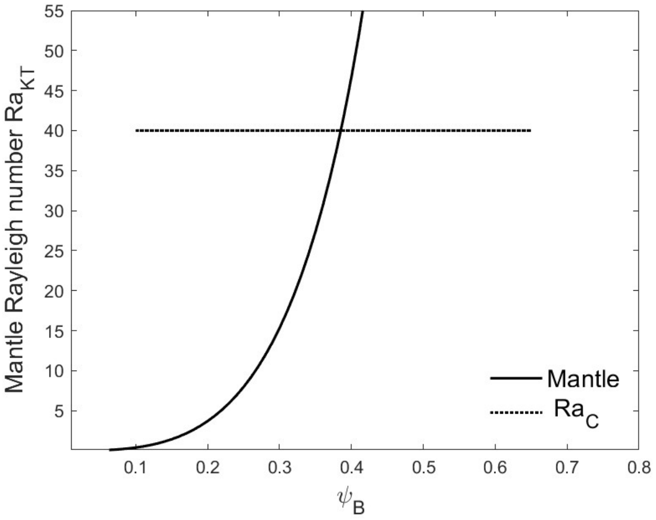

Figure 8.6: Raleigh number versus porosity for temperature differences mantle inner to mantle outer, with critical Raleigh number line Ra_c=40.

The results indicate that at porosities in the mantle and core of the cluster, natural convection either does not occur or only at very low velocities. Therefore for heat transfer purposes the mantle and core can be treated as solids with the effective conductivity related by equation 8.7. Further, pre-cluster state convection is likely to be weak as this has a porosity close to 0.5, especially if the hive is of low thermal conductance, with low internal temperature differences.

8.5.2 Honey bee body, pre–cluster, core and mantle thermal conductivity.

Because of the experimental uncertainty and the methods used by experimenters in table 8.2, the range of honey bee conductivities for 0.4 to 0.6 $Wm^{-1}K^{-1}$ will be considered. The variation of effective conductivity with porosity is shown in the graph in figure 8.7. This results in an effective thermal conductivity of the mantle when not clustered (porosity 0.5) (Mitchell, 2022) of around 0.2 $Wm^{-1}K^{-1}$ and when tightly clustered (porosity 0.05 (Li et al., 2010) i.e. sphero-cylinder packing limit with hair) of about 0.5 $Wm^{-1}K^{-1}$. This also shows that there is an increase in conductivity by ~ 2 in the transition from not clustered to tightly clustered over a wide range of honey bee body conductivity (from 0.4 to 0.6 $Wm^{-1}K^{-1}$) and mantle porosity (0.25 to 0.05). Therefore the cluster mantle does not meet the 2nd criteria $\frac{\delta k_{mantle}}{\delta \Gamma} < 0 \Rightarrow insulator$ i.e. conductivity definition of “insulating”.

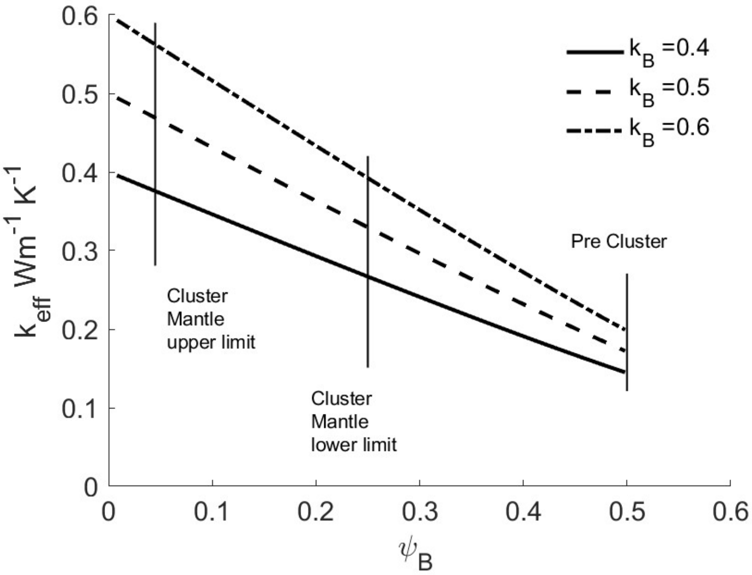

Figure 8.7: Effective conductivity k_{eff} of air honey bee mixtures versus porosity ψ_B using EMT where k_B=0.4, 0.5, 0.6 and k_{air}=0.026.

At lower ambient temperatures, the cluster core has been shown and described by many researchers to be of a lower density or higher porosity than the mantle, but of less porosity than the pre-cluster state (Southwick, 1985). Thus we can infer that, for heat transfer, the core can be treated as a solid, and that from figure 8.7, we can reliably infer that the thermal conductivity of the mantle is higher than that of the core. Therefore the 3rd criteria $k_{mantle} < k_{core} \Rightarrow insulator$ for insulation is not met and instead fulfils the criteria for a heat sink.

8.5.3 Heat loss, mantle size ratio determination

Using the principle of the conservation of energy this can be represented by a set of 3 non linear equations using convection correlations (Warrington and Powe, 1985; Bejan, 2013), and radiative heat transfer rules (Incropera and DeWitt, 2007). These can be iteratively solved (MATLAB, 2018) to yield the mantle heat flux i.e. heat loss, and hive surface temperatures from a known size of cluster, hive properties and outside conditions as shown in figure 8.8 (see methods).

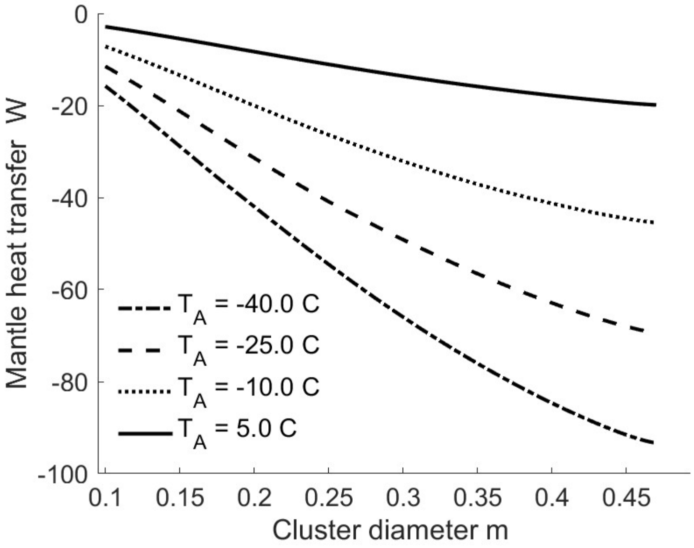

Figure 8.8: Cluster radius versus mantle heat flux (negative is heat loss) for varying air temperatures T_a in a bare landscape inside British National wooden hive with 19mm walls conductivity 0.12 $Wm^{-1}K^{-1}$. Effective sky temperatures derived for 1% humidity.

For all outside conditions heat transfer varies with mantle size at a rate between -70 to -450Wm^{-1} i.e. $\frac{\delta \dot{q}}{\delta r} < 0$. This means that the mantle does not fulfil the 1st criteria, i.e. heat loss versus size criteria for insulation, and instead acts like a heat sink.

8.5.4 R-value analysis

In figure 8.9, for isotherms from +5°C to -20°C and the values of temperature and cluster size from (Owens, 1971), the results from the model in section 8.4.3 were plotted against a) metabolic heat, b) R-value, c) air gap temperature difference as proportion of mantle to ambient temperature difference, d) mantle temperature difference as proportion of mantle to ambient temperature difference.

For material comparison, the mantle heat transfer was plotted (figure 8.10) for various hive materials at 16.7°C (wood 19mm k_{hive}=0.1, ϵ_{outer}=0.9; aluminium 1mm oxidised k_{hive}=200, ϵ_{outer}=0.2; polyisocyanurate (PIR) 50mm, k_{hive}=0.023, ϵ_{outer}=0.3; expanded polystyrene (EPS) 30mm), =k_{hive}0.03, ϵ_{outer}=0.9).

We can see that the cluster diminishes in diameter from 0.47m to 0.34m when the temperature falls from 6.7°C to -16.7°C with the reduction in diameter ceasing around -10°C at ~ 0.17m. This is reflected by an increase in metabolic power from 6.8W to 42.5W and a reduction in R value from 1.33 to 0.11. Over the same interval the proportion of the core to temperature difference supplied by the mantle falls from 80% to 33% while the air gap between the mantle and the hive inner surface grows from 10% to 41%.

The heat loss from the colony of ~36W when the temperature drops from +6.7°C to -16.7°C gives a gradient of ~1.53 WK^{-1}, which compares with a previously found gradient of 0.57 WK^{-1} kg^{-1} which would suggest Owens used a colony of ~2.7 kg, a realistic value for wintered colonies in that locale (Southwick, 1982; Ellis and Hammons, 2013). Unfortunately we do not know actual weight of the colony.

This means that the mantle does not fulfil the 4th criteria to be an insulator.

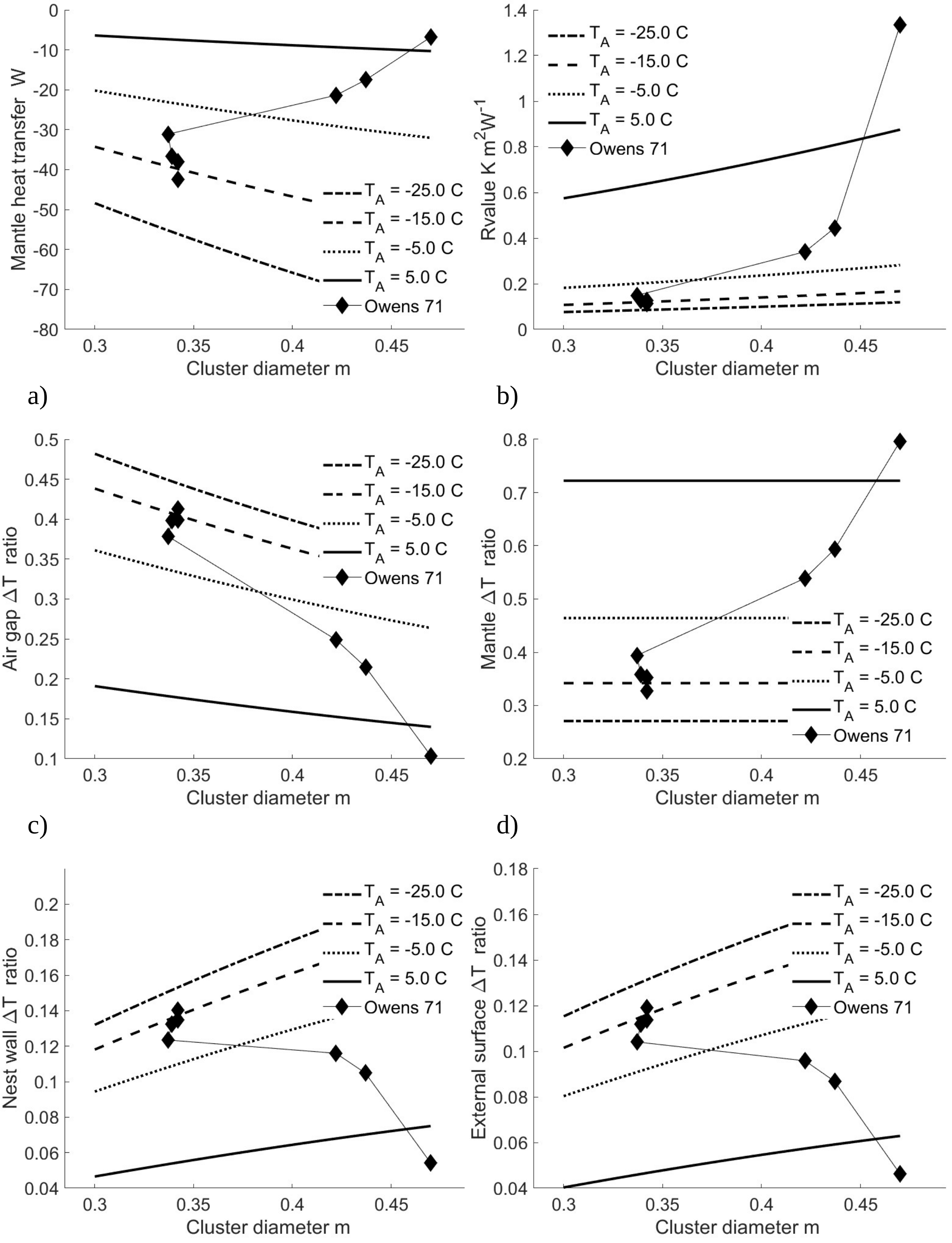

a) b) c) d) e) f)

Figure 8.9: For isotherms from +5°C to -20°C and the values of temperature and cluster size from (Owens, 1971) versus, a) metabolic heat, b) R-value, c) internal hive air gap ΔT as proportion of mantle to ambient ΔT, d) mantle ΔT as proportion of mantle to ambient ΔT, e) hive wall ΔT as proportion of mantle to ambient ΔT, f) external surface to ambient ΔT as proportion of mantle to ambient ΔT. Using the same size hive as (Owens, 1971) shaded from the sky in still air.

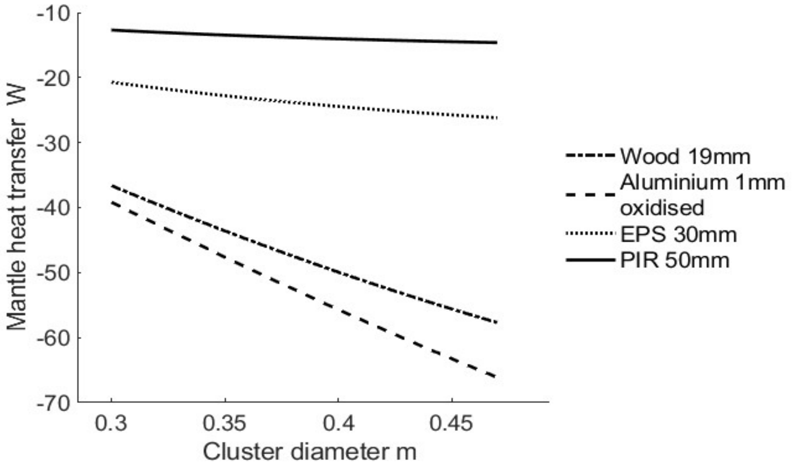

Figure 8.10: Metabolic heat versus cluster diameter T_A =-16.7C for various wall materials. Using the same size hive as (Owens, 1971) shaded from the sky in still air.

8.5.5 Alternative hive constructions

For isotherms from +5°C to -20°C, the results from the model in section 8.4.3 with the parameters for the various materials from table 8.3 were plotted against a) metabolic heat, b) R-value, c) air gap temperature difference as proportion of mantle to ambient temperature difference, d) mantle temperature difference as proportion of mantle to ambient temperature difference.

It can be seen that for the metabolic energy generation for the 19mm walled wooden hive (figure 8.9a) only differs by ~10% from the 1mm aluminium and the 1mm stainless steel (figures 8.11a and 8.12a). However, for the 30mm expanded polystyrene and the 50 mm PIR hives the metabolic heat generation is less than 60% and ~35% of that of wooden hive respectively (figures 8.13a and 8.14a).

The maximum proportion of the total temperature difference between core and ambient that is accounted for by the hive walls varies from 10-5 and 10-4 for aluminium and steel to 0.2,0.5 and 0.6 for wood, expanded polystyrene and PIR respectively.

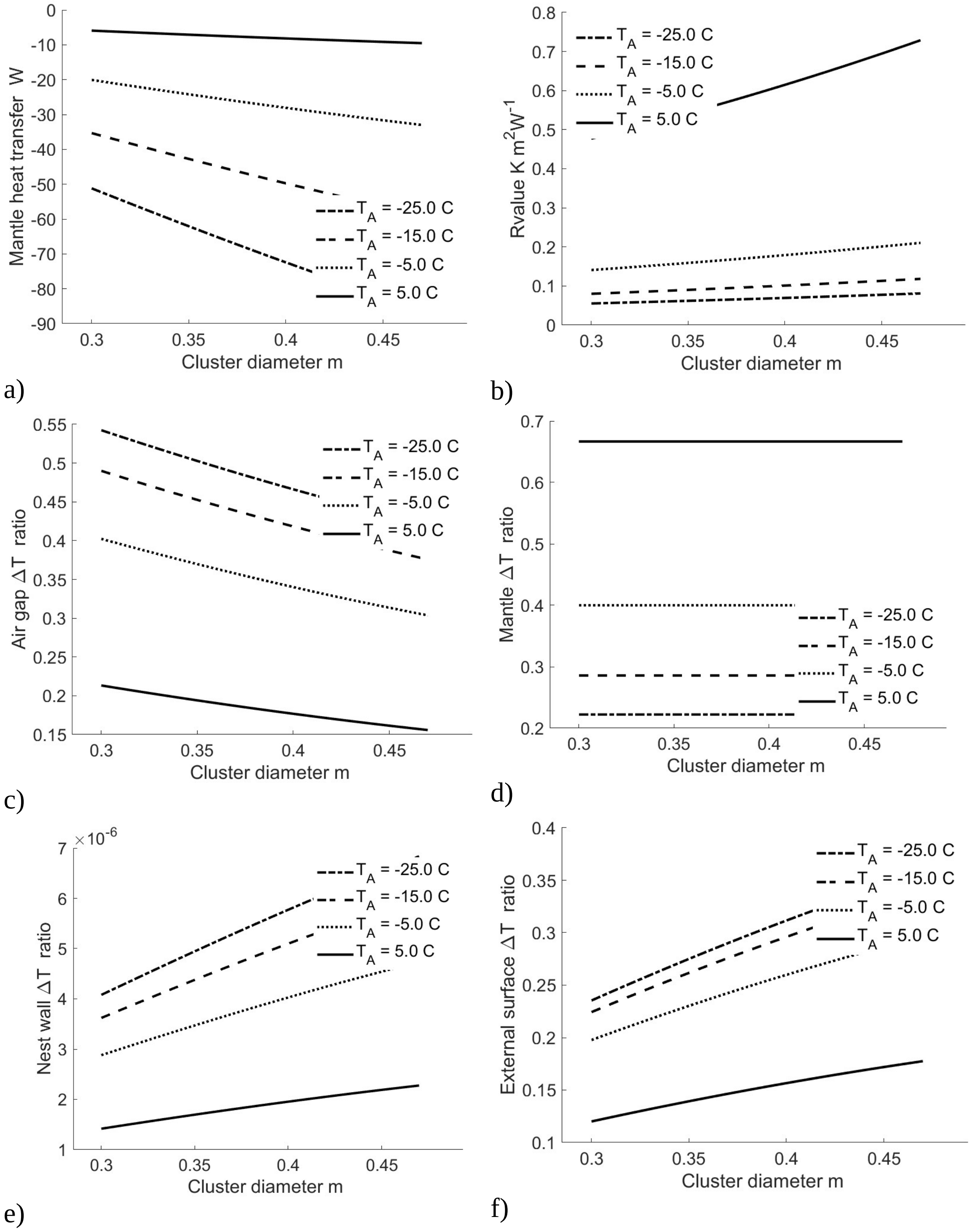

a)
b)
c)
d)
e)
f)

Figure 8.11:Aluminium 1mm walls using the same dimensions as (Owens, 1971) shaded from the sky in still air. For isotherms from +5°C to -20°C versus, a) metabolic heat, b) mantle R-value, c) internal hive air gap ΔT as proportion of mantle to ambient ΔT, d) mantle ΔT as proportion of mantle to ambient ΔT, e) hive wall ΔT as proportion of mantle to ambient ΔT, f) external surface to ambient ΔT as proportion of mantle to ambient ΔT.

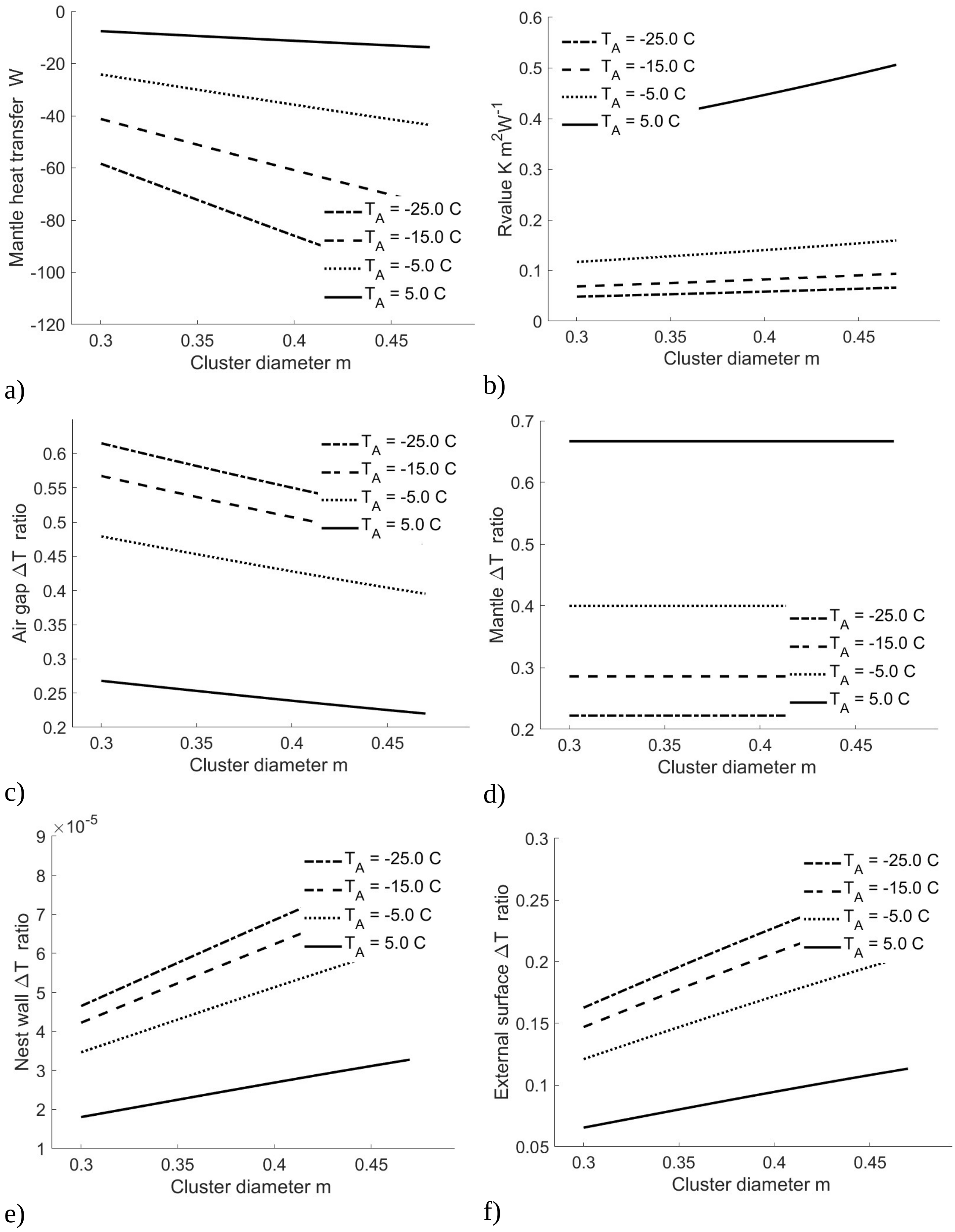

Figure 8.12: Stainless steel 1mm walls using the same dimensions as (Owens, 1971) shaded from the sky in still air. For isotherms from +5°C to -20°C versus, a) metabolic heat, b) mantle R-value, c) internal hive air gap ΔT as proportion of mantle to ambient ΔT, d) mantle ΔT as proportion of mantle to ambient ΔT, e) hive wall ΔT as proportion of mantle to ambient ΔT, f) external surface to ambient ΔT as proportion of mantle to ambient ΔT.

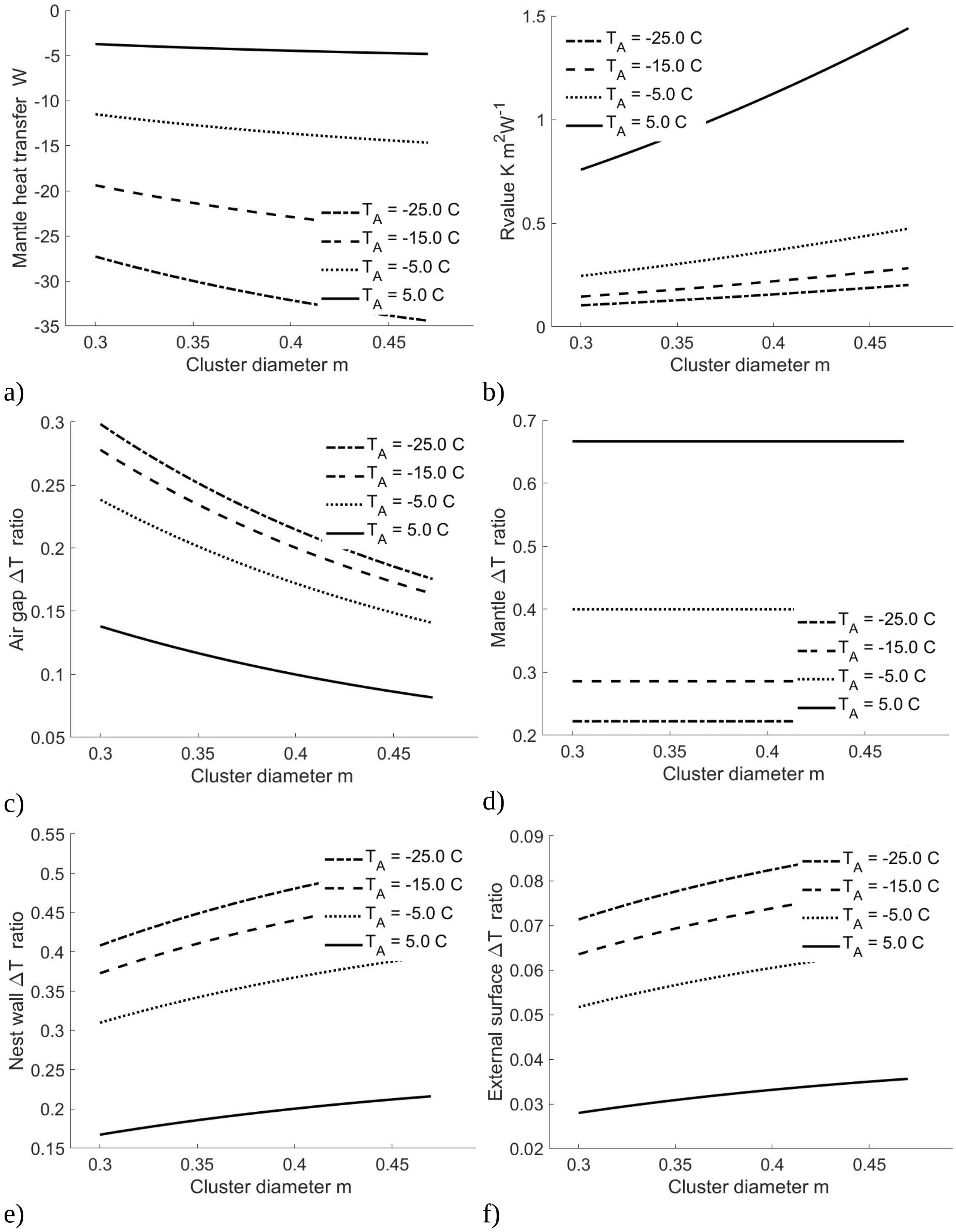

Figure 8.13: Expanded Polystyrene 30mm walls using the same dimensions as (Owens, 1971) shaded from the sky in still air. For isotherms from +5°C to -20°C versus, a) metabolic heat, b) mantle R-value, c) internal hive air gap ΔT as proportion of mantle to ambient ΔT, d) mantle ΔT as proportion of mantle to ambient ΔT, e) hive wall ΔT as proportion of mantle to ambient ΔT, f) external surface to ambient ΔT as proportion of mantle to ambient ΔT.

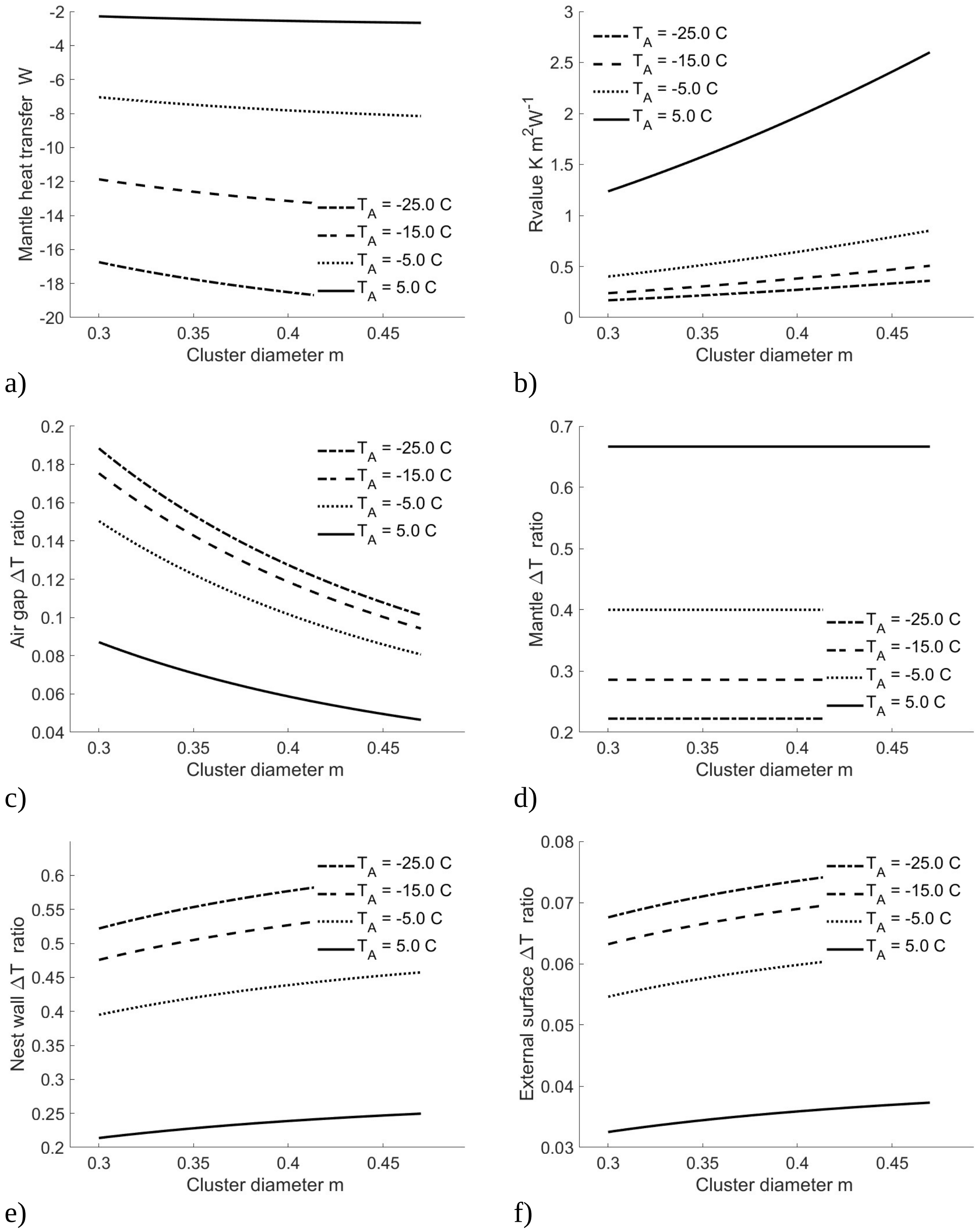

Figure 8.14: Polyisocyanurate (PIR) 50 mm walls using the same dimensions as (Owens, 1971) shaded from the sky in still air. For isotherms from +5°C to -20°C versus, a) metabolic heat, b) mantle R-value, c) internal hive air gap ΔT as proportion of mantle to ambient ΔT, d) mantle ΔT as proportion of mantle to ambient ΔT, e) hive wall ΔT as proportion of mantle to ambient ΔT, f) external surface to ambient ΔT as proportion of mantle to ambient ΔT.

8.6 Discussion

The cluster mantle does not meet any of the four insulation criteria identified and meets all three heat sink criteria.

So why cluster? Honey bees need 25°C to be at their best for heat producing, below 18°C their heating ability falls fast and at 10°C they are on the edge of life (Goller and Esch, 1990). So if the inside surface of the hive is 18°C+ (i.e. the 18°C contour is close to or in the hive walls), and the bees are comfortable producing the heat required to maintain it (figure 8.2a), then it is thermally like a summer swarm cluster (Heinrich, 1981), which rests with its periphery regulated to 18°C. This then requires little additional heat or bees to raise local temperatures to brood heat 34°C (Stabentheiner et al., 2021), as the brood is sitting in a volume in which convection is suppressed, with lower conductivity, and amongst honey bees able to deliver extra metabolic heat.

Once the outside temperature falls, the heat needed to sustain 18°C+ inside goes up. If it goes above sustainable heat production level, things start to happen. The temperature near the hive wall drops and so does that of the honey bees near it, when they rest from heating. For the individual bees which have been chilled, they have to get closer to honey bees that can still effectively produce heat, so they move inwards from the hive walls (Heinrich, 1981; Stabentheiner et al., 2003). This creates a bee-less gap next to the wall. As the outside temperature falls further, this eventually makes this 18°C contour move towards the centre of the hive (figure 8.2b). Convection currents occur in the growing gap between the hive walls and the honey bees. This increases the heat loss. The honey bees get closer together and their conductivity increases, which, while improving the survival of the outer honey bees, makes the heat loss greater. Now some of the core honey bees are cooled below 18°C, so more of those shutdown, and the collapse inwards continues. The outside conditions worsen and the 10°C contour now enters the hive internal space along with stronger convection currents (figure8.2c). Honey bees that stay outside this contour will die.

Where this 10°C contour lies now determines the thermal environment. The heat is now being produced by a few bees inside the 18°C contour that are at high levels of exertion. These produce heat for a short time and are then replaced by other honey bees (Stabentheiner et al., 2003). This shrinking of the cluster and reduction of the core goes on until heat passing through the surface area of bees at 10°C is reduced, to be in balance with the ability to produce heat by honey bees remaining at 18°C and above. As a consequence, the total heat production of the colony and the level of all other activity has collapsed (Southwick, 1982). Now instead of unstressed bees, we have bees alternately stressed by low temperature and high exertion.

In order to maintain mantle surface temperature, once the maximum density of the mantle is reached, further decreases in ambient temperature require one or more of the following: the mantle thinning by expansion of the core; the mantle thinning by honey bees on the outside dying and falling off; the core increasing its temperature.

In anthropomorphic terms, clustering as described above is not a “wrapping of a thick blanket” to keep warm, but more like a desperate struggle to crowd closer to the “fire” or otherwise die and fail the colony. Calling it an insulator gives a false impression of its role in the nest. A more accurate descriptive term may be “increased conduction mitigated by domain collapse”.

This is not the currently accepted view. This was shaped, first by Phillip and Demuth and then C.L Farrar, who commented that the cluster provided its own insulation, and then later by the work of E.E Southwick who describes, in several papers, clustering as an increase in thermal effectiveness (Southwick, 1985; Southwick, 1991), and stresses the close packing of the honey bees increasing the thermal resistance through interlocking hair and therefore several packed layers of bees as an effective insulating coat for the cluster. This led to some assuming that the thermal conductivity decreased with increasing density (Watmough and Camazine, 1995). Unfortunately this is incorrect as convection is suppressed when they are dispersed at a porosity of a round 50% i.e. about 1 to 2mm between bees (Mitchell, 2022), close to their pre-cluster state. At the densities Southwick refers to, the cluster is mostly honey bee and not air.

The difference in view resides primarily in the knowledge or assumption of pre-cluster state. Convention has used the long held assumption that the pre-cluster state is one where high value convection is dominant and clustering reduces the convection around the individual honey bees and replaces it with low value conduction.

However recent research (Mitchell, 2022), shows that the pre-cluster state is one of low value conduction and weak convection, which, on clustering, is replaced by high value convection around the cluster and doubling of the conduction within, that necessitates a dramatic partial shutdown of core heat production and other activities, offset by a reduction in surface area and an increase of stress on the individual honey bees.

In addition, some attribute the bulk of the core to ambient temperature difference to the properties of the mantle (Milbrath, 2020) giving as a reason the small temperature difference between the hive inner and outer surfaces. This is evident not only in direct statements (Milbrath, 2020), but also in the comparing of body weight to heat conductance of bee colonies to that of other animals. Those animals weights include the weight of the structure causing the temperature difference (i.e. fur, feathers), but the structure for the honey bees (i.e. the hive) has been omitted (Southwick, 1985). However, they have overlooked the high proportion of the heat difference being provided by the hive cavity (Air Gap figure 8.9). As the temperature drops the share of the temperature difference moves from the mantle (~33%) to the air cavity(~40%) and to a lesser extent the hive wall (~14%) and external surface air (~12%). This air gap makes this wooden hives performance not substantially different to one of metal (figure 8.11) (Moeller, 1977; Milbrath, 2020).

This can be summarised as either overlooking, or misunderstanding the complex interaction of the colony enclosure and thermofluids (heat, radiation, water vapour, air) with honey bee behaviour and physiology, i.e. not recognising the enclosure as within the extended phenotype.

The mathematical model of a hive used here to prove the mantle is a heat sink can also be used to estimate the thermal characteristics of potential hives design or place existing hives in context. This can be seen in summary in figure 8.10 and in detail in figures 8.9, 8.11, 8.12, 8.13, 8.14. This shows that the hive enclosure conductance has to change considerably in order to be thermally significant compared to he air gap i.e. 30mm Polystyrene or PIR. This may accounrt for some of ambigous results using honey beea and shows the importance of testing the physical significance of treatments before conducting animal experiments.

As regards the limitations of the model presented:

- The relation used here for heat transfer of the mantle to the cavity, is that of a sphere and not an ellipsoid interrupted by thermally conductive combs. However this is only likely to change the magnitude and not direction of the R value, as the observed increase in heat loss and decrease in surface area of the cluster will prevail.

- Owens had ventilation holes piercing the hive shell, if this had increased the rate of heat loss, one might have expected an increase in colony size (see section 8.5.4). Yet the predicted colony size is realistic for the locale (Ellis and Hammons, 2013). This is explained by such holes having little thermal impact in high thermal conductance enclosures (Mitchell, 2017).
- In determining the onset and magnitude of convection in the porous cluster, current heat transfer relations used here do not explicitly reflect: the isothermy of the core, the isothermy of the mantle outer surface and the boundary effects of the narrow space between the combs. Further the size of the honey bee being about half the gap between the combs adds further complexity. Thus the relations used are a simplification of a complex expanding subject (Nield and Bejan, 2006; Shruti et al., 2022).
- Anisotropy resulting from hair distribution.

All of which are subjects for further research.

8.7 Conclusion

All substances can create a temperature difference. The use of the word “insulation”, in connection with clusters, means more than that. It implies, in this case an unwarranted, positive value judgement about the substance or configuration and has, with its repetition, influenced interactions with honey bees, encouraging practices of using thin walled wooden hives and the North American refrigeration of honey bee colonies.

This study has shown that in any reasonable interpretation of the word "insulation" the clustering process results in its decrease and that a cluster is an increase in conduction, mitigated by collapsing the colony domain. A transition from a state where the honey bees can suppress internal convection within the nest, into a state of high internal convection and conduction, that results in increased individual honey bee stress. This is opposed to the conventional view that the cluster is a benign thermal improvement on the pre-cluster state.

The conventional view does not match the recent advances in research, and enables an avoidable increase in honey bee stress, (i.e. refrigeration and use of hives not significantly in different in performance from thin metal), when they are facing unavoidable increases in stress from pests, disease and climate change.

Imposing avoidable stresses on vertebrates by provoking behavioural survival responses for no benefit to the individual or groups of animals may be regarded as cruelty. Although present ethics standards for insects are different, changes in practice that reduce the frequency and duration of clustering should be urgently considered, researched and promoted (e.g. using hives from materials in figure 8.11).

8.8 References

Alburaki, M. and Corona, M. 2022. Polyurethane honey bee hives provide better winter insulation than wooden hives. *Journal of Apicultural Research*. **61**(2), pp.190–196.

Anderson, E.J. 1943. Some Research on the Wintering of Bees. *Gleanings in Bee Culture*. **71**, pp.681–683.

Basak, T., Rao, K.K. and Bejan, A. 1996. A model for heat transfer in a honey bee swarm. *Chemical Engineering Science*. **51**(3), pp.387–400.

Becher, M.A., Hildenbrandt, H., Hemelrijk, C.K. and Moritz, R.F.A. 2010. Brood temperature, task division and colony survival in honeybees: A model. *Ecological Modelling*. **221**(5), pp.769–776.

Bejan, A. 2013. *Convection Heat Transfer* 3rd Edition. New York: Wiley.

Bergman, T.L. and Lavine, A.S. 2017a. Empirical Correlations: Enclosures *In*: *Fundamentals of Heat Transfer*. Wiley.

Bergman, T.L. and Lavine, A.S. 2017b. The Conduction Shape Factor and the Dimensionless Conduction Heat Rate *In*: *Fundamentals of Heat Transfer*. Wiley, p.210.

Carson, J.K., Lovatt, S.J., Tanner, D.J. and Cleland, A.C. 2005. Thermal conductivity bounds for isotropic, porous materials. *International Journal of Heat and Mass Transfer*. **48**(11), pp.2150–2158.

Currie, R.W. and Spivak, M. 2015. Winter Management of HoneyBee Colonies *In*: J. Graham, ed. *Hive and the Honey bee*. Hamilton IL USA: Dadant.

Cushman, D. 2011. Drawings of Hives and Hive Parts. *Dave Cushman's Beekeeping and Bee Breeding Website*.

DeGrandi-Hoffman, G., Corby-Harris, V., Graham, H., Watkins-deJong, E., Chambers, M. and Snyder, L. 2023. The survival and growth of honey bee (Hymenoptera: Apidae) colonies overwintered in cold storage: the effects of time and colony location J. Rangel, ed. *Journal of Economic Entomology*., p.toad103.

Dodologlu, A., Dülger, C. and Genc, F. 2004. Colony condition and bee behaviour in honey bees (apis mellifera) housed in wooden or polystyrene hives and fed 'bee cake' or syrup. *Journal of Apicultural Research*. **43**(1), pp.3–8.

Elansari, A.M. and Hobani, A.I. 2009. Effect of temperature and moisture content on thermal conductivity of four types of meat. *International Journal of Food Properties*. **12**(2), pp.308–315.

Ellis, J.D. and Hammons, K. 2013. *Overwintering Honey Bee Colonies in Northern Climates*. University of Florida IFAS Extension.

Farrar, C.L. 1943. An interpretation of the problems in wintering the honey bee colony. *Gleanings in Bee Culture*. **September**, p.513.

Farrar, C.L. 1947. The overwintering of productive colonies *In*: R. A. Grout, ed. *Hive and the honey bee*. Chicago: Dadant and sons, pp.425–451.

Free, J.B. and Racey, P.A. 1968. The effect of the size of honeybee colonies on food consumption, brood rearing and the longevity of the bees during winter. *Entomologia Experimentalis et Applicata*. **11**(2), pp.241–249.

Glover, P.W.J. and Luo, M. 2020. The Porosity and Permeability of Binary Grain Mixtures. *Transport in Porous Media*. **132**.

Goforth, M.A., Gilchrist, G.W. and Sirianni, J.D. 2002. Cloud effects on thermal downwelling sky radiance *In*: X. P. Maldague and A. E. Rozlosnik, eds. *Thermosense XXIV* [Online]. International Society for Optics and Photonics, pp.203–213. Available from: https://doi.org/10.1117/12.459570.

Goller, F. and Esch, H. 1990. Comparative study of chill-coma temperatures and muscle potentials in insect flight muscles. *Journal of Experimental Biology*. **150**, pp.221–231.

Heinrich, B. 1981. The Mechanisms and Energetics of Honeybee Swarm Temperature Regulation. *J. Exp. Biol.* **91**(1).

Hopkins, B.K., Kulhanek, Kelly and Shved,Gregory 2023. Demographics of Indoor Bee Storage. *Project Apis m.* [Online]. [Accessed 15 September 2023]. Available from: https://www.projectapism.org/demographics-of-indoor-bee-storage.html.

Incropera, F.P. and DeWitt, D.P. 2007. *Fundamentals of Heat and Mass Transfer 6th Edition*. New Jersey US: John Wiley & Sons.

Jarimi, H., Tapia-Brito, E. and Riff, S. 2020. A review on thermoregulation techniques in honey bees' (Apis mellifera) beehive microclimate and its similarities to the heating and cooling management in buildings. *Future Cities and Environment*. **6**(1), pp.1–8.

Li, S.X., Zhao, J., Lu, P. and Xie, Y. 2010. Maximum packing densities of basic 3D objects. *Chinese Science Bulletin*. **55**(2), pp.114–119.

MATLAB 2018. *9.4.0.813654 (R2018a)*. Natick, Massachusetts: The MathWorks Inc.

Meikle, W.G., Corby-Harris, V., Ricigliano, V., Snyder, L. and Weiss, M. 2023. Cold storage as part of a Varroa management strategy: effects on honey bee colony performance, mite levels and stress biomarkers. *Scientific Reports*. **13**(1), p.11842.

Milbrath, M. 2020. The Greatest Generation : Winter Bees. *American Bee Journal*. **160**(1), pp.33–36.

Mitchell, D. 2017. Honey bee engineering: Top ventilation and top entrances. *American Bee Journal*. **157**(8), pp.887–889.

Mitchell, D.M. 2022. Honey bee (Apis mellifera) size determines colony heat transfer when brood covering or distributed. *International Journal of Biometeorology*. **66**(8), pp.1653–1663.

Mitchell, D.M. 2016. Ratios of colony mass to thermal conductance of tree and man-made nest enclosures of Apis mellifera: implications for survival, clustering, humidity regulation and Varroa destructor. *International Journal of Biometeorology*. **60**(5), pp.629–638.

Moeller, F.E. 1977. *Overwintering of Honey Bee Colonies*. Agricultural Research Service USDA.

Nield, D.A. and Bejan, A. 2006. *Convection in Porous Media*. Springer.

Norrström, N., Niklasson, M. and Leidenberger, S. 2021. Winter weight loss of different subspecies of honey bee Apis mellifera colonies (Linnaeus, 1758) in southwestern Sweden. *PLoS ONE*. **16**(10 October), pp.1–23.

Ocko, S.A. and Mahadevan, L. 2014. Collective thermoregulation in bee clusters. *Journal of the Royal Society Interface*. **11**(91).

Owens, C.D. 1971. *The thermology of the wintering honey bee*. U.S. Agricultural Research Service.

Phillips, E.F. and Demuth, G.S. 1914. *The temperature of the honeybee cluster in winter* [Online]. U.S. Dept. of Agriculture. Available from: https://doi.org/10.5962/bhl.title.64465.

Seeley, T.D. 2019a. Darwinian Beekeeping. *The Lives of Bees*. (March), pp.277–292.

Seeley, T.D. 1985. *Honeybee Ecology: A Study of Adaptation in Social Life*. New Jersey, United States: Princeton University Press.

Seeley, T.D. 2019b. *The Lives of Bees*. Princeton NJ US: Princeton University Press.

Shruti, B., Alam, M.M., Parkash, A. and Dhinakaran, S. 2022. LBM study of natural convection heat transfer from a porous cylinder in an enclosure. *Theoretical and Computational Fluid Dynamics*. **36**(6), pp.943–967.

Southwick, E.E. 1985. Allometric relations, metabolism and heat conductance in clusters of honey bees at cool temperatures. *Journal of Comparative Physiology B*. **156**(1), pp.143–149.

Southwick, E.E. 1982. Metabolic energy of intact honey bee colonies. *Comparative Biochemistry and Physiology -- Part A: Physiology*. **71**(2), pp.277–281.

Southwick, E.E. 1991. The colony as a thermoregulating superorganism *In*: *The Behaviour and Physiology of Bees*. Wallingford, England: C.A.B. International, pp.28–47.

Stabentheiner, A., Kovac, H. and Brodschneider, R. 2010. Honeybee colony thermoregulation - Regulatory mechanisms and contribution of individuals in dependence on age, location and thermal stress. *PLoS ONE*. **5**(1).

Stabentheiner, A., Kovac, H., Mandl, M. and Käfer, H. 2021. Coping with the cold and fighting the heat: thermal homeostasis of a superorganism, the honeybee colony. *Journal of Comparative Physiology A: Neuroethology, Sensory, Neural, and Behavioral Physiology*. **207**(3), pp.337–351.

Stabentheiner, A., Pressl, H., Papst, T., Hrassnigg, N. and Crailsheim, K. 2003. Endothermic heat production in honeybee winter clusters. *Journal of Experimental Biology*. **206**(2), pp.353–358.

Thermal Engineering 2019. What is R-value - Thermal Insulance Factor - Definition. *Thermal Engineering*. [Online]. [Accessed 1 August 2023]. Available from: https://www.thermal-engineering.org/what-is-r-value-thermal-insulance-factor-definition/.

Villumstad, E. 1974. Importance of hive insulation for wintering , development and honey Yield in Norway. *Apiacta*. **3**, pp.116–118.

Warrington, R.O. and Powe, R.E. 1985. The transfer of heat by natural convection between bodies and their enclosures. *International Journal of Heat and Mass Transfer*. **28**(2), pp.319–330.

Watmough, J. and Camazine, S. 1995. Self-organized thermoregulation of honeybee clusters. *Journal of Theoretical Biology*. **176**(3), pp.391–402.

Winston, M.L. 1987. Other Worker activities:Nest homeostatsis *In*: *The biology of the honey bee*. Cambridge, MASS: Harvard University Press, pp.118–119.

Xue, Y., Lofland, S. and Hu, X. 2019. Thermal conductivity of protein-based materials: A review. *Polymers*. **11**(3).

Chapter 9 Thesis Conclusions

This work has shown that the thermofluid properties of the nest enclosure of this important insect pollinator are bound up with efficiency in summer, survival in winter, geographical spread, and even the morphology of the honey bee subspecies and has demonstrated that the core hypothesis, that the nest enclosure is an intrinsic part of the honey bee colony, is proven. Also this work has shown that there are honey bee behaviours being masked by the lack of knowledge of how the colony manipulates its thermofluid environment of which the nest enclosure is an integral part. Further that the lack of knowledge is placing honey bee colonies under unnecessary stress when other stressors of parasites, climate change and disease are present. These long standing misconceptions about heat transfer in the cluster have effectively inhibited the design of new hives, which the models developed here should help to correct. This work has demonstrated that both CFD and classic engineering analysis can provide new insights in to the built environment of honey bees and in doing so has shown to human thermofluid engineers "We are not alone".

Chapter 10 Further work

This work is the first to date to look in depth with rigour into the thermofluid environment of honey bees in their nest. This has uncovered many lines of study that impact our knowledge of evolution of honey bees, their behaviour and that of thermofluids. The main challenge faced has been to constrain this enquiry into the time and space of a doctorate. The future areas are of such scope they have been further classified here into that which can be conducted as invitro/insilico and live honey bee experiments:

- In-vitro/in-silico:
    - Validating modified P1 radiation modelling with mixed optical widths.
    - Adding validated variable conductivity of porous solids to OpenFOAM.
    - Basic honey bee continuity modelling.
    - Advanced honey bee continuity modelling with honey bee thermotaxis.
    - Validated heat coefficient relation for a solid interrupted ellipsoid in narrow channels.
    - Validated Rayleigh numbers for a porous annulus about an isothermally heated porous core.
    - Impact of apertures and entrance in honey bee nests and hive design.
- Live honey bee:
    - Repeating Owens work for effective levels of insulation and for tree geometries.
    - Repeating Ellis work for Northern European honey bee subspecies.
    - Finding fluid dynamic valid sizes for the world's Apis mellifera subspecies.

10.1 In-vitro/in-silico

10.1.1 Validating modified P1 radiation modelling with mixed optical widths

The validation work showed radiation was significant, but this work did not use radiation in its CFD modelling as the current OpenFOAM models do not support the mixture of optical thickness found in and around a honey bee nest with the topological complexity. During the study some exploration of the feasibility of including computationally efficient radiation modelling was done. In summary the fvDOM model (discrete ordinates model (Modest, 2003)) is computationally intensive and requires a simple geometry, ViewFactors as implemented in OpenFOAM does not allow for fluids that absorb or emit and has been found to be inaccurate in narrow complex geometries and the P1 model is inaccurate in fluids with low absorptivity . In that exploration, the P1 model was found to have potential for modification, (See Appendices) and it proved feasible to modify the code and validate it against theory for a single geometry with zero honey bee occupancy.

The future work is to determine the emissivity correction factors for the P1 model for the geometries and honey bee number densities of the nests being simulated and then validate them using physical models. This will require 3D printing of honey bee phantoms for various honey bee number densities, inserting them in an instrumented test cell/hive and measuring the resulting heat transfer and correlating this against OpenFOAM CFD models with and without the adjusted/modified P1 model. The output from this will not only enable better OpenFOAM modelling, but increase the accuracy of hive design tools.

10.1.2 Adding validated variable conductivity of porous solids to OpenFOAM

The current study uses the fvOptions to modify the momentum equation of a fluid to simulate porous solids, but does not implement the modification of the energy equation to allow for the change in thermal conductivity of the fluid. In order to maintain accuracy the majority of this work used only thin (~10mm) porous layers beyond the isothermally heated solids, thus reducing or eliminating the inaccuracy of conductive effects within the fluid caused by the porosity. This future work needs the development of a new conjugate heat multi region solver and its validation against physical experiments. These physical experiments need to cover both the classical small bead large channel type and the circumstances which relate to honey bees. This is where the objects are not spherical, in a narrow channel, where channel width similar to the object length and twice the object girth. Some initial feasibility investigation has been done but has not been implemented in the code or validated (see Appendices).

10.1.3 Basic Honey bee continuity modelling.

The present work has not addressed finite number of bees in a colony within its CFD modelling. That is to say, it does not model the continuum of the change in densities as clustering proceeds. This new work requires the development of pre-processing to create valid cluster core/mantle number densities and porosities. This is to emulate the formation of clusters which decrease the "rest of the hive" number density as they form. This will enable a basic time series investigation of how heat transfer changes in the entire system as the cluster develops.

10.1.4 Advanced Honey bee continuity modelling with honey bee thermotaxis

This involves the adding to the governing equations, one for honey bee thermotaxis (Ocko and Mahadevan, 2014) and producing an OpenFOAM conjugate heat multi-region solver that incorporates this and the porosity conductivity model. This can then be used to investigate how the honey bee hive design impacts cluster formation and stability by simulating trees, current and proposed hive design for a range of climatic conditions, honey bee densities and honey bee sub-species.

10.1.5 A validated heat coefficient relation for a solid interrupted ellipsoid in narrow channels by conducting elements.

This work has shown that a simple model can direct decisions for hive design and bee keeping practices, however this relies on a relation for a sphere for the cluster in an empty box and does not take account of the differing shape (ellipsoid) or the interrupting comb. A more accurate relation could be found using CFD and enable determination of a valid critical dimension of an interrupted ellipsoid cluster similar to those know for a sphere or a cylinder, (Leung Wong et al., 2010; Totala, 2013). This work involves OpenFOAM simulation of the solid generic shape mentioned above within a hive structure, across a range of temperatures, hive geometries and conductances to determine the characteristic lengths and correlations. Validation would also be required by creating instrumented physical models.

10.1.6 Validated Rayleigh numbers for a porous annulus about an isothermally heated porous core with narrow channels and relatively large objects.

The porosity of honey bees between their combs has a rare set of conditions which has been assumed, in the current study and others, to be of a classical porous solid, but this assumption has not had its validity tested. The future work is to, via CFD and experiment, explore if the classical approach is valid and if not, produce a replacement. A more accurate knowledge of convection within the honey bee will serve to increase our understanding of honey bee behaviour.

10.1.7 Impact of apertures and entrance in honey bee nests and hive design.

The fluid mechanics of the current style of hive entrances, combined with additional vents and underfloor openings contrast dramatically with the high hydraulic resistance of the knot hole entrance in tree nests. The impact of these differences in high and low conductance nests can be investigated by in-silicio using CFD and in the field with honey bees. These CFD models will simulate tree and various hive designs, with a) range of apertures commonly found and b) high hydraulic resistance entrances, to measure the impact on heat transfer for a series of climatic conditions and honey bee occupancy.

10.2 Live honey bee based

10.2.1 Repeating Owen's work for effective levels of insulation and for tree geometries

The actual behaviour of honey bees in clustering and transitioning to cluster has only been examined in one set of thermal conditions i.e. high conductance conventional hives (Owens, 1971).Their behaviour in significantly low conductance or high aspect ratio trees or hives is not known.

In Owen's previous work he did not adequately quantify: the insulation, the thermal conductance, or the effect of the entrances and ventilation holes. His experiments did not consider entrances with significant hydraulic resistance, or differing hive aspect ratios. The current work has shown that if the cluster geometry changes, the thermofluid implications are significant. This new work involves instrumenting a range of hive designs with a large number of temperature sensing devices embedded in the combs within the nest. These hives are subject to a range of climatic conditions (by location and/or climate controlled chambers) and the comb temperatures data logged. This will determine how hive thermal characteristics, entrance hydraulic resistance and aspect ratio effect cluster occurrence and shape.

10.2.2 Repeating Ellis's work for Northern European honey bee subspecies

This work has shown the humidity conditions within the nest are dependent on the external conditions, the nest properties and the honey bee behaviour. This work suggests two possible hypotheses:

1. The fanning behaviour is determined by the water activity of honey which is independent of the nest location, honey bee behaviour and subspecies.
2. The fanning behaviour is determined by the climatic conditions and thus is susceptible to sub specifies adaptation.

The work was previously done on *Apis mellifera scutellata* (Ellis et al., 2008) an African sub tropical sub-species. Therefore repeating and comparing with the temperate maritime sub species *Apis mellifera mellifera* would resolve which of the two hypotheses is correct.

This new work places several samples of *Apis mellifera mellifera* honey bees in dark, constant temperature containers, each of which having a distinct constant humidity and then monitoring how many honey bees are fanning. This can be achieved, as per Ellis, by having in the containers, different salt solutions below a mesh. In addition to measuring fanning visually under red light, it is proposed to measure the intensity of the sound from the honey bee's wings.

10.2.3 Finding fluid dynamic valid sizes for the world's Apis mellifera subspecies.

This work has shown that subspecies size is a major adaptation to living within a nest by effecting the resistance to air flow and is more significant than size relationships commonly seen in mammals. However, size information on the worlds honey bee subspecies is lacking as the live fluid dynamic effective size has not been measured. A citizen science project in which bee keeper and bee enthusiasts around the world can measure bees using mobile phone photographs would rectify that lack of information.

10.3 References

Ellis, M.B., Nicolson, S.W., Crewe, R.M. and Dietemann, V. 2008. Hygropreference and brood care in the honeybee (Apis mellifera). *Journal of Insect Physiology*. **54**(12), pp.1516–1521.

Leung Wong, K., León Salazar, J.L., Lu, J.W.Z., Leung, A.Y.T., Iu, V.P. and Mok, K.M. 2010. The Critical Heat Transfer Characteristics of an Insulated Sphere Considering Heat Radiation *In*: Hong Kong- Macau (China), pp.1321–1326. [Accessed 2 September 2023]. Available from: https://pubs.aip.org/aip/acp/article/1233/1/1321-1326/914940.

Modest, M.F. 2003. *Radiative heat transfer, 2nd edition*.

Ocko, S.A. and Mahadevan, L. 2014. Collective thermoregulation in bee clusters. *Journal of the Royal Society Interface*. **11**(91).

Owens, C.D. 1971. The thermology of the wintering honey bee. *Technical Bulletin No.1429.*, p.32.

Totala, Prof.N.B. 2013. Analysis for critical radius of insulation for a cylinder. *IOSR Journal of Engineering*. **03**(09), pp.32–38.

Chapter 11 Appendices

Table 11.1: Appendix nomenclature.

Symbol	Description	Units
α'	Diffusivity density product	
$\alpha'_{laminar}$	Diffusivity density product laminar flow contribution	
$\alpha'_{turbulen}$	Diffusivity density product turbulent flow contribution	
β_v	Diffusivity density product scaling factor	
c_p	Heat capacity per unit mass	Jkg^{-1}
c_{beeEff}	Effective heat capacity per unit mass of honey bees and air in a porous region	Jkg^{-1}
h	enthalpy	Jkg^{-1}
h_{air}	Enthalpy of air phase	Jkg^{-1}
h_{bee}	Enthalpy of honey bee phase	Jkg^{-1}
k_x	Conductivity	$Wm^{-1}K^{-1}$
k_{eff}	Effect conductivity of porous region	$Wm^{-1}K^{-1}$
k_{air}	Conductivity of air phase of porous region	$Wm^{-1}K^{-1}$
k_{solid}	Conductivity of solid phase of porous region	$Wm^{-1}K^{-1}$
k_{beeEff}	Effective conductivity of honey bees and air in a porous region	$Wm^{-1}K^{-1}$
μ	Dynamic viscosity	$kgm^{-1}s^{-1}$
φ	Porosity	-
ρ	Density	kgm^{-3}
ρ_f	Density of fluid	kgm^{-3}
$\dot{q}$	Rate of heat input	W
$\dot{q}_{thermal}$	Rate of energy change due to thermal processes	W
T	Temperature	K

11.1 Other publications, conferences and outreach

The following were based on m the materials of this research.

11.1.1 Other publications:

1. Mitchell D. 2017 Honey bee engineering: Top ventilation and top entrances. *American Bee Journal* **157**, 887–889.
2. Mitchell D. 2017 Putting a Number on Natural. *Natural Bee Husbandry* **1**.
3. Mitchell D. 2019 To save honey bees we need to design them new hives. *The Conversation* , 10–12.

4. Mitchell, Derek. 2019 Changing human-made hives can help save the honey bees | The Independent | The Independent. *The Independent*, 18 September. See https://www.independent.co.uk/news/science/change-human-made-hives-honey-bees-a9098246.html.
5. Mitchell, Derek Morville (2019) ‘Thermal Efficiency’, *Bee Culture*, April. Available at: https://www.beeculture.com/thermal-efficiency/ (Accessed: 30 September 2023).
6. Mitchell, Derek. 2019 Physics and the Future of Hive Design. In *Variations on a Beehive*, Northern Bee Books.
7. Mitchell D. 2018 Surviving Winter and Making Honey needs ‘ A – Rated ’ Homes. *BBKA News* , 375–377.

11.1.2 CFD conference presentations

1. 17th OpenFOAM workshop University of Cambridge July 2022.
2. 6th Building Simulation and Optimisation, University of Bath, December 2022 (Awarded best paper)

11.1.3 International /national bee keeping events

1. Virtual Beekeeping Lecture: Garfield Park Conservatory Chicago IL USA
2. International podcast: Mitchell, D.M. (2021) ‘Insulating Your Hives in Summer & Sting Management’. (Two bees in a podcast). Available at: https://podcasters.spotify.com/pod/show/ufhbrel/episodes/Episode-67-Insulating-your-Hives-in-Summer--Sting-Management-e13mq41.
3. International conference presentation: Apimondia 2019 Montreal Canada.

11.1.4 Presentation/lectures to UK county and local beekeeping associations

Table 11.2: Lectures to UK county and local bee keeping associations

Date	**Association**
18/04/17	South Gloucestershire

Date	**Association**
06/09/17	North Staffs & South Cheshire
16/09/17	Taunton and District
13/11/17	Bridgend
16/11/17	New Forest and District
11/01/18	Fleet
26/01/18	Vale and Downland
06/10/18	Cheshire Autumn Convention
17/11/18	Dorchester and Weymouth
09/01/19	Sheffield Beekeeping
16/02/19	Somerset '
01/05/19	South West Hampshire
09/05/19	East Carmarthen
05/09/19	Harlow
19/09/19	Cambridgeshire .
17/01/20	Wantage
27/02/20	Newent
01/01/20	East Challow
01/02/20	Newent
01/04/20	Epping Forest
01/10/20	Bournmouth
01/03/21	Liskeard
01/03/21	North Hertfordshire
01/04/21	South West Hampshire
01/06/21	Aberystwyth
01/07/21	Laddingford
01/09/21	Basingstoke
01/10/21	Saffron Waldon
01/10/21	Lune Valley
01/10/21	Tavistock
01/11/21	Aylesbury
01/11/21	Ipswich
01/11/21	Winchester
01/01/22	York
22/04/22	Newbury
11/06/22	Worcestershire
01/09/22	Romford
23/10/22	Devon
07/10/22	Fareham

Date	**Association**
31/01/23	Yorkshire
23/02/23	Newent
24/03/23	East Dorset
01/04/23	N. Somerset
24/06/23	Suffolk
13/09/23	Wokingham
29/09/23	High Wycombe
24/10/23	Chalfont
03/11/23	Stratford
21/11/23	Bournemouth
02/12/23	Surrey

11.2 *P1* Radiation model validation and calibration

While this work has focused on a radiation-free approach following (Sudarsan et al., 2012) it has been shown (Mitchell, 2022) that radiation is considerable when considering the hive as a whole. The radiation models available in OpenFOAM include:

- *P1*
- Viewfactors
- *FVDOM*

The need to use participating media i.e. honey bees and wire meshes, and inability of the OpenFOAM implementation to cope with multiple narrow channels eliminated the *Viewfactors* model, and the requirement to keep computational time down eliminated *FVDOM*. However the *P1* model has limitations when used in optically thin applications e.g. no honey bees present or view factors are a consideration e.g. comb spacing. In particular, it over estimates the radiated heat loss of localised heat sources. The *P1* model and latter issue is described in (Sazhin et al., 1996) where the over estimation is quoted as factor of 1.67. To allow for this an approach of adjusting the emissivity to compensate was undertaken.

11.2.1 Determination of emissivity compensation

A CFD case of a 0.4m cube concentrically placed within a 1m cube with a temperature differential was used, to quantify the overestimation of the *P1* model and to select an emissivity that would give realistic results over the temperature differentials envisaged. The radiated power from the central cube was measured using the wallHeatFlux utility. This was compared to the theoretical radiated power (Table 11.3) (Bergman et al., 2017). The overestimation was found to be a factor of 1.91 for a central cube and outer cube emissivity of 1.0. To give the same power as theory for a central cube 0.9 and outer cube 1.0 emissivities, a *P1* model emissivity was determined by running a series of OpenFOAM cases with varying emissivity. This gave a value of ~0.6.

11.2.2 Non homogenous emissivity/absorptivity solver modifications

OpenFOAM has various radiation models to cater for either homogenous optical thickness (*constantAbsorptionEmission*) or optical thickness based on gas properties (*greyMeanAbsorptionEmission, greyMeanSolidAbsorptionEmission*, and *wideBandAbsorptionEmission*). There are no standard models that allow changes in optical thickness based on fixed locations. To cater for the radiation effects of honey bees and varroa mesh, an additional radiation model was created that varied the emissivity and absorptivity based on volumetric scalar fields (*nonHomogenousAbsorptionEmission*). The effect of the new radiation model can be seen in figure 11.1. There is a marked change in intensity around the varroa screen. This is also shown in the graph (figure 11.2) of the plot line that runs from the crown board to below the varroa screen. At y=-0.02 the intensity changes from ~1704 to 1715 W Sr^{-1} at the screen.

11.2.3 *P1* hive model validation

Using a *P1* radiation model for a hive with a low or zero number of bees has issues as the influence of view factors on the result is considerable. An approach analogous to non-radiation validation was taken to assume that all radiation emitted by a comb is absorbed by the adjacent comb thus leading to zero net emittance. This can then be implemented in the CFD model by setting comb emissivity to a very low value ~ 0.001. Varroa mesh radiation properties were set using the newly created *nonHomogenousAbsorptionEmission* model via the *setfields* utility. The simulations were run corresponding to the three set temperatures in the hive physical verification experiment and the emissivity of the hive, crownboard and roof set to 0.637. This gave resistance results (9.84, 15.09, 20.62) within 4% of the experimental findings (10.19, 15.08, 20.09).

Table 11.3: P1 CFD validation results

ID	Experimental W	P1 CFD W
rad-f8-10w	10.19 ± 1%	9.84
rad-f8-15w	15.08 ± 1%	15.09
rad-f8-20w	20.09 ± 1%	20.62

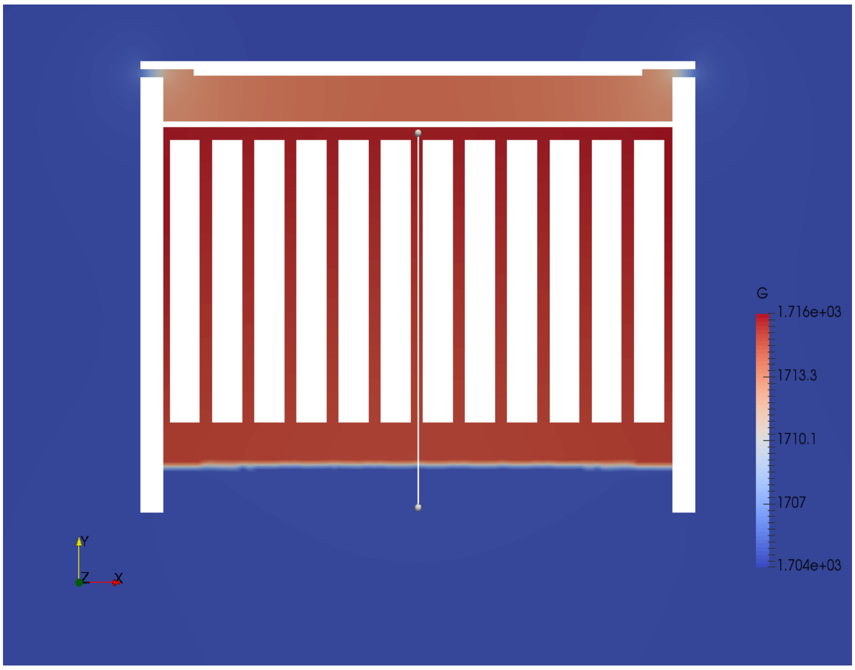

Figure 11.1: Cross section of hive showing Air phase radiation intensity with attenuation through the varroa screen and the plot line of the graph

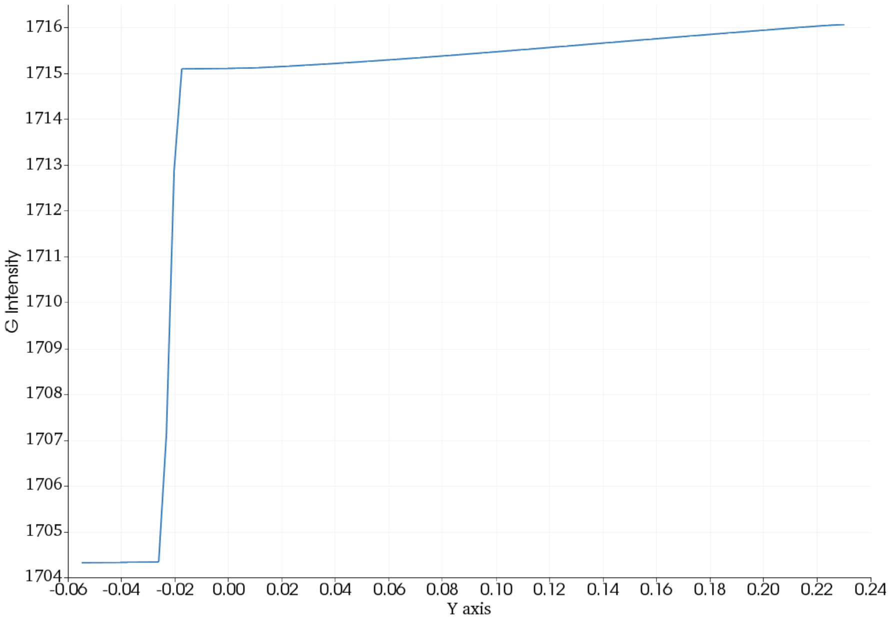

Figure 11.2: Plot of Air phase radiation intensity vs y displacment with attenuation through the varroa screen

11.3 Fluid phase vs Solid phase assumption test

The current work follows that of Sudarsan (Sudarsan et al., 2012) in treating the honey bees purely as flow resistance in a fluid phase. This is in contrast to some others (Basak et al., 1996; Humphrey and Dykes, 2008) ,which treat the clustered honey bees purely as a conducting solid phase. The reality is more complex. The honey bees covering the brood are a solid phase forming a porosity surrounded by air . At high porosities (above 0.8) convection currents move past the solid phase and convection dominates the heat transfer. At lower porosities (<0.6) drag from the solid phase stops natural convection then conduction dominates heat transfer. The question then is what is the value of conductivity to be used in future work? .

In the previous period the modelling was solely as gas with flow retarded by the solid phase. This meant that the thermal resistance increased monotonically with decreasing porosity, as conductance through the solid phase is ignored.

The literature shows that determining the effective conductance of the combination of the gas and solid is complex even when convection is eliminated. It has been shown that variation of conductivity with porosity is likely to between to that described as the second form of the Maxwell–Eucken equation (Carson et al., 2005) as shown in equation 11.1 and the EMT equation 11.2

$$k_{eff}=k_{air}\frac{2k_{air}+k_{solid}-2(k_{air}-k_{solid})(1-\varphi)}{2k_{air}+k_{solid}+(k_{air}-k_{solid})(1-\varphi)} \tag{11.1}$$

$$k_{eff}=\frac{1}{4}\Big((3\varphi-1)k_{air}+[3(1-\varphi)-1]k_{solid} + \sqrt{\{(3\varphi-1)k_{air}+[3(1-\varphi)-1]k_{solid}\}^2+8k_{air}k_{solid}}\Big) \tag{11.2}$$

For the known the conductivities of air and honey bees (Humphrey and Dykes, 2008) , this gives the relationship of effective conductivity and porosity as shown in figure 11.3

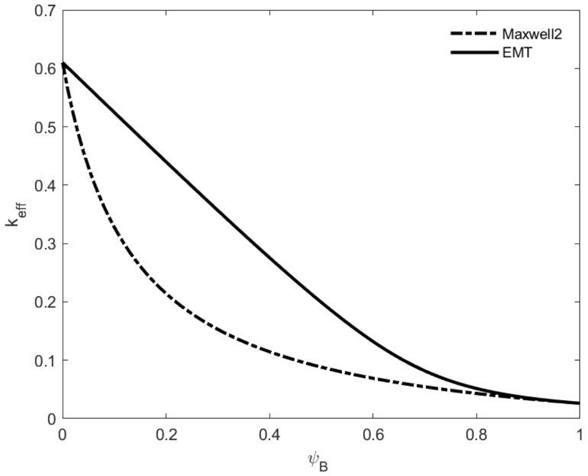

Figure 11.3: Effective conductance versus porosity for Maxwell Eucken and EMT equations where k_{solid}*=0.61 and* k_{air}*=0.026 versus brood covering porosity* ψ_B.

The actual values are dependent on the amount of thermal contact between the honey bees. It was investigated as to whether equation 11.1 or equation 11.2 could be incorporated into the gas phase of the solver. However is non trivial to achieve and validate in short time scales, so an alternate method was used of having a model that assumed the honey bee phase was a solid that obeyed the equation 11.1. This was then compared to the previous model, which assumed the honey bee phase was part of air but with retarded flow. This involved changing CAD model to fuse the brood bearing comb cell zone and the brood covering cell zones, altering the cell refinement as shown in figure 11.6, and applying the appropriate thermal conductivity to each part of the solid. A series of runs for varying ambient temperatures TA for both solid (eq. 11.1) and fluid brood covering assumptions were conducted. The plots of hive thermal resistance against porosity are show in figures 11.8 and 11.7. The difference between the two assumptions shows that further work is needed to investigate with a merged solid-fluid model.

11.3.1 Proposed solver modification

The following code is currently used in the fluid solver (figure 11.4).

```
fvScalarMatrix EEqn
(
    fvm::div(phi, he)
  + (
        he.name() == "e"
      ? fvc::div(phi, volScalarField("Ekp", 0.5*magSqr(U) + p/rho))
      : fvc::div(phi, volScalarField("K", 0.5*magSqr(U)))
    )
  - fvm::laplacian(turb.alphaEff(), he)
 ==
    rho*(U&g)
  + rad.Sh(thermo)
  + fvOptions(rho, he)
);
```

Figure 11.4: Energy equation for fluid regions

The line `- fvm::laplacian(turb.alphaEff(), he)` implements, for the steady state, the laplacian thermal terms of the energy equation (equation 11.3) where h_e is the enthalpy (equation 11.4) and α' the diffusivity density product as supplied by the function `turb.alphaEff()` i.e. equation 11.5. This function produces the sum of the turbulent and laminar modified diffusivities as in equation 11.6.

$$\dot{q}_{thermal} = -k \nabla^2 T \tag{11.3}$$

$$\text{If} \quad h = c_p T \quad \text{and} \quad diffusivity = \frac{k}{\rho c_p} \qquad \alpha' = \frac{k}{c_p} \quad \text{then} \tag{11.4}$$

$$\dot{q}_{thermal} = -\alpha' \nabla^2 h \tag{11.5}$$

$$\dot{q}_{thermal} = -(\alpha'_{laminar}{}' + \alpha'_{turbulent}) \nabla^2 h_{air} \tag{11.6}$$

When the honey bee phase is added, the effective conductivity is added to equation 11.3 which gives equation 11.7.

$$\dot{q}_{thermal} = -k_{air} \nabla^2 T - k_{beeEff} \nabla^2 T \tag{11.7}$$

Converting the combined thermal term in equation 11.7 to one expressed as enthalpies at equilibrium gives equation 11.8.

$$\dot{q}_{thermal} = -(\alpha'_{laminar} + \alpha'_{turbulent})\nabla^2 h_{air} - \alpha'_{beeEff}\nabla^2 h_{bee} \tag{11.8}$$

$$\dot{q}_{thermal} = -(\alpha'_{laminar} + \alpha'_{turbulent})\nabla^2 h_{air} - \alpha'_{beeEff}\frac{c_{beeEff}}{c_p}\nabla^2 h_{air} \tag{11.9}$$

However as solver is set up to solve for h_{air}, we can convert h_{bee} into h_{air} , as per equations 11.4 and 11.5, in equation 11.8 to give equation 11.9 . This is realised as yet unimplemented code in figure 11.5 with `alphaBeeEffCratio` as volume scalar field containing $\alpha'_{beeEff}\frac{c_{beeEff}}{c_p}$,

```
fvScalarMatrix EEqn
(
    fvm::div(phi, he)
  + (
       he.name() == "e"
      ? fvc::div(phi, volScalarField("Ekp", 0.5*magSqr(U) + p/rho))
      : fvc::div(phi, volScalarField("K", 0.5*magSqr(U)))
    )
  - fvm::laplacian(turb.alphaEff(), he)
  - fvm::laplacian(alphaBeeEffCratio, he)
  ==
    rho*(U&g)
  + rad.Sh(thermo)
  + fvOptions(rho, he)
);
```

Figure 11.5: Modified energy equation for fluid phase incorporating honey bees.

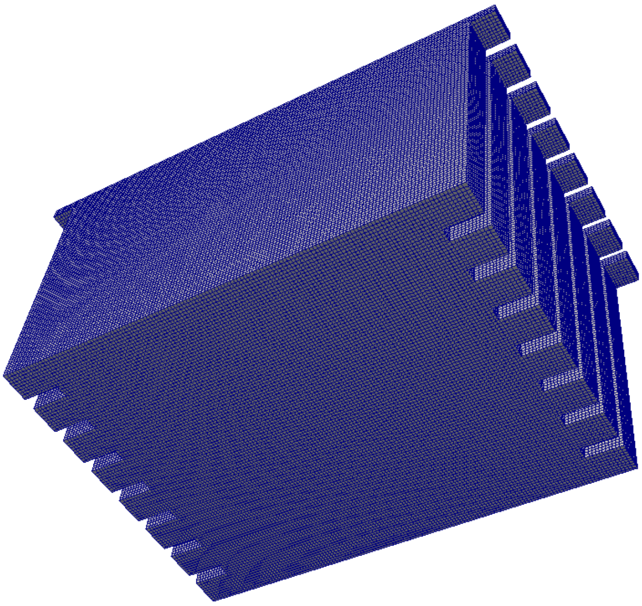

Figure 11.6: Fused brood combs and brood covering bees.

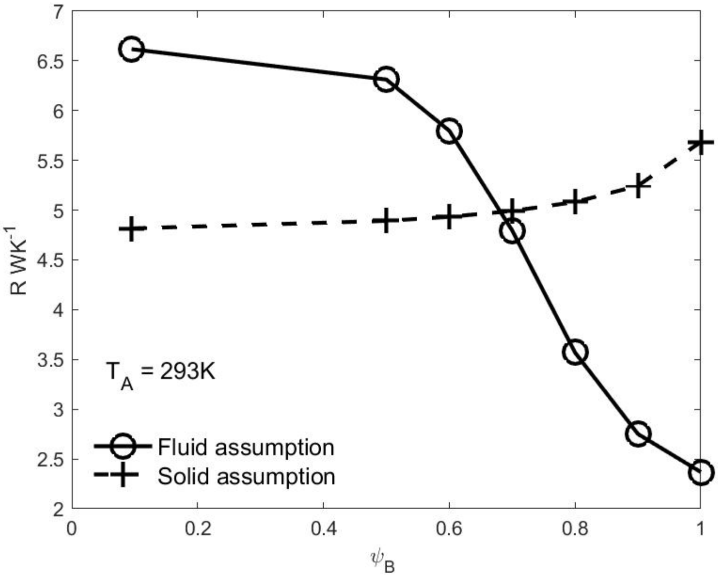

Figure 11.7: Resistance of hive R versus porosity for Brood covering assumptions at T_A= 293K

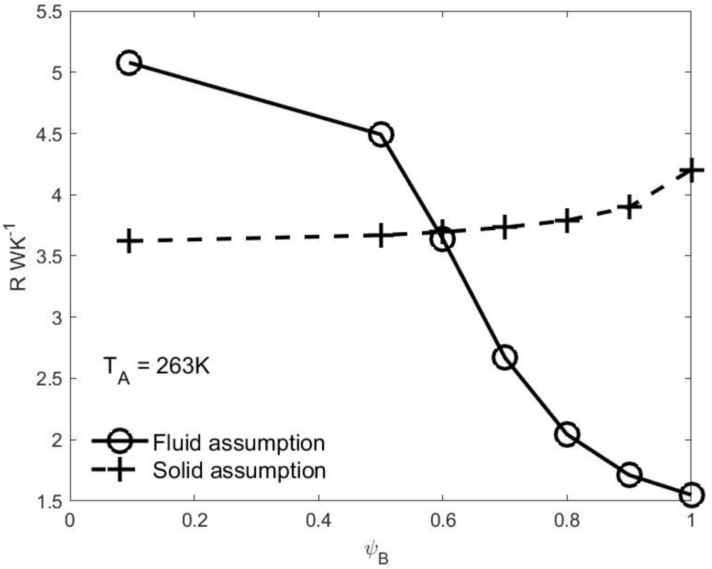

Figure 11.8: Resistance of hive R versus porosity for Brood covering assumptions at T_A=263K

11.3.2 References

Basak, T., Rao, K.K. and Bejan, A. 1996. A model for heat transfer in a honey bee swarm. *Chemical Engineering Science*. **51**(3), pp.387–400.

Bergman, T.L., Lavine, A.S., Incropera, F.P. and DeWitt, D.P. 2017. *Fundamentals of Heat and Mass Transfer* 8th ed. Wiley.

Carson, J.K., Lovatt, S.J., Tanner, D.J. and Cleland, A.C. 2005. Thermal conductivity bounds for isotropic, porous materials. *International Journal of Heat and Mass Transfer*. **48**(11), pp.2150–2158.

Humphrey, J.A.C. and Dykes, E.S. 2008. Thermal energy conduction in a honey bee comb due to cell-heating bees. *Journal of Theoretical Biology*. **250**(1), pp.194–208.

Mitchell, D. 2022. Honey bee (Apis mellifera) size determines colony heat transfer when brood covering or distributed. *International Journal of Biometeorology*. **in review**.

Sazhin, S.S., Sazhina, E.M., Faltsi-Saravelou, O. and Wild, P. 1996. The p-1 model for thermal radiation transfer: Advantages and limitations. *Fuel*. **75**(3), pp.289–294.

Sudarsan, R., Thompson, C., Kevan, P.G. and Eberl, H.J. 2012. Flow currents and ventilation in Langstroth beehives due to brood thermoregulation efforts of honeybees. *Journal of Theoretical Biology*. **295**, pp.168–193.